Roles of the MicroRNA miR-31 in Tumor Metastasis and an Experimental System for the Unbiased Discovery of Genes Relevant for Breast Cancer Metastasis

by

Scott J. Valastyan

B.S., Biological Sciences
Cornell University, 2006

SUBMITTED TO THE DEPARTMENT OF BIOLOGY IN PARTIAL FULFILLMENT OF
THE REQUIREMENTS FOR THE DEGREE OF

DOCTOR OF PHILOSOPHY IN BIOLOGY
AT THE
MASSACHUSETTS INSTITUTE OF TECHNOLOGY

SEPTEMBER 2010

Signature of Author:_____
Department of Biology
May 17, 2010

Certified by:_____
Robert A. Weinberg
Professor of Biology
Thesis Supervisor

Accepted by:_____
Stephen P. Bell
Professor of Biology
Chairperson, Graduate Committee

Roles of the MicroRNA miR-31 in Tumor Metastasis and an Experimental System
for the Unbiased Discovery of Genes Relevant for Breast Cancer Metastasis

by

Scott J. Valastyan

Submitted to the Department of Biology on August 7, 2010
in Partial Fulfillment of the Requirements for the Degree of Doctor of Philosophy in Biology

ABSTRACT

In these studies, the microRNA miR-31 was identified as a potent inhibitor of breast cancer metastasis. miR-31 expression levels were inversely associated with the propensity to develop metastatic disease in human breast cancer patients. Additionally, various functional analyses revealed that miR-31 expression was both necessary and sufficient to impede breast cancer metastasis. These effects did not involve confounding influences on primary tumor development; instead, miR-31 exerted its anti-metastatic activities by impinging upon at least three distinct steps of the invasion-metastasis cascade: local invasion, one or more early post-intravasation events, and metastatic colonization. At a mechanistic level, miR-31 impaired metastasis via the pleiotropic suppression of a cohort of target genes that otherwise operate to promote metastasis, including integrin α5, radixin, and RhoA. Significantly, the concomitant re-expression of integrin α5, radixin, and RhoA sufficed to override the full spectrum of miR-31's anti-metastatic activities. Moreover, the concurrent short hairpin RNA-conferred knockdown of endogenous integrin α5, radixin, and RhoA levels closely phenocopied the known consequences of ectopic miR-31 expression on metastasis. Integrin α5, radixin, and RhoA were found to act during at least partially unique steps of the invasion-metastasis cascade downstream of miR-31. Notably, the temporally controlled re-activation of miR-31 in already-established metastases elicited metastatic regression. These anti-metastatic therapeutic responses were attributable to the capacity of acutely re-expressed miR-31 to induce both cell cycle arrest and apoptosis; such effects arose specifically within the context of the foreign microenvironment present at a metastatic locus. When taken together, these findings provide mechanistic insights concerning the regulation of breast cancer metastasis and suggest that miR-31 may represent a clinically useful prognostic biomarker and/or therapeutic target in certain aggressive human carcinomas.

In addition, a novel experimental system for the unbiased identification of metastasis-relevant genes was described. The utility of this system was demonstrated in an initial proof-of-concept screen, which implicated RhoJ as a previously unappreciated modulator of cell motility. Collectively, these observations imply that the single-cell clone-based screening methodology outlined herein may represent a generally useful means by which to enumerate novel regulators of various metastasis-relevant processes.

Thesis Supervisor: Robert A. Weinberg
Title: Professor of Biology, MIT; Member, Whitehead Institute for Biomedical Research

Biographical Note

SCOTT JOHN VALASTYAN

60 Wadsworth Street, #8G
Cambridge, MA 02142
630-373-2625
scott_v@mit.edu

EDUCATION

2006-2010	Ph.D., Biology, Massachusetts Institute of Technology, Cambridge, MA
2002-2006	B.S., Biological Sciences, Cornell University, Ithaca, NY
1998-2002	Salutatorian, Wheaton Warrenville South High School, Wheaton, IL

HONORS AND DISTINCTIONS

2010	Poster Prize, Dana-Farber/Harvard Cancer Center Breast and Ovarian Cancer Symposium
2009	Trevigen Poster Prize, Beatson International Cancer Conference
2008	U.S. Department of Defense Breast Cancer Research Program Predoctoral Fellowship
2007, 2008	National Science Foundation Graduate Research Fellowship Honorable Mention
2006	Graduated Summa Cum Laude with High Honors in Research, Cornell University
2006	Merrill Presidential Scholar
2006	Paul Schreurs Memorial Award for Excellence in Undergraduate Research
2006	Cornell Chronicle Outstanding Senior Award
2004-2006	Presidential Research Scholar
2004	Howard Hughes Medical Institute Research Scholar
2003	Outstanding Freshman Award, Cornell University
2002-2006	Dean's List, Cornell University (all semesters)

RESEARCH EXPERIENCE

2010-present   Post-doctoral research fellow, Harvard Medical School, Advisor: Joan S. Brugge, Ph.D.
- Responsible for conducting independent research involving identification and characterization of novel molecular regulators of breast cancer metastasis

2007-2010   Doctoral thesis research, Massachusetts Institute of Technology and Whitehead Institute for Biomedical Research, Advisor: Robert A. Weinberg, Ph.D.
- Responsible for performing independent research regarding molecular mechanisms underlying breast cancer progression and metastasis, including the capacity of microRNAs to modulate metastatic dissemination
- Supervised and mentored two undergraduate students working on this project
- Extensive experience with peer reviewing manuscripts for high-impact journals, successfully applying for grants, and interviewing post-doctoral applicants

2003-2006   Undergraduate thesis research, Cornell University, Advisor: Danny Manor, Ph.D.
- Responsible for undertaking independent research investigating transcriptional regulation of cholesterol homeostasis by _-tocopherol
- Supervised and mentored three undergraduate students working on this project
- Selected to organize and moderate weekly group meetings for undergraduates

COMPETITIVE RESEARCH FUNDING AWARDED

10/08-10/11   W81XWH-08 (Department of Defense Breast Cancer Research Program Predoctoral Traineeship Award): Identification of a Putative Metastasis Suppressor MicroRNA in Human Breast Cancer

PUBLICATIONS

1. **<u>Valastyan S</u>**, Thakur V, Johnson A, Kumar K, and Manor D. 2008. Novel transcriptional activities of vitamin E: inhibition of cholesterol biosynthesis. *Biochemistry*. 47: 744-752.
2. **<u>Valastyan S</u>**, Reinhardt F, Benaich N, Calogrias D, Szász AM, Wang ZC, Brock JE, Richardson AL, and Weinberg RA. 2009. A pleiotropically acting microRNA, miR-31, inhibits breast cancer metastasis. *Cell*. 137: 1032-1046.
3. **<u>Valastyan S</u>** and Weinberg RA. 2009. MicroRNAs: crucial multi-tasking components in the complex circuitry of tumor metastasis. *Cell Cycle*. 8: 3506-3512.
4. **<u>Valastyan S</u>**, Benaich N, Chang A, Reinhardt F, and Weinberg RA. 2009. Concomitant suppression of three target genes can explain the impact of a microRNA on metastasis. *Genes and Development*. 23: 2592-2597.
5. **<u>Valastyan S</u>** and Weinberg RA. 2009. Assaying microRNA loss-of-function phenotypes in mammalian cells: emerging tools and their potential therapeutic utility. *RNA Biology*. 6: 541-545.
6. Ma L, Young JJ, Prabhala H, Mestdagh P, Muth D, Teruya-Feldstein J, Reinhardt F, Onder TT, **<u>Valastyan S</u>**, Westermann F, Speleman F, Vandsompele J, and Weinberg RA. 2010. miR-9, a MYC/MYCN-activated microRNA, regulates E-cadherin and cancer metastasis. *Nature Cell Biology*. 12: 247-256
7. **<u>Valastyan S</u>** and Weinberg RA. 2010. miR-31: a crucial overseer of tumor metastasis and other emerging roles. *Cell Cycle*. In press.
8. **<u>Valastyan S</u>**, Chang A, Benaich N, Reinhardt F, and Weinberg RA. 2010. Concurrent suppression of integrin _5, radixin, and RhoA phenocopies the effects of miR-31 on metastasis. *Cancer Research*. In press.
9. **<u>Valastyan S</u>**, Brugge JS, and Weinberg RA. Tumor metastasis: molecular insights and evolving paradigms. *Cell*. Invited review article in preparation.
10. **<u>Valastyan S</u>**, Chang A, Reinhardt F, Benaich N, and Weinberg RA. Restoration of miR-31 function in already-established metastases elicits metastatic regression in vivo. Manuscript in preparation.

PATENTS

Filed 12/5/08   U.S. Patent Application No. 61/120,322: COMPOSITIONS AND METHODS
                   RELATING TO miR-31

PRESENTATIONS AND TALKS

2011	20th Annual Meeting of the Japanese Association of Metastasis Research, invited seminar
2010	Universidade de São Paulo, invited seminar
2010	American Association for Cancer Research 101st Annual Meeting, invited seminar
2010	Cambridge Healthtech Institute Conference: MicroRNAs in Human Disease and Development, invited seminar
2010	Dana-Farber/Harvard Cancer Center Breast and Ovarian Cancer Symposium, invited seminar and poster presentation
2010	Nature Publishing Group Conference: Targeting Cancer Invasion and Metastasis, poster presentation
2010	Massachusetts Institute of Technology Department of Biology Research Symposium, invited seminar
2009	Beatson International Cancer Conference: Microenvironment, Motility, and Metastasis, poster presentation
2009	Harvard Cancer Center Specialized Programs of Research Excellence in Breast Cancer, invited seminar
2008	Whitehead Institute Forum, invited seminar
2006	Vertebrate Genomics Institute of Cornell, invited seminar
2005	Center for Vertebrate Genomics Conference, poster presentation

TEACHING EXPERIENCE
2010   Instructor, Understanding Tumor Metastasis: Historical Roots and Emerging Paradigms, Universidade de São Paulo
2010   Teaching Assistant, Graduate and Undergraduate Molecular Biology, Massachusetts Institute of Technology
2007   Teaching Assistant, Graduate Genetics, Massachusetts Institute of Technology

ACTIVITIES
2008-2010   Eastgate Executive Committee President
2008-2010   Massachusetts Institute of Technology Graduate Student Council Representative
2006-2007   Massachusetts Institute of Technology Association for Biology Graduate Students
2004-2006   Cornell University Biology Student Advisor and Academic Tutor
2004-2006   Presidential Research Scholar Peer Advisor
2003-2006   Phi Sigma Pi National Honor Fraternity, Beta Nu Chapter
- Executive Board member: President (2005), House Manager (2005), Historian and Parliamentarian (2004)

Acknowledgments

I would first like to thank my thesis advisor, Dr. Robert Weinberg, for his constant support and tutelage. I have learned a great deal during my time in the lab, and I am grateful for the freedom that I was granted to develop my scientific passions. At present, I can only appreciate that I cannot yet truly appreciate all of the wonderful opportunities that I have been given during the course of my Ph.D. training.

I also thank the members of my thesis committee, Dr. Michael Hemann and Dr. Phillip Sharp, for their many helpful discussions and sage guidance over the past three years.

I am grateful to Dr. Matthew Vander Heiden and Dr. Randolph Watnick for being so gracious with their time to serve on my thesis defense committee.

This research would not have been possible without the contributions of my collaborators at Brigham and Women's Hospital, Dr. Andrea Richardson, Dr. Jane Brock, Dr. Zhigang Wang, Dr. Marcell Szász, and Diana Calogrias. I would also like to express gratitude to Dr. Thomas Andl of Vanderbilt University, with whom I have recently forged a new collaboration. In addition, I was greatly assisted in this work by members of the MIT Koch Institute Histology Core Facility, the MIT Histology Lab, the MIT Koch Institute ES Cell and Transgenics Core Facility, and the Whitehead Institute Genome Technology Core.

I thank both past and present members of the Weinberg laboratory for providing an incredibly stimulating environment in which to conduct this research. Many thanks to Christina Scheel for first making me feel welcome back when I was a rotation student, as well as Sandra McAllister and Wenjun Guo for many fruitful discussions during my time in the lab. I would also like to acknowledge my current roommates, Brian Bierie and Wai Leong Tam, for helpful conversations, as well as their tolerance of cold temperatures and loud music.

I have had the distinct privilege of working with two exceptionally talented undergraduate students during the course of my Ph.D. training, Nathan Benaich and Amelia Chang. I have enjoyed these experiences immensely, and I can only hope that they have learned half as much from me as I have learned from them – their enthusiasm for science has been infectious.

I am grateful to Ferenc Reinhardt. Not only has he performed all of the mouse surgical procedures described in this thesis, but he is also a great benchmate and is a truly selfless person that I consider myself honored to know.

My sincere thanks to my "lab moms", Joana Liu Donaher, Ann Gifford, Mary Brooks, Elinor Eaton, and Christine Hickey, for their constant support and encouragement. In a profession that can be somewhat fast-paced and stressful, it is wonderful to have people who always take the time to genuinely care about me as a person. Also, what 25-year-old doesn't enjoy constantly hearing comments like "you're not sleeping enough" and "I hope you're not planning on wearing *that* to your post-doc interview"?

I am indebted to Matthew Saelzler and Lynne Waldman – my former roommates, fellow Weinberg lab graduate students, and good friends – from whom I have learned a great deal. One of my enduring memories from my time in the lab was the occasion when Matthew agreed to help me terminate a mouse experiment for the first time. Needless to say, I had a lot to learn and this must have been excruciatingly tedious for him – although I think he enjoyed a good laugh at my expense.

I would like to thank my parents-in-law, Anne and Steve Beckenstein, for always making me feel like a part of their family – even before I was officially a part of their family. Their years of unyielding love and support have meant a great deal to me. I am also grateful that a dedicated lineage of Yankees fans allowed their only daughter to marry a lowly Cubs fan.

I have been fortunate enough to have the love and encouragement of my grandparents, John and Cathy Schultz, and of my younger sister, Karen Valastyan. As a biologist, I am inclined to believe that my interest in the sciences must have some genetic basis – and one need look no further than their insatiable senses of curiosity, incredible creativity, and unwavering dedication to following projects through to completion to see that I have been the beneficiary of a set of genes that has indeed served me well in my scientific pursuits.

It is rare to find a scientific colleague whose intellect you respect so deeply that you immediately trust their opinion even more than you trust your own. It is rarer still to find someone who is willing to love you despite your many faults. It therefore must be "rare-est" for that valued scientific colleague and that person who loves you to be one and the same. Julie – I cannot possibly thank you enough for your years of love, advice, support, and patience. Who could have imagined that a chance meeting as two high school students would lead to all that has happened for us over these past nine years?

Finally, I would like to thank my mom, Lynn Valastyan. She has edited every paper that I have written since elementary school (including this thesis) – an act that can only be described as love. She is a source of strength during hard times, a person to laugh and celebrate with during good times, and a woman that I continue to learn from at all times. Mom – you are someone that I really look up to, and I thank you for everything that you have done for me.

This thesis is dedicated to the memory of my dad, John Valastyan, who died of metastatic colon cancer in 2001. The topic of my Ph.D. research has always held great personal significance for me, and I like to hope that my work would have made him proud.

Table of Contents

Chapter 1

Introduction

Portions of this chapter are excerpted from the following publications (copyright permissions obtained):

1. Valastyan S and Weinberg RA. (2009). MicroRNAs: crucial multi-tasking components in the complex circuitry of tumor metastasis. Cell Cycle *8*, 3506-3512.

2. Valastyan S and Weinberg RA. (2009). Assaying microRNA loss-of-function phenotypes in mammalian cells: emerging tools and their potential therapeutic utility. RNA Biology *6*, 541-545.

Cancer: Clinical Realities

Cancer is currently the second leading cause of mortality in the United States, and this disease is estimated to have claimed the lives of nearly 600,000 individuals during 2009 alone. Moreover, more than 1.5 million new cases of cancer are diagnosed within this country annually (The American Cancer Society, 2009). Unfortunately, despite a more sophisticated understanding of the etiology of cancer and a greater emphasis placed on early detection of the disease, overall mortality rates in the United States from cancer have not diminished greatly over the past 15 years (The American Cancer Society, 2009). As such, cancer continues to pose a major threat to human health and further research regarding the molecular basis of this disease is imperative in order to devise prognostic and/or therapeutic strategies that more effectively diagnose, control, and combat cancer.

Cancer is a Genetic Disease

The vast majority of human cancers arise via the accumulation of a series of genetic mutations and epigenetic changes that alter the ability of a cell to appropriately control its proliferation, survival, and differentiation (Kinzler and Vogelstein, 1996; Hanahan and Weinberg, 2000). Broadly speaking, there exist two basic classes of cancer-relevant genes: oncogenes and tumor suppressor genes. Oncogenes can promote cellular proliferation and/or survival; therefore, the aberrant activation of an oncogene can foster tumorigenic progression. In contrast, tumor suppressor genes normally function to inhibit inappropriate cellular proliferation and/or survival; accordingly, the inactivation of a tumor suppressor gene can drive tumor development. In many cases, oncogenes and tumor suppressor genes play biochemically antagonistic roles within signal transduction pathways that control numerous fundamental cell-

biologic functions (Kinzler and Vogelstein, 1996; Hanahan and Weinberg, 2000). Thus, genetic perturbations occurring within a cancer cell can lead to biochemical changes that ultimately manifest themselves as the altered cell-biologic properties characteristic of neoplastic cells.

Recent genome-wide sequencing of patient tumor specimens has revealed that a typical human tumor contains mutations in approximately 90 distinct genes (Sjöblom et al., 2006; Wood et al., 2007). While many of these mutations are likely to have arisen as passive byproducts of the intrinsic genetic instability of tumor cells (so called "passenger mutations"), it is generally believed that the deregulation of between four and eleven of these 90 mutated genes causally contribute to the pathogenesis of the disease (referred to as "driver mutations") (Hanahan and Weinberg, 2000; Sjöblom et al., 2006; Wood et al., 2007).

Traditionally, it has been posited that these mutation-bearing cancer genomes evolve via a process akin to Darwinian selection: variation is continuously introduced into the population via stochastic mutational events, and then those cell clones possessing variations that confer a proliferation and/or survival advantage become overrepresented within the population. Subsequently, this new, genetically altered population becomes the fodder for additional rounds of mutation and clonal selection (Nowell, 1976). Thus, cancer arises via a multi-step process that progressively converts normal cells of the body into highly malignant derivates via the accumulation of defined genetic alterations.

Breast Cancer

Breast cancer – the most commonly diagnosed cancer type in women in the United States, as well as the second leading cause of cancer-associated mortality in women in this country (The American Cancer Society, 2009) – is one such cancer that arises through the

progressive accumulation of genetic mutations. At a cell-biologic level, breast cancers are carcinomas, meaning that they originate from the neoplastic transformation of epithelial cells (Visvader, 2009). Epithelia are sheet-like layers of cells present throughout the body; breast epithelial cells are characterized by precisely defined apical-basal polarity, the presence of homotypic E-cadherin-mediated cell-cell junctions, and their topological location in close juxtaposition to a relatively thin layer of specialized extracellular matrix (ECM) known as the basement membrane. Within the context of intact breast tissue, the basement membrane separates the epithelium from a complex assemblage of underlying mesenchymal support cells, which are collectively referred to as the stroma (Nelson and Bissell, 2006).

Importantly, due to their acquired complement of genetic perturbations, breast carcinomas typically display a loss of cell polarity, altered expression of epithelial cell-cell adhesion molecules, disruption of the basement membrane and/or aberrations in its constituent components, and an altered cast of surrounding stromal cells (Nelson and Bissell, 2006). Indeed, emerging evidence indicates that the tissue architecture of normal breast epithelium can serve as an intrinsic barrier to tumor formation that must be overcome by incipient carcinoma cells before they can develop into overt neoplasias (Nelson and Bissell, 2006). Hence, molecular alterations that drive mammary carcinoma progression often alter the typical cell-biologic homeostasis of normal breast tissue.

At a genetic level, breast cancer is a heterogeneous disease comprised of at least five distinct molecularly defined subtypes (Sørlie et al., 2001). Importantly, these different subtypes of breast cancer differ markedly in terms of both prognosis for the development of terminal disease and responsiveness to rationally designed targeted therapeutic agents (Sørlie et al., 2001; Desmedt et al., 2008). However, despite these differences, one clinical reality shared by all of the

subtypes of breast cancer stems from the fact that the single most reliable predictor of ultimate

patient outcome is the presence of localized versus systemic disease at the time of initial

diagnosis (i.e., whether tumor cells remain confined solely within breast tissue or, instead, are

already also present at various anatomically distant organ sites) (Steeg, 2006). In fact, this poor-

prognosis criterion involving diagnosis with systemic disease is common to the overwhelming

majority of carcinomas originating from a wide spectrum of other epithelial tissues as well

(Steeg, 2006). Systemic disease occurs as a byproduct of metastasis – the spread of tumor cells

from their initial site of growth to secondary loci throughout the body.

Metastasis: the Major Obstacle to Effectively Treating Human Tumors

The association of metastasis-positivity with poor patient outcome across a diverse array

of carcinoma types is not an epiphenomenon of cancer progression; instead, distant metastases –

rather than the primary tumors from which these malignant lesions were initially spawned – are

responsible for greater than 90% of human mortality from carcinomas (Fidler, 2003; Gupta and

Massagué, 2006). Whereas essentially curative measures can be undertaken via surgical

resection and standard adjuvant therapy when patients present with well-confined primary

tumors, metastatic disease is largely inoperable given its systemic nature (Steeg, 2006).

Moreover, already-disseminated metastatic tumor cells appear to be more refractory to

conventional therapeutic agents than are the cells present in a corresponding primary tumor

(Dean et al., 2005). Accordingly, when taken together, these observations indicate that our ability

to effectively manage the impact of cancer on human health is quite dependent on our capacity to

interdict – and perhaps even reverse – the process of tumor metastasis.

The Invasion-Metastasis Cascade

At a cell-biologic level, metastases are the final end-products of a highly complex, step-wise process termed "the invasion-metastasis cascade", whereby the epithelial cells in a primary tumor (1) become motile, (2) invade locally through their surrounding ECM, (3) intravasate into the lumen of a blood vessel, (4) survive the rigors of vasculature mediated-transport, (5) arrest at a secondary organ site, (6) extravasate into the parenchyma of a distant tissue, (7) adapt to initially survive in a foreign microenvironment in order to form micrometastases, and finally (8) re-initiate their proliferative program at the site of metastasis to generate macroscopic and clinically detectable neoplastic growths (a step often referred to as "metastatic colonization") (Fidler, 2003; Gupta and Massagué, 2006). Importantly, as will be discussed below, each of these complex cell-biologic events is driven by the acquisition of defined molecular alterations that endow the incipient metastatic carcinoma cells with an ability to progress onward to the next step of the invasion-metastasis cascade.

1. Cell Motility

Attaining a motile phenotype is a crucial pre-requisite for achieving competence to complete subsequent steps of the invasion-metastasis cascade. In many forms of cell motility, individual tumor cells move along their substratum in response to contextual cues (Friedl and Wolf, 2003; Sahai, 2005). Therefore, one inherent barrier to single-cell motility imposed by the epithelial origin of carcinoma cells is the presence of intercellular, E-cadherin-mediated cell-cell junctions, which serve to prevent carcinoma cells from disaggregating from their neighbors.

As one solution toward overcoming this obstacle, tumor cells can opportunistically co-opt an evolutionarily conserved developmental program known as the epithelial-mesenchymal

transition (EMT) (Thiery, 2002; Polyak and Weinberg, 2009). The EMT converts otherwise-immotile epithelial cell clusters into single mesenchymal cells that possess a high migratory capacity. Genetically, the EMT is governed by a number of pleiotropically acting transcription factors – including Slug, Snail, Twist, Zeb1, and Zeb2 – all of which stimulate entrance into a mesenchymal state by, for example, transcriptionally repressing the expression of E-cadherin (Polyak and Weinberg, 2009). Thus, the actions of these EMT-promoting transcription factors allow cohorts of cohesive epithelial cells to disaggregate and subsequently move as individual units, thereby surmounting intrinsic physical barriers imposed by normal epithelial tissue architecture that oppose the process of cell motility.

Classically, the single-cell motility of carcinoma cells has been viewed as a four-step cyclical process involving (1) the polarized extension of actin-rich protrusions in the direction of intended migration, (2) formation of integrin-mediated adhesive focal contacts between these forward-reaching actin protrusions and the substratum, (3) stress fiber-dependent actomyosin-evoked contraction of the cell body, and (4) the release of focal contacts specifically at the rear, lagging edge of the cell and resulting propulsion of the cell body forward (Lauffenburger and Horwitz, 1996). More recently, this stress fiber- and integrin-dependent form of single-cell motility has been coined "mesenchymal migration", a name ascribed so as to distinguish it from an alternative single-cell migration-conferring pathway that operates independently of integrin-mediated focal adhesions and is termed "amoeboid migration" (Friedl and Wolf, 2003; Sahai, 2005). In the amoeboid single-cell motility program, cell movement arises due not to stress fiber- and integrin-dependent contractile forces, but instead as a consequence of the actions of the small GTPase Rho and its downstream effector kinase ROCK on the organization of more diffusely localized patches of cortical actin. These actions, in turn, allow highly deformable

individual cells to essentially glide along their substratum (Friedl and Wolf, 2003; Sahai, 2005). Consequently, there exist at least two molecularly distinct single-cell motility programs that can be hijacked by carcinoma cells to facilitate their locomotion.

As a third alternative, tumor cells can move as largely cohesive multi-cellular units through the process of "collective migration". In this form of motility, entire sheets of tumor cells linked by intact cell-cell adhesion molecules are able to execute in concert the repeating four-step cycle characteristic of mesenchymal single-cell motility (cells at the leading edge of the cluster extend protrusions and form focal contacts, contractile forces are generated, and cells at the rear of the cluster release their interfaces with the substratum to facilitate forward translocation) (Friedl and Wolf, 2003; Sahai, 2005). As in mesenchymal single-cell motility, collective migration is orchestrated by the actions of various integrins and actomyosin-regulating proteins (Friedl and Wolf, 2003; Sahai, 2005). Thus, tumor cells are capable of moving as either individual units or, instead, as cohesive multi-cellular cohorts via defined genetic and biochemical pathways involving cell-matrix interactions and the focalized control of actin dynamics.

The importance of these distinct cell motility programs within the context of metastasis derives from the capacity of tumor cells to interconvert between these various motility-promoting strategies in response to changing environmental conditions (Friedl and Wolf, 2003; Sahai, 2005). For example, if a tumor cell population that typically migrates via single-cell mesenchymal-type motility is treated with an antibody that blocks integrin function, the cells in the population can undergo a mesenchymal-to-amoeboid transition, thus allowing the tumor cells to continue their translocation by shifting to an integrin-independent migration program (Friedl and Wolf, 2003; Sahai, 2005). For this reason, it has been proposed that anti-migratory

therapeutic strategies must be capable of simultaneously inhibiting mesenchymal motility, amoeboid motility, and collective motility in order to demonstrate true efficacy (Friedl and Wolf, 2003; Sahai, 2005). Hence, tumor cells have evolved a variety of molecular mechanisms by which to achieve motility, thus enabling them to successfully translocate even in the wake of insults that abrogate entire individual migration pathways.

2. Local Invasion

Once tumor cells have become motile, they are then able to begin to invade locally. Local invasion refers to the ability of carcinoma cells that formerly resided within an intact epithelial tissue to physically enter into the surrounding tumor-associated stroma (Fidler, 2003; Gupta and Massagué, 2006). In order to reach the stroma, the tumor cells must first penetrate the basement membrane – a thin layer of specialized ECM that separates the epithelial and stromal tissue compartments (Nelson and Bissell, 2006).

The basement membrane surrounding most carcinoma cells is comprised of a complex array of glycoproteins and proteoglycans, including various collagens, laminins, and fibronectin (Nelson and Bissell, 2006). In addition to the structural roles played by the basement membrane – essentially serving as a physical barrier between carcinoma cells arising within an epithelium and the adjacent stromal compartment – components of this ECM also play vital roles in signal transduction events within the carcinoma cells via pathways initiated by integrin-mediated cell-matrix interfaces. Moreover, the ECM contains a rich repository of tethered growth factor molecules, which can subsequently be liberated by the actions of extracellular proteases secreted by carcinoma cells (Nelson and Bissell, 2006). Therefore, disruption of the basement membrane

by carcinoma cells profoundly alters both the physical and biochemical microenvironment within which tumor cells reside.

During carcinoma progression, degradation of the basement membrane is principally executed by members of the matrix metalloproteinase (MMP) family. These substrate-specific proteolytic enzymes efficiently degrade well-defined ECM components; consequently, in normal epithelial tissue, the activity of MMPs is carefully controlled via a combination of transcriptional and post-translational regulatory events (Coussens et al., 2002). Carcinoma cells have devised a number of means by which to derail this tight modulation of MMP activity, almost invariably leading to enhanced MMP function and thus degradation of ECM components that lie in the path of invading tumor cells (Coussens et al., 2002).

Hence, once carcinoma cells have attained both cell motility and the ability to dissolve constituents of the ECM, they are able to successfully traverse the basement membrane and enter into the neighboring tumor-associated stroma. The cancer cells are then able to engage in heterotypic signaling events with a complex milieu of stromal cells – including fibroblasts, myofibroblasts, macrophages and other immune cells, adipocytes, mesenchymal stem cells, and endothelial cells – that are capable of further enhancing the aggressive behaviors of carcinoma cells (Joyce and Pollard, 2009). For example, stromal myofibroblasts can promote primary tumor growth and angiogenesis in breast cancer xenograft models by secreting stromal cell-derived factor-1 (SDF-1) (Orimo et al., 2005); similarly, mesenchymal stem cells recruited to the tumor stroma can secrete chemokine ligand-5 (CCL5) to enhance the migration and invasion of breast carcinoma cells (Karnoub et al., 2007). More generally, microarray gene expression profiling of the tumor-associated stroma reveals characteristic expression signatures that are associated with patient metastatic outcome in human breast tumors (Finak et al., 2008) Thus, genetic influences

on the cell-biologic processes of metastasis are not solely tumor cell-intrinsic; rather, the molecular composition of tumor-adjacent stromal cells can also play a critical role in dictating metastatic progression.

Importantly, in addition to the malignancy-promoting attributes that certain stromal cell types can impart to invading carcinoma cells, entry of the epithelial tumor cells into the stroma – driven by the genetic events outlined above – also provides abundant opportunities for the cancer cells to physically gain access to either the lymphatic or hematogenous circulation and thereby disseminate systemically.

3. Intravasation

Intravasation refers to the process of locally invasive carcinoma cells exiting their surrounding stroma and entering into the lumen of a lymphatic vessel or a blood vessel (Fidler, 2003; Gupta and Massagué, 2006). Although lymphatic spread of carcinoma cells is routinely observed in human tumors – and, in fact, represents an important prognostic biomarker for the propensity for disease progression – cancer cell dissemination via the bloodstream appears to represent the major mechanism by which incipient metastatic carcinoma cells broadly disperse throughout the body (Fidler, 2003; Gupta and Massagué, 2006).

The detailed molecular mechanisms by which tumor cells complete the cell-biologic task of intravasating into the lumina of blood vessels remains an area of active investigation. However, it is likely that this process can be facilitated by defined genetic changes occurring within carcinoma cells that promote their ability to cross the endothelial cell barrier that lines blood vessels. For example, the EMT-promoting transcription factor Twist was shown to enhance the intravasation of murine mammary carcinoma cells (Yang et al., 2004), ostensibly by

either increasing the ability of tumor cells to invade through endothelial cell sheets or more generally augmenting the invasive and/or migratory capacity of carcinoma cells.

Of perhaps even more widespread relevance to the process of intravasation is the physical nature of tumor-associated blood vessels. Through a variety of cellular mechanisms – many of which converge on members of the vascular endothelial growth factor (VEGF) family – tumor cells are capable of stimulating the formation of new blood vessels within their local microenvironment through a process known as neo-angiogenesis (Hanahan and Folkman, 1996). In contrast to the blood vessels present in non-tumor-containing tissues, the neo-vasculature created by cancer cells is quite tortuous and is prone to vascular leakiness (Jain, 2005; Stockmann et al., 2008). Accordingly, because the intercellular interactions between endothelial cells lining the lumina of tumor-associated blood vessels are inherently weak, it is probable that locally invasive carcinoma cells can often cross into the lumen of a tumor-proximal blood vessel without substantial difficulty – and perhaps even in the absence of additional acquired molecular alterations.

4. Survival in the Circulation

Once they have successfully intravasated into the lumen of a blood vessel, tumor cells can be broadly disseminated throughout the body via transit through the hematogenous circulation. Recent technological advances have facilitated the direct detection of tumor cells within the bloodstream of human cancer patients (Nagrath et al., 2007; Pantel et al., 2008). Of interest, it has been demonstrated that quantitation of the overall numbers of circulating tumor cells present in patients afflicted with any of a variety of carcinoma types provides a prognostic indicator of likely disease outcome (Pantel et al., 2008), as well as a means by which to rapidly

gauge the responsiveness of a given tumor to neo-adjuvant or adjuvant therapies (Maheswaran et al., 2008). Thus, tumor cells can indeed be detected in the bloodstream of carcinoma patients; ostensibly, these isolates contain the precursor cells of eventual overt metastases that are actively in the process of disseminating.

Carcinoma cells present in the hematogenous circulation must survive a variety of cellular stresses in order to reach a secondary organ site intact. First, tumor cells in the circulation are deprived of integrin-conferred adhesion to the ECM (Reddig and Juliano, 2005). Because this integrin-mediated signaling provides a source of essential survival-promoting signals, epithelial cells that lack proper cell-matrix adhesion normally undergo anoikis – a form of apoptotic cell death triggered by the loss of anchorage to a substratum (Reddig and Juliano, 2005). At a molecular level, anoikis is regulated by a number of cell surface receptors, including various integrins (Gupta and Massagué, 2006). Thus, in order for tumor cells to survive vasculature-mediated transport, it appears that they may first have to become refractory to anoikis-mediated cell death by constitutively activating pro-survival signaling pathways that are otherwise dampened upon matrix detachment.

Additionally, tumor cells in the systemic circulation must overcome two additional threats in order to survive until they reach a secondary organ site: (1) the damages imposed by hemodynamic shear forces and (2) detection by predatory cells of the immune system (Gupta and Massagué, 2006). Conveniently, carcinoma cells seem to be capable of simultaneously evading both of these cytotoxic influences through the utilization of a single mechanism involving the co-option of platelets. More specifically, by forming relatively large emboli via interactions with blood platelets, tumor cells are able to both shield themselves from shear forces and also evade immune detection (Nash et al., 2002). Thus, platelet-coated tumor cells that have also become

resistant to anoikis are able to persist in a viable state within the circulation until they arrest at a secondary tissue locus.

5. Arrest at a Distant Organ Site

Eventually, tumor cells that retain viability within the systemic circulation will become lodged in the microvasculature present at an anatomically distant organ site. Despite the theoretical ability of metastasizing carcinoma cells traveling through the hematogenous circulation to disseminate to a wide variety of secondary loci, clinicians have long-noted that individual carcinoma types stereotypically form metastases at only a limited subset of these sites (Fidler, 2003; Gupta and Massagué, 2006). Of relevance to this observation, one point of contention within the metastasis research community concerns whether tumor cells actively "home" to specific distant organs at an appreciable frequency via genetically driven ligand-receptor interactions or, instead, predominantly simply arrest within capillary beds stochastically due to size restrictions imposed by the diameters of those blood vessels (Gupta and Massagué, 2006). To be certain, the anatomical layout of the vasculature precludes the arrest of carcinoma cells within the capillary beds of certain distant organ sites when those capillary beds lie downstream of other microvessels whose diameter is insufficient to permit the passage of circulating tumor cells (Fidler, 2003; Gupta and Massagué, 2006).

However, compelling evidence has also been obtained indicating that at least certain populations of carcinoma cells are capable of forming specific adhesive interactions – mediated by cell-matrix adhesion molecules, cell-cell adhesion molecules, or chemokine receptors – at particular secondary organ sites, which preferentially favor entrapment of the disseminating tumor cells there (Gupta and Massagué, 2006). For example, expression of _3_1 integrin

heterodimers on the membranes of disseminating breast carcinoma cells and fibrosarcoma cells has been proposed to mediate their lung-selective arrest via interactions with the cognate ligand of _3_1 integrin – laminin-5 – which lies exposed on the surface of the pulmonary vascular basement membrane (Wang et al., 2004). The relative prevalence of these and analogous molecularly driven strategies that facilitate the organ-specific arrest of disseminated carcinoma cells awaits future study.

6. Extravasation

Regardless of the particular mechanism by which cancer cells initially become trapped within the microvasculature at a distant organ site, tumor cells lodged in blood vessels are likely to attempt to extravasate from the lumen of those vessels into the parenchyma of that tissue. In order to do so, carcinoma cells must cross the endothelial cell layer that separates vessel lumina from the stromal microenvironment of that organ (Fidler, 2003; Gupta and Massagué, 2006).

Superficially, extravasation seems to represent the exact reverse of the process of intravasation; however, there are reasons to believe that these processes may, in fact, be mechanistically quite distinct from one another. As discussed previously, the neo-vasculature formed by a tumor at its primary site of growth is tortuous and leaky (Jain, 2005; Stockmann et al., 2008); conversely, endothelial cell permeability at a secondary organ site can be very low (Nguyen et al., 2009). For example, incipient metastatic carcinoma cells attempting to reach the brain parenchyma must traverse the blood-brain barrier; similarly, the endothelial cells lining the lumina of pulmonary microvessels are largely impermeable. In contrast, however, carcinoma cells arriving in the bone encounter fenestrated sinusoids that likely pose only a minor obstacle to extravasating tumor cells (Nguyen et al., 2009). Thus, the nature of the specific tissue

microenvironment present at the site of metastasis holds great consequences for the progression and fate of disseminated tumor cells – a critically important point that will be revisited in greater detail below.

Molecular mediators of extravasation have historically proven difficult to identify. However, a recent study discovered that angiopoietin-like 4 (Angptl4) promotes lung metastasis in human breast cancer xenograft models via disruption of pulmonary vascular endothelial cell cell-cell junctions, thereby increasing retention of the carcinoma cells at this metastatic locus (Padua et al., 2008). Of note, Anglptl4 did not augment the metastatic abilities of these same breast cancer cells to the bone, nor did Anglptl4 enhance their intravasation efficiency (Padua et al., 2008); hence, Anglptl4 specifically promoted the process of extravasation, and did so only within the particular microenvironmental context of the lung. These findings provide empirical evidence for a model in which extravasation at certain secondary organ sites necessitates defined genetic programs that are not required for either intravasation away from a primary tumor or extravasation at alternative secondary organ sites.

7. Initial Survival in a Foreign Microenvironment and Micrometastasis Formation

Although examples of intraluminal metastatic growth have been reported (Al-Mehdi et al., 2000), metastases predominantly arise following the extravasation of tumor cells into the parenchyma of a secondary organ site. A critical pre-requisite for metastasis formation therefore becomes an acquired ability of disseminated carcinoma cells that have successfully extravasated to survive within the foreign microenvironment afforded by the tissue parenchyma present at the site of metastasis (Fidler, 2003; Gupta and Massagué, 2006). At first glance, this may seem to represent a rather trivial hurdle for a metastasizing carcinoma cell that has already endured

numerous perils in order to translocate systemically; however, the cells that populate a primary tumor were evolutionarily selected on the basis of accumulated genetic alterations that promoted their ability to survive and proliferate specifically within their orthotopic site of growth (Hanahan and Weinberg, 2000). Thus, if the microenvironment at the site of metastasis differs substantially from that previously encountered by the carcinoma cells at the primary tumor locus – in terms of either the representation of heterotypically signaling stromal cells, the constituency of the surrounding ECM, or the spatial architecture of the tissue itself – then the disseminated tumor cells are unlikely to be able to sufficiently activate certain requisite pro-survival molecular signaling pathways within this novel microenvironment.

Some have proposed that carcinoma cells can solve this problem of an incompatible microenvironment at the metastatic site via the establishment of a "pre-metastatic niche" (Kaplan et al., 2005). According to this model, cancer cells residing in a primary tumor induce the mobilization of hematopoietic progenitor cells from the bone marrow to the future site of metastasis formation, and these hematopoietic cells then modify the local microenvironment of that site by secreting matrix metallopeptidase 9 (MMP-9) – all of this occurring prior to the carcinoma cells ever arriving at the secondary locus (Kaplan et al., 2005). Activation of MMP-9 at the future site of metastasis is believed to result in the stimulation of various integrins, as well as the liberation of sequestered SDF-1 (Kaplan et al., 2005). Thus, tumor cells reaching this modified anatomically distant microenvironment are able to more readily adapt to form retention- and survival-promoting interactions with their new stromal milieu.

Notably, the creation of a supportive pre-metastatic niche could potentially represent a broadly important determinant of metastatic propensity, as the organ site spectrum of metastases formed by lung carcinoma cells can be altered simply by re-routing the niche-forming

hematopoietic cells to different organs (Kaplan et al., 2005). It is worth noting that aspects of the molecular details underlying the pre-metastatic nice concept have recently been questioned (Dawson et al., 2009), and thus this model remains controversial. More generally, however, it is clear that tumor cells must deploy genetically driven cell-autonomous or cell-non-autonomous means to modify the novel microenvironment encountered at the site of metastasis in order for them to initially survive at an ectopic location and form small micrometastases.

8. Metastatic Colonization

Once disseminated tumor cells adapt to initially survive within an ectopic, secondary microenvironment, the carcinoma cells usually do not rapidly progress from small micrometastases into large, robustly growing macroscopic metastases. Instead, most of the disseminated tumor cells persist in a state of apparent dormancy – retaining viability in the absence of any net gain or net loss in overall cell number (Chambers et al., 2002). Two models – which are not mutually exclusive – have been proposed to rationalize the behavior of these occult micrometastases. In the first model, the tumor cells continue to proliferate within the parenchyma of the new tissue, yet an increase in total cell number does not occur due to the counterbalancing effects of a high rate of apoptosis in these actively dividing cells; a failure of the disseminated cells to trigger neo-angiogenesis at the secondary locus has been proposed as a possible mechanistic explanation for this phenomenon (Holmgren et al., 1995). The second model holds that the disseminated tumor cells are largely quiescent, with their proliferation at the metastatic site greatly impaired due to incompatibilities with the foreign microenvironment encountered at the site of metastasis (Chambers et al., 2002).

This appreciation that disseminated tumor cells often encounter significant difficulties as they attempt to form macroscopic metastases is not a new concept. In fact, more than 120 years ago, Stephen Paget articulated his "seed and soil" hypothesis of metastatic outgrowth based upon clinical observations detailing preferential metastasis of a given type of cancer to one or more particular distant organ sites (Paget, 1889). This viewpoint posits that, while tumor cells are broadly disseminated during the course of malignant progression, detectable metastases only develop at those sites ("soils") where the tumor cells ("seeds") are suitably adapted for survival and proliferation (Paget, 1889). Importantly, the "seed and soil" hypothesis does not distinguish between the proliferation/apoptosis counterbalance model and the quiescence model of micrometastatic dormancy.

Consistent with the "seed and soil" hypothesis, evidence emanating from a number of laboratories – most notably the work of Fidler and colleagues – has directly documented that specific organ microenvironments are indeed inherently more or less hospitable to certain types of disseminated tumor cells, independent of influences stemming from the anatomical layout of the vasculature (Hart and Fidler, 1980; Fidler, 2003). For example, melanoma cells readily metastasized to sub-cutaneous grafts of lung tissue but failed to metastasize to identically placed – and identically vascularized – sub-cutaneous grafts of renal tissue, thereby reflecting the known proclivity of melanomas to form pulmonary metastases (Hart and Fidler, 1980; Fidler, 2003). More recently, the Massagué laboratory has identified a number of genes whose expression facilitates the metastatic colonization of breast cancer cells specifically to either bone (Kang et al., 2003), lung (Minn et al., 2005), or brain (Bos et al., 2009). Ostensibly, these genetic factors favor outgrowth in an organ-selective manner due to their ability to allow disseminated tumor cells to overcome specific obstacles to macroscopic metastasis formation imposed by the

tissue microenvironment of a particular organ. Indeed, many of these genes play crucial roles of apparent relevance to the colonization of only a single specific microenvironment. One example of this is provided by the osteoclastic cytokine interleukin-11 (IL-11), which facilitates the formation of osteolytic bone metastases by breast cancer cells (Kang et al., 2003). The observation that these genetic factors act in a highly tissue site-specific manner further underscores the reality that successful metastatic colonization requires a delicate interplay between disseminated tumor cells and the particular microenvironment within which these cells come to reside.

An additional consideration pertinent to the topic of metastatic colonization derives from an appreciation that the precursor cells of macroscopic metastases must possess a relatively high self-renewal capacity in order to form large malignant growths. On the basis of research carried out over the last decade, some have proposed that only a sub-population of the neoplastic cells present in a tumor – the so-called "tumor-initiating cells" (TICs) – possess the extensive self-renewal capacity required to seed new tumors (Rosen and Jordan, 2009). Indeed, xenograft serial transplantation studies involving several human tumor types lend support to this model, although the applicability of these findings to all types of human malignancies remains a subject of intensive ongoing debate (Rosen and Jordan, 2009). Of particular relevance to metastatic colonization, the TIC hypothesis asserts that one or more TICs must disseminate from a primary tumor during the course of disease progression in order for a macroscopic metastasis to develop; accordingly, if a non-TIC disseminates to a secondary locus, its limited self-renewal capacity precludes it from spawning a macroscopic metastasis (Brabletz et al., 2005). At a molecular level, one class of molecules that has been implicated in regulating the TIC-state are EMT-promoting transcription factors, such as Snail, Twist, and Zeb1 (Polyak and Weinberg, 2009);

this unexpected convergence between a single molecular pathway that appears to promote both motility and self-renewal is noteworthy, as the pleiotropic actions of these transcription factors may concomitantly facilitate multiple distinct aspects of the metastatic process.

By concurrently solving microenvironmental incompatibilities and activating self-renewal pathways via the actions of the genetic factors outlined above, some carcinoma cells succeed in completing the endeavor of metastatic colonization and thereby generate macroscopic, clinically detectable metastases (Fidler, 2003; Gupta and Massagué, 2006). The formation of robustly growing macroscopic metastases represents the endpoint of the invasion-metastasis cascade. In many respects, only those foci that have completed the process of metastatic colonization truly ought to be referred to as "metastases", as these are the only malignant growths that have overcome the complex series of obstacles – from physical barriers associated with preventing the initial escape of cancer cells from a primary tumor all of the way through to the ability of disseminated carcinoma cells to adapt to survive and thrive within a novel microenvironment – that normally operate to oppose metastasis formation. Hence, via the accumulation of acquired genetic alterations, cancer cells are capable of completing an intricate, multi-step cell-biologic process that culminates in the formation of macroscopic – and oftentimes life-threatening – malignant growths at a secondary organ site.

Metastasis is a Highly Inefficient Process

The invasion-metastasis cascade – which, as detailed above, is the cell-biologic program that governs the creation of metastases – is extraordinarily inefficient (Chambers et al., 2002). For example, large numbers of circulating tumor cells can be detected within the bloodstream of human cancer patients that possess few – if any – overt metastases (Nagrath et al., 2007). Thus,

the ability of tumor cells to exit from their initial site of growth and intravasate into the systemic circulation does not guarantee the subsequent formation of clinically detectable metastases.

This point was vividly demonstrated by observing ovarian cancer patients who were provided palliative remediation via the insertion of peritoneovenous shunts (Tarin et al., 1984). In addition to relieving pain, this treatment – which evacuates ascites fluid into the venous circulation – liberated millions of cancer cells into the systemic circulation; nevertheless, these patients largely failed to develop detectable metastases even several years after installation of the shunts (Tarin et al., 1984). Taken together, these observations begin to suggest that later steps of the invasion-metastasis cascade – namely, survival in the circulation, arrest at a distant organ site, extravasation, initial survival in a foreign microenvironment to permit micrometastasis formation, and/or metastatic colonization – are successfully completed at only a very low frequency.

Detailed work in experimental model systems has further defined the particular steps of the metastatic process that appear to be rate-limiting. More specifically, the Chambers laboratory discovered that survival in the circulation, arrest at a distant organ site, and extravasation occurred quite efficiently in multiple carcinoma cell types (Luzzi et al., 1998; Chambers et al., 2002). In contrast, however, once tumor cells exited the lumen of a microvessel into the parenchyma of a distant tissue, high rates of attrition were observed. Importantly, although a significant number of successfully extravasated tumor cells failed to initially survive within a foreign microenvironment and form micrometastases, the subsequent process of metastatic colonization was substantially more inefficient – perhaps even by several orders of magnitude (Luzzi et al., 1998; Chambers et al., 2002). Hence, it appears likely that metastatic colonization typically represents the rate-limiting step of the invasion-metastasis cascade.

Further support for this supposition is provided by clinical observations in carcinoma patients concerning the kinetics of distant relapse and disease recurrence. In many human tumor types – for example, breast cancers – detectable metastases often arise only many years or even decades after the apparent complete resection of a patient's primary tumor (Nguyen et al., 2009). Because the metastatic cells must have been shed by the primary tumor prior to its surgical removal, this implies that these cells persisted in an occult – yet viable – state for many years. The most parsimonious interpretation of these clinical observations is that, although the incipient metastatic precursor cells were capable of disseminating to a distant organ site and retaining viability at that locus, the appearance of clinically detectable metastases was substantially delayed due to the gross inefficiency of the process of metastatic colonization (Nguyen et al., 2009). Ostensibly, during this long period of latency, the disseminated tumor cells underwent gradual genetic evolution in order to overcome obstacles that initially precluded successful metastatic colonization.

When taken together, these observations reveal that only an extremely small minority of the cells that initially enter into the invasion-metastasis cascade ultimately complete the process and yield macroscopic metastases. However, despite the high rates of cellular attrition that accompany various steps of the metastatic process, metastasis-competent cells nevertheless ultimately arise in many human cancer patients – where they often represent the source of terminal disease (Fidler, 2003; Gupta and Massagué, 2006). Together, these points naturally draw attention to questions regarding the cellular origin of the precursor cells of overt metastases, as well as the timing and spatial localization of the genetic events that drive the molecular evolution of these cells toward metastatic competence.

How, When, and Where Do the Precursor Cells of Overt Metastases Arise During the Course of Tumor Progression?

The above discussions indicate that (1) metastatic colonization is often the rate-limiting step of the invasion-metastasis cascade and (2) the genetic and cell-biologic requirements for a tumor cell to thrive at an orthotopic site versus an ectopic site can be quite different. It is therefore reasonable to ponder how – under the Darwinian clonal selection model of cancer pathogenesis – metastasis-competent cells can initially arise at the requisite frequency within a primary tumor (Bernards and Weinberg, 2002). In some instances, the answer may be somewhat trivial: certain genetic changes can confer acquired abilities that promote cellular proliferation and/or survival at both the primary site of growth and at a metastatic locus. Genes whose altered activities participate in tumor progression in this manner have been termed "metastasis initiation genes" and "metastasis progression genes" (Nguyen et al., 2009). In the case of pleiotropically acting factors, even if the specific biochemical function responsible for endowing these growth-promoting attributes differs between the context of a primary tumor and an ectopic microenvironment, selection for heightened overall activity of the factor may still occur during primary tumor development. This might lead, in turn, to enrichment of cells possessing this genetic alteration within the primary tumor and thus an increased probability for those cells to initiate the invasion-metastasis cascade.

More puzzling is the problem of how cells expressing "metastasis virulence genes" – i.e., genetic factors that confer a proliferation and/or survival advantage only within the context of specific ectopic, secondary microenvironments (Nguyen et al., 2009) – can arise at an appreciable frequency during the course of malignant progression. Because altered activity of these gene products – by definition – does not impact primary tumor development, cells

expressing these factors cannot possibly be selected for during the evolution of a primary tumor under the Darwinian model (Bernards and Weinberg, 2002). Nevertheless, in light of the fact that metastatic disease often involves the aberrant activity of such metastasis virulence genes (Nguyen et al., 2009), it is clear that cells bearing these genetic alterations do arise at a reasonably high frequency. One possible explanation for this observation involves the stochastic accumulation of genetic changes affecting metastasis virulence genes as "passenger mutations" within tumor cell populations that possess unrelated "driver mutations" (Sjöblom et al., 2006; Wood et al., 2007) that serve as the basis for the initial clonal expansion of these cells within a primary tumor. Accordingly, purely by chance, sub-populations of cells that inadvertently possess a high proclivity for metastasis formation might come to exist within a primary tumor.

An alternative model to explain how cells expressing metastasis virulence genes can arise at a frequency sufficient to induce metastasis formation considers the possibility that cells might disseminate from a primary cancerous lesion relatively early during the course of tumor progression. These early disseminating cells are then proposed to undergo multiple rounds of clonal selection already within the specific microenvironment where overt metastases will ultimately develop – notably, a microenvironment where genetic alterations in metastasis virulence genes can now be evolutionarily selected for (Klein, 2009). This so-called "parallel progression model" was recently put forth by Klein and coworkers in light of several independent observations from human carcinoma patients and experimental animal models: (1) not-yet fully neoplastic cells are routinely disseminated in a systemic manner from even the earliest pre-malignant lesions (Nagrath et al., 2007; Hüsemann et al., 2008), (2) untransformed epithelial cells present in the systemic circulation can survive within the vasculature, arrest at a distant organ site, extravasate, and initially survive in a foreign tissue microenvironment

(Podsypanina et al., 2008), (3) early-disseminating pre-neoplastic cells retain at least some capacity for cell proliferation at a secondary organ site (Hüsemann et al., 2008; Podsypanina et al., 2008), and (4) patient-matched primary tumors and distant metastases can harbor significantly different spectra of genetic alterations (Schmidt-Kittler et al., 2003). Thus, it is possible that only partially aberrant cells disseminated relatively early during the course of disease progression represent the precursor cells of overt metastases, owing to the gradual clonal evolution of these cells at the site of eventual metastasis formation – all of this occurring independently from the clonal expansion transpiring within the population of cells that comprise the primary tumor from which these disseminated cells were initially spawned. If ultimately proven correct, the parallel progression model would represent a major paradigm shift, and would hold major implications for the design of effective therapeutic agents aimed at the remediation of metastatic disease.

Importantly, the parallel progression model is not disproved by the observation that gene expression signatures predictive of the propensity for metastatic progression can be identified by microarray analysis of carcinoma patient primary tumors (v'ant Veer et al., 2002; Ramaswamy et al., 2003). This is because the "metastasis signatures" could, in actuality, represent "dissemination signatures" that facilitate the escape of not-yet fully neoplastic cells to an ectopic secondary organ site, where these cells would then serve as the fodder for Darwinian selection. Instead, the major conceptual incongruence that must be reconciled by proponents of the parallel progression model concerns how the quasi-normal cells shed to distant organ sites can possibly undergo enough successive cell divisions within a foreign microenvironment that does not inherently support their proliferation to generate the genetic diversity required for subsequent clonal selection. Further resolution of this point represents an important topic of ongoing

research; until a mechanistic rationale for this issue can be provided, the parallel progression model is likely to remain controversial.

Progress Toward a Detailed Molecular Understanding of Tumor Metastasis

As outlined in the preceding discussions, although a number of fundamental questions concerning the basic nature of metastasis remain unresolved, research conducted over the past decade has begun to implicate the actions of specific genetic factors in the regulation of discrete cell-biologic aspects of the invasion-metastasis cascade. A diverse array of approaches have been undertaken to this end, including a number of genomics- and functional-genomics-based strategies, which have yielded a bevy of novel regulators of the metastatic phenotype (Clark et al., 2000; van't Veer et al., 2002; Ramaswamy et al., 2003; Kang et al., 2003; Minn et al., 2005; Bos et al., 2009). Together, these studies have generated promising candidates for the development of clinically informative prognostic biomarkers for metastatic progression, as well as putative therapeutic targets for the remediation of metastatic disease. Also of interest, the first two whole-genome sequences of patient-matched primary breast tumors and distant metastases have recently been reported (Shah et al., 2009; Ding et al., 2010); while sample sizes are, at present, too limited for meaningful interpretation of these findings, it is highly likely that additional sequencing-based cataloging of the full roster of genetic alterations present in clinically arising primary tumors and paired metastases will succeed in enumerating previously unappreciated regulators of the metastatic process.

Importantly, however, despite intensive investigation, the currently assembled list of metastasis-relevant genes is quite rudimentary, and alternative approaches for the identification of molecular regulators of metastasis are required in order to more fully comprehend the highly

complex etiology of metastatic disease. Moreover, the bulk of the prior work conducted on

molecular mediators of tumor metastasis has focused on the roles of traditional protein-encoding

genes. More recently, however, additional classes of regulatory molecules of putative importance

to the regulation of metastatic progression have been uncovered. One prominent class of

understudied potential modulators of metastasis are microRNAs (miRNAs).

MicroRNAs

miRNAs are an evolutionarily conserved family of short regulatory RNAs that modulate

gene expression post-transcriptionally via sequence-specific interactions with the 3' untranslated

regions (UTRs) of cognate mRNA targets (Ambros, 2004; Bartel, 2004). miRNAs were

originally identified by Ambros and Ruvkun through forward genetic screens in the nematode

worm *C. elegans* (Lee et al., 1993; Wightman et al., 1993). Initially considered a peculiarity of

worm development, it was only years later – after the discovery of RNA-interference

technologies (Fire et al., 1998) and elucidation of the first miRNA that was evolutionarily

conserved from nematodes to humans (Reinhart et al., 2000) – that miRNAs began to attract

widespread attention. Although this field is still in its infancy, remarkable progress has been

made over the past decade; consequently, we are now beginning to comprehend in significant

detail the mechanisms underlying miRNA biogenesis, miRNA targeting specificity, and the

biochemical means by which miRNAs silence gene expression post-transcriptionally (Filipowicz

et al., 2008; Bartel, 2009).

At present, more than 650 human miRNAs have been identified (Bartel, 2009). Because

each individual miRNA is capable of simultaneously modulating the expression levels of dozens

of distinct mRNA targets, current estimates posit that greater than half of the total mRNA species

encoded in the human genome are subject to miRNA-mediated regulation (Friedman et al., 2009). Therefore, it is perhaps not surprising that the pleiotropic actions of individual miRNAs enable them to function as crucial regulators of cell and organismal homeostasis; indeed, specific miRNAs critically modulate a variety of normal physiologic processes (Ambros, 2004; Bartel, 2004). Additionally, aberrant miRNA activity contributes to a number of pathological states, including tumorigenic development (Esquela-Kerscher and Slack, 2006; Ventura and Jacks, 2009; Sotiropoulou et al., 2009).

MicroRNAs and Cancer

A role for miRNAs in cancer was first revealed by the work of Croce and associates, who discovered that miR-15 and miR-16 were frequently deleted in human chronic lymphocytic leukemias (Calin et al., 2002). Subsequent analyses revealed that these two miRNAs function as *bona fide* tumor suppressor genes by inducing cell cycle arrest and apoptosis (Calin and Croce, 2006). Provocatively, more than 50% of miRNA-encoding genomic loci reside in chromosomal regions that are known to be altered during the course of tumor pathogenesis (Calin et al., 2004), and global downregulation of miRNA levels in human tumors has been reported (Lu et al., 2005). Furthermore, characteristic aberrant miRNA expression profiles that are strongly associated with both disease status and ultimate clinical outcome have been identified in many types of neoplasias (Calin and Croce, 2006). Alterations in miRNA levels occurring during tumor development are not epiphenomena of cancer pathogenesis, since genetic inhibition of the miRNA biogenesis machinery accelerates tumor progression (Kumar et al., 2007; Kumar et al., 2009). Consequently, modulation of the expression levels of certain miRNAs is likely to play a causal role in tumorigenesis.

In fact, research conducted over the past five years has revealed that the genes encoding a number of miRNAs behave as classically defined oncogenes or tumor suppressor genes. Mechanistically, many of these cancer-relevant miRNAs appear to exert their influences on tumor progression via the downregulation of previously appreciated components of the integrated circuit of a cancer cell (Esquela-Kerscher and Slack, 2006; Ventura and Jacks, 2009; Sotiropoulou et al., 2009). Thus, miRNAs are likely to represent critical control nodes within neoplastic signaling circuitry whose overall design is already well-established. Together, these cancer-relevant miRNAs function in myriad distinct aspects of tumorigenesis (Esquela-Kerscher and Slack, 2006; Ventura and Jacks, 2009; Sotiropoulou et al., 2009). As such, miRNAs participate in critical ways in the regulation of essentially all aspects of tumor biology, including metastatic progression.

MicroRNAs and Metastasis

miR-10b was the first miRNA recognized to alter the metastatic potential of human cancer cells (Ma et al., 2007). Via gain-of-function approaches, it was demonstrated that ectopic miR-10b expression endowed otherwise-non-aggressive human breast cancer cells with the capacity to become motile and invasive, as well as seed distant micrometastases when implanted as tumor xenografts (Ma et al., 2007). Subsequently, an unbiased functional genetic screen involving the overexpression of approximately 450 miRNAs identified the miR-373/520c seed family as pro-metastatic miRNAs in human breast cancer cells; once again, these effects were ostensibly due to the ability of these miRNAs to promote cell motility and invasiveness (Huang et al., 2008). Soon thereafter, miR-21 was highlighted as yet another motility- and metastasis-

promoting miRNA in human breast and colorectal carcinoma cells (Asangani et al., 2008; Zhu et al., 2008).

By combining *in vivo* selection for highly metastatic variants with gene expression profiling, Massagué and co-workers implicated miR-126, miR-206, and miR-335 as the first metastasis-suppressing miRNAs (Tavazoie et al., 2008). When ectopically expressed in breast cancer xenograft models, these three miRNAs exerted unique effects on distinct aspects of the metastatic process: whereas miR-126 acted as a general inhibitor of tumor cell proliferation (at both the primary site and in distant organs), miR-206 and miR-335 instead specifically inhibited cell motility and invasiveness (Tavazoie et al., 2008). Additionally, in a study comparing metastasis-specific methylation of the promoters of human miRNA genes, miR-34b/c and miR-148a were implicated as miRNAs whose overexpression was sufficient to impair metastasis formation in human head-and-neck carcinoma xenografts by virtue of their ability to impede cell motility and invasiveness (Lujambio et al., 2008).

While gain-of-function approaches in xenograft assays have demonstrated that each of the aforementioned miRNAs was capable of altering metastatic capacity, it has remained unclear whether these effects could be attributed specifically to influences on one or more steps of the invasion-metastasis cascade. Resolution of this question has been obscured by the potentially confounding reported influences of each of these miRNAs on primary tumor development, cell proliferation, and/or apoptosis (Voorhoeve et al., 2006; Ma et al., 2007; Sathyan et al., 2007; Si et al., 2007; Kondo et al., 2008; Tavazoie et al., 2008; Lujambio et al., 2008). Hence, the extent to which miRNAs are capable of specifically regulating metastasis has remained incompletely understood.

Importantly, because an individual miRNA is capable of simultaneously regulating the expression levels of dozens of target genes – and thus controlling numerous different signaling networks together in parallel – deregulation of a single miRNA can potentially affect the completion of multiple distinct steps of the invasion-metastasis cascade. This, in turn, would carry significant implications for our understanding of the pathogenesis of high-grade malignancies, as the functional pleiotropy of individual miRNAs might provide one explanation for how tumor cells can accumulate the requisite genetic and epigenetic aberrations needed to override the multiple safeguards that normally operate to prevent metastasis over the course of a typical human lifespan.

Main Questions Addressed

As indicated above, our knowledge regarding the identity of molecular regulators of the complex process of tumor metastasis remains only fragmentary. Hence, the studies that I conducted – and which will be described herein – strived to identify novel regulators of metastatic progression via the implementation of two distinct experimental approaches. Moreover, the cell-biologic consequences of perturbing the expression levels of several of these newly identified modulators of metastasis were investigated, as were the molecular mechanisms underlying these observed responses.

First, I attempted to discern whether particular miRNAs played a vital role in controlling breast cancer metastasis. At the time that these studies were initially undertaken, a role for miRNAs in the regulation of tumor metastasis remained unexplored. In light of the pleiotropic nature of gene regulation exhibited by miRNAs, I hypothesized that certain miRNAs might be endowed with a capacity to crucially modulate metastatic progression. An expression-based

screen for miRNAs whose levels were associated with metastatic potential in human breast cancer cells uncovered the miRNA miR-31 as a putative regulator of metastasis. I then investigated the possibility that miR-31 might function as a *bona fide* overseer of breast cancer metastasis due to a capacity to intervene during multiple distinct steps of the invasion-metastasis cascade via the pleiotropic suppression of a cohort of downstream effector molecules.

Second, I hypothesized that prior approaches for the identification of genetic factors involved in metastatic progression had failed to enumerate a number of crucially important metastasis-regulatory molecules due to the inability of these previous strategies to properly preserve and assay the extensive – and functionally critical – heterogeneity intrinsic to tumor cell populations. Therefore, I devised a novel experimental system for the unbiased discovery of genes whose encoded products contribute to tumor metastasis and associated cell-biologic pre-requisites for metastasis formation. Importantly, this new experimental approach was capable of maintaining and investigating the profound phenotypic heterogeneity and genetic diversity that pre-exists within tumor cell populations.

Collectively, these studies provide mechanistic insights regarding the genetic events that drive the complex cell-biologic processes underlying the invasion-metastasis cascade. These findings have implications for our comprehension of the etiology of metastatic disease. Additionally, this work identifies novel genes that may one day serve as clinically useful prognostic biomarkers and/or potential therapeutic targets for certain metastatic human carcinomas.

REFERENCES

Al-Mehdi AB, Tozawa K, Fisher AB, et al. (2000). Intravascular origin of metastasis from the proliferation of endothelium-attached tumor cells: a new model for metastasis. Nat Med *6*, 100-102.

Ambros V. (2004). The functions of animal microRNAs. Nature *431*, 350-355.

Asangani IA, Rasheed SA, Nikolova DA, et al. (2008). MicroRNA-21 post-transcriptionally downregulates tumor suppressor Pdcd4 and stimulates invasion, intravasation and metastasis in colorectal cancer. Oncogene *27*, 2128-2136.

Bartel DP. (2004). MicroRNAs: Genomics, biogenesis, mechanism, and function. Cell *116*, 281-297.

Bartel DP. (2009). MicroRNAs: target recognition and regulatory functions. Cell *136*, 215-233.

Bernards R and Weinberg RA. (2002). A progression puzzle. Nature *418*, 823.

Bos PD, Zhang XH, Nadal C, et al. (2009). Genes that mediate breast cancer metastasis to the brain. Nature *459*,1005-1009.

Brabletz T, Jung A, Spaderna S, Hlubek F, and Kirchner T. (2005). Migrating cancer stem cells – an integrated concept of malignant tumour progression. Nat Rev Cancer *5*, 744-749.

Calin GA and Croce CM. (2006). MicroRNA signatures in human cancers. Nat Rev Cancer *6*, 857-866.

Calin GA, Dumitru CD, Shimizu M, et al. (2002). Frequent deletions and down-regulation of micro-RNA genes miR15 and miR16 at 13q14 in chronic lymphocytic leukemia. Proc Natl Acad Sci USA *99*, 15524-15529.

Calin GA, Sevignani C, Dumitru CD, et al. (2004). Human microRNA genes are frequently located at fragile sites and genomic regions involved in cancers. Proc Natl Acad Sci USA *101*, 2999-3004.

Chambers AF, Groom AC, and MacDonald IC. (2002). Dissemination and growth of cancer cells in metastatic sites. Nat Rev Cancer *2*, 563-572.

Clark EA, Golub TR, Lander ES, and Hynes RO. (2000). Genomic analysis of metastasis reveals an essential role for RhoC. Nature *406*, 532-535.

Coussens LM, Fingleton B, and Matrisian LM. (2002). Matrix metalloproteinase inhibitors and cancer: trials and tribulations. Science *295*, 2387-2392.

Dawson MR, Duda DG, Fukumura D, and Jain RK. (2009). VEGFR1-activity-independent metastasis formation. Nature 461, E4-E5.

Dean M, Fojo T, and Bates S. (2005). Tumour stem cells and drug resistance. Nat Rev Cancer *5*, 275-284.

Desmedt C, Haibe-Kains B, Wirapati P, et al. (2008). Biological processes associated with breast cancer clinical outcome depend on the molecular subtypes. Clin Cancer Res. *14*, 5158-5165.

Ding L, Ellis MJ, Li S, et al. (2010). Genome remodelling in a basal-like breast cancer metastasis and xenograft. Nature *464*, 999-1005.

Esquela-Kerscher A, Slack FJ. (2006). Oncomirs - microRNAs with a role in cancer. Nat Rev Cancer *6*, 259-269.

Fidler IJ. (2003). The pathogenesis of cancer metastasis: the 'seed and soil' hypothesis revisited. Nat Rev Cancer *3*, 453-458.

Filipowicz W, Bhattacharyya SN, and Sonenberg N. (2008). Mechanisms of post-transcriptional regulation by microRNAs: are the answers in sight? Nat Rev Genet *9*,102-114.

Finak G, Bertos N, Pepin F, et al. (2008). Stromal gene expression predicts clinical outcome in breast cancer. Nat Med *14*, 518-527.

Fire A, Xu S, Montgomery MK, et al. (1998). Potent and specific genetic interference by double-stranded RNA in Caenorhabditis elegans. Nature *391*, 806-811.

Friedl P and Wolf K. (2003). Tumour-cell invasion and migration: diversity and escape mechanisms. Nat Rev Cancer *3*, 362-374.

Friedman RC, Farh KK, Burge CB, and Bartel DP. (2009). Most mammalian mRNAs are conserved targets of microRNAs. Genome Res *19*, 92-105.

Gupta GP and Massagué J. (2006). Cancer metastasis: building a framework. Cell *127*, 679-695.

Hanahan D and Folkman J. (1996). Parameters and emerging mechanisms of the angiogenic switch during tumorigenesis. Cell *86*, 353-364.

Hanahan D and Weinberg RA. (2000). The hallmarks of cancer. Cell *100*, 57-70.

Hart IR and Fidler IJ. (1980). Role of organ selectivity in the determination of metastatic patterns of B16 melanoma. Cancer Res *40*, 2281-2287.

Holmgen L, O'Reilly MS, and Folkman J. (1995). Dormancy of micrometastases: balanced proliferation and apoptosis in the presence of angiogenesis suppression. Nat Med *1*, 149-153.

Huang Q, Gumireddy K, Schrier M, et al. (2008). The microRNAs miR-373 and miR-520c promote tumour invasion and metastasis. Nat Cell Biol *10*, 202-210.

Hüsemann Y, Geigl JB, Schubert F, et al. (2008). Systemic spread is an early step in breast cancer. Cancer Cell *13*, 58-68.

Jain RK. (2005). Normalization of tumor vasculature: an emerging concept in antiangiogenic therapy. Science *307*, 58-62.

Joyce JA and Pollard JW. (2009). Microenvironmental regulation of metastasis. Nat Rev Cancer *9*, 239-252.

Kang Y, Siegel PM, Shu W, et al. (2003). A multigenic program mediating breast cancer metastasis to bone. Cancer Cell *3*,537-549.

Kaplan RN, Riba RD, Zacharoulis S, et al. (2005). VEGFR1-positive haematopoietic bone marrow progenitors initiate the pre-metastatic niche. Nature *438*, 820-827.

Karnoub AE, Dash AB, Vo AP, et al. (2007). Mesenchymal stem cells within tumour stroma promote breast cancer metastasis. Nature *449*, 557-563.

Kinzler KW and Vogelstein B. (1996). Lessons for hereditary colorectal cancer. Cell *87*, 159-170.

Klein CA. (2009). Parallel progression of primary tumours and metastases. Nat Rev Cancer *9*, 302-312.

Kondo N, Toyama T, Sugiura H, Fujii Y, and Yamashita H. (2008). miR-206 Expression is down-regulated in estrogen receptor _-positive human breast cancer. Cancer Res. *68*, 5004-5008.

Kumar MS, Lu J, Mercer KL, Golub TR, and Jacks T. (2007). Impaired microRNA processing enhances cellular transformation and tumorigenesis. Nat Genet *39*, 673-677.

Kumar MS, Pester RE, Chen CY, et al. (2009). Dicer1 functions as a haploinsufficient tumor suppressor. Genes Dev *23*, 2700-2704.

Lauffenburger DA and Horwitz AF. (1996). Cell migration: a physically integrated molecular process. Cell *84*, 359-369.

Lee RC, Feinbaum RL, and Ambros V. (1993). The *C. elegans* heterochronic gene *lin-4* encodes small RNAs with antisense complementarity to *lin-14*. Cell *75*, 843–854.

Lu J, Getz G, Miska EA, et al. (2005). MicroRNA expression profiles classify human cancers. Nature *435*, 834-838.

Lujambio A, Calin GA, Villanueva A, et al. (2008). A microRNA DNA methylation signature for human cancer metastasis. Proc Natl Acad Sci USA *105*, 13556-13561.

Luzzi KJ, MacDonald IC, Schmidt EE, et al. (1998). Multistep nature of metastatic inefficiency: dormancy of solitary cells after successful extravasation and limited survival of early micrometastases. Am J Pathol *153*, 865-873.

Ma L, Teruya-Feldstein J, and Weinberg RA. (2007). Tumour invasion and metastasis initiated by microRNA-10b in breast cancer. Nature *449*, 682-688.

Maheswaran S, Sequist LV, Nagrath S, et al. (2008). Detection of mutations in EGFR in circulating lung-cancer cells. N Engl J Med *359*, 366-377.

Minn AJ, Gupta GP, Siegel PM, et al. (2005). Genes that mediate breast cancer metastasis to lung. Nature *436*, 518-524.

Nagrath S, Sequist LV, Maheswaran S, et al. (2007). Isolation of rare circulating tumour cells in cancer patients by microchip technology. Nature *450*, 1235-1239.

Nash GF, Turner LF, Scully MF, and Kakkar AK. (2002). Platelets and cancer. Lancet Oncol *3*, 425-430.

Nelson CM and Bissell MJ. (2006). Of extracellular matrix, scaffolds, and signaling: tissue architecture regulates development, homeostasis, and cancer. Annu Rev Cell Dev Biol *22*, 287-309.

Nguyen DX, Bos PD, and Massagué J. (2009). Metastasis: from dissemination to organ-specific colonization. Nat Rev Cancer *9*, 274-284.

Nowell PC. (1976). The clonal evolution of tumour cell populations. Science *194*, 23-28.

Orimo A, Gupta PB, Sgroi DC, et al. (2005) Stromal fibroblasts present in invasive human breast carcinomas promote tumor growth and angiogenesis through elevated SDF-1/CXCL12 secretion. Cell *121*, 335-348.

Padua D, Zhang XH, Wang Q, et al. (2008). TGFbeta primes breast tumors for lung metastasis seeding through angiopoietin-like 4. Cell *133*, 66-77.

Paget S. (1889). The distribution of secondary growths in cancer of the breast. Lancet *1*, 99-101.

Pantel K, Brakenhoff RH, and Brandt B. (2008). Detection, clinical relevance and specific biological properties of disseminating tumour cells. Nat Rev Cancer *8*, 329-340.

Podsypanina K, Du YC, Jechlinger M, et al. (2008). Seeding and propagation of untransformed mouse mammary cells in the lung. Science *321*, 1841-1844.

Polyak K and Weinberg RA. (2009). Transitions between epithelial and mesenchymal states: acquisition of malignant and stem cell traits. Nat Rev Cancer *9*, 265-273.

Ramaswamy S, Ross KN, Lander ES, and Golub TR. (2003). A molecular signature of metastasis in primary solid tumors. Nat Genet *33*, 49-54.

Reddig PJ and Juliano RL. (2005). Clinging to life: cell to matrix adhesion and cell survival. Cancer Metastasis Rev *24*, 425-439.

Reinhart BJ, Slack FJ, Basson M, et al. (2000). The 21 nucleotide let-7 RNA regulates developmental timing in Caenorhabditis elegans. Nature *403*, 901–906.

Rosen JM and Jordan CT. (2009). The increasing complexity of the cancer stem cell paradigm. Science *324*, 1670-1673.

Sahai E. (2005). Mechanisms of cancer cell invasion. Curr Opin Genet Dev *15*, 87-96.

Sathyan P, Golden HB, and Miranda RC. (2007). Competing interactions between micro-RNAs determine neural progenitor survival and proliferation after ethanol exposure. J Neurosci. *27*, 8546-8557.

Schmidt-Kittler O, Ragg T, Daskalakis A, et al. (2003). From latent disseminated cells to overt metastasis: genetic analysis of systemic breast cancer progression. Proc Natl Acad Sci USA *100*, 7737-7742.

Shah SP, Morin RD, Khattra J, et al. (2009). Mutational evolution in a lobular breast tumour profiled at single nucleotide resolution. Nature *461*, 809-813.

Si ML, Zhu S, Wu H, Lu Z, Wu F, and Mo, YY. (2007). miR-21-mediated tumor growth. Oncogene *26*, 2799-2803.

Sjöblom T, Jones S, Wood LD, et al. (2006). The consensus coding sequences of human breast and colorectal cancers. Science *314*, 268-274.

Sørlie T, Perou CM, Tibshirani R, et al. (2001). Gene expression patterns of breast carcinomas distinguish tumor subclasses with clinical implications. Proc Natl Acad Sci USA *98*, 10869-10874.

Sotiropoulou G, Pampalakis G, Lianidou E, and Mourelatos Z. (2009). Emerging roles of microRNAs as molecular switches in the integrated circuit of the cancer cell. RNA *15*, 1443-1461.

Steeg PS. (2006). Tumor metastasis: mechanistic insights and clinical challenges. Nat Med *12*, 895-904.

Stockmann C, Doedens A, Weidemann A, et al. (2008). Deletion of vascular endothelial growth factor in myeloid cells accelerates tumorigenesis. Nature *456*, 814-818.

Tarin D, Price JE, Kettlewell MG, et al. (1984). Mechanisms of human tumor metastasis studied in patients with peritoneovenous shunts. Cancer Res *44*, 3584-3592.

Tavazoie SF, Alarcón C, Oskarsson T, et al. (2008). Endogenous human microRNAs that suppress breast cancer metastasis. Nature *451*, 147-152.

The American Cancer Society. "Cancer Facts and Figures 2009". 2009. www.cancer.org.

Thiery JP. (2002). Epithelial-mesenchymal transitions in tumour progression. Nat Rev Cancer *2*, 442-454.

van't Veer, Dai H, van de Vijver MJ, et al. (2002). Gene expression profiling predicts clinical outcome of breast cancer. Nature *415*, 530-536.

Ventura A and Jacks T. (2009). MicroRNAs and cancer: short RNAs go a long way. Cell *136*, 586-591.

Visvader JE. (2009). Keeping abreast of the mammary epithelial hierarchy and breast tumorigenesis. Genes Dev *23*, 2563-2577.

Voorhoeve PM, le Sage C, Schrier M, et al. (2006). A genetic screen implicates miRNA-372 and miRNA-373 as oncogenes in testicular germ cell tumors. Cell *124*, 1169-1181.

Wang H, Fu W, Im JH, et al. (2004). Tumor cell alpha3beta1 integrin and vascular laminin-5 mediate pulmonary arrest and metastasis. J Cell Biol *164*, 935-941.

Wood LD, Parsons DW, Jones S, et al. (2007). The genomic landscapes of human breast and colorectal cancers. Science *318*, 1108-1113.

Wightman B, Ha I, and Ruvkun G. (1993). Posttranscriptional regulation of the heterochronic gene *lin-14* by lin-4 mediates temporal pattern formation in C. elegans. Cell *75*, 855–862.

Yang J, Mani SA, Donaher JL, et al. (2004). Twist, a master regulator of morphogenesis, plays an essential role in tumor metastasis. Cell *117*, 927-939.

Zhu S, Wu H, Wu F, et al. (2008). MicroRNA-21 targets tumor suppressor genes in invasion and metastasis. Cell Res *18*, 350-359.

Chapter 2

A Pleiotropically Acting MicroRNA, miR-31, Inhibits Breast Cancer Metastasis

Scott Valastyan[1,2], Ferenc Reinhardt[1], Nathan Benaich[1,3], Diana Calogrias[4], Attila M. Szász[4], Zhigang C. Wang[5,6], Jane E. Brock[4], Andrea L. Richardson[4], and Robert A. Weinberg[1,2,7]

[1]Whitehead Institute for Biomedical Research, Cambridge, MA 02142, USA
[2]Department of Biology, Massachusetts Institute of Technology, Cambridge, MA 02139, USA
[3]Department of Biology, Williams College, Williamstown, MA 01267, USA
[4]Department of Pathology, Brigham and Women's Hospital, Boston, MA 02115, USA
[5]Department of Surgery, Brigham and Women's Hospital, Boston, MA 02115, USA
[6]Department of Cancer Biology, Dana-Farber Cancer Institute, Boston, MA 02115, USA
[7]MIT Ludwig Center for Molecular Oncology, Cambridge, MA 02139, USA

This chapter is excerpted from the following publication (copyright permissions obtained):

INTRODUCTION

As described in Chapter One, metastases account for 90% of human cancer deaths (Gupta and Massagué, 2006), yet our understanding of the molecular circuitry that governs metastatic dissemination remains fragmentary. The invasion-metastasis cascade, which leads to these growths, is a complex, multi-step process involving the escape of neoplastic cells from a primary tumor (local invasion), intravasation into the systemic circulation, survival during transit through the vasculature, extravasation into the parenchyma of distant tissues, the establishment of micrometastases, and ultimately the outgrowth of macroscopic secondary tumors (colonization) (Fidler, 2003).

MicroRNAs (miRNAs) constitute an evolutionarily conserved class of pleiotropically acting small RNAs that suppress gene expression post-transcriptionally via sequence-specific interactions with the 3' untranslated regions (UTRs) of cognate mRNA targets (Bartel, 2009), as was discussed previously in Chapter One. In mammalian cells, miRNAs effect gene silencing via both translational inhibition and mRNA degradation; an individual miRNA is capable of regulating dozens of distinct mRNAs, and together the >650 human miRNAs are believed to modulate greater than one-third of the mRNA species encoded in the genome (Bartel, 2009).

As outlined in Chapter One, a central role for miRNAs in the establishment and progression of human tumors has begun to emerge. More than 50% of miRNA-encoding loci reside in chromosomal regions altered during tumorigenesis (Calin et al., 2004), and expression profiling reveals characteristic miRNA signatures for many tumor types – including breast neoplasias – that predict disease status and clinical outcome (Calin and Croce, 2006). In addition, miRNAs have been identified that function as classical oncogenes or tumor suppressor genes (Ventura and Jacks, 2009), as well as a limited number that act at late stages of tumor

progression (Ma et al., 2007; Tavazoie et al., 2008; Huang et al., 2008; Asangani et al., 2008; Zhu et al., 2008; Lujambio et al., 2008).

The extent to which miRNAs specifically affect metastasis remains unclear, as all the miRNAs reported to affect metastasis also exert potentially confounding influences on primary tumor development, apoptosis, and/or cell proliferation (Voorhoeve et al., 2006; Sathyan et al., 2007; Ma et al., 2007; Si et al., 2007; Tavazoie et al., 2008; Kondo et al., 2008; Lujambio et al., 2008) – a point that was highlighted previously in Chapter One. Moreover, a role for miRNAs in steps of the invasion-metastasis cascade subsequent to local invasion has not been described.

The pleiotropic nature of gene regulation exhibited by miRNAs led me to hypothesize that certain miRNAs might be endowed with a capacity to function as crucial modulators of tumor metastasis. Here, I identify an anti-metastatic human miRNA, miR-31, that acts at multiple steps of the invasion-metastasis cascade via repression of a cohort of pro-metastatic targets.

RESULTS

miR-31 Expression is Specifically Attenuated in Metastatic Breast Cancer Cell Lines

To identify miRNAs that might regulate breast cancer metastasis, I selected 10 cancer-associated miRNAs for further characterization due to their concordant identification among expression profiling studies of clinical breast tumors (Iorio et al., 2005; Volinia et al., 2006), global analysis of miRNA copy-number variation in human breast carcinomas (Zhang et al., 2006), and localization of miRNA loci to cancer-relevant sites of chromosomal aberration (Calin et al., 2004) (Supplementary Table 1). These studies did not stratify patients based on metastasis status.

Expression of the 10 candidate miRNAs was assayed in 15 human and mouse mammary cell lines, which included normal epithelial cells, tumorigenic but non-metastatic cells, and metastatic tumor cells (Supplementary Table 2). The levels of a single miRNA, miR-31, were specifically attenuated in aggressive human breast cancer cells when compared to primary normal human mammary epithelial cells (HMECs). While non-metastatic tumor cells (HMLER, MCF7-Ras, and SUM-149) exhibited four-fold reduced miR-31, expression of this miRNA in metastatic SUM-159 and MDA-MB-231 cells was diminished by >100-fold (Figure 1A).

Relative to its expression in normal murine mammary gland (NMuMG) cells, miR-31 levels in sub-lines derived from a single murine mammary tumor reflected their capacities to metastasize: miR-31 was reduced by two-fold in metastatic D2.1 and D2A1 cells, but not in non-aggressive D2.OR cells (Figure 1B). miR-31 levels were also inversely proportional to metastatic ability in four mouse mammary carcinoma sub-lines derived from a single spontaneously arising tumor: while miR-31 levels in non-aggressive 67NR cells were similar to those in NMuMG, miR-31 expression was progressively diminished upon acquisition of the capacity to invade locally (168FARN), to form micrometastases (4TO7), and to yield macroscopic metastases (4T1) (Figure 1B). Thus, miR-31 levels are specifically attenuated in aggressive breast cancer cells.

miR-31 expression was heterogeneous in 4T1 cell primary mammary tumors; of note, the proportion of cells expressing miR-31 was 10-fold reduced in lung metastases relative to the fraction of miR-31-positive cells in the primary tumors from which they were derived (Figure 1C). Also, five-fold fewer cells located near the invasive front of 4T1 cell mammary tumors expressed miR-31, compared to cells in the interior of these tumors (Figure 1D). These data raise the possibility that selective pressures diminish the prevalence of miR-31-expressing cells within the pool of successfully metastasizing cells during the course of metastatic progression.

miR-31 Expression Suppresses Metastasis-Relevant Traits *in vitro*

Given these inverse correlations between miR-31 levels and malignant phenotypes, I assessed the potential for anti-metastatic roles for miR-31. Thus, I stably expressed miR-31 in metastatic MDA-MB-231 human breast cancer cells ("231 cells"). This overexpression resulted in miR-31 levels comparable to those in HMECs (Supplementary Figure 1A).

Ectopic miR-31 did not affect proliferation *in vitro*, but did reduce invasion by 20-fold and motility by 10-fold (Figure 2A and Supplementary Figures 1B and 1C). These effects were specifically attributable to the biological activities of miR-31, as equivalent overexpression of a control miRNA, miR-145, failed to influence invasion or motility (Figure 2A and data not shown). Also, miR-31-expressing cells exhibited 60% diminished resistance to anoikis-mediated cell death (Figure 2B).

These defects could not be ascribed to toxicity resulting from ectopic miR-31 (Supplementary Figure 1D). The consequences of miR-31 expression were not unique to 231 cells: miR-31 reduced invasion, motility, and anoikis resistance, yet did not affect proliferation, in aggressive SUM-159 human breast cancer cells (Supplementary Figure 2). Hence, miR-31 impairs *in vitro* surrogates of metastatic ability.

miR-31 Expression Suppresses Metastasis *in vivo*

Due to its effects on *in vitro* traits associated with high-grade malignancy, I asked if ectopic miR-31 could inhibit metastasis in otherwise-aggressive cells. Thus, 231 cells expressing miR-31 were injected into the orthotopic site – the mammary fat pad – of mice. Unexpectedly, miR-31 enhanced primary tumor growth by 1.5-fold and correspondingly increased cell proliferation (Figure 2C and Supplementary Figure 3A). Control 231 cell primary tumors

displayed evidence of local invasion; however, miR-31-expressing tumors were well-encapsulated and non-invasive (Figures 2D and 2E). These changes were not accompanied by altered neo-vascularization (Supplementary Figure 3B).

Despite their ability to generate larger primary tumors, 231 cells expressing miR-31 were strikingly impaired in their capacity to seed lung metastases. miR-31-expressing cells formed 95% fewer lesions than did controls 62 days post-implantation (Figure 2F). Thus, miR-31 suppresses metastasis from an orthotopic site, ostensibly due, at least in part, to its ability to impede local invasion.

I addressed the possibility that miR-31's impact on these parameters was attributable to clonal variation in 231 cells by expressing miR-31 in a single-cell-derived population isolated from the parental 231 cells (Supplementary Figure 4A) (Minn et al., 2005). As before, when injected orthotopically, miR-31-expressing cells formed large, well-encapsulated primary tumors and also reduced lung metastasis by five-fold (Supplementary Figures 4B-4D). Orthotopic injection of SUM-159 cells expressing miR-31 further corroborated my earlier findings: miR-31 enhanced primary tumor growth, yet miR-31-expressing tumors were more well-confined than control tumors (Supplementary Figure 5). These observations indicated that the ability of miR-31-expressing cells to form larger, less invasive primary tumors, as well as to seed fewer metastases, is a specific consequence of the biological activities of miR-31.

I determined if miR-31's impact on metastasis was also attributable to effects on later steps of the invasion-metastasis cascade, independent of its influence on local invasion. Thus, I injected miR-31-expressing 231 cells directly into the circulation of mice, thereby circumventing the initial steps of local invasion and intravasation. After one day, miR-31-expressing cells were four-fold impaired in their ability to persist in the lungs (Figure 2G). This difference was not a

consequence of an inability of miR-31-expressing cells to become lodged initially in the lung microvasculature, as equal numbers of miR-31-expressing and control cells were detected in the lungs 10 minutes and two hours post-injection (Figure 2G and Supplementary Figure 6A). These observations suggested that miR-31 regulates early post-intravasation events, such as intraluminal viability, extravasation, and/or initial survival in the lung parenchyma.

Three months after tail vein injection, miR-31-expressing 231 cells generated 40-fold fewer lung metastases than did controls (Figure 2G). I also observed a dramatic effect on the size of eventually formed lesions: after three months, miR-31-expressing cells generated only small micrometastases while control cells formed macroscopic metastases; this occurred despite the fact that miR-31-expressing and control cells established comparably sized micrometastases one month post-injection (Figure 2G and Supplementary Figure 6B). Such effects on lesion size implied that miR-31 affects metastatic colonization in addition to its influences on local invasion and early post-intravasation events.

Inhibition of miR-31 Promotes Metastasis-Relevant Traits *in vitro*

The preceding observations demonstrated that miR-31 expression deprives metastatic cells of attributes associated with high-grade malignancy. I next asked if miR-31 also prevents the acquisition of aggressive traits by otherwise-non-metastatic human breast cancer cells. To do so, I transiently inhibited miR-31 in non-invasive MCF7-Ras cells with either antisense oligonucleotides or miRNA sponges. The latter are expression constructs that carry miRNA recognition motifs in their 3' UTR that bind and thus titer miRNAs (Ebert et al., 2007). Both approaches inhibited miR-31 function by >4.5-fold (Supplementary Figure 7A). Suppression of

miR-31 enhanced invasion by 20-fold and motility by five-fold, but cell viability was unaffected by either inhibitor (Figure 3A and Supplementary Figure 7B).

Techniques for stable miRNA inhibition have been unavailable (Krützfeldt et al., 2006). To address this problem, I modified elements derived from the transiently expressed miRNA sponges, cloned them into a retroviral vector, and created MCF7-Ras cells that stably express the modified miRNA sponges. The miR-31 sponge reduced miR-31 function by 2.5-fold, but did not affect the activity of other known anti-metastatic miRNAs (Supplementary Figures 8A and 8B). The relatively modest suppression of miR-31 conferred by stable sponge expression elicited strong responses: invasion was enhanced by 12-fold, motility by eight-fold, and anoikis resistance by 2.5-fold (Figure 3B and Supplementary Figure 8C). The miR-31 sponge failed to alter *in vitro* proliferation (Supplementary Figure 8D).

When stably expressed in immortalized HMECs or tumorigenic but non-metastatic SUM-149 human breast cancer cells, the miR-31 sponge elicited increased invasion, motility, and anoikis resistance without affecting proliferation (Supplementary Figure 9 and data not shown). Collectively, these data indicated that sustained miR-31 activity is necessary to prevent the acquisition of aggressive traits by both tumor cells and untransformed breast epithelial cells.

Inhibition of miR-31 Promotes Metastasis *in vivo*

I exploited my ability to stably inhibit miRNAs in order to assess whether miR-31 activity is required to prevent metastasis *in vivo*. To do so, otherwise-non-metastatic MCF7-Ras cells stably expressing the miR-31 sponge were orthotopically implanted into mice. Inhibition of miR-31 failed to alter *in vivo* proliferation and primary tumor growth (Figure 3C and Supplementary Figure 10A). Primary tumors derived from miR-31 sponge-expressing cells were

poorly encapsulated and locally invasive, while control MCF7-Ras tumors appeared well-confined and non-invasive (Figures 3D and 3E). Again, neo-vascularization did not differ (Supplementary Figure 10B).

Strikingly, miR-31 sponge-expressing MCF7-Ras cells metastasized to the lungs in significant numbers, while control tumor-bearing host lungs were largely devoid of tumor cells; cells with impaired miR-31 activity formed 10-fold more lesions than did controls (Figure 3F). Hence, continuous miR-31 function is required to prevent metastasis from an orthotopic site.

I asked if loss of miR-31 activity also promoted metastasis by intervening at steps of the invasion-metastasis cascade subsequent to local invasion. Thus, I intravenously injected mice with miR-31 sponge-expressing MCF7-Ras cells. Within one day, miR-31 inhibition enhanced cell number in the lungs by six-fold; similarly, at later times after injection, miR-31 sponge-expressing cells were 10-fold more prevalent in the lungs than were controls (Figure 3G). The differing metastatic abilities of control and miR-31 sponge-expressing cells did not arise due to failure of control cells to become lodged initially in the lung vasculature, as equal numbers of cells from each cohort were present 10 minutes after injection (Figure 3G and Supplementary Figure 11).

Suppression of miR-31 also affected lesion size four months after tail vein injection: whereas control cells formed only small micrometastases, miR-31 sponge-expressing cells produced macroscopic metastases (Figure 3G). Together, these data extended and reinforced my ectopic expression studies by demonstrating that miR-31 affects local invasion, early post-intravasation events, and metastatic colonization.

miR-31 Directly Regulates a Cohort of Pro-Metastatic Genes

miR-31's ability to impede multiple steps of the invasion-metastasis cascade might derive from its ability to pleiotropically regulate genes involved in diverse aspects of metastatic dissemination. To identify effectors of miR-31, I used two algorithms that predict the mRNA targets of a miRNA – PicTar (Krek et al., 2005) and TargetScan (Grimson et al., 2007). Based on the representation of miR-31 sites in their 3' UTRs, >200 mRNAs were predicted to be regulated by miR-31. Gene Ontology (Ashburner et al., 2000) revealed that these targets included a disproportionately large number of genes encoding proteins with roles in motility-related processes, such as cell adhesion, cytoskeletal remodeling, and cell polarity (data not shown).

Guided by this Gene Ontology analysis, I cloned the 3' UTRs of 16 putative miR-31 targets from these overrepresented categories, including several implicated in tumor invasion (Sahai and Marshall, 2002; McClatchey, 2003), into a luciferase construct. Reporter assays using miR-31-expressing 231 cells revealed that miR-31 repressed six of the UTRs: frizzled3 (Fzd3), integrin _5 (ITGA5), myosin phosphatase-Rho interacting protein (M-RIP), matrix metallopeptidase 16 (MMP16), radixin (RDX), and RhoA (Figure 4A). Mutation of the putative miR-31 site(s) in these six 3' UTRs (Supplementary Table 3) abrogated responsiveness to miR-31 (Figure 4B). In the case of RhoA, whose UTR contains two miR-31 sites separated by 152 nucleotides, mutation of either motif abolished miR-31-responsiveness (Figure 4B), suggesting functional interaction between the sites (Grimson et al., 2007).

Endogenous Fzd3, ITGA5, MMP16, RDX, and RhoA protein levels were assayed in miR-31-expressing 231 cells. miR-31 repressed the levels of these proteins by 40-60% (Figure 4C). miR-31's effects on levels of the M-RIP protein could not be evaluated due to the lack of appropriate antibodies. Also, miR-31 reduced the endogenous mRNA levels of these six targets

by two-fold in SUM-159 cells, as well as Fzd3, ITGA5, MMP16, RDX, and RhoA mRNA levels in 231 cells (Figure 4D). miR-31 did not affect CXCL12 mRNA levels – a computationally predicted miR-31 target found not to be regulated by this miRNA – in either cell type (Figures 4A and 4D). These data indicated that miR-31 directly regulates endogenous Fzd3, ITGA5, M-RIP, MMP16, RDX and RhoA expression in human breast cancer cells.

I determined if concomitant repression of Fzd3, ITGA5, M-RIP, MMP16, RDX, and RhoA correlated with disease progression in clinical breast cancers by examining expression profiling data from 295 primary breast tumors (Supplementary Table 4) (van de Vijver et al., 2002). To do so, I constructed a miR-31 target signature based on coordinate differential expression of these six genes. Within this cohort, high expression of the miR-31 target signature was associated with metastasis, as well as poor survival, relative to signature-negative tumors; five-year survival among patients negative for the target signature was 90%, while >35% of target signature-positive patients succumbed to their disease over this interval (Figures 5A and 5B). Thus, coordinate repression of Fzd3, ITGA5, M-RIP, MMP16, RDX, and RhoA correlated with more favorable outcome in clinical breast tumors.

To assess the functional contributions of these miR-31 targets to aggressive phenotypes, I first examined if their inhibition affected the invasion or motility of 231 cells. Transfection with siRNAs potently reduced target protein levels without affecting cell viability (Supplementary Figures 12A and 12B). siRNAs targeting Fzd3, ITGA5, RDX, or RhoA reduced invasion and motility, while siRNAs against M-RIP or MMP16 failed to affect these traits (Figure 5C and Supplementary Figure 12C).

I asked if inhibition of these effectors compromised resistance to anoikis. siRNAs against ITGA5, RDX, or RhoA sensitized 231 cells to anoikis; in contrast, siRNAs targeting Fzd3, M-

RIP, or MMP16 had no effect on anoikis resistance (Figure 5D). Hence, suppression of Fzd3, ITGA5, RDX, or RhoA impaired metastasis-relevant traits *in vitro*.

Re-Expression of Fzd3, ITGA5, RDX, and RhoA Reverses miR-31-Dependent Metastasis-Relevant Phenotypes *in vitro*

To determine whether *in vitro* phenotypes associated with miR-31 expression could be reversed via restoration of Fzd3, ITGA5, M-RIP, MMP16, RDX, or RhoA levels, I transfected miR-31-expressing 231 cells with individual expression constructs rendered miRNA-insensitive by deletion of their 3' UTRs; this was not cytotoxic (Supplementary Figures 13A and 13B and data not shown). In miR-31-expressing cells, Fzd3, ITGA5, RDX, or RhoA reversed, at least partially, miR-31-imposed invasion and motility defects; in contrast, M-RIP or MMP16 had no effect on these traits (Figure 5E and Supplementary Figure 13C). Surprisingly, re-expression of RDX or RhoA completely rescued miR-31-mediated invasion and motility defects. Expression of the six targets failed to enhance the invasion or motility of control 231 cells (Figure 5E and Supplementary Figure 13C).

I evaluated if re-expression of any of the six targets rescued miR-31's effects on anoikis. ITGA5, RDX, or RhoA reversed, at least in part, anoikis susceptibility resulting from ectopic miR-31; in contrast, Fzd3, M-RIP, or MMP16 failed to affect this trait (Figure 5F). In fact, ITGA5 or RhoA completely rescued miR-31-dependent anoikis phenotypes. The six targets did not enhance anoikis resistance in control 231 cells (Figure 5F). Hence, Fzd3, ITGA5, RDX, and RhoA are functionally relevant effectors of miR-31 for conferring malignant traits *in vitro*.

Re-Expression of RhoA Partially Reverses miR-31-Imposed Metastasis Defects *in vivo*

RhoA afforded the most pronounced reversal of miR-31-mediated phenotypes. Thus, I stably re-expressed miRNA-resistant RhoA in 231 cells that already had been infected with either miR-31 or control vector (Supplementary Figures 14A and 14B). RhoA did not affect proliferation *in vitro*, but did abrogate miR-31-imposed invasion, motility, and anoikis resistance defects (Supplementary Figures 14C-14F).

To ascertain if restored RhoA levels reversed *in vivo* metastasis phenotypes ascribable to miR-31, I orthotopically injected mice with 231 cells expressing combinations of miR-31, RhoA, and control vectors. As observed previously, miR-31 enhanced primary tumor growth (Figure 6A). RhoA initially augmented primary tumor growth in the presence of ectopic miR-31, but failed to do so in control 231 cells (Figure 6A). In consonance with my earlier findings, control 231 primary tumors were locally invasive, while miR-31-expressing tumors were non-invasive (Figures 6B and 6C). In control 231 cells, ectopic RhoA failed to exacerbate the extent of local invasion; in contrast, RhoA abolished the previously encapsulated appearance of miR-31-expressing tumors and enabled invasion into surrounding normal tissue (Figures 6B and 6C).

Re-expression of RhoA restored lung metastasis in miR-31-expressing 231 cells to 75% of control cell levels, while RhoA failed to enhance metastasis in control 231 cells (Figure 6D). Thus, re-expression of RhoA partially, yet robustly, reverses metastasis-suppression imposed by miR-31. The observed magnitude of rescue is surprising, as RhoA is only one member of a larger cohort of metastasis-relevant genes repressed by miR-31.

By intravenously injecting mice with 231 cells expressing miR-31 and/or RhoA, I gauged if RhoA-mediated reversal of miR-31-imposed metastasis defects was solely attributable to effects on local invasion. While expression of miR-31 and/or RhoA failed to affect the initial

lodging of tumor cells in the lung vasculature, the number of cells that persisted in the lungs differed within one day of injection (Figure 6E and Supplementary Figure 15). As before, miR-31 inhibited both the number of metastases formed and their eventual size (Figure 6E). While expression of RhoA in control 231 cells failed to enhance metastasis, RhoA restored the number of lung metastases to 60% of control cell levels in miR-31-expressing cells; however, RhoA did not facilitate the formation of macroscopic metastases in cells with ectopic miR-31 (Figure 6E).

Together, these data indicated that miR-31's ability to inhibit metastasis is attributable, in significant part, to its capacity to inhibit RhoA. miR-31-mediated repression of RhoA affects both local invasion and early post-intravasation events. However, these data also implied that the full spectrum of miR-31's effects on metastasis are elicited only via the coordinate repression of multiple targets, as suppression of RhoA alone could not explain the complete impact of miR-31 on the number of metastases formed or its effects on metastatic colonization.

miR-31 Expression Correlates Inversely with Metastasis in Human Breast Tumors

Because established cell lines and xenograft studies cannot fully recapitulate clinical malignancy, I extended my analyses by assaying miR-31 expression in specimens from 56 human breast cancer patients (Supplementary Table 5; Median follow-up = 59 months). Relative to grade-matched estrogen receptor (ER)$^+$ tumors, which are associated with more favorable disease outcome (Sørlie et al., 2001), basal-like tumors exhibited 40% reduced miR-31; no difference in miR-31 levels was observed between ER$^+$ and HER2$^+$ tumors (Supplementary Figure 16).

When these 56 tumors were stratified based on clinical progression, I found that miR-31 expression was diminished in primary tumors that subsequently metastasized, when compared to

normal breast tissue and primary tumors that did not recur; moreover, low miR-31 levels correlated strongly with reduced distant disease-free survival relative to tumors with high miR-31 (Figures 7A and 7B). Similarly, within this cohort of tumors, high RhoA expression was associated with an increased incidence of distant metastasis (Supplementary Figure 17).

The association of low miR-31 levels with metastasis persisted independent of both tumor grade and molecular subtype (Supplementary Figure 18). Such grade- and subtype-independence is quite surprising, as clinically utilized prognostic markers for breast cancer largely correlate with these parameters; furthermore, currently available markers do not identify a worse-prognosis group within the more aggressive basal-like or HER2^{+} subtypes (Desmedt et al., 2008). Thus, miR-31 may represent a marker for metastasis in a variety of breast cancer subtypes; however, its utility as a prognostic indicator will depend on extension of these initial observations.

I next assessed the heterogeneity of miR-31 expression in human primary breast tumors, as well as distant metastases arising in the same patients. miR-31 was expressed in 65% of the cells in these primary tumors; however, miR-31 was detected in only 12-30% of cells in patient-matched distant metastases (Figure 7C). These data raise the possibility that selective pressures operating over the course of breast cancer progression diminish the representation of miR-31-expressing cells within the population of successfully metastasizing cells.

Finally, I asked if expression of ITGA5, RDX, and RhoA was also heterogeneous in primary human breast tumors. RDX and RhoA were expressed in 60-75% of cells in the primary tumors examined, while ITGA5 was detected in >80% of cells (Figure 7D). Distant metastases were more homogeneous for the expression of RDX and RhoA than the primary tumors from which they were derived, as >90% of cells in the metastases expressed RDX and RhoA (Figure

7D). Similarly, >90% of cells in the metastases expressed ITGA5; however, the widespread

ITGA5 expression observed in the patient-matched primary tumors complicates interpretation of

its expression in distant metastases (Figure 7D).

MATERIALS AND METHODS

Plasmid Construction and Generation of Stable Cell Lines

The human miR-31 gene was PCR-amplified from genomic DNA and cloned into

pcDNA3.1 (Invitrogen), then subcloned into the BamHI and SalI sites of the pBABE-puro

retroviral vector (Morgenstern and Land, 1990). Synthetic miR-31, miR-126, miR-206, and miR-

335 binding site-containing *Renilla* luciferase reporter genes were constructed by annealing,

purifying, and cloning corresponding short oligonucleotides into the SacI and AgeI sites of the 3'

UTR of a pIS1 vector backbone provided by D. Bartel (Farh et al., 2005). Transient CMV-driven

miRNA sponge backbones were provided by P. Sharp; a control sponge containing tandem non-

targeting binding sites was identical to that utilized previously (Ebert et al., 2007), while the

miR-31 sponge was constructed by annealing, purifying, and cloning oligonucleotides containing

seven tandem "bulged" (at positions 9-12) miR-31 binding motifs into the XhoI and ApaI sites of

the CMV sponge backbone. For stable expression studies, the BamHI-ApaI fragments of the

miR-31 and control CMV sponge constructs were subcloned into the pBABE-puro retroviral

vector. Luciferase reporter genes driven by the 3' UTRs of the indicated computationally

predicted miR-31 targets were created via PCR-based amplification from human genomic DNA,

and then cloned into AgeI, SacI, SpeI, and/or XbaI sites within the 3' UTR of the pIS1 *Renilla*

luciferase reporter backbone. The indicated mutagenized miR-31 recognition site-containing

luciferase reporter genes were generated with a QuikChange II XL Site-Directed Mutagenesis

Kit (Stratagene), in accordance with the manufacturer's instructions. For transient

overexpression experiments, previously described constructs encoding Fzd3 (Deardorff et al.,

2001), ITGA5 (Kuwada and Li, 2000), M-RIP (Surks et al., 2003), MMP16 (Hotary et al., 2006),

RDX (Batchelor et al., 2004), and RhoA (Subauste et al., 2000) were provided by P. Klein, S.

Kuwada, H. Surks, S. Weiss, S. Crouch, and G. Bokoch, respectively. For stable overexpression

studies, RhoA was directly subcloned from pcDNA3 (Invitrogen) into the retroviral vector

pBABE-zeo (Morgenstern and Land, 1990).

All stable cell lines were generated via retroviral infection using HEK293T cells, as has

been previously described (Elenbaas et al., 2001). GFP-labeled MDA-MB-231 and MCF7-Ras

cells were created via infection with pWZL-blast-EGFP.

Cell Culture

MDA-MB-231 and MCF7-Ras cells were obtained from the ATCC and cultured under

standard conditions. HMEC and HME cells have been described (Ma et al., 2007). SCP3 cells

were obtained from J. Massagué (Minn et al., 2005). SUM-149 and -159 cells were provided by

S. Ethier (Ma et al., 2007). D2 cells have been described (Morris et al., 1993). 67NR, 168FARN,

4TO7, and 4T1 cells were obtained from F. Miller (Aslakson and Miller, 1992).

miRNA Detection

Total RNA, inclusive of the small RNA fraction, was extracted from cultured cells with a

*mir*Vana miRNA Isolation Kit (Ambion). RT-PCR-based detection of mature miR-31 and 5S

rRNA was achieved with a *mir*Vana miRNA Detection Kit and gene-specific primers (Ambion).

miRNA *in situ* Hybridization

miRNA expression was assessed from paraffin sections using a protocol adapted from Silahtaroglu et al. (2007). Briefly, after a four hour pre-hybridization, a 5' FITC-labeled miRCURY LNA probe targeting miR-31 (Exiqon) was hybridized to proteinase K-treated 10 _m sections at 55°C for 12 hours. Slides were then incubated with anti-FITC-HRP (PerkinElmer), and the resulting signal was intensified with the TSA Plus Fluorescein System (PerkinElmer).

Invasion and Motility Assays

For invasion assays, 1.0×10^5 cells were seeded in a Matrigel-coated chamber with 8.0 _m pores (BD Biosciences); for motility assays, 5.0×10^4 cells were plated atop uncoated membranes with 8.0 _m pores (BD Biosciences). Cells were seeded in serum-free media, and translocated toward complete growth media for 20 hours. Fugene6 (Roche) was used to transfect cells 24 hours prior to plating. 200 nM miRIDIAN miRNA Inhibitors (Dharmacon) were employed to transiently inhibit miR-31. SMARTpool siRNAs against Fzd3, ITGA5, M-RIP, MMP16, RDX, or RhoA (Dharmacon) were provided at 100 nM. Antisense oligonucleotides and siRNAs were transfected 48 hours prior to seeding using Oligofectamine (Invitrogen).

Anoikis Assays

Anoikis resistance was evaluated by seeding 7.5×10^4 cells in ultra-low attachment plates (Corning). After 24 hours of anchorage-independent culture, cells were resuspended in 0.4% trypan blue (Sigma) and cell viability was assessed.

Animal Studies

All research involving animals complied with protocols approved by the MIT Committee on Animal Care. For spontaneous metastasis assays, age-matched female NOD/SCID mice (propagated on-site) were bilaterally injected into the mammary fat pad with the indicated number of tumor cells in 1:2 Matrigel (BD Biosciences) plus normal growth media. For experimental metastasis assays, age-matched female NOD/SCID mice were injected with 5.0 x 10^5 cells (resuspended in PBS) via the tail vein. Metastasis was quantified using a fluorescent microscope within three hours of specimen isolation.

Luciferase Assays

5.0 x 10^4 cells were co-transfected with 50 ng of the indicated pIS1 *Renilla* luciferase construct and 50 ng of a pIS0 firefly luciferase normalization control. Lysates were collected 24 hours post-transfection, and *Renilla* and firefly luciferase activities were measured with a Dual-Luciferase Reporter System (Promega).

Immunoblots

Lysates were resolved by electrophoresis, transferred to a PVDF membrane, and probed with antibodies against _-actin (Santa Cruz), Fzd3 (Abcam), ITGA5 (Santa Cruz), MMP16 (Abcam), RDX (Cell Signaling), or RhoA (Santa Cruz).

miR-31 Target Signature

Expression profiling of 295 human breast tumors (van de Vijver et al., 2002) was used to categorize tumors as miR-31 target signature-positive or -negative. Tumors were considered

target signature-positive or -negative if the normalized expression of multiple of the six miR-31 targets herein identified resided in the top or bottom 15% of tumors in this cohort, respectively.

Immunohistochemistry

Detection of Ki-67 (Pharmingen), MECA-32 (U. of Iowa), ITGA5 (Santa Cruz), RDX (Santa Cruz), or RhoA (Abcam) was performed on 5 _m paraffin sections using the indicated antibodies, Vectastain Elite ABC kits (Vector), and ImmPACT DAB Substrate (Vector).

Human Breast Tumors

Primary breast tumors, distant metastases, and normal breast tissue were collected and processed in compliance with a protocol approved by the Brigham and Women's Hospital IRB. Fresh tissue was harvested from patients, OCT-embedded, snap-frozen, and preserved at -80°C. Recurrent cases were primary tumors from patients that developed distant metastases. For each recurrent case, two non-recurrent cases were selected to control for date of diagnosis, molecular subtype, lymph node status, and time of follow-up. Total RNA was isolated from 35 _m sections via TRIzol extraction and a *mir*Vana miRNA Isolation Kit. To discern if miR-31 levels correlate with distant metastasis, primary tumors were classified as miR-31-positive or -negative. Tumors were considered miR-31-positive or -negative if the normalized expression of miR-31 resided in the top or bottom 30% of tumors in this cohort, respectively. Similarly, tumors were classified as RhoA-high or -low if their RhoA levels were in the top or bottom 30% of tumors examined.

Statistical Analyses

Data are presented as mean ± s.e.m. Unless otherwise noted, Student's t-test was used for comparisons, with $P < 0.05$ considered significant.

Measurements of *in vitro* Cell Proliferation

In vitro proliferative kinetics were assayed by seeding 7.5×10^4 cells per well in 6-well plates. Total cell number was assessed every two to three days, as indicated, by trypsinization and manual counting with a hemocytometer.

Cell Viability Assays

The impact of transient transfection with various constructs and reagents on cell viability was assessed by a trypan blue dye exclusion assay. Briefly, in parallel to the corresponding invasion, motility, and anoikis assays, 2.0×10^5 cells were seeded in 6-well plates, and then transfected with the indicated expression constructs, siRNAs, or antisense oligonucleotides, as described in the Experimental Procedures. After 24 hours (expression constructs) or 48 hours (siRNAs and antisense oligonucleotides), cells were trypsinized, resuspended in 0.4% trypan blue staining solution (Sigma), and manually counted using a hemocytometer.

cDNA Synthesis and Real Time RT-PCR

Where indicated, cDNA was prepared from 200 ng of total RNA using the SuperScript III First-Strand Synthesis System (Invitrogen), and target levels were assessed via SYBR Green-based real time RT-PCR (Applied Biosystems).

Oligonucleotide Sequences

Oligonucleotides employed in this study were: cloning miR-31 from genomic DNA, ACAATACATAGCAGGACAGGAAGTAAGGAAGGTG and CATCTTCAAAAGCGGACACTCTAAGGAAGACTATGTTG; cloning miR-145 from genomic DNA, TGCTACAGATGGGGCTGGATGCAGAA and TAAGCCCTCTTACCTCCAGGGACAGC; miR-31 synthetic binding site, AATGGCGAGCTCAGGCAAGATGCTGGCATAGCTACCGGTAATGGC and GCCATTACCGGTAGCTATGCCAGCATCTTGCCTGAGCTCGCCATT; cloning modified miRNA sponges to pBABE-puro, AGACCCAAGCTGGCTAGCGTTTAAACTTAAGCTTG and AATGGCGTCGACTAGAAGGCACAGTCGAGGCT; miR-126 synthetic binding site, GCCATTGAGCTCTCGTACCGTGAGTAATAATGCGACCGGTGCCATT and AATGGCACCGGTCGCATTATTACTCACGGTACGAGAGCTCAATGGC; miR-206 synthetic binding site, GCCATTGAGCTCTGGAATGTAAGGAAGTGTGTGGACCGGTGCCATT and AATGGCACCGGTCCACACACTTCCTTACATTCCAGAGCTCAATGGC; miR-335 synthetic binding site, GCCAGTGAGCTCTCAAGAGCAATAACGAAAAATGTACCGGTGCCAGT and ACTGGCACCGGTACATTTTTCGTTATTGCTCTTGAGAGCTCACTGGC; cloning Arp2/3s5 3' UTR from genomic DNA, TTAACCGAGCTCTCTGGCAGGAAGTGGAT and TTGGCCTCTAGAGAGTTTATAGAATTTCTGCACCAGTTTGC; cloning CXCL12 3' UTR from genomic DNA, TTAAGGACCGGTGCACAACAGCCAAAAAGGA and TGGGCCACTAGTAAGCTCCATCACTAACAACTAATGA; cloning Ets-1 3' UTR from genomic DNA, TTAACCGAGCTCTGGCACTGAAGGGGCT and TCGGCCACCGGTATGAATGAAATTCTTTGT; cloning Fzd3 3' UTR from genomic DNA, TTGGCCGAGCTCTTTGTCTTGTCTAAGGT and TTGGCCACCGGTAAGAAAGCTACCAATTCTTATTTG; cloning HoxC13 3' UTR from genomic DNA, TTAATAGAGCTCCCACCCACCCGCTGCT and TTAATAGAGCTCCCACCCACCCGCTGCT; cloning ITGA5 3' UTR from genomic DNA, TTAACCGAGCTCGTCCTCCCAATTTCAGACTC and TTAACCACCGGTCTAGTTCTGGTCAGTGGGGGCACT; cloning JAZF1 3' UTR from genomic DNA, TTGGCCGAGCTCCATGCTGGTCATAACTG and TTAACCACCGGTGGGTCAGAGGCAGTTTA; cloning

74

KLF13 3' UTR from genomic DNA, TATATAACCGGTGCCCGCCACAGCCATGA and TGCGGCCGCGCCCGGACTAGTAAAATAATGAATCATAAATTTTAT; cloning M-RIP 3' UTR from genomic DNA, TTAACCGAGCTCAGAGTCTGAAGGAAGGCCT and TTAAATACCGGTACCAAGAAAGGAACGAGCGGA; cloning MMP16 3' UTR from genomic DNA, TTAACCGAGCTCGCAGGAGTTTGTGGTAACTT and TTGGCCACCGGTATCCACCACATTGTGTT; cloning NFAT5 3' UTR from genomic DNA, TTGGCCACCGGTAAATTCCACGAAGAAAATCCTG and TGGGCCTCTAGAAACTTTCAGTGTTTTATTTTTGACTGCAGCTG; cloning Numb 3' UTR from genomic DNA, TTCCGGACCGGTAAGCAATCATTATGGCTATGT and TCGGCCACTAGTAAAAGCTTCTACCATGAACATT; cloning RDX 3' UTR from genomic DNA, TTGGCCACCGGTGAGCTGTTATTTTGCATATATG and TTGGCCACTAGTGAAGGCATGAGCTTTTGTCACTTTATTG; cloning Ret 3' UTR from genomic DNA, TTGGCCACCGGTCATTTCTTTGTGAAAGGT and TTGGCCACTAGTGCAATGAAGAATGACAAGAAGCT; cloning RhoA 3' UTR from genomic DNA, TTAACCGAGCTCAACCTTGCTGCAAGCACA and TTGGCCACCGGTAGAAAACTGCCTTTATTCTATTAGTAGTTGG; cloning YY1 3' UTR from genomic DNA, TTGGCCGAGCTCAAAGAAGAGAGAAGACCCTTCT and TTGGCCACCGGTCTTTAGGATTGCTATTTTATTGTTGCCCT; Fzd3 3' UTR mutagenesis, CTACAGTGAGATGTGATCGGCGCAAAGCCACCAGACCTTGGCTTCC and GGAAGCCAAGGTCTGGTGGCTTTGCGCCGATCACATCTCACTGTAG; ITGA5 3'UTR mutagenesis, CTGCAAAGATCTGTCCTCAGCCAAAAGAGAGATCCAAAAGAAGCCCCCAG and CTGGGGGCTTCTTTTGGATCTCTCTTTTGGCTGAGGACAGATCTTTGCAG; M-RIP 3' UTR mutagenesis, GTTTGTTTTTTATTAAATCGGCGACAAAATCCCCGGCCCCTCTCC and GGAGAGGGGCCGGGGATTTTGTCGCCGATTTAATAAAAAACAAAC; MMP16 3' UTR mutagenesis, GTGTTTATAACAAACAGAAATGATGTTACCGGCCAAAATTTTTCTGGC and GCCAGAAAAATTTTGGCCGGTAACATCATTTCTGTTTGTTATAAACAC; RDX 3' UTR mutagenesis, GATATGATGGAATGCATCCCACCAGCGGAAAGCACTTACACCAGTTTGACTGTG and

CACAGTCAAACTGGTGTAAGTGCTTTCCGCTGGTGGGATGCATTCCATCATATC; RhoA 3' UTR site

one mutagenesis, CCTAAGATTACAAATCAGAAGTCAGGCGGCTACCAGTATTTAGAAGCCAAC and

GTTGGCTTCTAAATACTGGTAGCCGCCTGACTTCTGATTTGTAATCTTAGG; RhoA 3' UTR site two

mutagenesis, GGCGCTAATTCAAGGAATTTCTTAACTCGCCGCTTCTTTCTAGAAAGAGAAACAGTGG

and CCAACTGTTTCTCTTTCTAGAAAGAAGCGGCGAGTTAAGAAATTCCTTGAATTAGCG CC;

CXCL12 RT-PCR, TGAGAGCTCGCTTTGAGTGACTGGGT and ATACCACCAGGACCTTCTGTGGATCGCA;

Fzd3 RT-PCR, TCCATCCCTGCACAATATAAGGCTTCCACA and TCTCAATGCATCAACATCGTAGAGGCCAAC;

GAPDH RT-PCR, TCACCAGGGCTGCTTTTAAC and GACAAGCTTCCCGTTCTCAG; ITGA5 RT-

PCR, AACTCATCATGGCCAGTGAGGGTAAGGGT and ATCCTTAATGGCTCAGACATTCGATCCCTCTACAACT;

M-RIP RT-PCR, AGGCAGAGCACATGGAGACCAATGCA and AGTCAGCCAGCCTTTCTTGAAATTCAGCA;

MMP16 RT-PCR, AGTACGGCTACCTTCCACCGACTGA and TACCTCTTGTCTGGTCAGGTACACCGCAT;

RDX RT-PCR, GAATCAGGAGCAGCTAGCAGCAGAACTT and TTGGTCTTTTCCAAGTCTTCCTGGGCTGCA;

RhoA RT-PCR, AGGTGGATGGAAAGCAGGTAGAGTTGGCT and AGGATGATGGGCACGTTGGGACAGA.
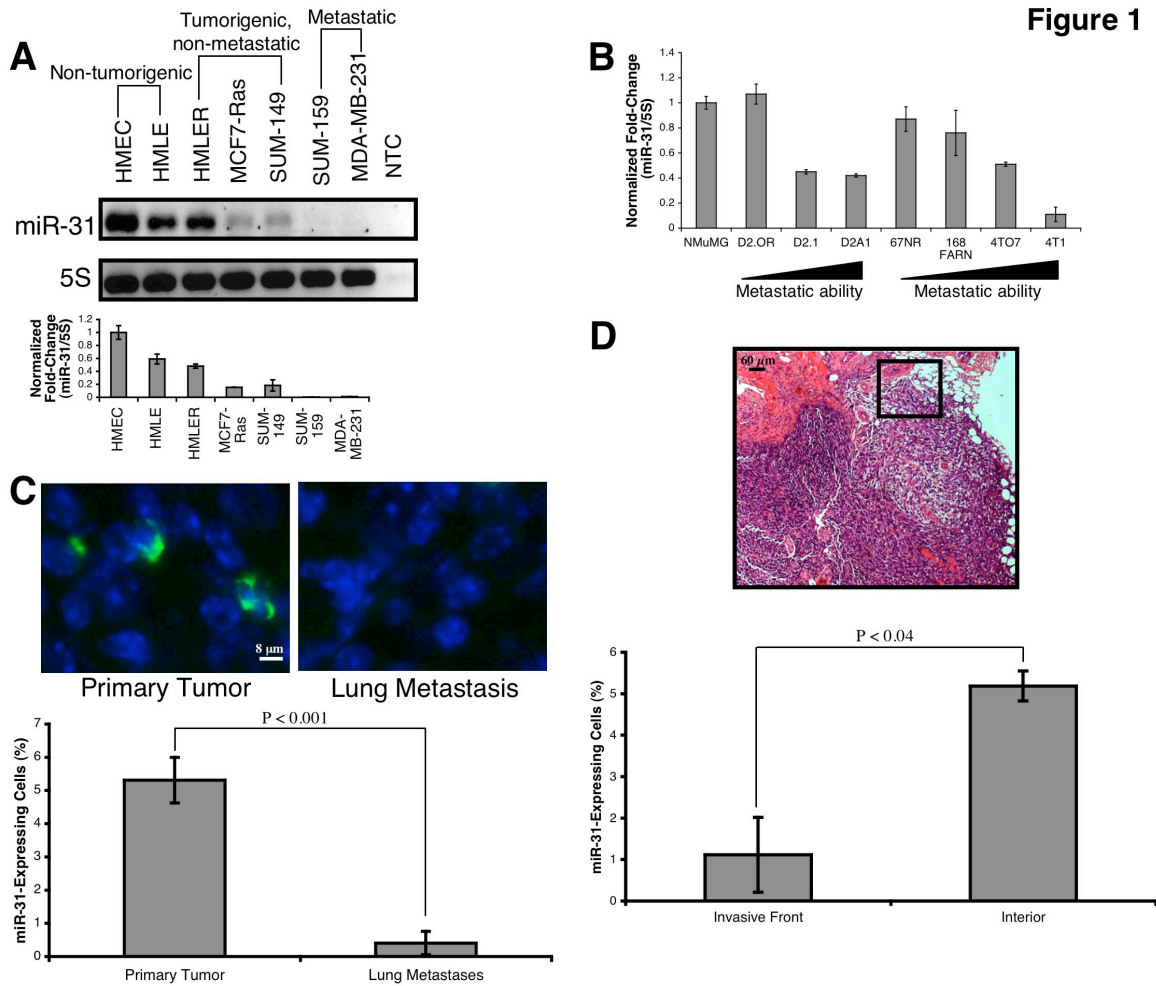
FIGURES

Figure 1. miR-31 Levels Correlate Inversely with Metastatic Ability in Breast Cell Lines.

(A) RT-PCR for miR-31 in seven human breast cell lines. 5S rRNA was a loading control. NTC: no template control. n = 3. **(B)** miR-31 RT-PCR in eight murine mammary cell lines. 5S rRNA was a loading control. n = 3. **(C)** *In situ* hybridization for miR-31 (green) in animal-matched 4T1 cell primary mammary tumors and lung metastases; DAPI counterstain (blue). n = 4. **(D)** Hematoxylin and eosin (H&E) stain of a 4T1 cell primary mammary tumor (top); box: invasive front. miR-31 *in situ* hybridization in 4T1 cells located near the invasive front or the interior of the primary tumors (bottom). n = 3.
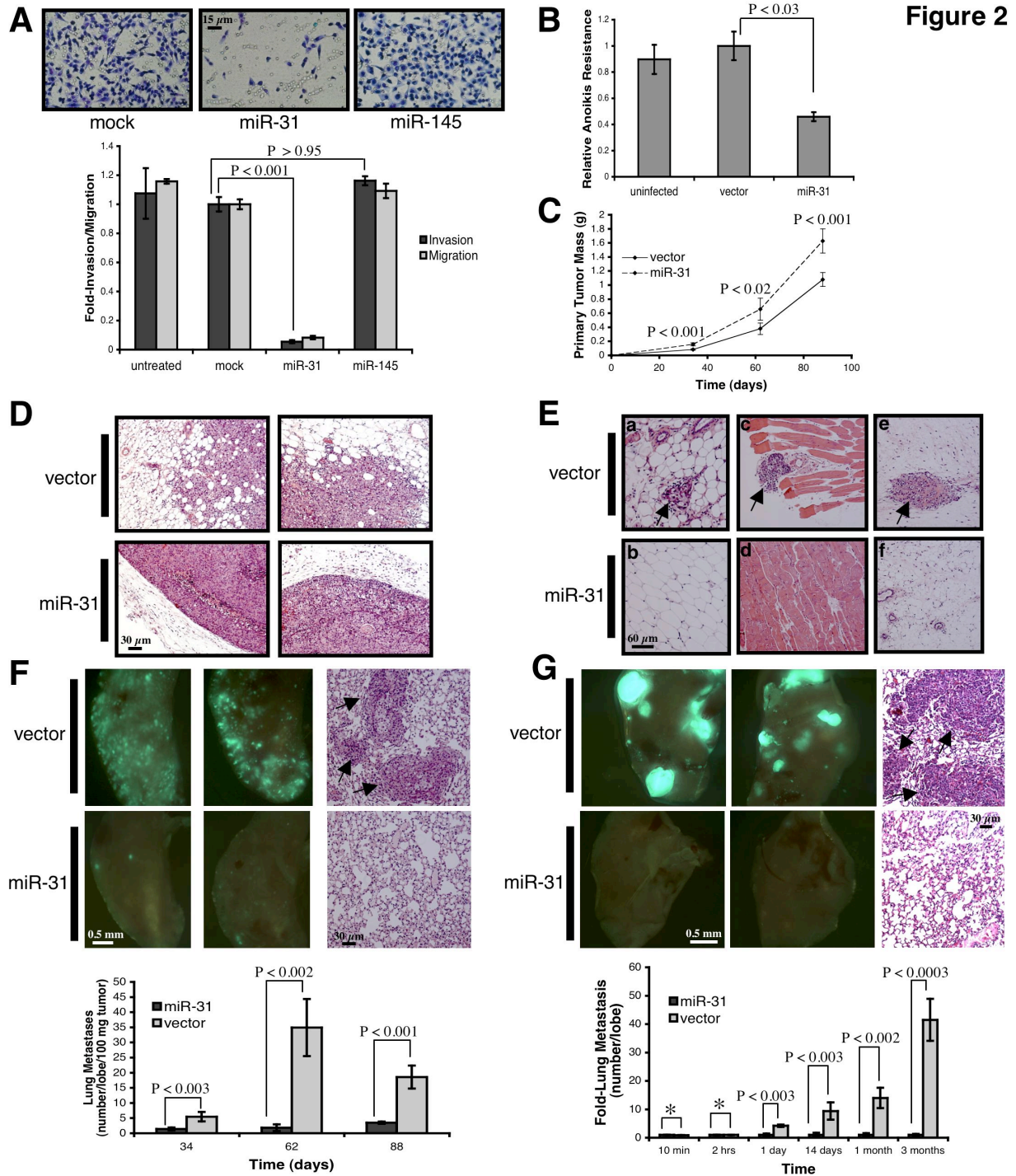
Figure 2. miR-31 Expression Inhibits Metastasis. (A) Invasion and motility assays after

transfection of MDA-MB-231 (231) cells with the indicated constructs. n = 3. **(B)** Anoikis assays

using 231 cells infected as indicated. n = 3. **(C)** Primary tumor growth upon orthotopic injection

of 1.0 x 10^6 GFP-labeled 231 cells infected as indicated. The experiment was terminated after 13 weeks due to primary tumor burden. n = 5 per group per timepoint. **(D)** H&E stain of 231 primary tumors 62 days after orthotopic injection. **(E)** H&E stain of tissue adjacent to the indicated 231 primary mammary tumors 62 days after injection. Arrows: disseminated tumor cells in normal fat (a, b), muscle (c, d), and subcutis (e, f). **(F)** Images of murine lungs to visualize GFP-labeled 231 cells 62 days after orthotopic implantation (left). H&E stain of lungs from animals bearing the indicated tumors (right); arrows: metastatic foci. n = 5. **(G)** Images of murine lungs to detect GFP-labeled 231 cells 88 days after tail vein injection (left). H&E stain of lungs (right); arrows: metastatic foci. Asterisks: P >0.66. n = 5, except for 10 min and two hrs (n = 4).
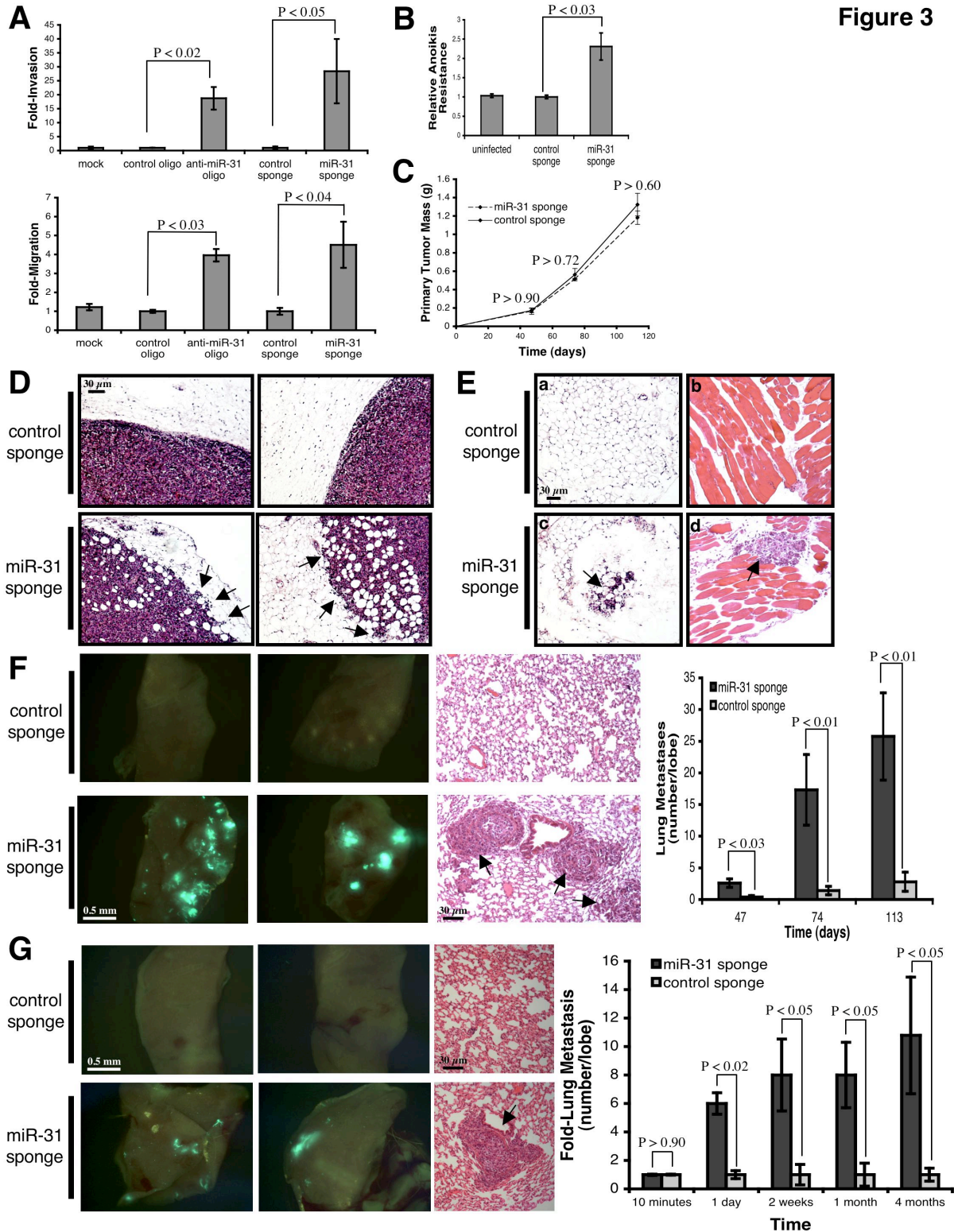
Figure 3. Inhibition of miR-31 Promotes Metastasis. (A) Invasion and motility assays using

MCF7-Ras cells transfected with the indicated transient miR-31 inhibitors. n = 3. **(B)** Anoikis

assays with MCF7-Ras cells stably expressing the indicated sponge. n = 3. **(C)** Primary tumor

growth upon orthotopic implantation of 5.0 x 10^5 GFP-labeled MCF7-Ras cells infected as

indicated. The experiment was terminated after 16 weeks due to primary tumor burden. n = 5 per

group per timepoint. **(D)** H&E stain of MCF7-Ras primary tumors 47 days after orthotopic

injection. Arrows: regions of poor encapsulation. **(E)** H&E stain of tissue adjacent to the

indicated MCF7-Ras primary tumors 47 days post-injection. Arrows: disseminated tumor cells in

normal fat (a, c) and muscle (b, d). **(F)** Images of murine lungs to visualize GFP-labeled MCF7-

Ras cells 113 days after orthotopic injection (left). H&E stain of lungs from animals bearing the

indicated tumors (middle); arrows: metastatic foci. n = 5. **(G)** Images of murine lungs to detect

GFP-labeled MCF7-Ras cells 122 days after tail vein injection (left). H&E stain of lungs

(middle); arrow: metastasis. n = 4, except for one day (n = 3).
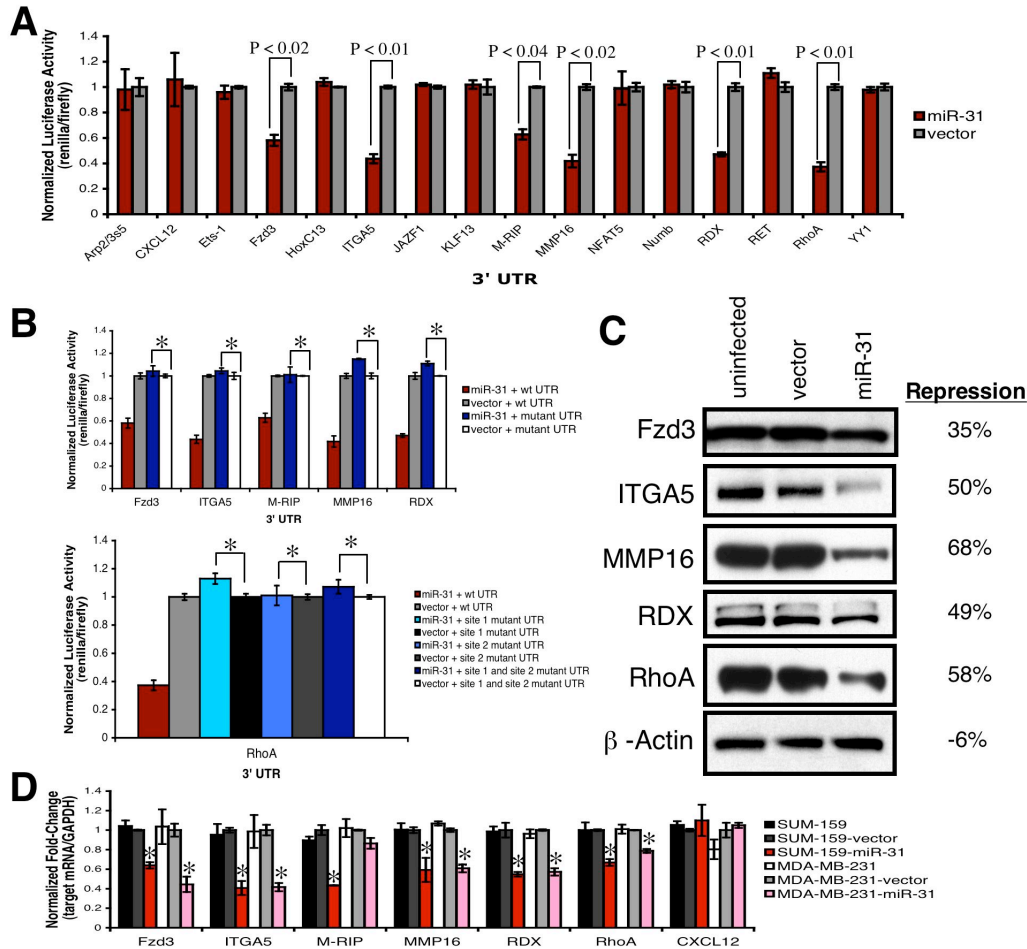
Figure 4. miR-31 Directly Regulates a Cohort of Pro-Metastatic Genes. (A) Luciferase

activity in 231 cells infected with miR-31 or control vector after transfection of the indicated 3'

UTR-driven reporter constructs. n = 3. **(B)** Luciferase activity in the indicated 231 cells upon

transfection of miR-31 site mutant 3' UTR-driven reporter constructs. wt: wild type; site 1: the

miR-31 motif at nt 145-151 of the RhoA 3' UTR; site 2: the motif spanning nt 303-309.

Asterisks: $P >0.80$ relative to mutant-UTR + vector controls. n = 3. **(C)** Immunoblots for

endogenous Fzd3, ITGA5, MMP16, RDX, and RhoA in the indicated 231 cells. _-actin was a

loading control. Repression: protein levels in miR-31-expressing cells relative to vector controls.

(D) RT-PCR for endogenous CXCL12, Fzd3, ITGA5, M-RIP, MMP16, RDX, and RhoA.

GAPDH was a loading control. Asterisks: $P <0.03$ relative to vector controls. n = 3.
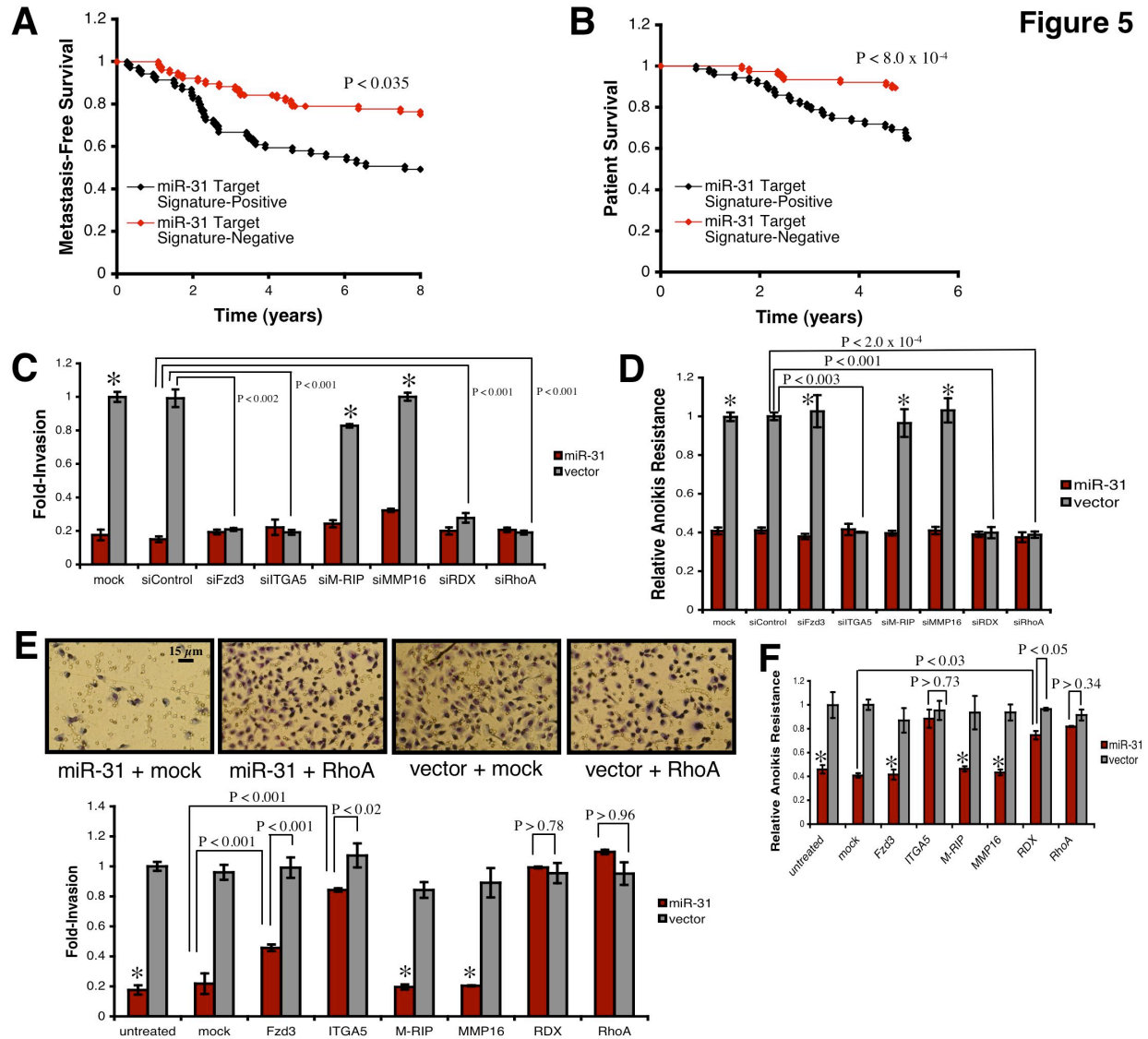
Figure 5. Repression of Fzd3, ITGA5, RDX, and RhoA Underlies miR-31-Dependent Phenotypes *in vitro*. (A) Kaplan-Meier curves for 295 human primary breast tumors depicting metastasis-free survival, stratified based on expression of the six-gene miR-31 target signature. P-value based on a logrank test. **(B)** Kaplan-Meier five-year survival curves for 295 breast cancer patients, stratified based on miR-31 target signature expression in their primary tumors. P-value based on a logrank test. **(C)** Invasion assays with miR-31-expressing or control 231 cells transfected as indicated. Asterisks: P >0.19 relative to vector + siControl cells. n = 3. **(D)**

Anoikis assays using 231 cells transfected with the indicated siRNAs. Asterisks: P >0.80 relative

to vector + siControl cells. n = 3. **(E)** Invasion assays using the indicated 231 cells transfected

with miRNA-resistant expression constructs. Asterisks: P >0.61 relative to miR-31 + mock cells.

n = 3. **(F)** Anoikis assays with the indicated 231 cells transfected as noted. Asterisks: P >0.11

relative to miR-31 + mock cells. n = 3.

Figure 6
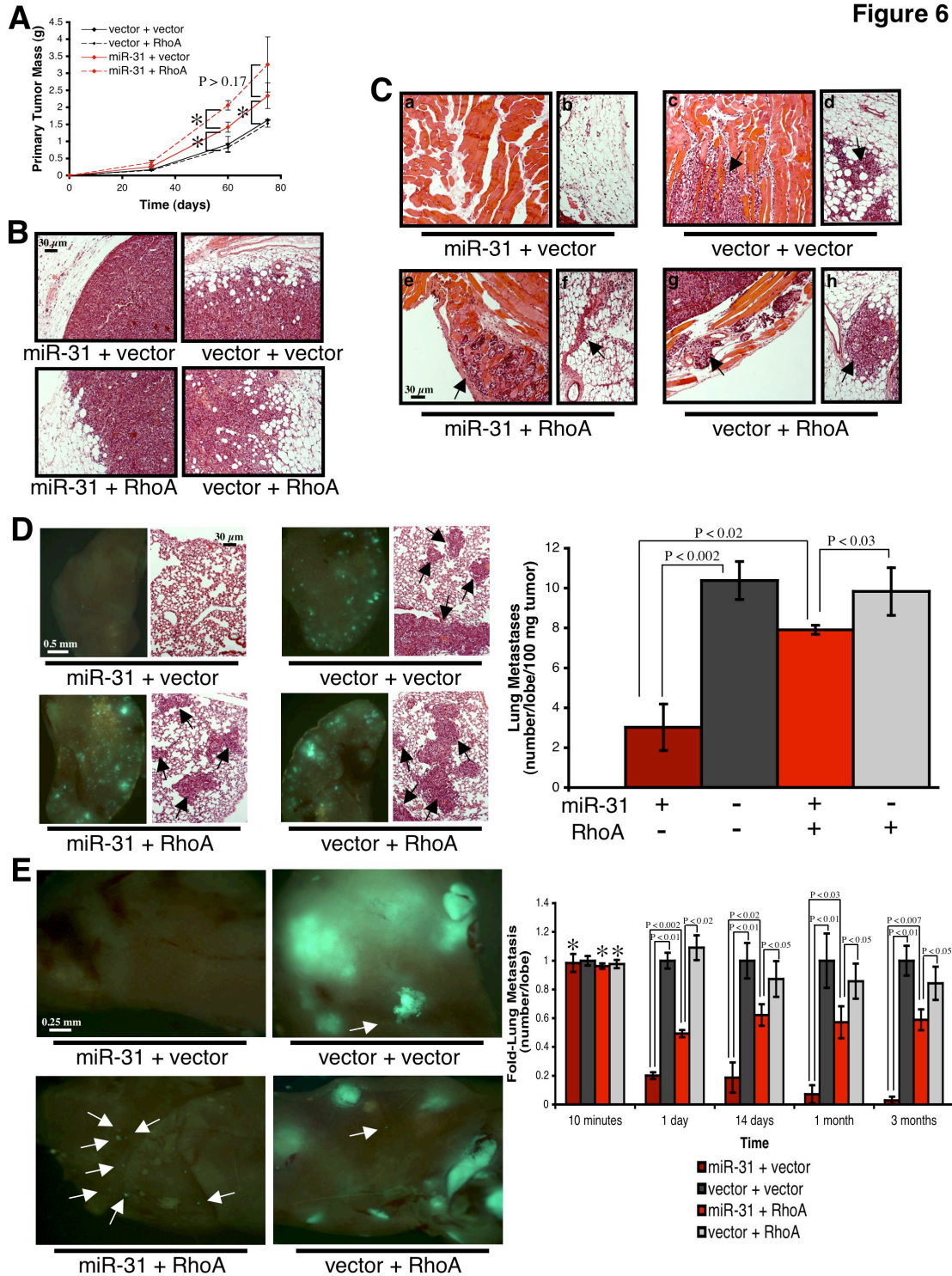
Figure 6. Re-Expression of RhoA Partially Reverses miR-31-Imposed Metastasis Defects *in*

vivo. **(A)** Primary tumor growth upon orthotopic injection of 5.0 x 10^5 GFP-labeled 231 cells.

The experiment was terminated after 11 weeks due to primary tumor burden. Asterisks: P <0.02.

n = 5 per group per timepoint. **(B)** H&E stain of 231 primary tumors 60 days after orthotopic injection. **(C)** H&E stain of tissue adjacent to the indicated 231 primary mammary tumors 60 days after injection. Arrows: disseminated tumor cells in normal muscle (a, c, e, g) and fat (b, d, f, h). **(D)** Images of murine lungs to visualize GFP-labeled 231 cells 60 days after orthotopic injection (left). H&E stain of lungs from animals bearing the indicated tumors (right); arrows: metastatic foci. n = 5. **(E)** Images of murine lungs to detect GFP-labeled 231 cells 86 days after tail vein injection (left); arrows: micrometastatic lesions. Asterisks: P >0.87 relative to vector + vector controls. n = 4, except for 2 weeks (n = 3).
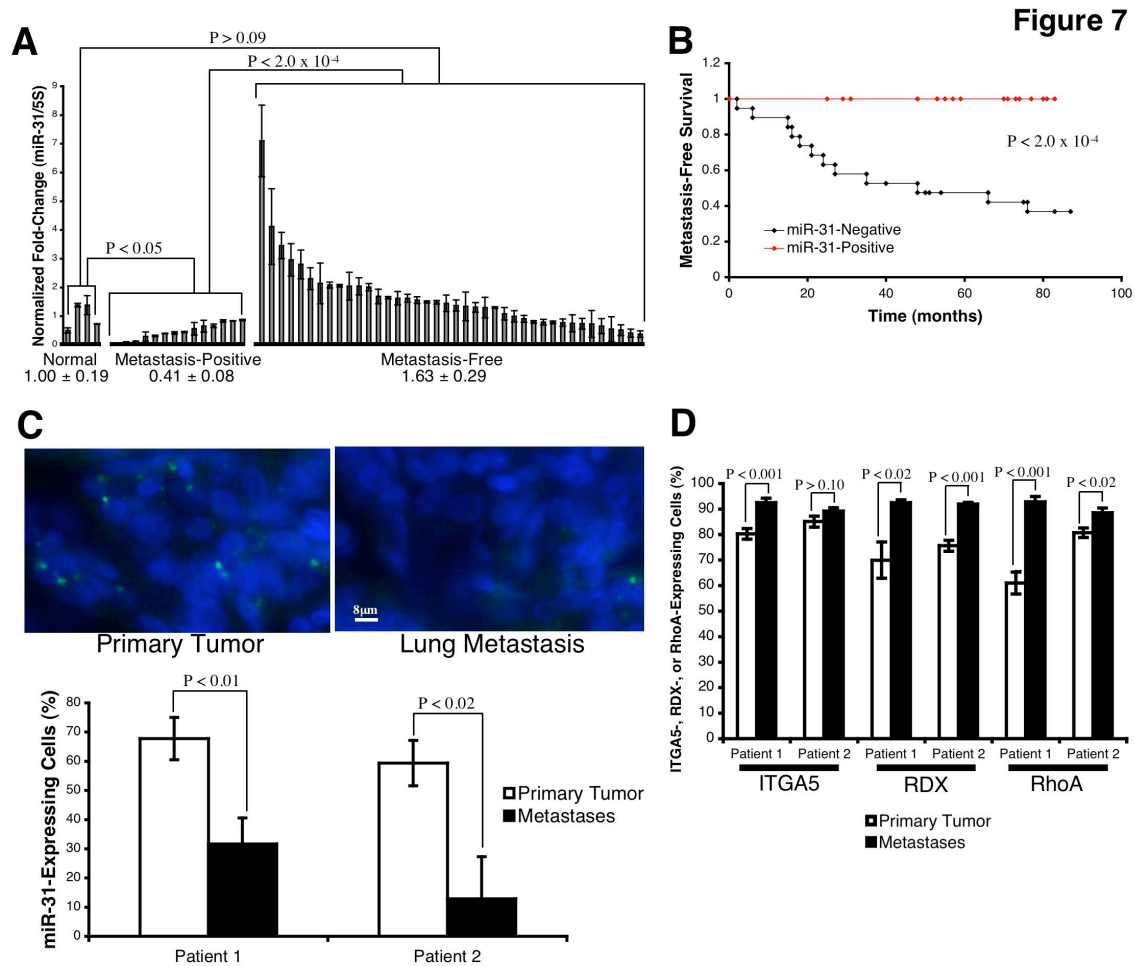
Figure 7. miR-31 Levels Correlate Inversely With Metastasis in Human Breast Tumors.

(A) miR-31 RT-PCR in 54 primary breast tumors. Normal: tissue from non-diseased individuals; metastasis-positive and -free: tumors of the indicated distant metastasis outcome. 5S rRNA was a loading control. n = 4 (normal); n = 14 (metastasis-positive); n = 40 (metastasis-free). **(B)** Kaplan-Meier distant metastasis-free survival curves for 54 breast cancer patients, stratified based on miR-31 levels in their primary tumors. P-value based on a chi-square test. **(C)** *In situ* hybridization for miR-31 (green) in patient-matched primary breast tumors and distant metastases (patient 1 = lung; 2 = pleura); DAPI counterstain (blue). n = 8 fields. **(D)** Immunohistochemical detection of ITGA5, RDX, and RhoA in patient-matched primary breast tumors and distant metastases (patient 1 = lung; 2 = pleura). n = 8 fields.
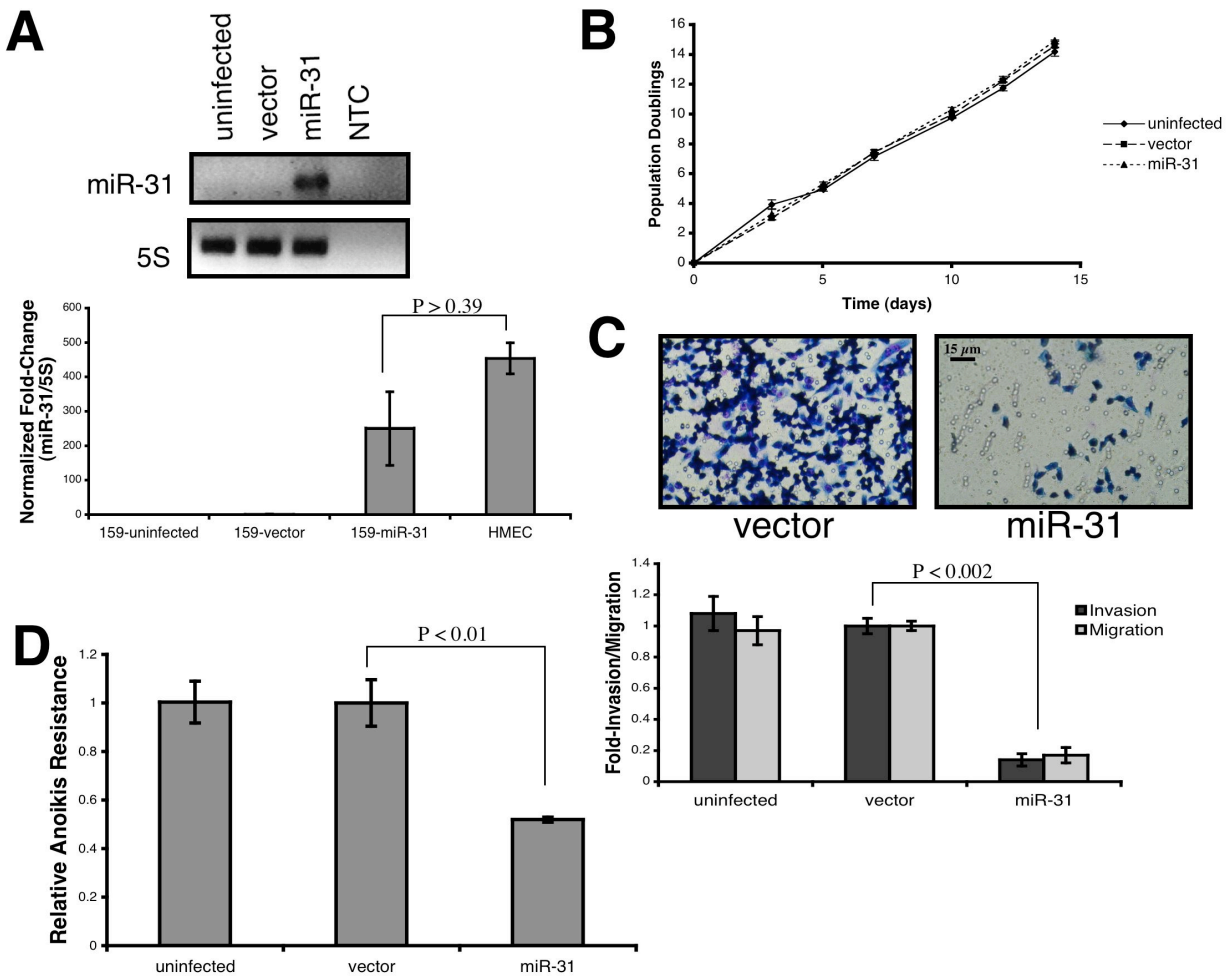
SUPPLEMENTARY FIGURES
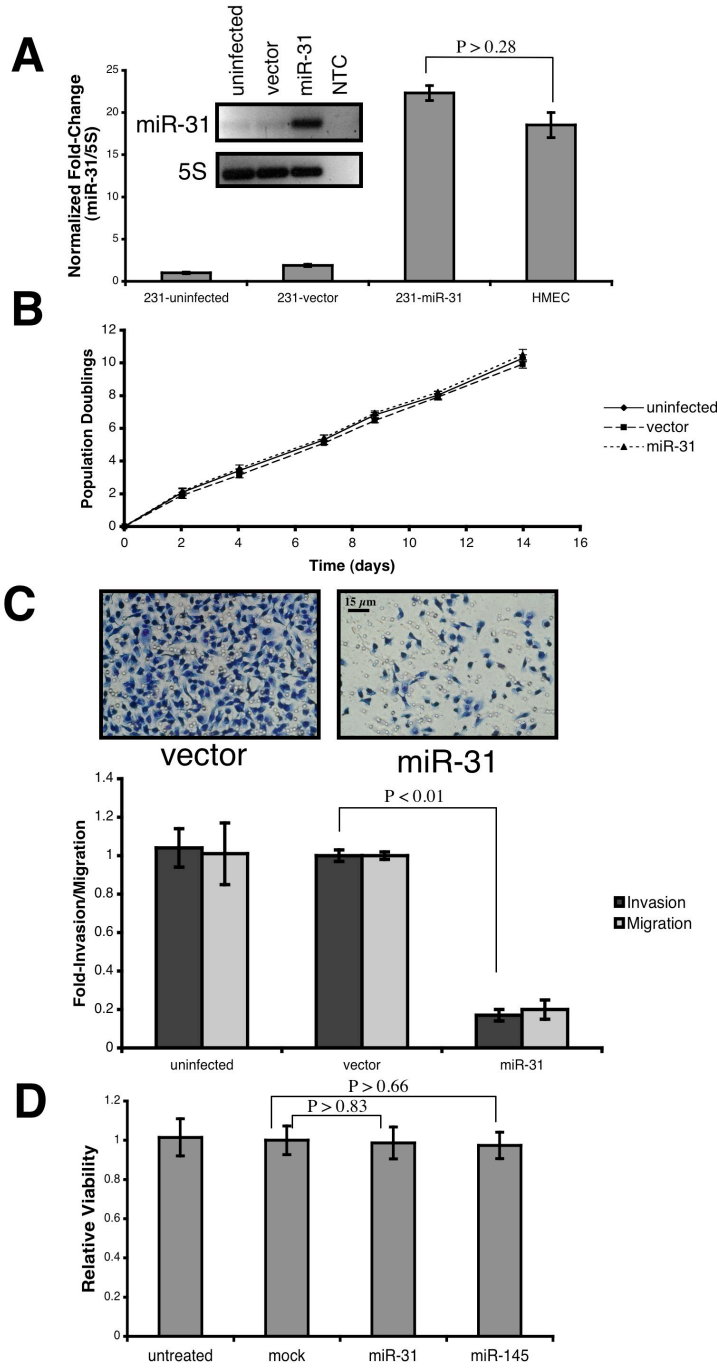
Supplementary Figure 1. miR-31 Does Not Affect MDA-MB-231 Cell Viability and

Proliferation *in vitro*. (A) RT-PCR for miR-31 in MDA-MB-231 (231) cells infected with

human miR-31 or control vector, as well as endogenous miR-31 levels in normal human

mammary epithelial cells (HMECs). 5S rRNA was a loading control. NTC: no template control.

n = 3. **(B)** *In vitro* growth curves of 231 cells expressing miR-31 or control vector. Triplicate

wells from each cohort were counted for 14 days, as indicated. n = 3. **(C)** Invasion and motility

assays using 231 cells infected with miR-31 or vector control. n = 3. **(D)** Trypan blue dye

exclusion assay using 231 cells transfected with the indicated expression constructs for 24 hrs. n

= 3.

Supplementary Figure 2. miR-31 Inhibits SUM-159 Invasion, Motility, and Anoikis Resistance *in vitro*. (A) RT-PCR for miR-31 in SUM-159 (159) cells infected with miR-31 or control vector, as well as endogenous miR-31 in normal HMECs. 5S rRNA was a loading control. n = 3. **(B)** *In vitro* growth curves of 159 cells infected with miR-31 or vector control. Triplicate wells from each cohort were c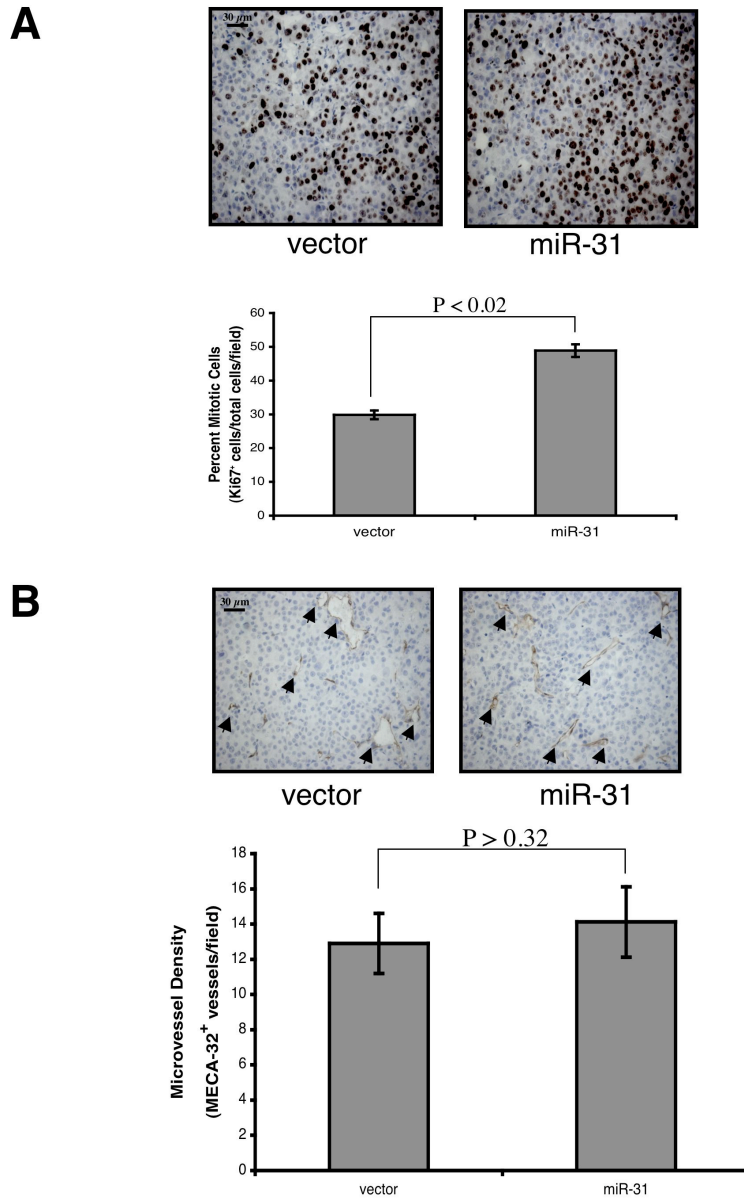ounted for 14 days, as indicated. n = 3. **(C)** Invasion and motility assays utilizing 159 cells expressing miR-31 or control vector. n = 3. **(D)** Anoikis assays using 159 cells infected with miR-31 or vector control. Cells were cultured in anchorage-independence for 24 hrs, and then cell viability was assessed by trypan blue stain. n = 3.

A

vector   miR-31

B

vector   miR-31

Supplementary Figure 3. miR-31 Does Not Impact MDA-MB-231 Primary Tumor Neo-vascularization. (A) Ki-67 staining of primary mammary tumors derived from 231 cells expressing miR-31 or control vector 62 days post-implantation. Cells were counterstained with hematoxylin. n = 5. **(B)** MECA-32 stain of 231 cell primary mammary tumors expressing miR-31 or control vector 62 days post-implantation. Arrows: intact intratumoral vessels. Cells were counterstained with hematoxylin. n = 5.
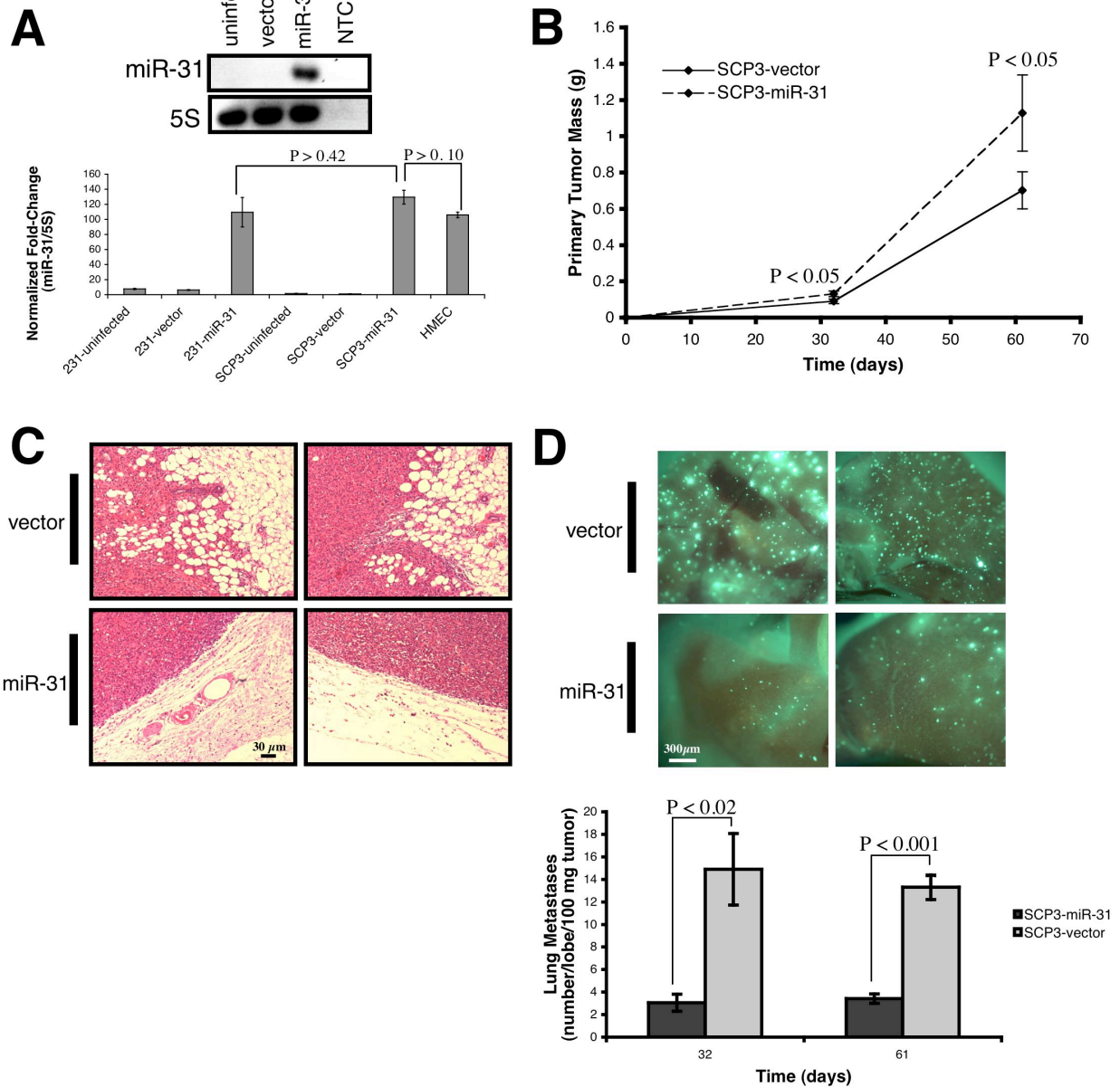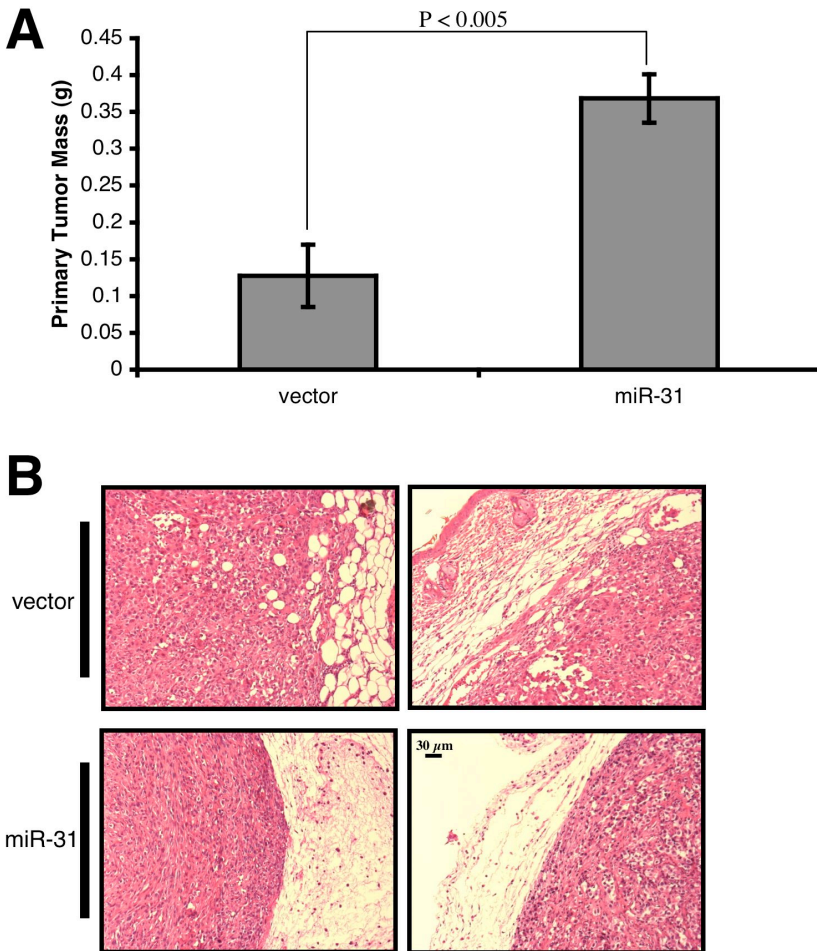
Supplementary Figure 4. miR-31 Promotes Primary Tumor Growth and Inhibits Both Local Invasion and Lung Metastasis in a Single-Cell-Derived Population of MDA-MB-231 Cells. (A) RT-PCR for miR-31 in SCP3 cells overexpressing miR-31 or control vector, the parental population of 231 cells infected as indicated, and endogenous miR-31 levels in normal HMECs. 5S rRNA was a loading control. n = 3. **(B)** Primary tumor growth kinetics upon

orthotopic injection of 1.0 x 10^6 GFP-labeled SCP3 cells infected as indicated. n = 5 per group

per timepoint. **(C)** Hematoxylin and eosin (H&E) stain of the indicated SCP3 primary tumors 32

days after orthotopic injection. **(D)** Fluorescent images of murine lungs to visualize the indicated

GFP-labeled SCP3 cells 61 days after orthotopic implantation (top panels). n = 5 per cohort per

timepoint.

Supplementary Figure 5. miR-31 Promotes Primary Tumor Growth and Inhibits Local Invasion in SUM-159 Cells. (A) Primary tumor burden 32 days after orthotopic injection of 1.0 x 10^6 SUM-159 cells infected as indicated. n = 5 per group per timepoint. **(B)** H&E stain of the indicated SUM-159 primary tumors 32 days after orthotopic implantation.
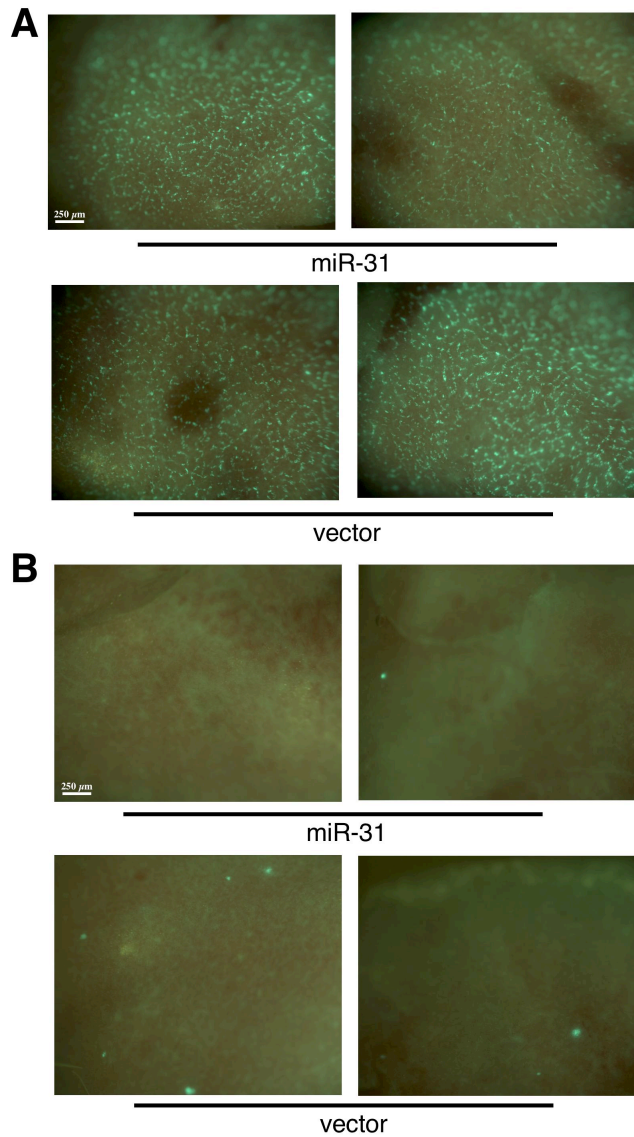
Supplementary Figure 6. miR-31 Fails to Alter the Initial Vascular Lodging of Intravenously Injected MDA-MB-231 Cells and the Size of Eventually Established Micrometastases. (A) Fluorescent images of murine lungs to visualize GFP-labeled 231 cells expressing miR-31 or control vector 10 minutes subsequent to tail vein injection of 5.0×10^5 cells. **(B)** Fluorescent images of murine lungs to visualize the indicated GFP-labeled 231 cells one month after intravenous injection.
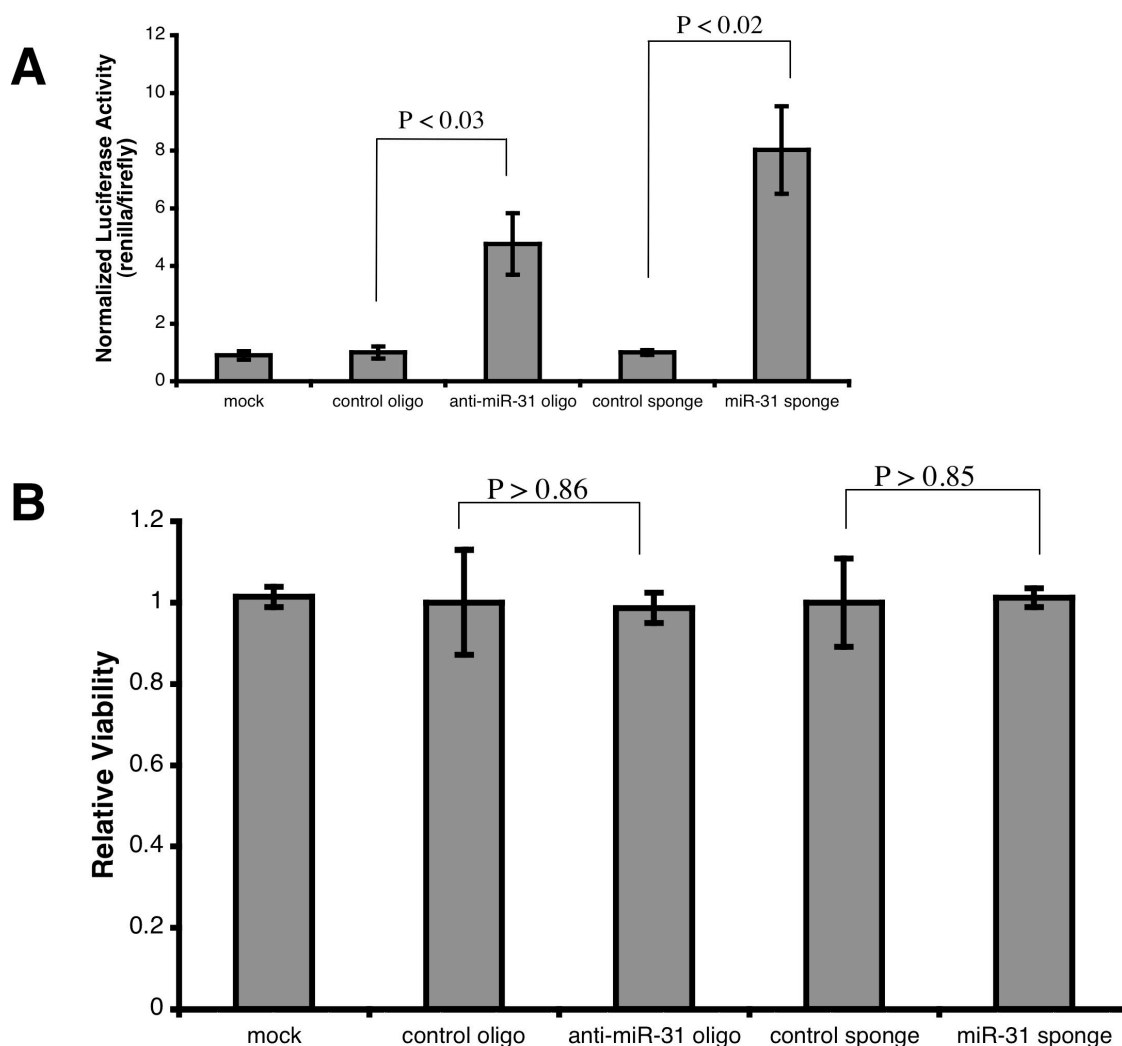
Supplementary Figure 7. Transient Inhibition of miR-31 Does Not Affect MCF7-Ras Cell Viability. (A) Luciferase assays in MCF7-Ras cells upon transfection of the indicated transient miRNA inhibitors. Cells were transfected with the inhibitors for 48 hrs, then co-transfected with a *Renilla* luciferase reporter containing a miR-31 motif in its 3' UTR and a control firefly luciferase reporter. 24 hrs after transfection with the reporters, cell lysates were harvested and luciferase activity was quantitated. n = 3. **(B)** Trypan blue dye exclusion assay employing MCF7-Ras cells transfected with the indicated antisense oligonucleotides or miRNA sponges for 48 hrs. n = 3.

A

B

C

D
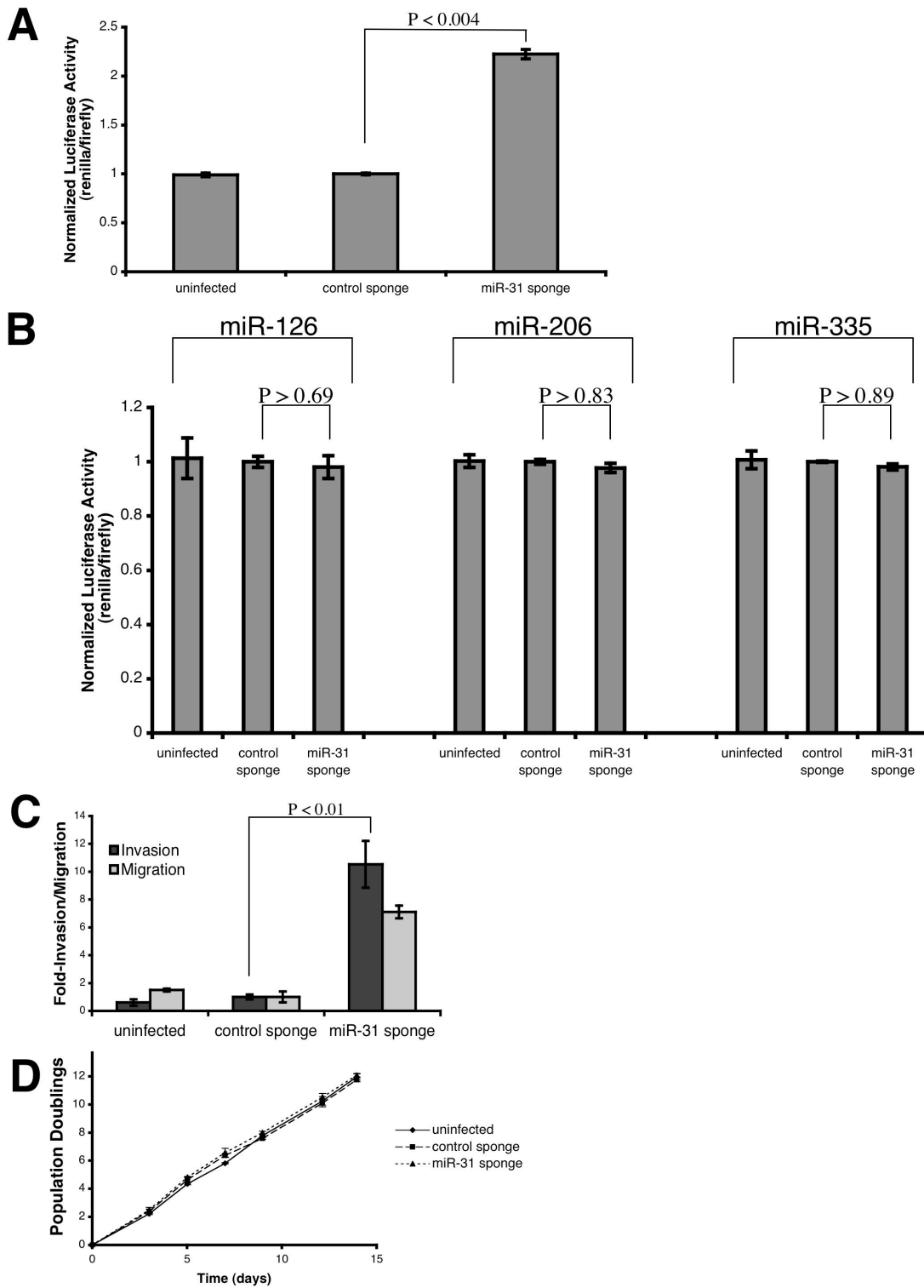
Supplementary Figure 8. Modified miRNA Sponges Stably and Specifically Inhibit miR-31 in MCF7-Ras Cells. (A) Luciferase assays upon stable infection of MCF7-Ras cells with a

modified miR-31 sponge or control sponge. Cells were co-transfected with a *Renilla* luciferase reporter containing a miR-31 motif in its 3' UTR and a control firefly luciferase reporter. 24 hrs after transfection with the reporter genes, cell lysates were harvested and luciferase activity was quantitated. n = 3. **(B)** Luciferase assays using MCF7-Ras cells stably infected with a miR-31 or control sponge. Cells were co-transfected with a *Renilla* luciferase reporter containing either a miR-126, miR-206, or miR-335 motif in its 3' UTR and a control firefly luciferase reporter. 24 hrs after transfection with the reporters, lysates were harvested and luciferase activity quantified. n = 3. **(C)** Invasion and motility assays using MCF7-Ras cells stably expressing a miR-31 sponge or control sponge. n = 3. **(D)** *In vitro* growth curves of MCF7-Ras cells infected with a miR-31 sponge or control sponge. Triplicate wells from each cohort were counted for 14 days, as indicated. n = 3.
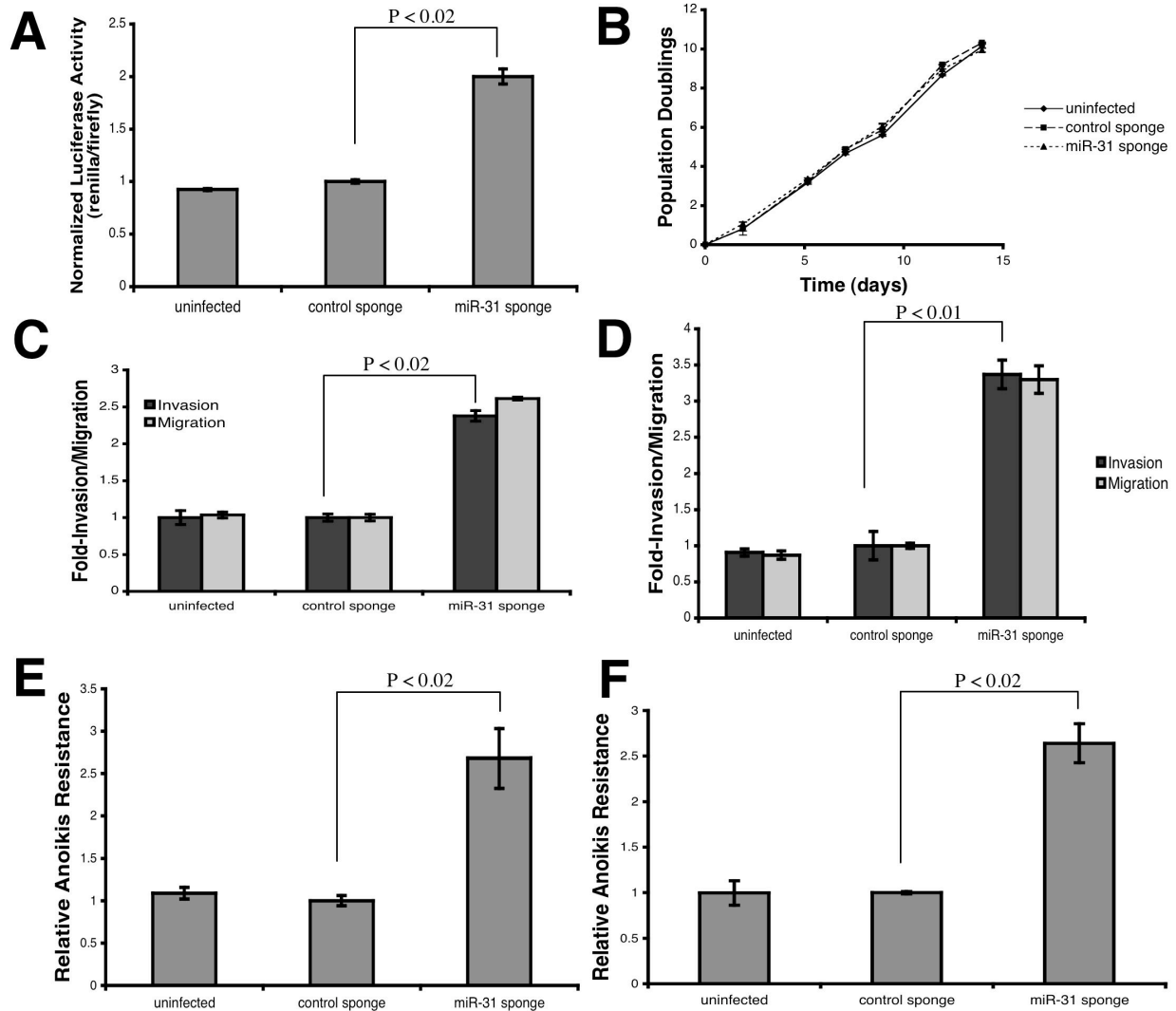
Supplementary Figure 9. miR-31 Inhibits HME and SUM-149 Invasion, Motility, and Anoikis Resistance *in vitro*. (A) Luciferase assays upon infection of HME cells with a miR-31 or control sponge. Cells were co-transfected with a *Renilla* luciferase reporter containing a miR-31 motif in its 3' UTR and a control firefly luciferase reporter. 24 hrs after transfection with the reporters, cell lysates were harvested and luciferase activity was quantitated. n = 3. **(B)** *In vitro* growth curves of HME cells infected with a miR-31 or control sponge. Triplicate wells from each cohort were counted for 14 days, as indicated. n = 3. **(C)** Invasion and motility assays using

HME cells infected with the indicated sponges. n = 3. **(D)** Invasion and motility assays utilizing SUM-149 cells infected with a miR-31 or control sponge. n = 3. **(E)** Anoikis assays with HME cells infected as indicated. Cells were cultured in anchorage-independence for 24 hrs, and then cell viability was assessed by trypan blue stain. n = 3. **(F)** Anoikis assays using SUM-149 cells infected as indicated. Cells were cultured in anchorage-independence for 24 hrs then cell viability was assessed via trypan blue stain. n = 3.

A

control sponge   miR-31 sponge

B

control sponge   miR-31 sponge
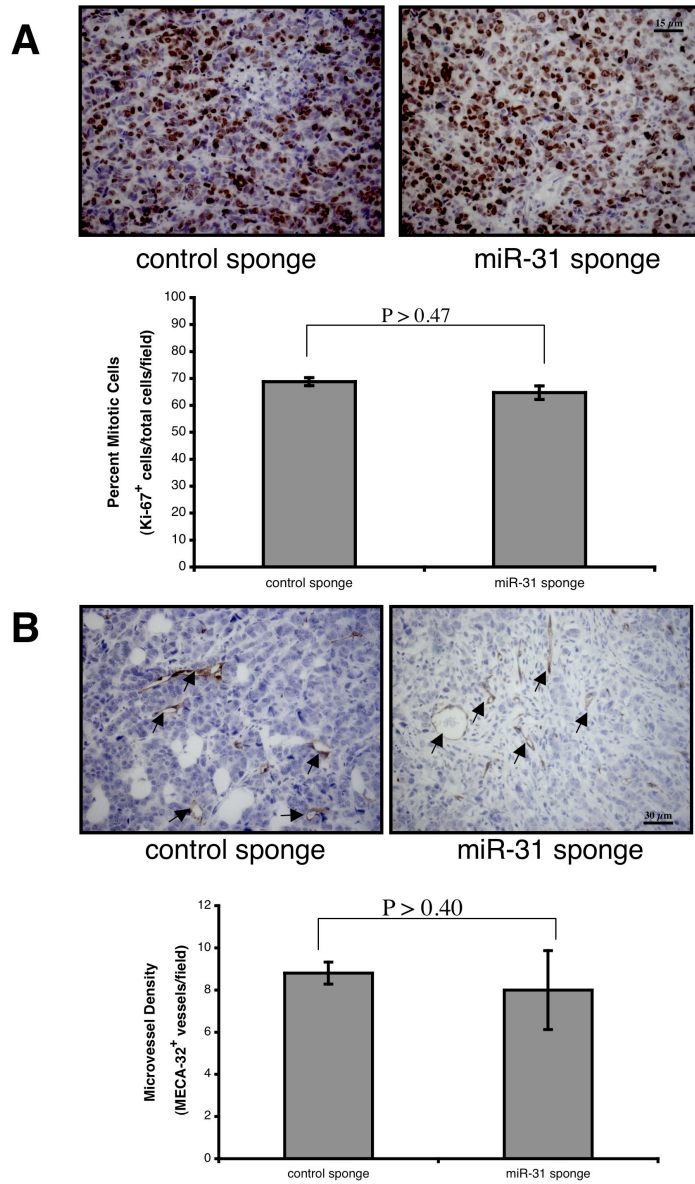
Supplementary Figure 10. Loss of miR-31 Fails to Affect MCF7-Ras Cell Primary Tumor Proliferation or Neo-vascularization. (A) Ki-67 staining of primary mammary tumors derived from the indicated MCF7-Ras cells 47 days post-injection of 5.0×10^5 cells. Cells were counterstained with hematoxylin. n = 5. **(B)** MECA-32 staining of primary mammary tumors derived from MCF7-Ras cells expressing a miR-31 or control sponge 47 days after injection. Arrows: intact intratumoral vessels. Cells were counterstained with hematoxylin. n = 5.

miR-31 sponge
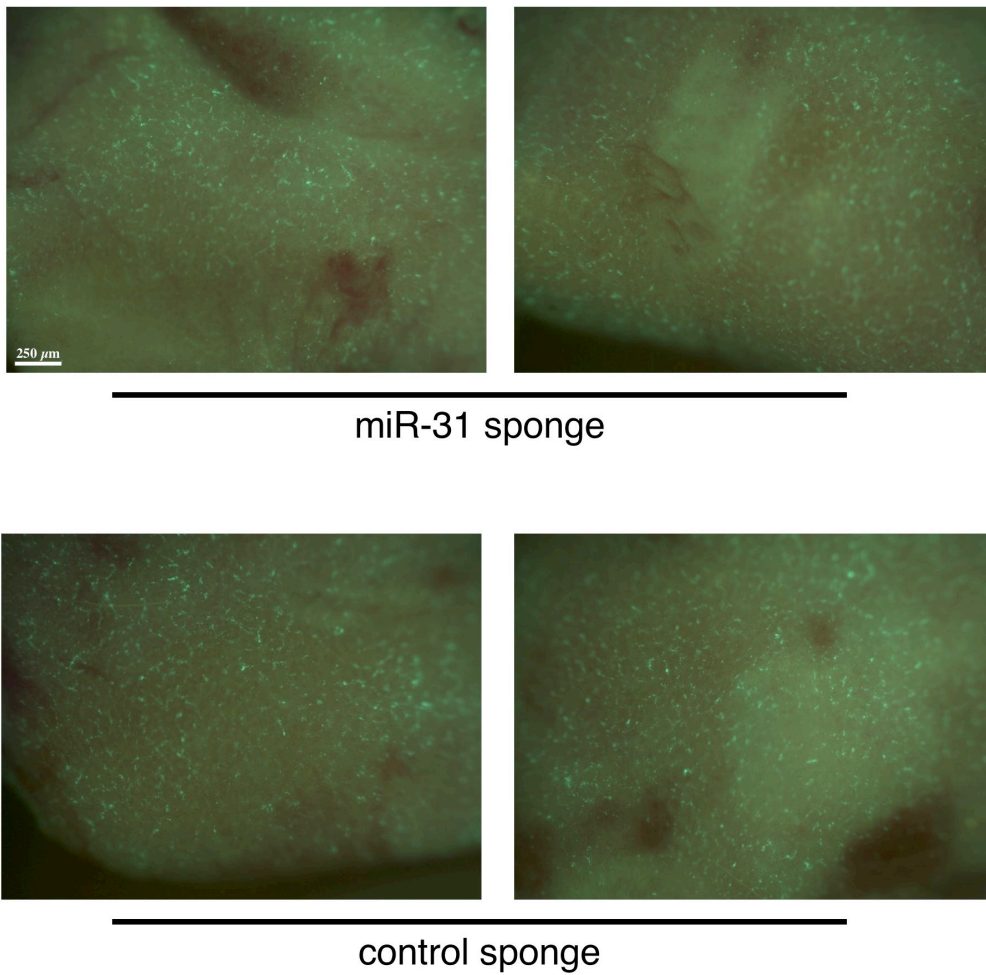
control sponge

Supplementary Figure 11. Loss of miR-31 Does Not Influence the Initial Vascular Lodging of Intravenously Injected MCF7-Ras Cells. Fluorescent images of murine lungs to visualize GFP-labeled MCF7-Ras cells expressing a miR-31 or control sponge 10 minutes after tail vein injection of 5.0 x 10^5 cells.
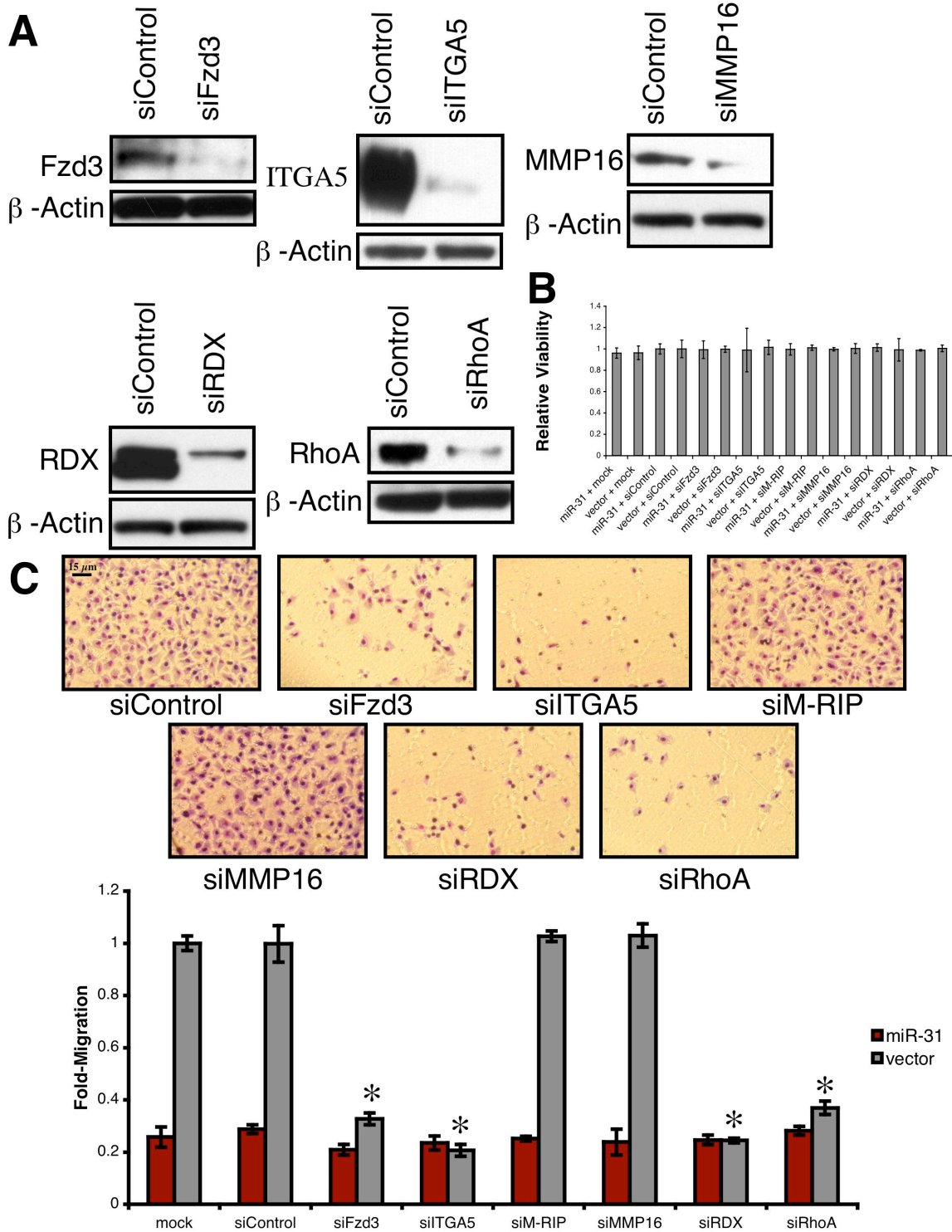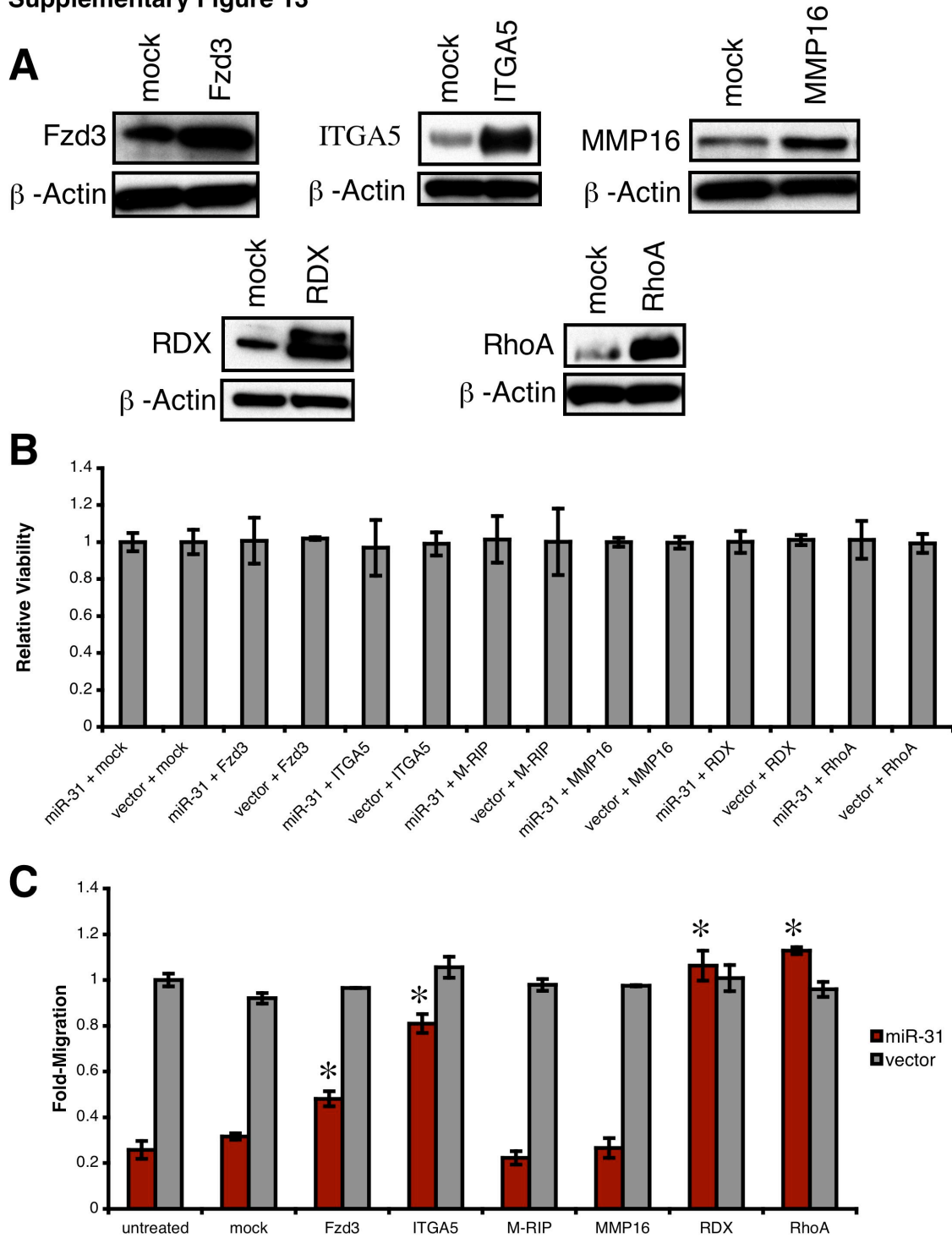
Supplementary Figure 12. Fzd3, ITGA5, RDX, and RhoA are Necessary for MDA-MB-231

Cell Motility. (A) Immunoblots for endogenous Fzd3, ITGA5, MMP16, RDX, and RhoA in

control 231 cells transfected with the indicated siRNAs for 48 hours. _-actin was a loading

control. Knockdown was >75% for all gene-specific siRNAs relative to siControl-treated cells.

(B) Trypan blue stain of 231 cells transfected with the indicated siRNAs for 48 hours. All P-

values are >0.80 relative to mock-treated vector control cells. n = 3. **(C)** Motility assays with

miR-31-expressing or control 231 cells transfected as indicated for 48 hrs. Asterisks: P <0.03

relative to siControl-treated vector control cells. n = 3.
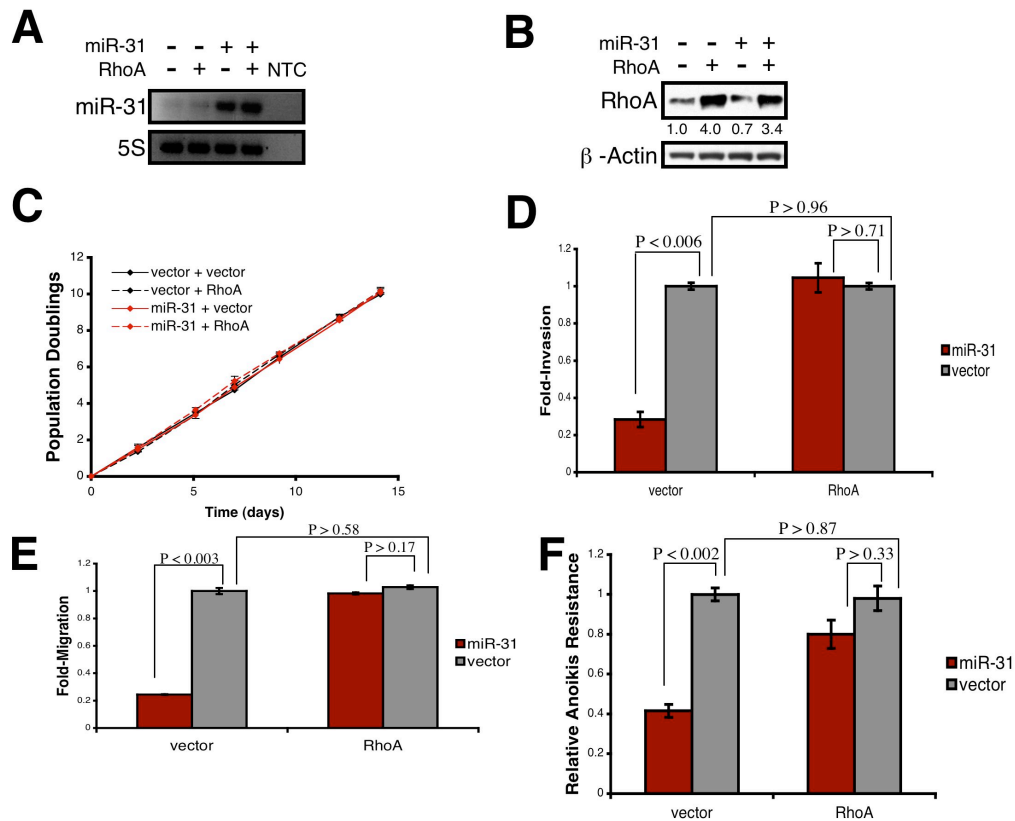
Supplementary Figure 13

Supplementary Figure 13. Restored Expression of Fzd3, ITGA5, RDX, and RhoA Rescues miR-31-Dependent Motility Phenotypes in MDA-MB-231 Cells. (A) Immunoblots for total

Fzd3, ITGA5, MMP16, RDX, and RhoA in 231 cells stably expressing miR-31 and transfected as indicated for 48 hrs. _-actin was a loading control. Overexpression was approximately five-fold for all constructs relative to mock-treated controls. **(B)** Trypan blue stain of miR-31-expressing or control 231 cells transfected as indicated for 24 hrs. All P-values are >0.86 relative to mock-treated vector control cells. n = 3. **(C)** Motility assays using miR-31-expressing or control 231 cells transfected as indicated for 24 hrs. Asterisks: P <0.02 relative to mock-treated miR-31-expressing cells. n = 3.

Supplementary Figure 14. Stable Re-Expression of RhoA Rescues miR-31-Mediated Inhibition of MDA-MB-231 Cell Invasion, Motility, and Anoikis Resistance *in vitro*. (A) RT-PCR for miR-31 in 231 cells infected with RhoA, miR-31, and/or control vectors. 5S rRNA was a loading control. **(B)** Immunoblot for total RhoA in 231 cells infected with RhoA, miR-31, and/or control vectors. _-actin was a loading control. Values: RhoA protein levels relative to vector + vector controls. **(C)** *In vitro* growth curves of 231 cells infected with miR-31, RhoA, and/or vector controls. Triplicate wells from each cohort were counted for 14 days, as indicated. n = 3. **(D)** Invasion assays using 231 cells infected with miR-31, RhoA, and/or control vectors. n = 3. **(E)** Motility assays with 231 cells infected with miR-31, RhoA, and/or vector controls. n = 3. **(F)** Anoikis assay with 231 cells infected as indicated. Cells were cultured in anchorage-independence for 24 hrs, and then viability was assessed via trypan blue staining. n = 3.
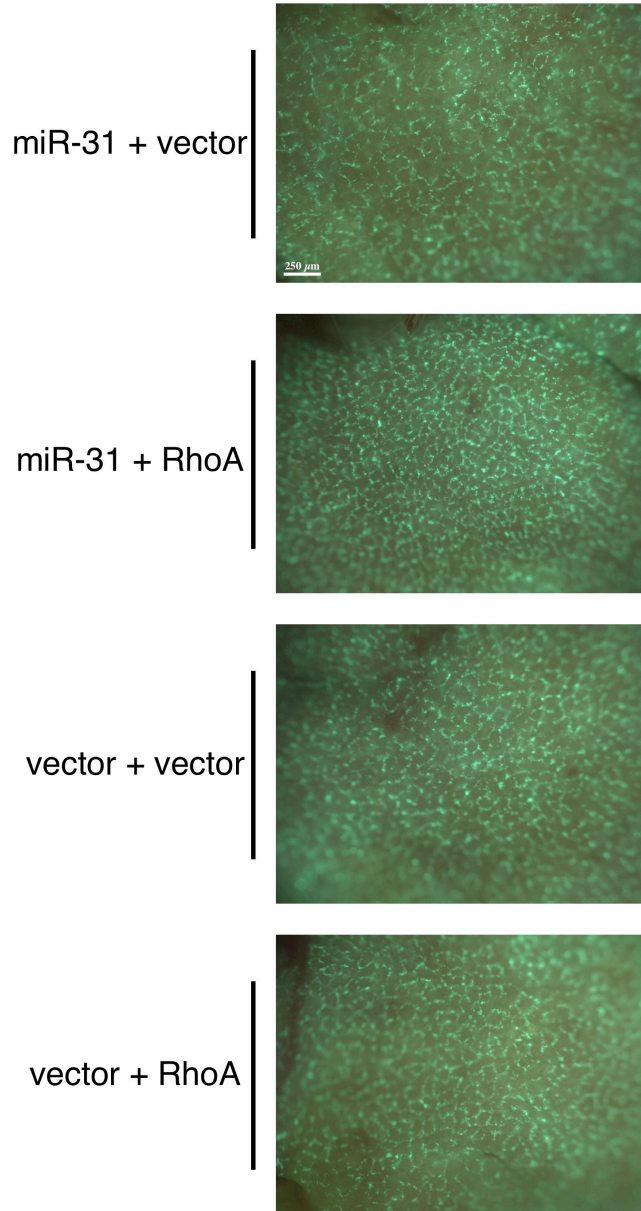
Supplementary Figure 15. miR-31 and RhoA Fail to Affect the Initial Vascular Lodging of Intravenously Injected MDA-MB-231 Cells. Fluorescent images of murine lungs to visualize 231 cells expressing miR-31, RhoA, and/or control vectors 10 minutes subsequent to tail vein injection of 5.0×10^5 GFP-labeled cells.
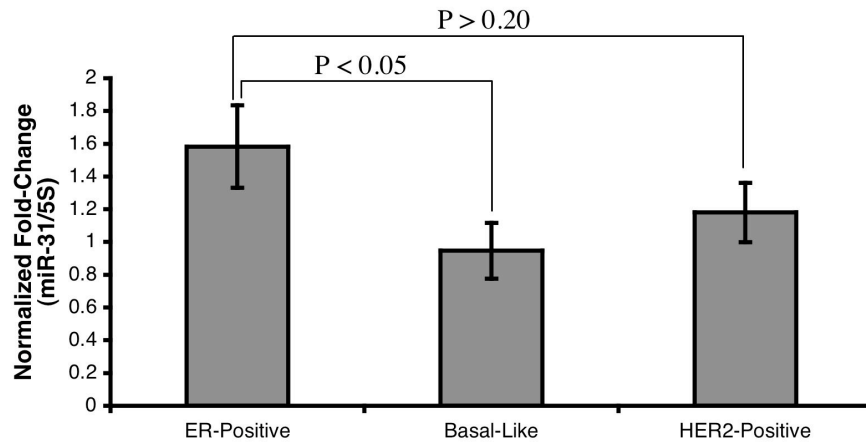
Supplementary Figure 16. miR-31 Levels in Primary Human Breast Tumors Partially Correlate With Molecular Subtype. miR-31 levels in the indicated Grade II and Grade III primary breast tumors, as assessed by RT-PCR. 5S rRNA was a loading control. n = 13 (ER$^+$); n = 19 (basal-like); n = 16 (HER2$^+$).
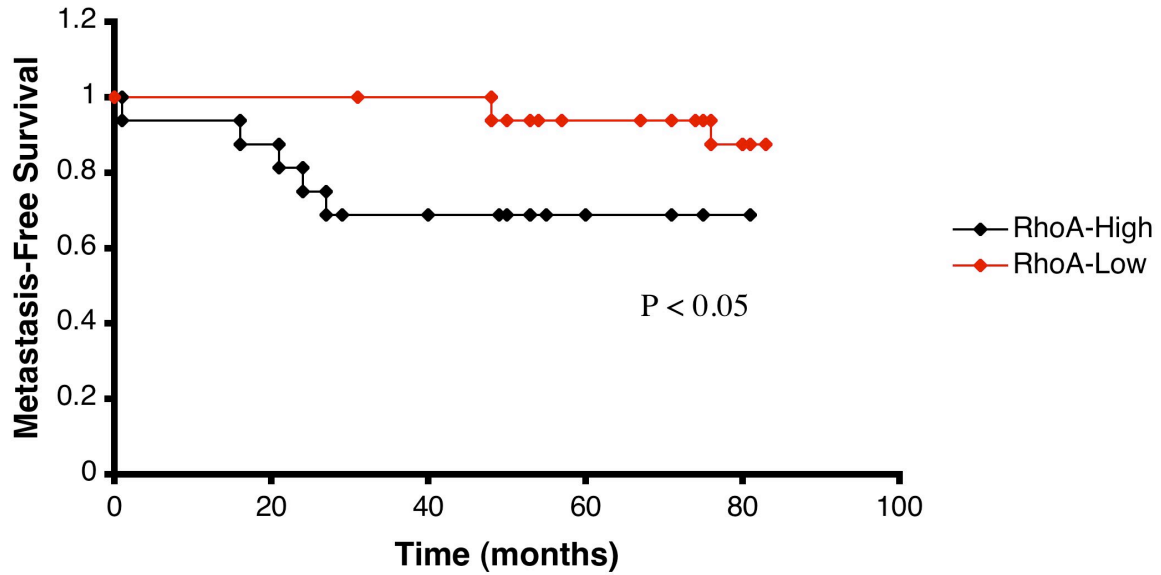
Supplementary Figure 17. RhoA Levels in Human Breast Tumors are Associated With Distant Metastasis. Kaplan-Meier distant metastasis-free survival curves for 54 breast cancer patients, stratified based on RhoA mRNA levels in their primary tumors. P-value based on a logrank test.

A

B
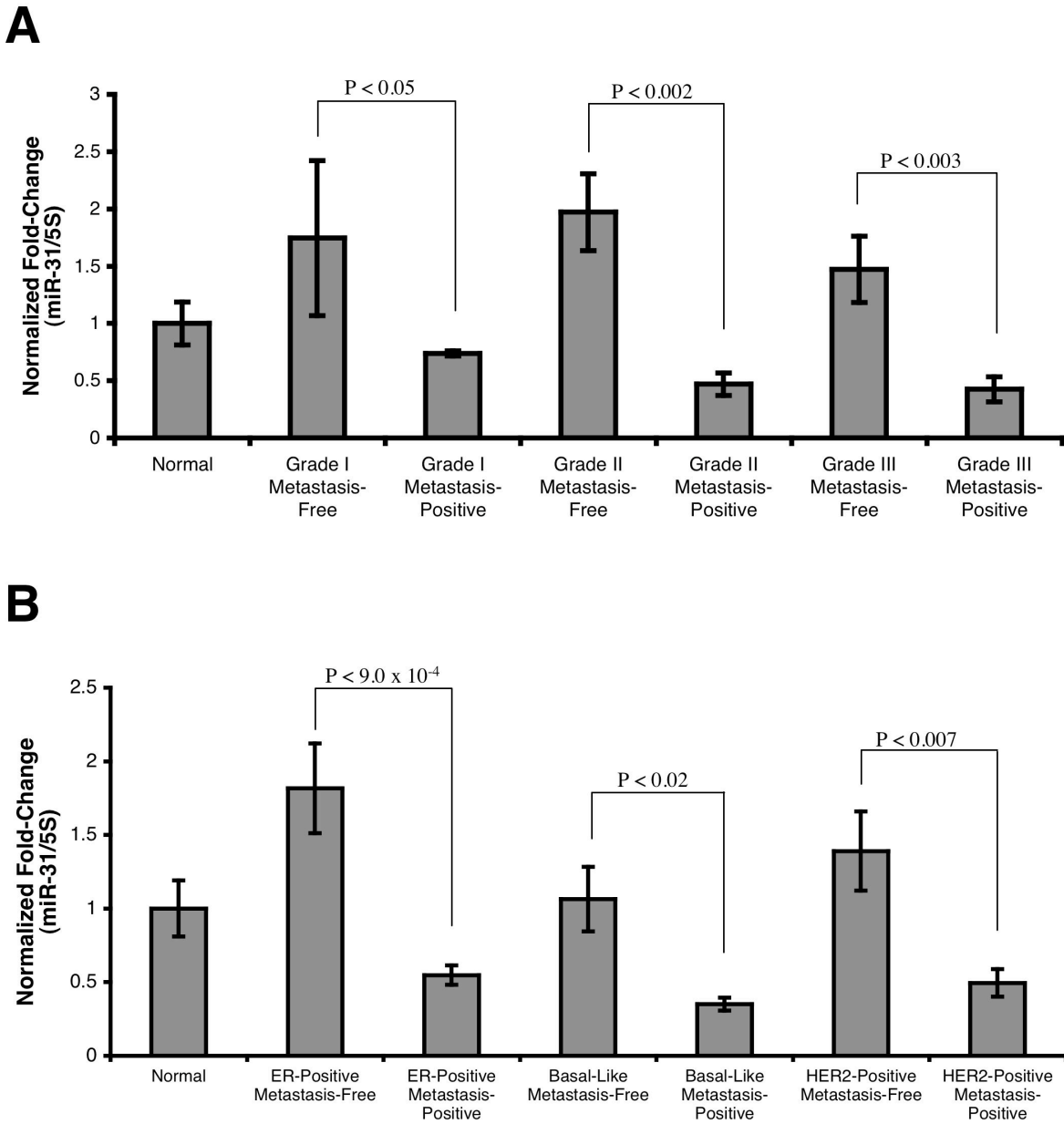
Supplementary Figure 18. miR-31 Expression in Primary Human Breast Carcinomas

Correlates with Metastatic Recurrence Independent of Tumor Grade and Subtype. (A)

miR-31 levels in primary breast tumors of the indicated grade and metastasis status, as assessed

by RT-PCR. 5S rRNA was a loading control. Normal: RNA derived from tissue of non-diseased

individuals; metastasis-positive and -free: RNA from primary tumors of the indicated distant

metastasis outcome. n = 4 (normal); n = 6 (Grade I, metastasis-free); n = 1 (Grade I, metastasis-positive); n = 9 (Grade II, metastasis-free); n = 5 (Grade II, metastasis-positive); n = 25 (Grade III, metastasis-free); n = 9 (Grade III, metastasis-positive). **(B)** RT-PCR for miR-31 in primary breast tumors of the indicated molecular subtype and metastasis status. 5S rRNA was a loading control. Normal: RNA derived from tissue of non-diseased individuals; metastasis-positive and -free: RNA from primary tumors of the indicated distant metastasis outcome. n = 4 (normal); n = 16 (ER-positive, metastasis-free); n = 4 (ER-positive, metastasis-positive); n = 10 (basal-like, metastasis-free); n = 5 (basal-like, metastasis-positive); n = 13 (HER2-positive, metastasis-free); n = 6 (HER2-positive, metastasis-positive).

SUPPLEMENTARY TABLES

Supplementary Table 1. Known Expression Patterns of Candidate miRNAs in Human Breast Tumors

miRNA	Calin et al., 2004	Iorio et al., 2005	Zhang et al., 2006	Volinia et al., 2006
miR-31	downregulated[a]	no change	downregulated	upregulated
miR-100	downregulated	no change	upregulated	no change
miR-101	downregulated	downregulated	downregulated	no change
miR-125b1	downregulated	downregulated	downregulated	downregulated
miR-125b2	downregulated	downregulated	downregulated	downregulated
miR-143	downregulated	downregulated	downregulated	no change
miR-145	downregulated	downregulated	downregulated	downregulated
miR-149	downregulated	downregulated	downregulated	no change
miR-210	downregulated	upregulated	downregulated	upregulated
miR-213	no change	upregulated	upregulated	upregulated

[a]Downregulated, upregulated, and no change refer to expression of the indicated miRNA in primary human breast tumor specimens relative to normal mammary tissue.

Supplementary Table 2. Characteristics of Mammary Epithelial Cell Lines Employed in this Study

Cell Line	Origin	Tumorigenic[a]?	Locally invasive[a]?	Capable of forming micrometastases[a]?	Capable of forming macrometastases[a]?
HMEC	Human; Primary mammary epithelial cells	No	No	No	No
HMLE	Human; Experimentally transformed	No	No	No	No
HMLER	Human; Experimentally transformed	Yes	No	No	No
MCF7-Ras	Human; Pleural effusion	Yes	No	No	No
SUM-149	Human; Primary ductal carcinoma	Yes	No	No	No
SUM-159	Human; Primary carcinoma	Yes	Yes	Yes	No
MDA-MB-231	Human; Pleural effusion	Yes	Yes	Yes	Yes
NMuMG	Murine; Primary mammary epithelial cells	No	No	No	No
D2.OR	Murine; Spontaneously arising carcinoma	Yes	Yes	No	No
D2.1	Murine; Spontaneously arising carcinoma	Yes	Yes	Yes	No
D2A1	Murine; Spontaneously arising carcinoma	Yes	Yes	Yes	Yes
67NR	Murine; Spontaneously arising carcinoma	Yes	No	No	No
168FARN	Murine; Spontaneously arising carcinoma	Yes	Yes	No	No
4TO7	Murine; Spontaneously arising carcinoma	Yes	Yes	Yes	No
4T1	Murine; Spontaneously arising carcinoma	Yes	Yes	Yes	Yes

[a]Upon orthotopic implantation into immune-deficient host mice (human cell lines) or a syngenic background (murine cell lines).

Supplementary Table 3. Site-Specific Mutation of miR-31 Binding Sites in 3' UTR Reporter Constructs

3' UTR	Wild Type Sequence	Mutagenized Sequence
Fzd3	TCTTGCCA	TC**GGCG**CA
ITGA5	CTTGCCA	C**AAAAG**A
M-RIP	ATCTTGC	ATC**GGCG**
MMP16	CTTGCCA	C**AAACAG**
RDX	CTTGCCA	**TCCA**CCA
RhoA (site 1)[a]	ATCTTGC	**GGTAG**GC
RhoA (site 2)[b]	TCTTGC	**CGCC**GC

[a]The miR-31 motif at nucleotides 145-151 of the human RhoA 3' UTR. [b]The miR-31 motif spanning nucleotides 303-309 of the RhoA 3' UTR. Red: nucleotides altered in the mutagenized reporter constructs.

Supplementary Table 4. Fold-Change Values in 295 Human Breast Tumors (van de Vijver et al., 2002)

Gene	Fold-Change (Range)	Fold-Change (Quartile$_3$ – Quartile$_1$)	Fold-Change (Target Signature-Positive vs. Signature-Negative)
Fzd3	7.21	1.62	2.75
ITGA5	11.56	1.61	3.38
M-RIP	8.24	1.37	2.32
MMP16	14.15	1.28	2.54
RDX	13.18	1.62	3.75
RhoA	5.7	1.43	2.39

Supplementary Table 5. Annotation of Clinical Breast Tumor Specimens

#	Age[a]	Histological Subtype	Molecular Subtype	Grade	ER	PR	HER2	LN Status	Metastatic Recurrence?	Sites of Metastasis
1	54	D	HER	II	n	n	p	n	No	None
2	57	D	HER	II	n	n	p	p	Yes	Viscera
3	85	D	HER	II	n	n	p	U	Yes	Pleura
4	63	D	HER	III	n	n	p	p	No	None
5	41	D	HER	III	n	n	p	n	No	None
6	44	D	HER	III	n	n	n	n	No	None
7	37	D	HER	III	n	n	p	n	No	None
8	55	D	HER	III	n	n	p	p	No	None
9	42	D	HER	III	p	n	p	p	No	None
10	45	D	HER	III	n	n	p	n	No	None
11	47	D	HER	III	p	p	p	p	No	None
12	56	D	HER	III	n	n	p	n	No	None
13	49	D	HER	III	p	p	p	n	No	None
14	53	D	HER	III	n	n	p	p	Yes	Viscera
15	45	D	HER	III	n	n	p	p	Yes	Viscera
16	62	D	ERLG	I	p	p	n	n	No	None
17	40	D	ERLG	I	p	n	n	p	No	None
18	37	D	ERHG	I	p	p	n	p	No	None
19	30	D	ERHG	II	p	p	p	p	No	None
20	37	D	ERHG	II	p	p	n	p	No	None
21	74	D	ERHG	II	n	n	n	n	No	None
22	64	D	ERHG	III	p	p	p	n	No	None
23	57	D	ERHG	III	p	p	lp	p	No	None
24	78	D	ERHG	III	p	p	n	p	No	None
25	55	D	ERHG	III	p	p	n	p	Yes	Bone only
26	57	D	Basal	II	n	n	n	n	No	None
27	41	D	Basal	III	n	n	n	n	No	None
28	40	D	Basal	III	n	n	n	n	No	None
29	49	D	Basal	III	n	n	p	n	No	None
30	78	D	Basal	III	n	n	n	n	No	None
31	48	D	Basal	III	n	n	n	n	No	None
32	48	D	Basal	III	n	n	n	n	No	None
33	65	D	Basal	III	n	n	n	n	No	None
34	U	D	Basal	III	n	n	n	n	No	None
35	79	D	Basal	III	n	n	n	n	Yes	Bone only
36	42	D	Basal	III	n	n	n	p	Yes	Viscera
37	43	D	Basal	III	n	n	n	n	Yes	Viscera
38	53	D	Basal	III	n	n	n	n	Yes	Viscera
39	64	D	Basal	III	n	n	n	n	Yes	Viscera
40	72	D	U	III	n	n	n	n	U	U
41	71	L	HER	III	p	p	p	p	No	None
42	62	L	ERLG	I	p	p	n	n	No	None
43	81	L	ERLG	I	p	pl	n	p	No	None
44	62	L	ERLG	I	p	p	n	n	No	None
45	45	L	ERLG	II	p	p	n	p	No	None
46	45	L	ERLG	II	p	p	n	n	No	None

47	60	L	ERHG	I	p	n	n	p	Yes	Bone only
48	46	L	ERHG	III	p	p	lp	p	No	None
49	32	M	HER	II	p	p	p	p	No	None
50	44	M	HER	II	p	pl	p	p	Yes	Viscera
51	44	M	HER	II	p	p	p	p	Yes	Viscera
52	46	M	ERLG	II	p	p	n	p	Yes	Bone only
53	58	M	ERHG	II	p	p	n	p	No	None
54	38	M	ERHG	III	pl	pl	n	p	Yes	Viscera
55	48	M	Basal	III	p	p	n	p	No	None
56	68	M	Basal	III	n	n	p	p	No	None

[a]At time of initial presentation. ER = Estrogen receptor; PR = Progesterone receptor; LN = lymph node; U = Unknown; D = Ductal; L = Lobular; M = Mixed type; ERLG = ER-positive low-grade; ERHG = ER-positive high-grade; p = positive; n = negative; pl = positive-low; lp = low-positive.

ACKNOWLEDGMENTS

REFERENCES

Asangani IA, Rasheed SA, Nikolova DA, et al. (2008). MicroRNA-21 post-transcriptionally downregulates tumor suppressor Pdcd4 and stimulates invasion, intravasation and metastasis in colorectal cancer. Oncogene *27*, 2128-2136.

Ashburner M, Ball CA, Blake JA, et al. (2000). Gene ontology: tool for the unification of biology. Nat Genet *25*, 25-29.

Aslakson CJ and Miller FR. (1992). Selective events in the metastatic process defined by analysis of the sequential dissemination of subpopulations of a mouse mammary tumor. Cancer Res. *52*, 1399-1405.

Bartel DP. (2009). MicroRNAs: target recognition and regulatory functions. Cell *136*, 215-233.

Batchelor CL, Woodward AM, and Crouch DH. (2004). Nuclear ERM (ezrin, radixin, moesin) proteins: regulation by cell density and nuclear import. Exp Cell Res *296*, 208-222.

Calin GA and Croce CM. (2006). MicroRNA signatures in human cancers. Nat Rev Cancer *6*, 857-866.

Calin GA, Sevignani C, Dumitru CD, et al. (2004). Human microRNA genes are frequently located at fragile sites and genomic regions involved in cancers. Proc Natl Acad Sci USA *101*, 2999-3004.

Deardorff MA, Tan C, Saint-Jeannet JP, and Klein PS. (2001). A role for frizzled 3 in neural crest development. Development *128*, 3655-3663.

Desmedt C, Haibe-Kains B, Wirapati P, et al. (2008). Biological processes associated with breast cancer clinical outcome depend on the molecular subtypes. Clin Cancer Res. *14*, 5158-5165.

Ebert MS, Neilson JR, and Sharp PA. (2007). MicroRNA sponges: competitive inhibitors of small RNAs in mammalian cells. Nat Methods *4*, 721-726.

Elenbaas B, Spirio L, Koerner F, et al. (2001). Human breast cancer cells generated by oncogenic transformation of primary mammary epithelial cells. Genes Dev *15*, 50-65.

Farh KK, Grimson A, Jan C, et al. (2005). The widespread impact of mammalian MicroRNAs on mRNA repression and evolution. Science *310*, 1817-1821.

Fidler IJ. (2003). The pathogenesis of cancer metastasis: the 'seed and soil' hypothesis revisited. Nat Rev Cancer *3*, 453-458.

Grimson A, Farh KK, Johnston WK, Garrett-Engele P, Lim LP, and Bartel DP. (2007). MicroRNA targeting specificity in mammals: determinants beyond seed pairing. Mol Cell *27*, 91-105.

Gupta GP and Massagué J. (2006). Cancer metastasis: building a framework. Cell *127*, 679-695.

Hotary K, Li XY, Allen E, Stevens SL, and Weiss SJ. (2006). A cancer cell metalloprotease triad regulates the basement membrane transmigration program. Genes Dev *20*, 2673-2686.

Huang Q, Gumireddy K, Schrier M, et al. (2008). The microRNAs miR-373 and miR-520c promote tumour invasion and metastasis. Nat Cell Biol *10*, 202-210.

Iorio MV, Ferracin M, Liu CG, et al. (2005). MicroRNA gene expression deregulation in human breast cancer. Cancer Res. *65*, 7065-7070.

Kondo N, Toyama T, Sugiura H, Fujii Y, and Yamashita H. (2008). miR-206 Expression is down-regulated in estrogen receptor _-positive human breast cancer. Cancer Res. *68*, 5004-5008.

Krek A, Grün D, Poy MN, et al. (2005). Combinatorial microRNA target predictions. Nat Genet *37*, 495-500.

Krützfeldt J, Poy MN, and Stoffel M. (2006). Strategies to determine the biological function of microRNAs. Nat Genet *38*, S14-S19.

Kuwada SK and Li X. (2000). Integrin alpha5/beta1 mediates fibronectin-dependent epithelial cell proliferation through epidermal growth factor receptor activation. Mol Biol Cell *11*, 2485-2496.

Lujambio A, Calin GA, Villanueva A, et al. (2008). A microRNA DNA methylation signature for human cancer metastasis. Proc Natl Acad Sci USA *105*, 13556-13561.

Ma L, Teruya-Feldstein J, and Weinberg RA. (2007). Tumour invasion and metastasis initiated by microRNA-10b in breast cancer. Nature *449*, 682-688.

McClatchey AI. (2003). Merlin and ERM proteins: unappreciated roles in cancer development? Nat Rev Cancer *3*, 877-883.

Minn AJ, Kang Y, Serganova I, et al (2005). Distinct organ-specific metastatic potential of individual breast cancer cells and primary tumors. J Clin Invest *115*, 44-55.

Morgenstern JP and Land H. (1990). Advanced mammalian gene transfer: high titre retroviral vectors with multiple drug selection markers and a complementary helper-free packaging cell line. Nucleic Acids Res *18*, 3587-3596.

Morris VL, Tuck AB, Wilson SM, Percy D, and Chambers AF. (1993). Tumor progression and metastasis in murine D2 hyperplastic alveolar nodule mammary tumor cell lines. Clin Exp Metastasis *11*, 103-112.

Sahai E and Marshall CJ. (2002). Rho-GTPases and cancer. Nat Rev Cancer *2*, 133-142.

Sathyan P, Golden HB, and Miranda RC. (2007). Competing interactions between micro-RNAs determine neural progenitor survival and proliferation after ethanol exposure. J Neurosci. *27*, 8546-8557.

Si ML, Zhu S, Wu H, Lu Z, Wu F, and Mo, YY. (2007). miR-21-mediated tumor growth. Oncogene *26*, 2799-2803.

Silahtaroglu AN, Nolting D, Dyrskjøt L, et al. (2007). Detection of microRNAs in frozen tissue sections by fluorescence in situ hybridization using LNA probes and tyramide signal amplification. Nat Protoc *2*, 2520-2528.

Sørlie T, Perou CM, Tibshirani R, et al. (2001). Gene expression patterns of breast carcinomas distinguish tumor subclasses with clinical implications. Proc Natl Acad Sci USA *98*, 10869-10874.

Subauste MC, Von Herrath M, Benard V, et al. (2000). Rho family proteins modulate rapid apoptosis induced by cytotoxic T lymphocytes and Fas. J Biol Chem *275*, 9725-9733.

Surks HK, Richards CT, and Mendelsohn ME. (2003). Myosin phosphatase-Rho interacting protein. A new member of the myosin phosphatase complex that directly binds RhoA. J Biol Chem *27*, 51484-51493.

Tavazoie SF, Alarcón C, Oskarsson T, et al. (2008). Endogenous human microRNAs that suppress breast cancer metastasis. Nature *451*, 147-152.

van de Vijver MJ, He YD, van't Veer LJ, et al. (2002). A gene-expression signature as a predictor of survival in breast cancer. N Engl J Med *347*, 1999-2009.

Ventura A and Jacks T. (2009). MicroRNAs and cancer: short RNAs go a long way. Cell *136*, 586-591.

Volinia S, Calin GA, Liu CG, et al. (2006). A microRNA expression signature of human solid tumors defines cancer gene targets. Proc Natl Acad Sci USA *103*, 2257-2261.

Voorhoeve PM, le Sage C, Schrier M, et al. (2006). A genetic screen implicates miRNA-372 and miRNA-373 as oncogenes in testicular germ cell tumors. Cell *124*, 1169-1181.

Zhang L, Huang J, Yang N, et al. (2006). microRNAs exhibit high frequency genomic alterations in human cancer. Proc Natl Acad Sci USA *103*, 9136-9141.

Zhu S, Wu H, Wu F, et al. (2008). MicroRNA-21 targets tumor suppressor genes in invasion and metastasis. Cell Res *18*, 350-359.

Chapter 3

Concomitant Suppression of Three Target Genes Can Explain the Impact of a MicroRNA on Metastasis

Scott Valastyan[1,2], Nathan Benaich[1,3], Amelia Chang[1,2], Ferenc Reinhardt[1], and Robert A. Weinberg[1,2,4]

[1]Whitehead Institute for Biomedical Research, Cambridge, MA 02142, USA
[2]Department of Biology, Massachusetts Institute of Technology, Cambridge, MA 02139, USA
[3]Department of Biology, Williams College, Williamstown, MA 01267, USA
[4]MIT Ludwig Center for Molecular Oncology, Cambridge, MA 02139, USA

This chapter is excerpted from the following publication (copyright permissions obtained):

N. Benaich is a Williams College summer student who assisted with several experiments. A. Chang is an MIT undergraduate who assisted with several experiments. F. Reinhardt provided technical assistance for the mouse studies. R.A. Weinberg supervised the research and assisted with the writing of the manuscript. All other experiments, data analysis, and writing were carried out by the thesis author, S. Valastyan.

<u>INTRODUCTION</u>

As described in Chapter One, microRNAs (miRNAs) are an evolutionarily conserved

family of regulatory RNAs that inhibit their mRNA targets post-transcriptionally, leading to

modulation of diverse biological processes including the development and progression of cancer

(Ambros, 2004; Bartel, 2009; Ventura and Jacks, 2009). An individual miRNA is capable of

regulating dozens of distinct mRNAs (Selbach et al., 2008; Baek et al., 2008), and it is thought

that pleiotropic suppression of multiple downstream effectors may underlie the phenotypic

changes observed upon perturbing the levels of certain miRNAs (Zhao et al., 2007; van Rooij et

al., 2007; Thai et al., 2007; Rodriguez et al., 2007; Johnnidis et al., 2008; Ventura et al., 2008). It

remains unclear, however, whether these consequences depend on simultaneous deregulation of

the entire repertoire of targets of a given miRNA or instead the altered activity of only a small

subset of effectors.

Metastases, which are responsible for 90% of human cancer deaths, arise via a complex

series of events, collectively termed the invasion-metastasis cascade (Fidler, 2003; Gupta and

Massagué, 2006), as has been previously outlined in Chapter One. In order to metastasize, cells

in a primary tumor must become motile, degrade surrounding extracellular matrix (local

invasion), intravasate into the vasculature, retain viability during transit through the circulation,

extravasate into the parenchyma of a distant tissue, survive in this foreign microenvironment to

form micrometastases, and finally thrive in their new milieu and establish macroscopic

secondary tumors (colonization) (Fidler, 2003). Colonization is the rate-limiting step of the

invasion-metastasis cascade, yet the molecular underpinnings of this process are poorly

understood (Gupta and Massagué, 2006).

As described in Chapter Two, I recently determined that expression of the miRNA miR-31 was both necessary and sufficient to inhibit the metastasis of human breast cancer xenografts, and that miR-31 levels correlated inversely with metastatic relapse in breast carcinoma patients (Valastyan et al., 2009). I attributed these effects to miR-31's ability to pleiotropically suppress a cohort of pro-metastatic targets; however, I did not identify a minimal set of downstream effectors whose concomitant re-expression is sufficient to fully override miR-31's influences on metastasis. For this reason, I undertook to determine whether the impact of miR-31 on metastasis could be explained by its ability to pleiotropically modulate a defined subset of its >200 predicted targets.

RESULTS

Individual Suppression of ITGA5, RDX, or RhoA Impairs Metastasis-Relevant Traits *in vitro* and Metastatic Capacity *in vivo*

I previously demonstrated that miR-31 regulates six mRNAs that encode proteins with roles in cell motility and tumor progression: frizzled3 (Fzd3), integrin-_5 (ITGA5), matrix metallopeptidase 16 (MMP16), myosin phosphatase-Rho interacting protein (M-RIP), radixin (RDX), and RhoA (Valastyan et al., 2009). To begin to address whether miR-31-imposed inhibition of one or more of these effectors might be responsible for mediating miR-31's anti-metastatic influences, I stably suppressed these six mRNAs individually in otherwise-metastatic MDA-MB-231 human breast cancer cells ("231 cells") using short hairpin RNAs (shRNAs). 231 cells are largely devoid of endogenous miR-31 and robustly express these six effectors; moreover, ectopic miR-31 impairs metastasis by these cells (Valastyan et al., 2009).

For each gene, I derived multiple cell lines that stably expressed a distinct shRNA targeting unique sequences in the encoded mRNA in order to minimize confounding influences from shRNA off-target effects (Supplementary Figures 1A and 2A). At least one shRNA against each of the six effectors reduced its target's level by a factor comparable to that elicited by miR-31 expression (Valastyan et al., 2009). This allowed me to reasonably approximate the consequences of miR-31's actions on each individual downstream effector.

These shRNA-expressing 231 cells were subjected to *in vitro* assays that model traits important for metastasis. I observed that individual suppression of ITGA5, RDX, or RhoA reduced invasion, motility, and resistance to anoikis-mediated cell death *in vitro*; in contrast, the Fzd3, MMP16, or M-RIP shRNAs failed to substantially affect these behaviors (Supplementary Figures 1B-1D and 2B-2D). For shRNAs that conferred measurable responses, the magnitude of these responses was directly correlated with the extent of knock-down achieved, suggesting that these effects arose as a specific consequence of reduced levels of the targeted protein. Inhibition of Fzd3, ITGA5, MMP16, M-RIP, RDX, or RhoA failed to affect *in vitro* proliferation (Supplementary Figures 1E and 2E). Also, the responses evoked by the ITGA5, RDX, and RhoA shRNAs could not be ascribed to saturation of the miRNA biogenesis machinery, as mature levels of eight control miRNAs were unaffected in these cells (Supplementary Figure 3).

I determined whether suppression of these six mRNAs altered metastatic capacity *in vivo* by intravenously injecting the shRNA-expressing 231 cells into mice. One month later, cells bearing shRNAs targeting ITGA5, RDX, or RhoA had generated 80%, 85%, and 55% fewer lung metastases than controls, respectively; however, downregulation of Fzd3, MMP16, or M-RIP did not affect the number of metastases spawned (Supplementary Figure 4). Thus, inhibition of

ITGA5, RDX, or RhoA – but not Fzd3, MMP16, or M-RIP – affects *in vitro* surrogates of metastatic capacity as well as *in vivo* metastasis.

Individual Re-Expression of ITGA5, RDX, or RhoA Partially Reverses miR-31-Imposed Metastasis Defects *in vivo*

To extend these analyses, I stably re-expressed miRNA-insensitive versions of the mRNAs encoding Fzd3, ITGA5, MMP16, M-RIP, RDX, or RhoA individually in 231 cells that already expressed either miR-31 or control vector (Supplementary Figure 5A). This allowed me to gauge the ability of each of these effectors – when re-expressed – to reverse miR-31's impact on *in vivo* metastasis. When introduced into the venous circulation of mice, miR-31-expressing cells formed 85% fewer lung metastases than controls one month post-injection (Supplementary Figure 5B), consistent with my prior findings (Valastyan et al., 2009). Individual re-expression of ITGA5, RDX, or RhoA restored the number of lung metastases in miR-31-expressing cells to 55%, 50%, and 65% of control levels, respectively; in contrast, Fzd3, MMP16, or M-RIP failed to increase lesion number (Supplementary Figure 5B). Overexpression of ITGA5, RDX, or RhoA did not further enhance metastasis in control 231 cells (Supplementary Figure 5B), suggesting that signaling from these pathways was already saturated in 231 cells, as has previously been established for RhoA-controlled networks (Pillé et al., 2005). Together, these findings implied that although miR-31 is capable of suppressing numerous mRNA species, its ability to regulate only a subset of these effectors appears to be crucial for its capacity to impair metastasis.

In support of this notion, when stably re-expressed in 231 cells, Fzd3, MMP16, or M-RIP failed to reverse miR-31-imposed attenuation of invasion, motility, and anoikis resistance *in vitro*

(Supplementary Figure 6); in contrast, my prior work revealed that restored levels of ITGA5, RDX, or RhoA rescued, at least partially, miR-31-evoked defects in these phenotypes (Valastyan et al., 2009). Based on these *in vitro* and *in vivo* re-expression data, as well as the above-described *in vitro* and *in vivo* loss-of-function findings, I focused my subsequent analyses on the ability of inhibition of ITGA5, RDX, and RhoA to account for miR-31's anti-metastatic activities.

Individual Suppression of ITGA5, RDX, or RhoA Impairs Metastasis, But Fails to Phenocopy the Full Spectrum of miR-31's Anti-Metastatic Activities *in vivo*

To this end, I investigated the consequences of suppressing ITGA5, RDX, or RhoA individually in an orthotopic injection assay. Accordingly, I implanted 231 cells expressing shRNAs targeting either ITGA5, RDX, or RhoA into the mammary fat pads of mice. Suppression of ITGA5 or RhoA did not affect primary tumor growth; conversely, inhibition of RDX reduced the size of resulting mammary tumors (Figure 1A). After normalizing for differences in primary tumor growth, cells expressing shRNAs against ITGA5, RDX, or RhoA formed 85%, 70%, and 50% fewer lung metastases than controls 2.5 months after injection, respectively (Figure 1B). Thus, inhibition of ITGA5, RDX, or RhoA each impedes metastasis; however, this assay did not reveal the particular step(s) of the invasion-metastasis cascade that were impaired due to suppression of ITGA5, RDX, or RhoA.

In my previous work, I observed that miR-31 impinges upon three steps of the invasion-metastasis cascade *in vivo*: local invasion, early post-intravasation events (intraluminal viability, extravasation, and/or initial survival in distant tissues), and colonization (Valastyan et al., 2009). Consequently, I evaluated whether the individual suppression of ITGA5, RDX, or RhoA was

sufficient to recapitulate one or more of miR-31's multiple effects on the metastatic process. I found that 231 cells containing shRNAs against either ITGA5, RDX, or RhoA formed primary tumors that appeared histologically invasive and were indistinguishable from controls (Figure 1C). Thus, inhibition of ITGA5, RDX, or RhoA alone does not abolish local invasion *in vivo*.

Putative effects on early post-intravasation events were examined by quantifying shRNA-expressing 231 cells in the lungs one day after intravenous injection. Cells with either suppressed ITGA5 or RhoA were 40% and 30% less prevalent than controls, respectively; however, RDX knock-down did not reduce persistence in the lungs (Figure 1D). These effects were not attributable to a differential ability of the cells to become lodged initially in the lung microvasculature, as equal numbers of cells were detected in the lungs 10 minutes after intravenous injection (Supplementary Figure 7). These data indicated that inhibition of either ITGA5 or RhoA impairs early post-intravasation events *in vivo*.

To investigate potential effects on colonization (i.e., the capacity of disseminated single cells to yield large, multi-cellular metastases), the sizes of lung metastases in intravenously injected animals was analyzed three months after implantation. 231 cells expressing either ITGA5 or RDX shRNAs formed only small micrometastases, while RhoA shRNA-containing cells generated macroscopic metastases comparable to those spawned by control cells (Figure 1E). Hence, suppression of either ITGA5 or RDX alone prevents colonization *in vivo*.

Together, these observations revealed that while individual suppression of ITGA5, RDX, or RhoA impairs one or more steps of the invasion-metastasis cascade, inhibition of any one of these proteins alone is unable to phenocopy the full spectrum of miR-31's impact on metastasis. This suggested that miR-31 may achieve its influences on multiple distinct stages of the metastatic process via concomitant suppression of several downstream effectors. Provocatively,

my loss-of-function analyses indicated that ITGA5, RDX, and RhoA act during at least partially distinct steps of the invasion-metastasis cascade (e.g., RhoA affected early post-intravasation events but not colonization, while RDX had no impact on early post-intravasation events but altered colonization); hence, their concurrent regulation provides a plausible mechanism by which miR-31 might elicit its multiple anti-metastatic effects.

Simultaneous Re-Expression of ITGA5, RDX, and RhoA Abrogates miR-31-Imposed Metastasis Suppression *in vivo*

To test this hypothesis, I stably re-expressed miRNA-insensitive mRNAs encoding ITGA5, RDX, and RhoA together in combination – along with either miR-31 or control vector – in 231 cells. When these cells were orthotopically injected into mice, miR-31 enhanced primary tumor growth, recapitulating my prior findings (Valastyan et al., 2009); simultaneous re-expression of ITGA5, RDX, and RhoA failed to alter the size of miR-31-containing or control primary tumors (Figure 2A). Despite their ability to generate larger primary tumors, miR-31-expressing 231 cells were impaired by >80% in their ability to spawn lung metastases (Figure 2B). ITGA5, RDX, and RhoA did not enhance metastasis in control 231 cells; however, concomitant re-expression of ITGA5, RDX, and RhoA in 231 cells containing miR-31 completely abrogated miR-31-imposed metastasis suppression (Figure 2B). These data implied that the impact of miR-31 on *in vivo* metastasis can be explained by miR-31's capacity to inhibit a cohort of three downstream effectors. This was quite surprising, as computational algorithms predict that miR-31 regulates >200 mRNAs, many of which encode proteins that function in metastasis-relevant processes (Krek et al., 2005; Grimson et al., 2007).

131

Re-Expression of ITGA5, RDX, and/or RhoA Affords Both Unique and Partially

Overlapping Reversal of miR-31-Evoked Inhibition of Spontaneous Metastasis *in vivo*

Since the combined re-expression of ITGA5, RDX, and RhoA entirely abolished miR-31-evoked metastasis suppression, I also determined whether these three effectors were able to reverse a subset of miR-31's influences on metastasis when re-expressed either individually or in different combinations. Thus, I created 231 cells stably expressing miR-31 or control vector plus all possible permutations of zero, one, two, or three of these miR-31 targets (all rendered miRNA-resistant) (Supplementary Figure 8). miR-31, ITGA5, RDX, and RhoA failed to affect cell proliferation *in vitro* (Supplementary Figure 9A). However, individual re-expression of ITGA5, RDX, or RhoA rescued, at least partially, *in vitro* defects in invasion, motility, and anoikis resistance conferred by ectopic miR-31; the extent of reversal was more pronounced when multiple effectors were re-expressed in combination (Supplementary Figures 9B-9D).Thus, ITGA5, RDX, and RhoA control *in vitro* behaviors important for metastasis downstream of miR-31.

To assay the respective abilities of all possible combinations of re-expressed ITGA5, RDX, and/or RhoA to reverse miR-31's influences on *in vivo* metastasis, 231 cells expressing miR-31, ITGA5, RDX, and/or RhoA were orthotopically implanted into mice. miR-31 generally promoted primary tumor growth, while restored levels of ITGA5, RDX, and RhoA failed to consistently affect the growth of primary tumors (Figure 3A and Supplementary Table 1). miR-31 reduced the incidence of metastatic lesions in the lungs by >90% (Figure 3B). When individually re-expressed in miR-31-containing cells, ITGA5, RDX, or RhoA increased metastasis to 40%, 45%, and 65% of control levels, respectively; re-expression of any two of these targets in miR-31-positive cells yielded 85% as many metastases as controls (Figure 3B).

As before, concomitant re-expression of ITGA5, RDX, and RhoA in cells containing miR-31 restored the number of lung metastases to 100% of that observed in controls (Figure 3B). Hence, these three effectors make distinct contributions to *in vivo* metastasis that can collaborate to explain miR-31's influence on this process; however, these observations failed to delineate the specific step(s) of the invasion-metastasis cascade affected by various combinations of re-expressed ITGA5, RDX, and/or RhoA.

miR-31 affects three steps of the invasion-metastasis cascade *in vivo*: local invasion, early post-intravasation events, and colonization (Valastyan et al., 2009). To investigate whether ITGA5, RDX, and RhoA – when overexpressed – could synergize to reverse miR-31's effects on local invasion, I examined the histological appearance of primary tumors that developed in orthotopically injected mice. Whereas control 231 cell tumors displayed clear evidence of invasion, miR-31-expressing tumors were well-confined (Figure 3C), as I previously documented (Valastyan et al., 2009). While ITGA5, RDX, and RhoA did not alter invasion in control 231 cell tumors, combined re-expression of these three targets abolished the previously well-encapsulated phenotype of miR-31-expressing tumors (Figure 3C). miR-31-containing cells with restored levels of either RDX or RhoA alone formed primary tumors that appeared invasive, though reversal of miR-31-imposed invasion defects was incomplete; ITGA5 did not affect encapsulation (Figure 3C). These observations revealed that miR-31-dependent attenuation of local invasion can be attributed to miR-31's ability to regulate RDX and RhoA. Ostensibly, in light of my shRNA studies (Figure 1C), RDX and RhoA function redundantly – either with one another or with additional, still-unidentified miR-31 targets – to promote invasion *in vivo*.

Re-Expression of ITGA5, RDX, and/or RhoA Affords Both Unique and Partially

Overlapping Reversal of miR-31-Mediated Inhibition of Experimental Metastasis *in vivo*

I also examined whether re-expression of these three targets could reverse the impact of miR-31 on early post-intravasation events. To do so, I introduced 231 cells into the venous circulation of mice and assayed the number of cells in the lungs one day after injection. Consistent with my previous findings (Valastyan et al., 2009), miR-31-expressing cells were five-fold impaired in their ability to persist in the lungs (Figure 4A), indicating that miR-31 impeded one or more early post-intravasation events. ITGA5, RDX, and RhoA failed to affect early post-intravasation events in control 231 cells (Figure 4A). In contrast, individual re-expression of either ITGA5 or RhoA restored the number of miR-31-expressing cells in the lungs to 50% of control levels; RDX did not augment the ability of cells containing miR-31 to persist in the lungs at this timepoint (Figure 4A). Simultaneous re-introduction of ITGA5 and RhoA in miR-31-expressing cells sufficed to completely override miR-31-imposed obstruction of early post-intravasation events (Figure 4A). These effects were not a consequence of an altered ability of ITGA5-, RDX-, RhoA-, and/or miR-31-expressing cells to become lodged initially in the lung microvasculature, as equal numbers of cells were detected in the lungs 10 minutes after intravenous injection (Supplementary Figure 10). These data provided evidence that miR-31-evoked suppression of early post-intravasation events can be ascribed to miR-31's ability to modulate ITGA5 and RhoA.

Three months after intravenous injection, control 231 cells generated large macroscopic metastases while miR-31-expressing cells yielded only small micrometastases (Figure 4B). Hence, miR-31 prevented disseminated tumor cells from re-initiating their proliferative program at the site of metastasis, in consonance with miR-31's reported influence on colonization

(Valastyan et al., 2009). Concomitant re-expression of ITGA5, RDX, and RhoA in miR-31-containing cells abrogated miR-31-imposed suppression of colonization, yet overexpression of these three targets in control 231 cells failed to increase lesion size (Figure 4B). Individually restored levels of either ITGA5 or RDX in miR-31-expressing cells reversed miR-31's effects on colonization; RhoA did not affect this parameter (Figure 4B). Thus, the ability of miR-31 to inhibit colonization can derive from its capacity to suppress ITGA5 and RDX.

In this same assay, miR-31-expressing 231 cells formed 20-fold fewer lung metastases than controls (Figure 4C). When individually re-expressed in miR-31-containing cells, ITGA5, RDX, or RhoA increased the number of metastases formed to 60%, 60%, and 50% of control levels, respectively (Figure 4C). Restored levels of pairwise combinations of these three targets in miR-31-expressing cells enhanced lesion number to >70% of controls; importantly, simultaneous re-expression of ITGA5, RDX, and RhoA in miR-31-containing cells completely abolished miR-31-mediated metastasis suppression (Figure 4C). Taken together, the preceding experiments indicated that the impact of miR-31 on metastasis can be entirely explained by miR-31's capacity to regulate ITGA5, RDX, and RhoA; these three targets act at partially overlapping steps of the invasion-metastasis cascade downstream of miR-31 *in vivo* (Table 1).

The Effects of ITGA5, RDX, and RhoA Re-Expression on miR-31-Evoked Metastasis-Relevant Phenotypes are Not Confined to 231 Cells

It remained possible that the ability of ITGA5, RDX, and RhoA to override miR-31's actions arose due to some peculiarity of the 231 cell system. To address this, I extended my analyses to SUM-159 human breast cancer cells. Like 231 cells, SUM-159 cells lack endogenous miR-31, are highly aggressive *in vitro*, and display impaired invasion, motility, and anoikis

resistance upon ectopic miR-31 (Valastyan et al., 2009). I created SUM-159 cells stably

expressing all 16 potential combinations of either miR-31 or control vector plus miRNA-resistant

mRNAs encoding ITGA5, RDX, and/or RhoA; all lines displayed comparable *in vitro*

proliferative kinetics (Supplementary Figures 11A and 11B). Consistent with my observations in

231 cells, individual re-expression of ITGA5, RDX, or RhoA in miR-31-containing SUM-159

cells rescued, at least partially, *in vitro* defects in invasion, motility, and anoikis resistance

attributable to ectopic miR-31; as before, the extent of rescue was more pronounced when

multiple effectors were concomitantly re-expressed (Supplementary Figures 11C-11E). Hence,

the ability of ITGA5, RDX, and RhoA re-expression to override the actions of miR-31 is not

confined to 231 cells.

MATERIALS AND METHODS

Plasmid Construction

     miR-31 was expressed from pBABE-puro, as I have elaborated upon (Valastyan et al.,

2009). Constructs encoding Fzd3 (Deardorff et al., 2001), ITGA5 (Kuwada and Li, 2000),

MMP16 (Hotary et al., 2006), M-RIP (Surks et al., 2003), RDX (Batchelor et al., 2004), and

RhoA (Subauste et al., 2000) – but lacking endogenous 3' UTR sequences and thus rendering

them miRNA-resistant – were subcloned into pBABE-hygro, pBABE-neo, pBABE-hygro,

pBABE-hygro, pBABE-hygro, and pBABE-zeo, respectively (Elenbaas et al., 2001). shRNAs

targeting Fzd3, ITGA5, MMP16, M-RIP, RDX, and RhoA were expressed from pLKO.1-puro

(Open Biosystems).

Cell Culture

Green fluorescent protein (GFP)-labeled 231 cells have been described (Valastyan et al., 2009). SUM-159 cells were provided by S. Ethier (Ma et al., 2007). Stable expression was achieved via retroviral (expression constructs) or lentiviral (shRNAs) transduction, followed by selection with puromycin, neomycin, hygromycin, and/or zeocin (Elenbaas et al., 2001).

Animal Studies

All research involving animals complied with protocols approved by the MIT Committee on Animal Care. Age-matched NOD/SCID (propagated on-site) or nude (Taconic) mice were utilized in the xenograft studies, as indicated. For spontaneous metastasis assays, the indicated female mice were bilaterally injected into the mammary fat pads with 1.0×10^6 tumor cells resuspended in 1:2 Matrigel (BD Biosciences) plus normal growth media. In spontaneous metastasis assays employing nude mice, primary tumor diameter was measured every seven days using precision calipers; tumor volume was calculated according to the formula $V = (4/3)\Pi r^3$. For experimental metastasis assays, the indicated mice were injected intravenously with 5.0×10^5 tumor cells (in PBS) via the tail vein. Lung metastasis was quantified using a fluorescent dissecting microscope within three hours of specimen isolation. Tumor histology was assessed by staining paraffin-embedded tissue sections with hematoxylin and eosin (H&E).

Statistical Analysis

Data are presented as mean ± s.e.m; Student's two-tailed t-test was used for comparisons, with $P < 0.05$ considered significant.

Immunoblotting

Lysates were resolved by NuPAGE gel electrophoresis (Invitrogen), transferred to a PVDF membrane, and probed with antibodies against _-actin (Santa Cruz), ITGA5 (Santa Cruz), RDX (Cell Signaling), or RhoA (Abcam).

miRNA Detection and RT-PCR

Total RNA, including small RNAs, was extracted from the indicated 231 cells with a *mir*Vana MicroRNA Isolation Kit (Ambion). RT-PCR-based detection of mature microRNAs and the 5S rRNA was achieved via use of a *mir*Vana MicroRNA Detection Kit and gene-specific primer sets (Ambion). For detection of Fzd3, GAPDH, ITGA5, MMP16, M-RIP, RDX, and RhoA transcript levels, cDNA was prepared from 200 ng of total RNA using the SuperScript III First-Strand Synthesis System (Invitrogen), and quantitated by SYBR Green real time RT-PCR (Applied Biosystems).

Invasion and Motility Assays

For invasion assays, 1.0×10^5 cells were plated in Matrigel-coated chambers with 8.0 _m pores (BD Biosciences); for motility assays, 5.0×10^4 cells were seeded atop uncoated membranes with 8.0 _m pores (BD Biosciences). Cells were seeded in serum-free media, and translocated toward complete growth media for 20 hours. Non-invaded or non-migrated cells were then physically removed; successfully translocated cells were visualized using a Diff-Quick Staining Set (Dade) and counted.

Anoikis Assays

Anoikis resistance was evaluated by seeding 7.5 x 10^4 cells in ultra-low attachment plates (Corning). After 24 hours, cells were resuspended in 0.4% trypan blue (Sigma) and the proportion of viable cells was quantified using a hemocytometer.

Measurements of *in vitro* Cell Proliferation

Unless otherwise denoted, proliferative kinetics were assayed by seeding 1.0 x 10^5 cells per well in 6-well plates. Total cell number was assessed every two to three days by trypsinization and manual counting with a hemocytometer. Alternatively, cell proliferation was measured by seeding 5.0 x 10^2 or 1.0 x 10^3 cells per well in 96-well plates and utilizing a CellTiter96 AQ$_{ueous}$ One Solution MTS Cell Proliferation Assay (Promega); cells were incubated with the MTS reagent for 1.5 hours, then total cell number was quantitated by measuring absorbance at 492 nm on a 96-well plate reader.

Oligonucleotide Sequences

Oligonucleotides employed in this study were: subcloning Fzd3 into pBABE-hygro, TGGCGAGAATTCATGGCTATGACTTGGATTGTCTTCTCTCTTTGGCCCT and TTGCGGGTCGACTTAAGCACTGGTTCCATCTTCTTCAATAACCCGA; subcloning ITGA5 into pBABE-neo, TTATAAGTCGACATGGGGAGCCGGACGCCAGAGTCCCCTCT and TTTATAGTCGACTCAGGCATCAGAGGTGGCTGGAGGCTTGAGCTGA; subcloning MMP16 into pBABE-hygro, AACCACTTTGTCGACATGATCTTACTCACATTCAGCACTGGAAGACGG and AACCACTTTGTCGACTCACACCCACTCTTGCATAGAGCGTTTACAGTAC; subcloning M-RIP into pBABE-hygro, AACCACTTTGAATTCATGTCGGCAGCCAAGGAGAAC and AACCACTTTGTCGACTCAGGTATCCCACGAGACCTGCTCAATTAC; subcloning RDX into pBABE-hygro, TGGCACGGATCCATGCCGAAACCAATCAACGTAAGAGTAACTACAATG and GGTCGAGTCGACTCACATTGCTTCAAACTCATCGATACGCTGCT;

Fzd3 RT-PCR, TCCATCCCTGCACAATATAAGGCTTCCACA and TCTCAATGCATCAACATCGTAGAGGCCAAC; GAPDH RT-

PCR, TCACCAGGGCTGCTTTTAAC and GACAAGCTTCCCGTTCTCAG; ITGA5 RT-PCR, AACTCATCATGGCCAGTGAGGGTAAGGGT

and ATCCTTAATGGCTCAGACATTCGATCCCTCTACAACT; MMP16 RT-PCR, AGTACGGCTACCTTCCACCGACTGA and

TACCTCTTGTCTGGTCAGGTACACCGCAT; M-RIP RT-PCR, AGGCAGAGCACATGGAGACCAATGCA and

AGTCAGCCAGCCTTTCTTGAAATTCAGCA; RDX RT-PCR, GAATCAGGAGCAGCTAGCAGCAGAACTT and

TTGGTCTTTTCCAAGTCTTCCTGGGCTGCA; RhoA RT-PCR, AGGTGGATGGAAAGCAGGTAGAGTTGGCT and

AGGATGATGGGCACGTTGGGACAGA.
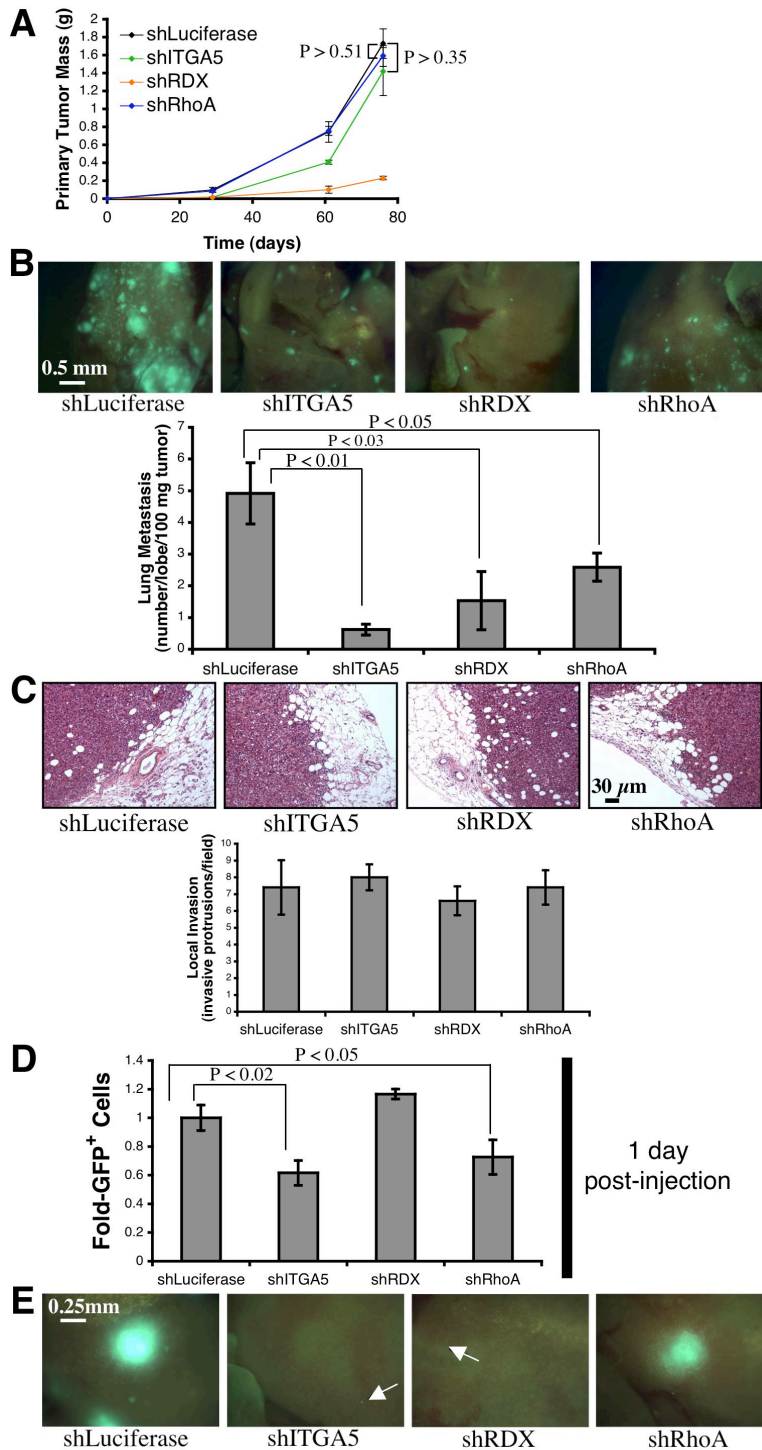
FIGURES

Figure 1. Individual Suppression of ITGA5, RDX, or RhoA Impairs Metastasis *in vivo*. (A)

Primary tumor growth upon orthotopic injection of the indicated GFP-labeled 231 cells into

NOD/SCID mice. The assay was terminated after 11 weeks due to primary tumor burden. n = 5 per timepoint. **(B)** Fluorescent images of murine lungs to visualize 231 cells 76 days after orthotopic implantation (top panels). Quantification of metastatic burden (bottom panel). n = 5. **(C)** H&E stain of 231 cell primary mammary tumors 57 days after injection (top panels). Quantification of local invasion (bottom panel). n = 5. All P-values are >0.67 relative to shLuciferase. **(D)** Prevalence of GFP-labeled 231 cells in the lungs one day after intravenous introduction into NOD/SCID mice. n = 4. **(E)** Fluorescent images of murine lungs to visualize 231 cells 89 days after intravenous injection. Arrows: micrometastases. shRNAs utilized in these assays: shITGA5 #4, shRDX #3, and shRhoA #5. All error bars represent mean ± s.e.m.

Figure 2

A

Primary Tumor Mass (g)

- vector + vector + vector + vector
- vector + RhoA + RDX + ITGA5
- miR-31 + vector + vector + vector
- miR-31 + RhoA + RDX + ITGA5

$P > 0.06$

$P < 0.005$

$P > 0.33$

Time (days)

B

0.5 mm

| miR-31 + vector + vector + vector | miR-31 + RhoA + RDX + ITGA5 | vector + vector + vector + vector | vector + RhoA + RDX + ITGA5 |

Lung Metastases (number/lobe/100 mg tumor)

$P < 0.001$ $P > 0.61$

miR-31	+	–	+	–
RhoA	–	–	+	+
RDX	–	–	+	+
ITGA5	–	–	+	+
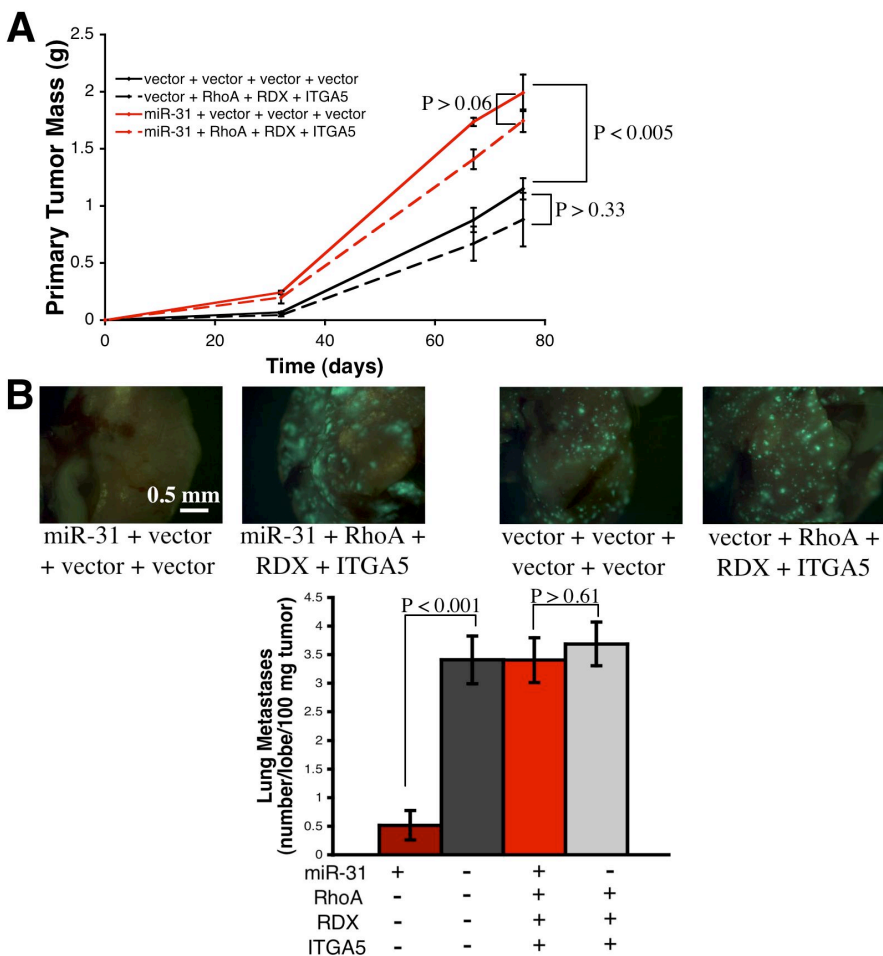
Figure 2. Simultaneous Re-Expression of ITGA5, RDX, and RhoA Abrogates miR-31-Imposed Metastasis Suppression *in vivo*. (A) Primary tumor growth upon orthotopic injection of the indicated GFP-labeled 231 cells into NOD/SCID mice. The assay was terminated after 11 weeks due to primary tumor burden. n = 5 per timepoint. **(B)** Fluorescent images of murine lungs to visualize 231 cells 67 days after orthotopic implantation (top panels). Quantification of metastatic burden (bottom panel). n = 5. All error bars represent mean ± s.e.m.

143

Figure 3

A

B

C
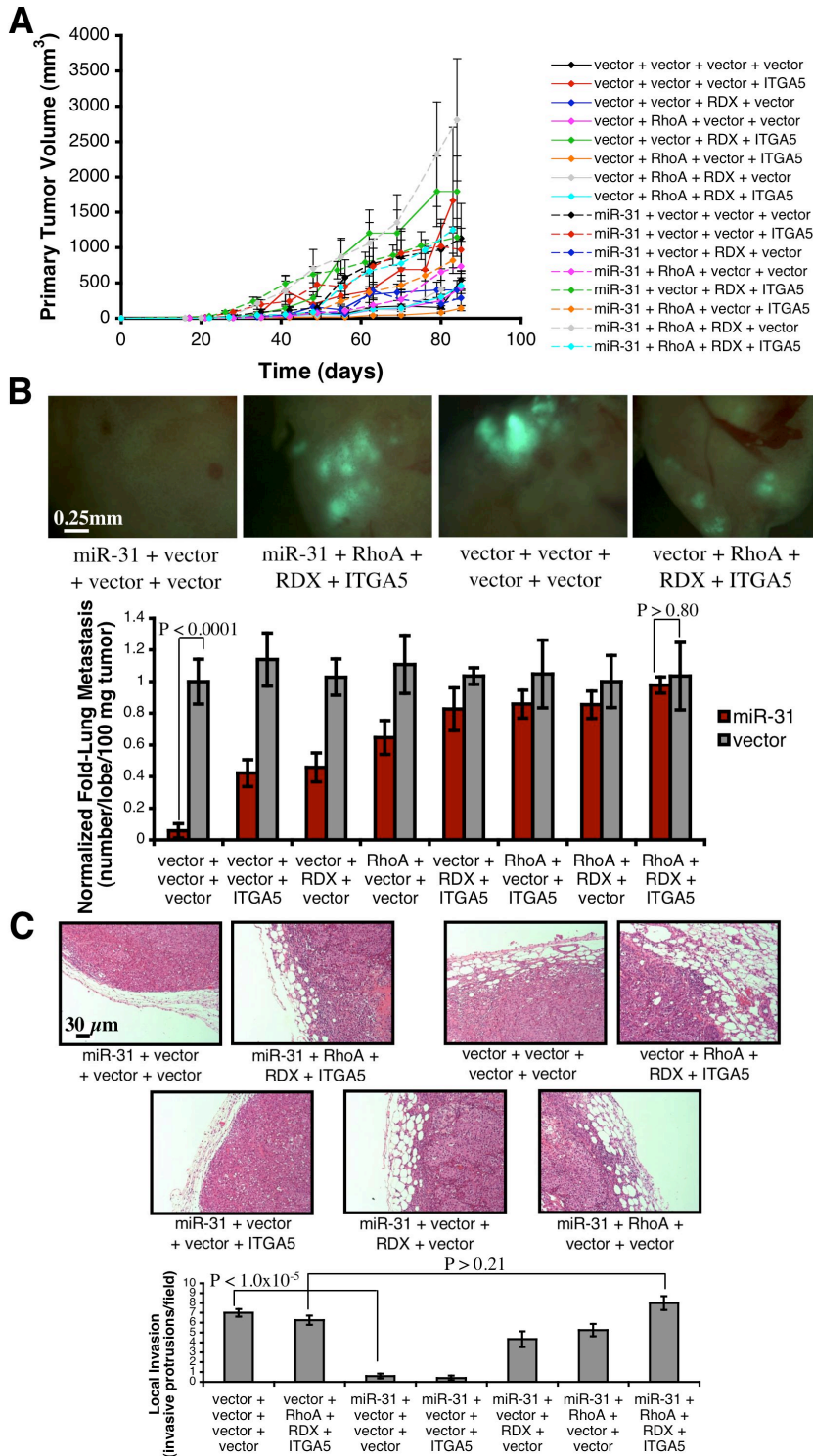
Figure 3. Re-Expression of ITGA5, RDX, and/or RhoA Affords Both Unique and Partially Overlapping Reversal of miR-31-Evoked Inhibition of Spontaneous Metastasis *in vivo*. (A) Primary tumor growth upon orthotopic implantation of the indicated GFP-labeled 231 cells into

144

nude mice. The assay was terminated after 13 weeks due to primary tumor burden. n = 5. **(B)** Fluorescent images of murine lungs to visualize 231 cells 88 days after orthotopic injection (top panels). Quantification of metastatic burden (bottom panel). n = 5. **(C)** H&E stain of 231 cell primary mammary tumors 54 days after injection. Quantification of local invasion (bottom panel). n = 5. All error bars represent mean ± s.e.m.
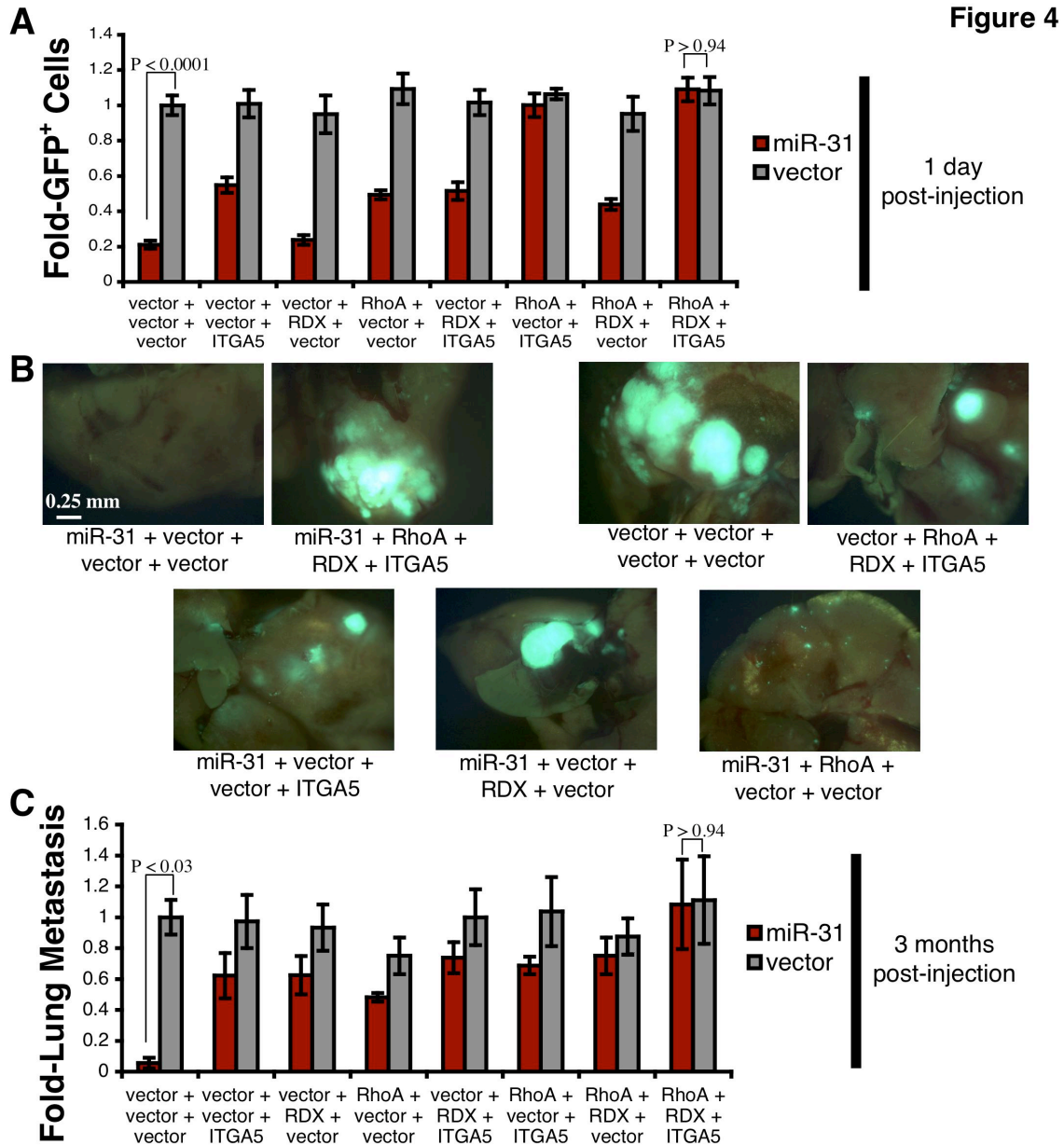
Figure 4. Re-Expression of ITGA5, RDX, and/or RhoA Affords Both Unique and Partially Overlapping Reversal of miR-31-Mediated Inhibition of Experimental Metastasis *in vivo*. **(A)** Prevalence of the indicated GFP-labeled 231 cells in the lungs one day after intravenous introduction into NOD/SCID mice. n = 4. **(B)** Fluorescent images of murine lungs to visualize 231 cells 84 days after tail vein injection. **(C)** Lung metastatic burden 84 days subsequent to intravenous injection. n = 5. All error bars represent mean ± s.e.m.

TABLES

Table 1

Table 1. Summary of Ability of Re-Expressed Targets to Rescue miR-31-Imposed Metastasis Suppression

Target	Local Invasion	Early Post-Intravasation Events	Metastatic Colonization
ITGA5	no rescue	√	√
RDX	√	no rescue	√
RhoA	√	√	no rescue

147

SUPPLEMENTARY FIGURES

A   **Supplementary Figure 1**
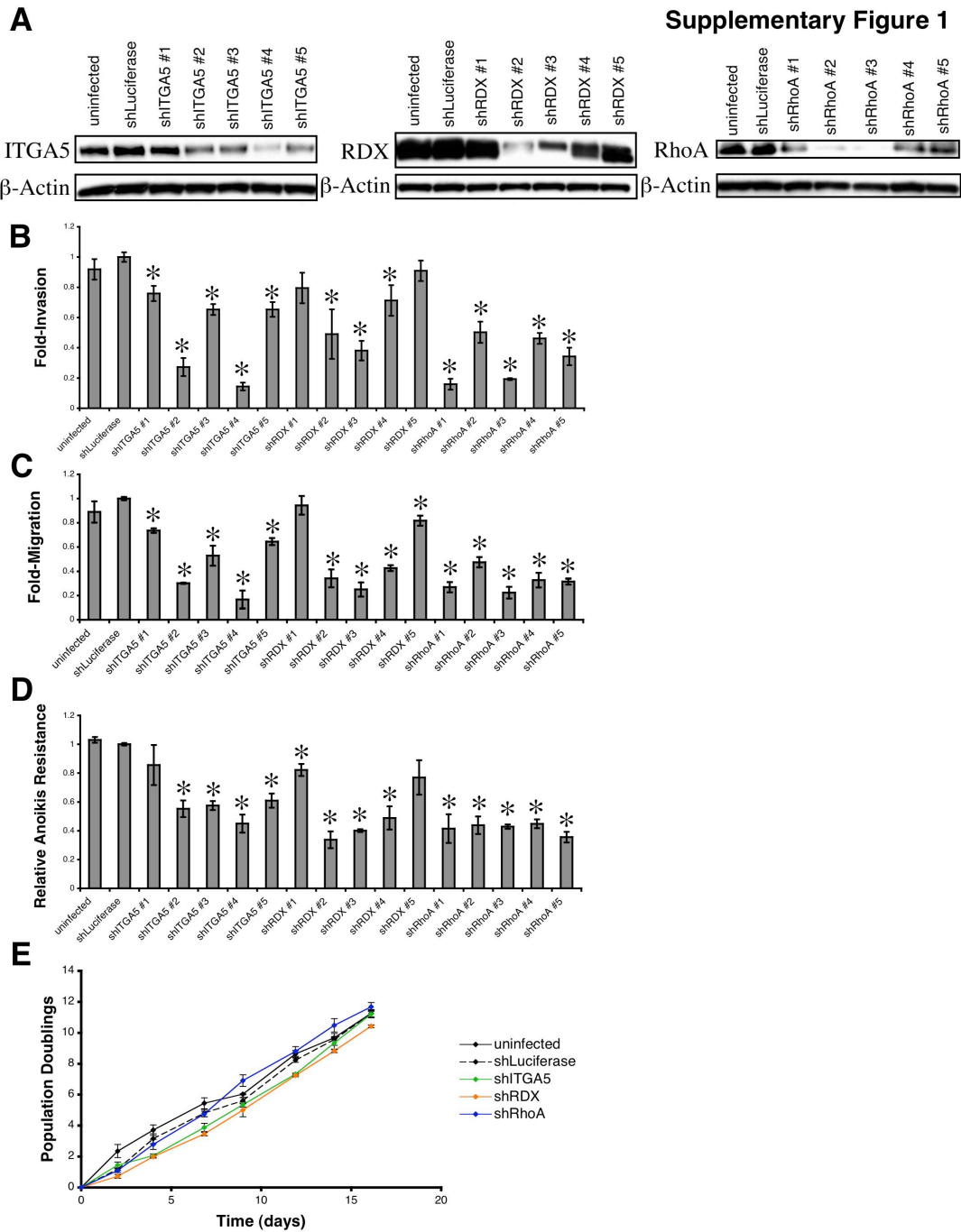
Supplementary Figure 1. Suppression of ITGA5, RDX, or RhoA Impairs Metastasis-

Relevant Traits *in vitro*. (A) Immunoblots for total ITGA5, RDX, or RhoA in the indicated

MDA-MB-231 (231) cells. _-actin was a loading control. **(B)** Invasion assays using the indicated

231 cells. n = 3. **(C)** Motility assays employing 231 cells infected as denoted. n = 3. **(D)** Anoikis

assays with the indicated 231 cells. n =3. **(E)** *In vitro* proliferation of the indicated 231 cells. n =

3. Asterisks: P <0.05 relative to shLuciferase. All error bars represent mean ± s.e.m.
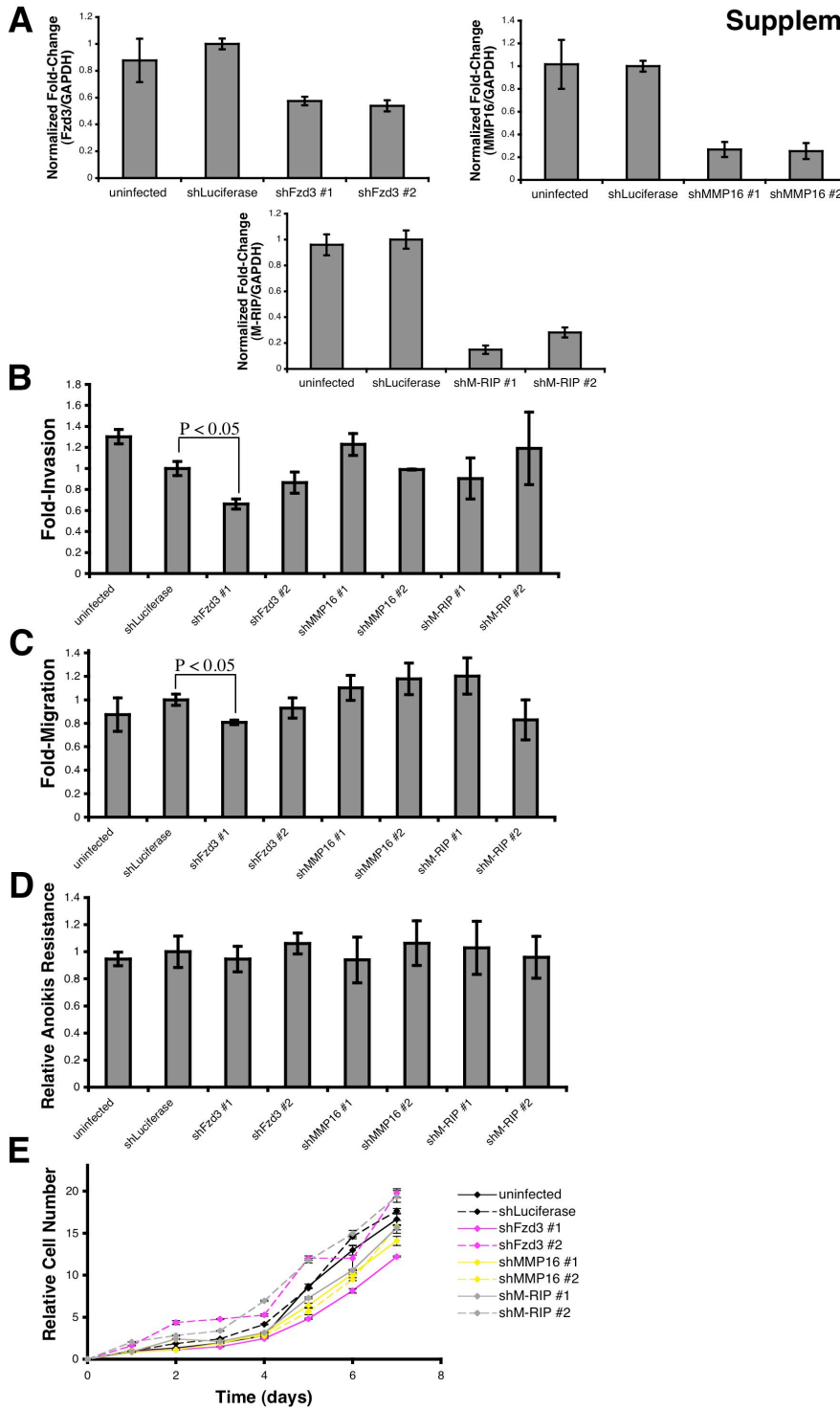
Supplementary Figure 2. Suppression of Fzd3, MMP16, or M-RIP Does Not Affect

Metastasis-Relevant Traits *in vitro*. (A) Real time RT-PCR for Fzd3, MMP16, and M-RIP in

the indicated 231 cells. GAPDH was a loading control. n = 3. **(B)** Invasion assays using the

indicated 231 cells. n = 3. **(C)** Motility assays employing 231 cells infected as denoted. n = 3.

(D) Anoikis assays with the indicated 231 cells. n =3. All P-values are >0.65 relative to

shLuciferase. **(E)** *In vitro* proliferation of the indicated 231 cells, as measured by an MTS assay.

n = 3. All error bars represent mean ± s.e.m.
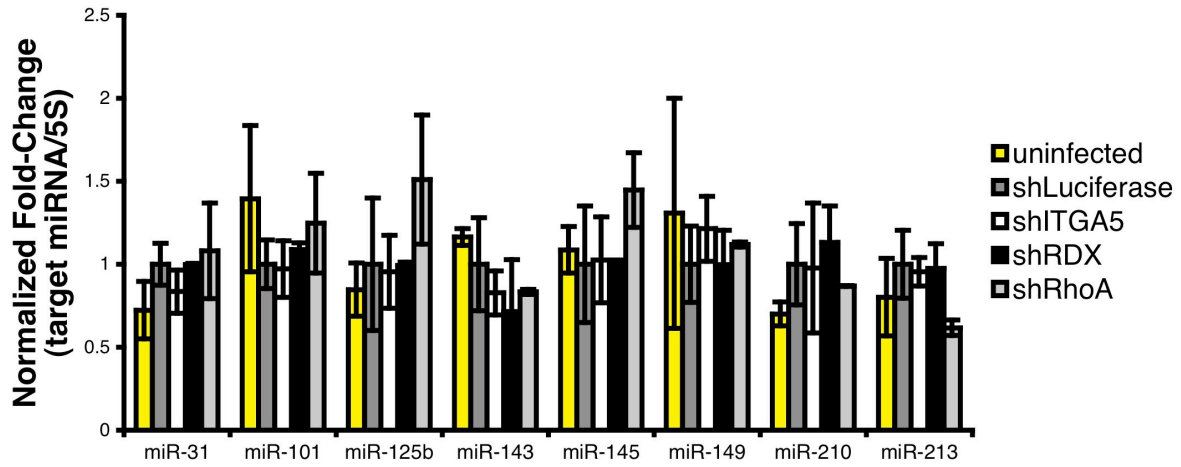
Supplementary Figure 3. shRNA Expression Does Not Interfere with MicroRNA Biogenesis. Real time RT-PCR for various mature microRNAs in the indicated 231 cells. 5S rRNA was a loading control. n = 3. All P-values are >0.32 relative to shLuciferase. shRNAs utilized in these assays: shITGA5 #4, shRDX #3, and shRhoA #5. All error bars represent mean ± s.e.m.
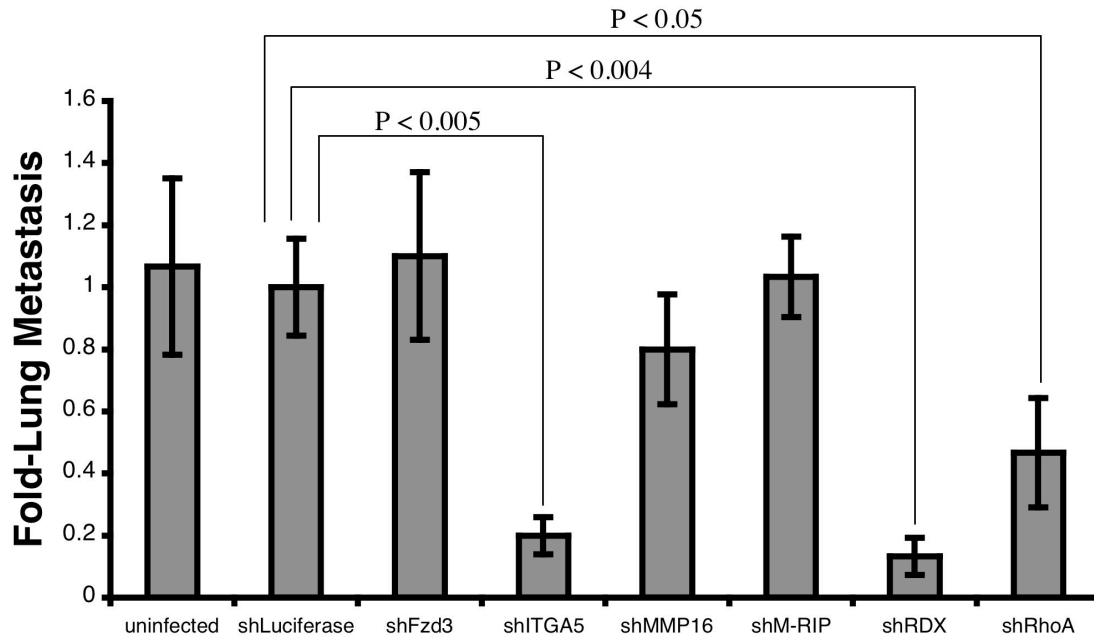
Supplementary Figure 4. Suppression of ITGA5, RDX, or RhoA Impairs *in vivo* Metastasis, while Inhibition of Fzd3, MMP16, or M-RIP Fails to Impact this Phenotype. Quantification of metastatic burden in the lungs of nude mice one month after intravenous injection of the indicated green fluorescent protein (GFP)-labeled 231 cells. n = 5. shRNAs utilized in these assays: shFzd3 #1, shITGA5 #4, shMMP16 #2, shM-RIP #2, shRDX #3, and shRhoA #5. All error bars represent mean ± s.e.m.
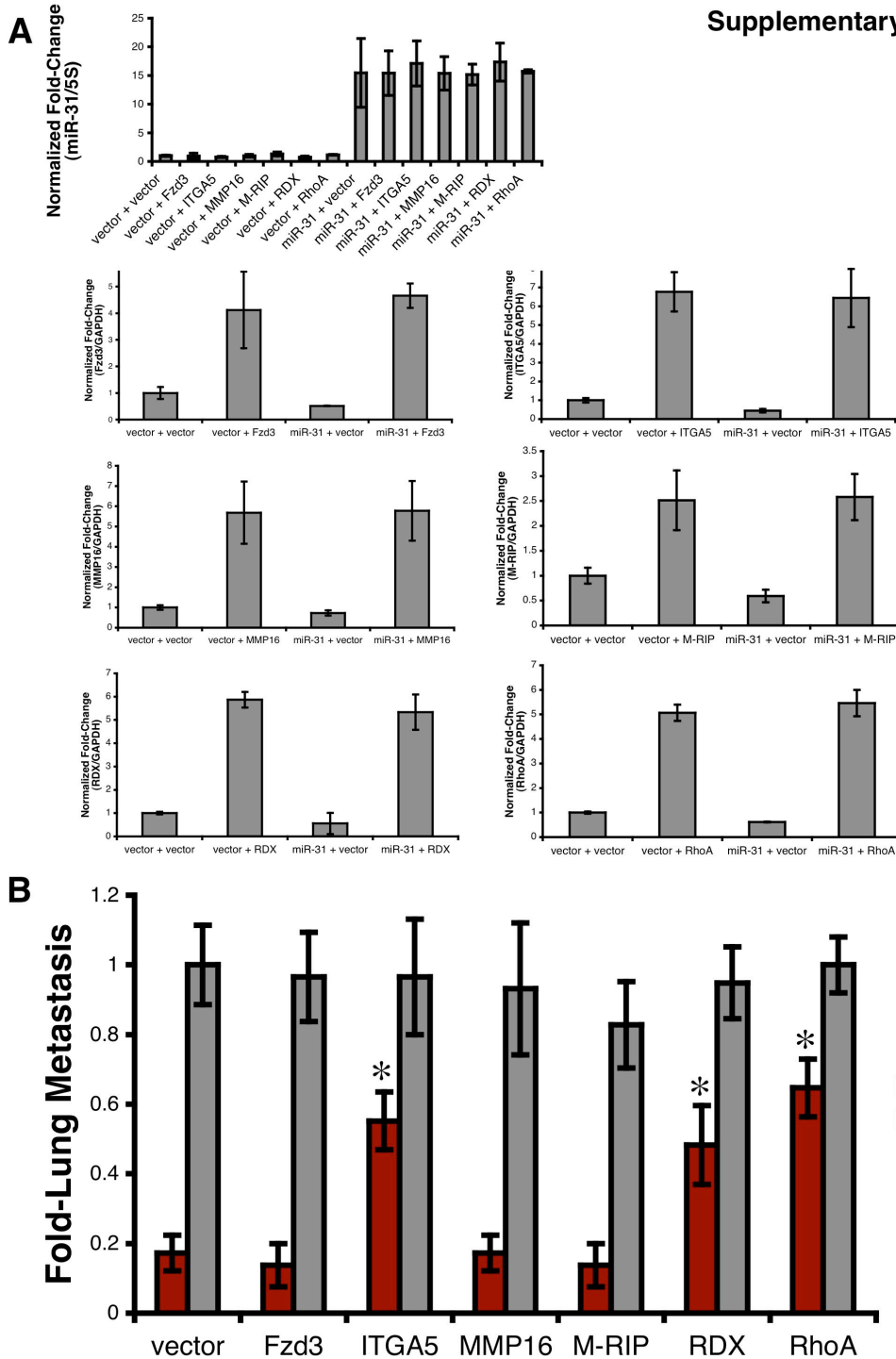
Supplementary Figure 5. Re-Expression of ITGA5, RDX, or RhoA Partially Reverses miR-31-Imposed Metastasis Suppression *in vivo*, while Re-Expression of Fzd3, MMP16, or M-RIP Fails to Rescue this Phenotype. (A) Real time RT-PCR for miR-31, Fzd3, ITGA5,

MMP16, M-RIP, RDX, and RhoA in the indicated 231 cells. 5S rRNA (for miR-31) and

GAPDH (for Fzd3, ITGA5, MMP16, M-RIP, RDX, and RhoA) were loading controls. n = 3. **(B)**

Quantification of metastatic burden in the lungs of nude mice one month after intravenous

injection of the indicated GFP-labeled 231 cells. n = 5. Asterisks: P <0.05 relative to miR-31 +

vector. All error bars represent mean ± s.e.m.
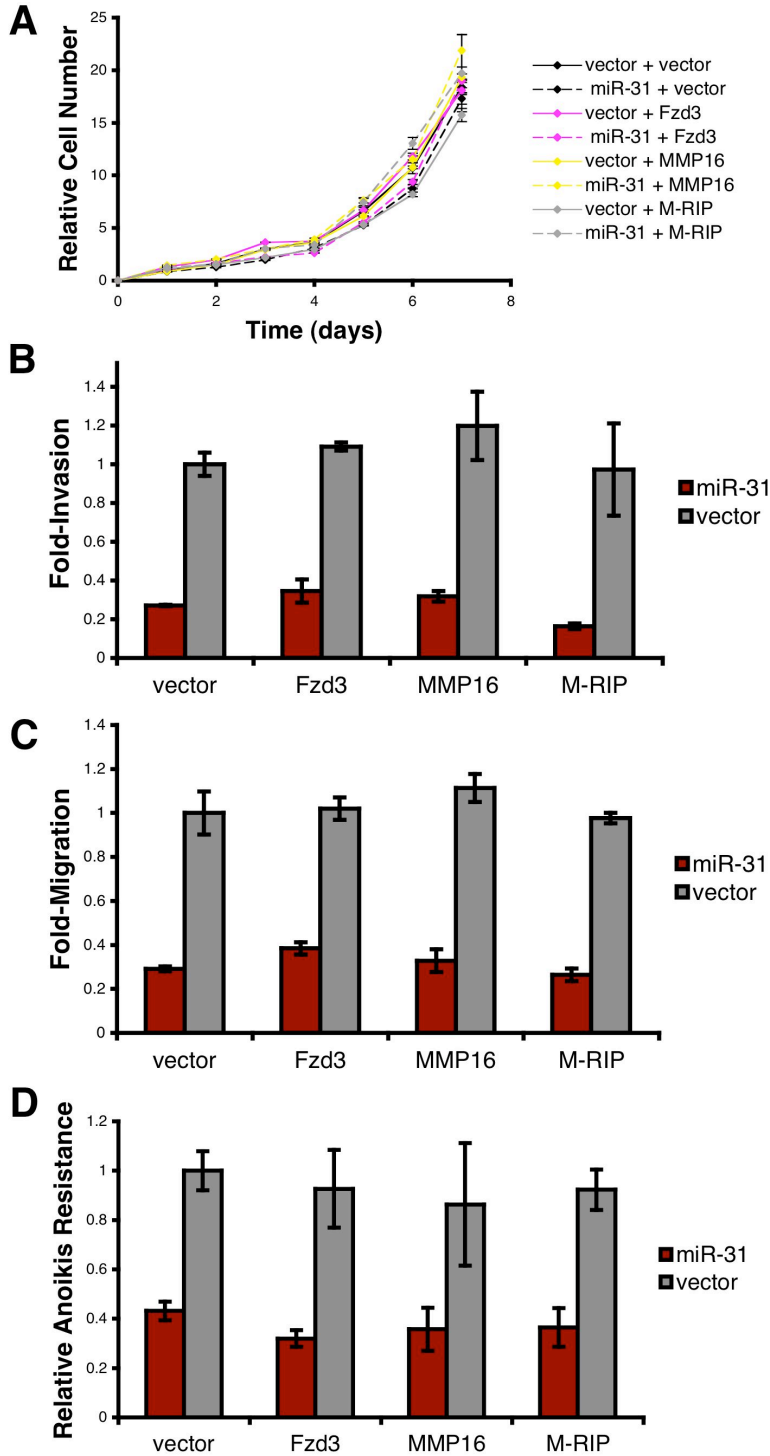
Supplementary Figure 6. Re-Expression of Fzd3, MMP16, or M-RIP Fails to Reverse miR-31-Imposed Metastasis-Relevant Phenotypes *in vitro*. (A) *In vitro* proliferation of the indicated 231 cells, as measured by an MTS assay. n = 3. **(B)** Invasion assays using the indicated

231 cells. n = 3. **(C)** Motility assays employing 231 cells infected as denoted. n = 3. **(D)** Anoikis

assays with the indicated 231 cells. n =3. All P-values indicated no significant difference

between miR-31 + vector and miR-31 + Fzd3, miR-31 + MMP16, or miR-31 + M-RIP in any of

these assays. All error bars represent mean ± s.e.m.
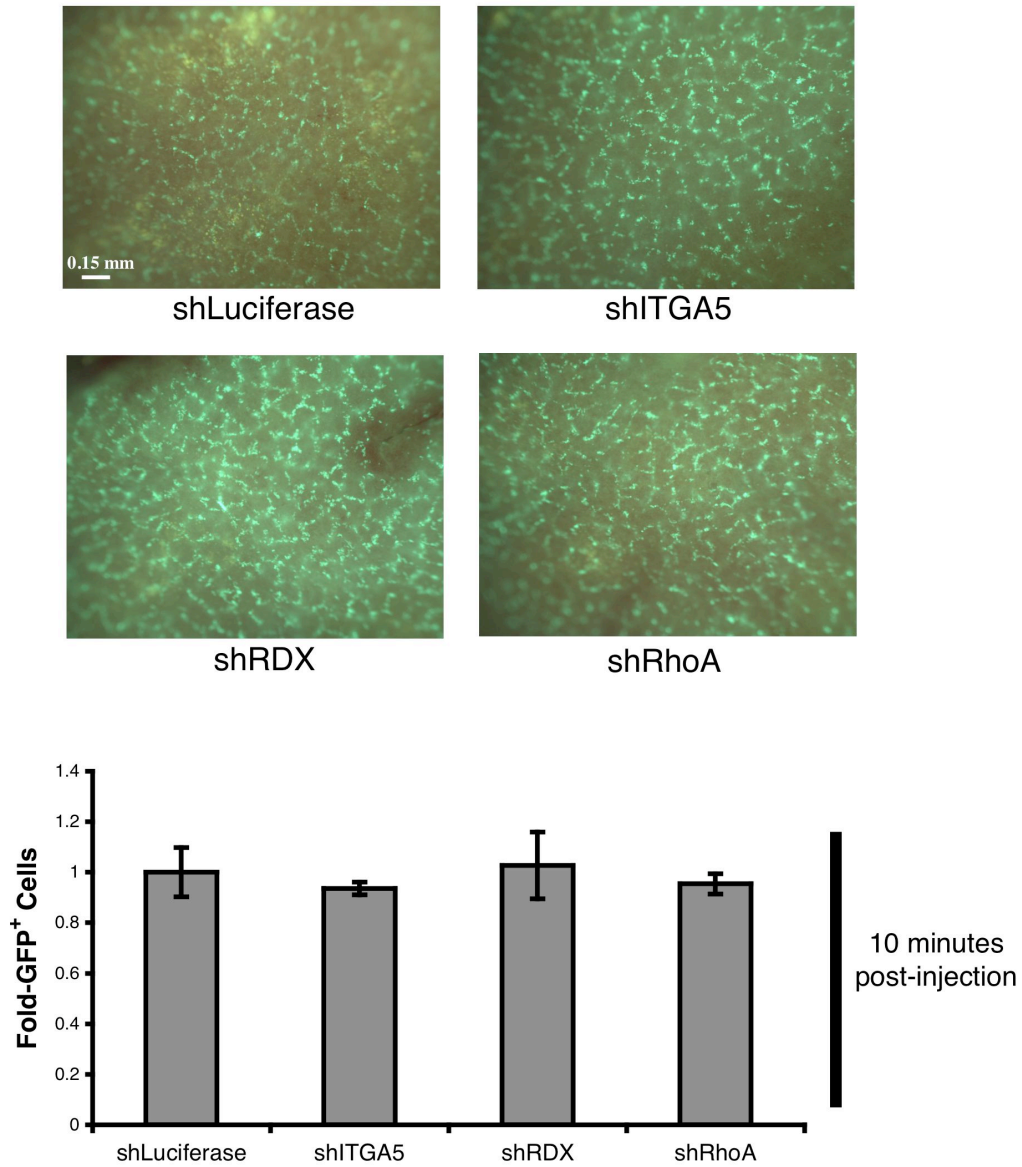
Supplementary Figure 7. Suppression of ITGA5, RDX, or RhoA Fails to Affect the Initial Vascular Lodging of Intravenously Injected 231 Cells *in vivo*. Fluorescent images of murine lungs to visualize GFP-labeled 231 cells 10 minutes subsequent to tail vein injection into NOD/SCID mice (top panels). Quantification of the relative prevalence of these cells in the lungs (bottom panel). n = 3. All P-values are >0.56 relative to shLuciferase. shRNAs utilized in these assays: shITGA5 #4, shRDX #3, and shRhoA #5. All error bars represent mean ± s.e.m.

A

B
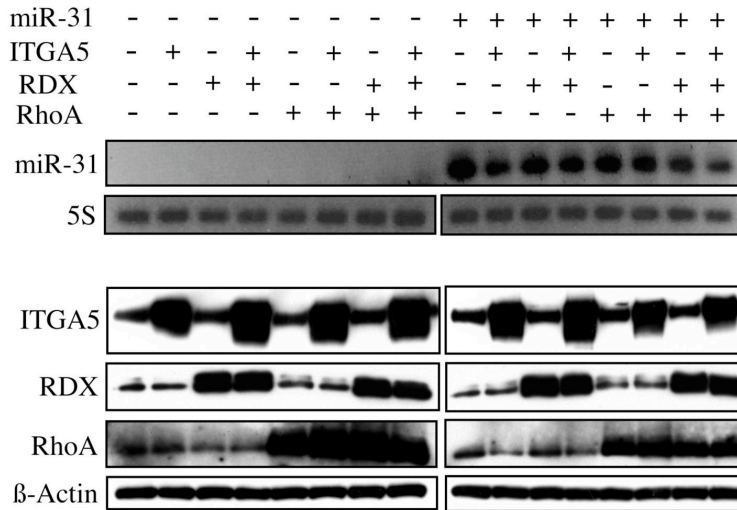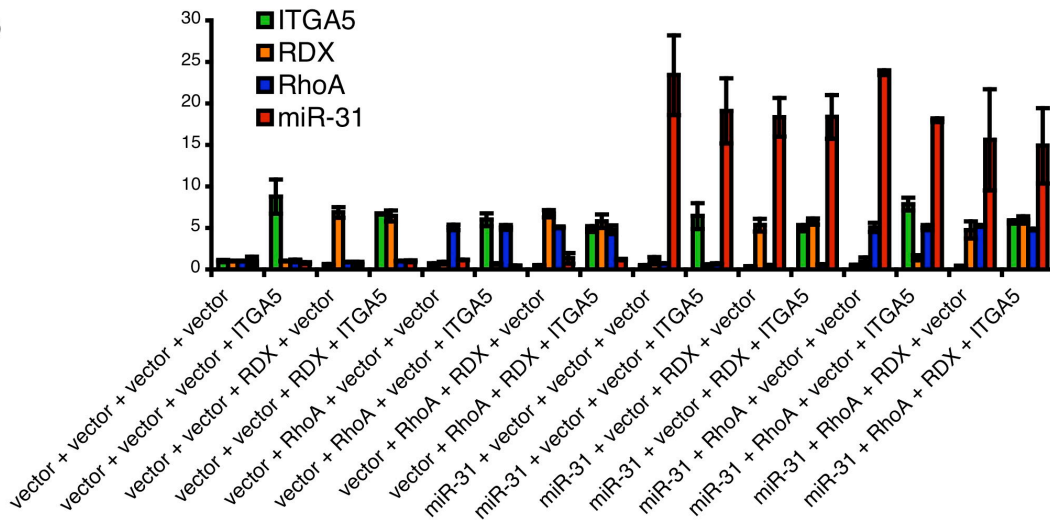
Supplementary Figure 8. Generation of 231 Cells Stably Expressing miR-31, ITGA5, RDX, and/or RhoA. (A) RT-PCR (top two rows) or immunoblots (bottom four rows) for total miR-31, ITGA5, RDX, or RhoA in the indicated 231 cells. 5S rRNA and _-actin were loading controls for the RT-PCR and immunoblots, respectively. **(B)** Real time RT-PCR for miR-31, ITGA5, RDX, and RhoA in the indicated 231 cells. 5S rRNA (for miR-31) and GAPDH (for ITGA5, RDX, and RhoA) were loading controls. n = 3. All error bars represent mean ± s.e.m.
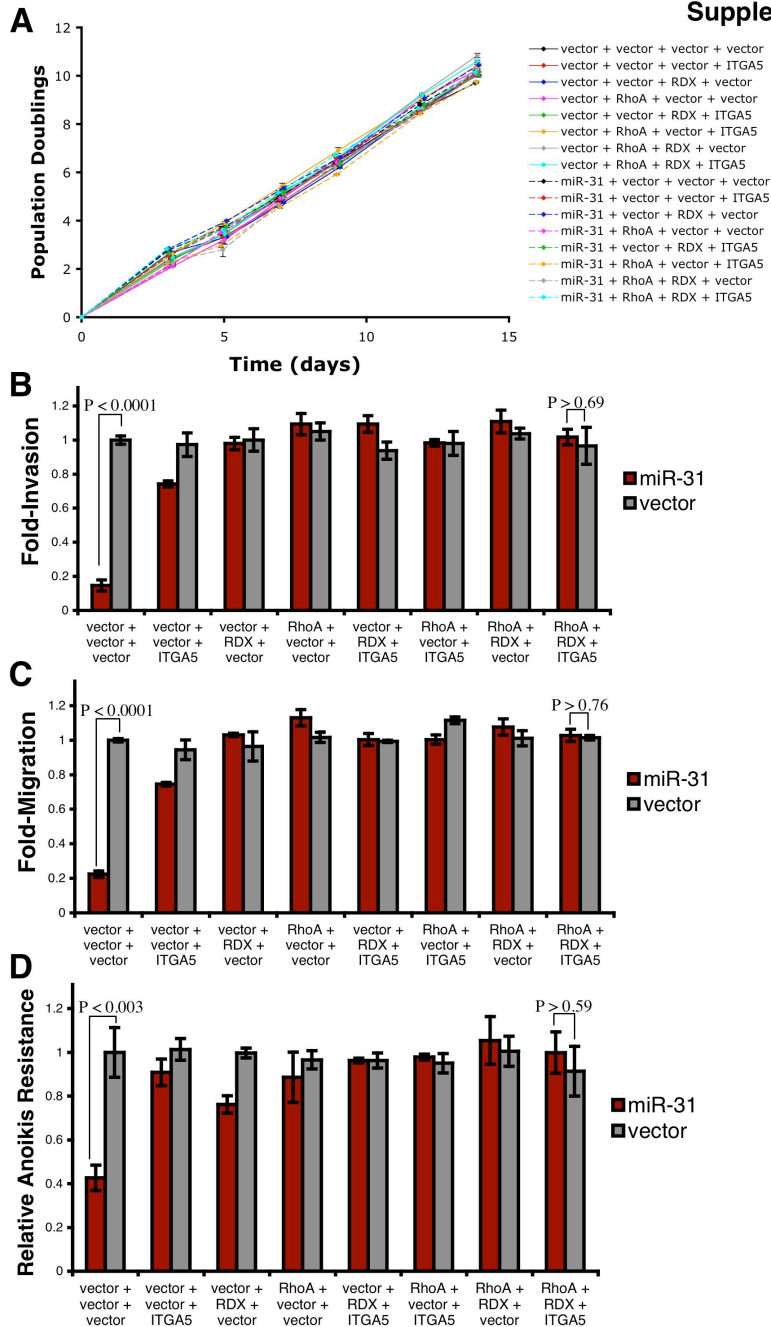
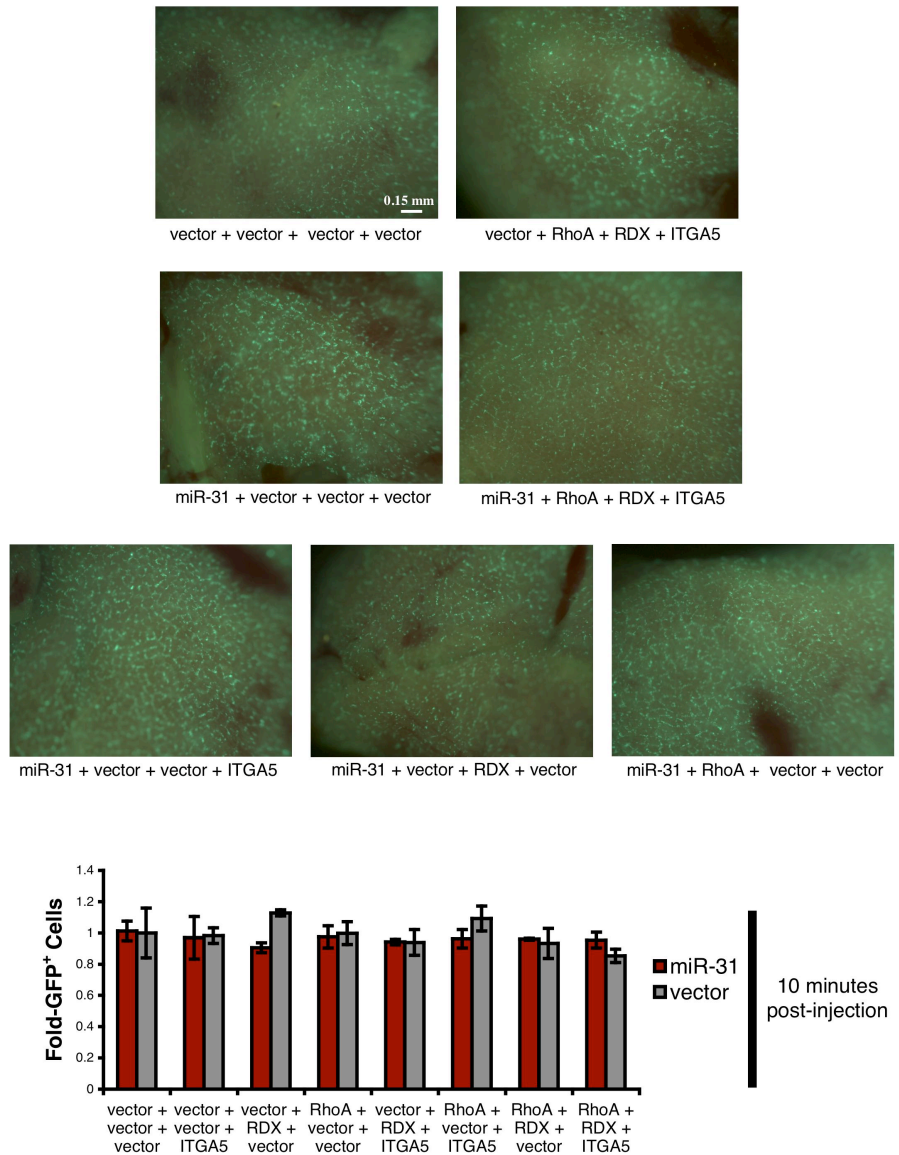**Supplementary Figure 9. Concomitant Re-Expression of ITGA5, RDX, and RhoA Reverses miR-31-Imposed Metastasis-Relevant Phenotypes in 231 Cells *in vitro*. (A)** *In vitro* proliferation of the indicated 231 cells. n = 3. **(B)** Invasion assays using the indicated 231 cells. n = 3. **(C)** Motility assays employing 231 cells infected as denoted. n = 3. **(D)** Anoikis assays with the indicated 231 cells. n =3. All error bars represent mean ± s.e.m.
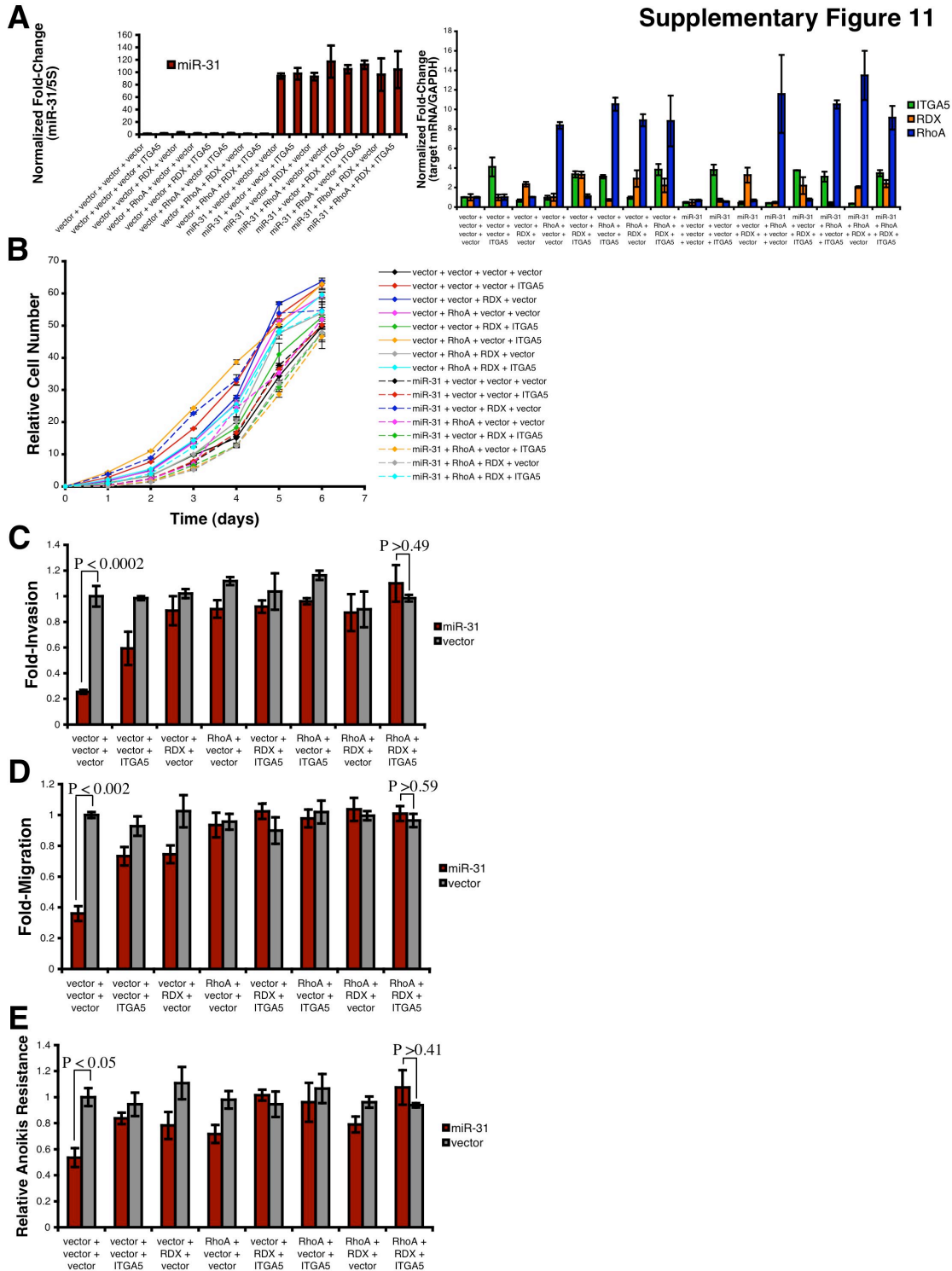
Supplementary Figure 10. miR-31, ITGA5, RDX, and RhoA Fail to Affect the Initial Vascular Lodging of Intravenously Injected 231 Cells *in vivo*. Fluorescent images of murine lungs to visualize GFP-labeled 231 cells 10 minutes subsequent to tail vein injection into NOD/SCID mice (top panels). Quantification of the relative prevalence of these cells in the lungs (bottom panel). n = 2. All P-values are >0.52 relative to vector + vector + vector + vector. All error bars represent mean ± s.e.m.

Supplementary Figure 11. Concomitant Re-Expression of ITGA5, RDX, and RhoA

Reverses miR-31-Imposed Metastasis-Relevant Phenotypes in SUM-159 Cells *in vitro*. (A)

Real time RT-PCR for miR-31, ITGA5, RDX, and RhoA in the indicated SUM-159 cells. 5S

rRNA (for miR-31) and GAPDH (for ITGA5, RDX, and RhoA) were loading controls. n = 3. **(B)**

In vitro proliferation of the indicated SUM-159 cells, as measured by an MTS assay. n = 3. **(C)**

Invasion assays using the indicated SUM-159 cells. n = 3. **(D)** Motility assays employing SUM-

159 cells infected as denoted. n = 3. **(E)** Anoikis assays with the indicated SUM-159 cells. n =3.

All error bars represent mean ± s.e.m.

Supplementary Table 1. Effects of miR-31, ITGA5, RDX, and RhoA on Primary Tumor Size

Cell Line	Relative Final Tumor Volume[a]	p-value[a]
vector + vector + vector + vector	1.0 ± 0.06[b]	-
vector + vector + vector + ITGA5	3.06 ± 1.90	>0.33
vector + vector + RDX + vector	0.73 ± 0.24	>0.33
vector + RhoA + vector + vector	0.80 ± 0.19	>0.36
vector + vector + RDX + ITGA5	3.30 ± 0.91	>0.06
vector + RhoA + vector + ITGA5	0.26 ± 0.06	<0.01
vector + RhoA + RDX + vector	0.74 ± 0.24	>0.34
vector + RhoA + RDX + ITGA5	0.84 ± 0.20	>0.48
miR-31 + vector + vector + vector	2.08 ± 0.37	<0.05
miR-31 + vector + vector + ITGA5	1.78 ± 0.27	<0.05
miR-31 + vector + RDX + vector	0.52 ± 0.19	>0.06
miR-31 + RhoA + vector + vector	1.35 ± 0.64	>0.61
miR-31 + vector + RDX + ITGA5	2.10 ± 0.34	<0.04
miR-31 + RhoA + vector + ITGA5	1.50 ± 0.18	<0.05
miR-31 + RhoA + RDX + vector	5.16 ± 1.58	<0.05
miR-31 + RhoA + RDX + ITGA5	2.30 ± 0.07	<0.01

[a]Relative to vector + vector + vector + vector. [b]All error bars represent mean ± s.e.m.

ACKNOWLEDGMENTS

REFERENCES

Ambros V. (2004). The functions of animal microRNAs. Nature *431*, 350-355.

Baek D, Villén J, Shin C, et al. (2008). The impact of microRNAs on protein output. Nature *455*, 64-71.

Bartel DP. (2009). MicroRNAs: target recognition and regulatory functions. Cell *136*, 215-233.

Batchelor CL, Woodward AM, and Crouch DH. (2004). Nuclear ERM (ezrin, radixin, moesin) proteins: regulation by cell density and nuclear import. Exp Cell Res *296*, 208-222.

Deardorff MA, Tan C, Saint-Jeannet JP, and Klein PS. (2001). A role for frizzled 3 in neural crest development. Development *128*, 3655-3663.

Elenbaas B, Spirio L, Koerner F, et al. (2001). Human breast cancer cells generated by oncogenic transformation of primary mammary epithelial cells. Genes Dev *15*, 50-65.

Fidler IJ. (2003). The pathogenesis of cancer metastasis: the 'seed and soil' hypothesis revisited. Nat Rev Cancer *3*, 453-458.

Grimson A, Farh KK, Johnston WK, Garrett-Engele P, Lim LP, and Bartel DP. (2007). MicroRNA targeting specificity in mammals: determinants beyond seed pairing. Mol Cell *27*, 91-105.

Gupta GP and Massagué J. (2006). Cancer metastasis: building a framework. Cell *127*, 679-695.

Hotary K, Li XY, Allen E, Stevens SL, and Weiss SJ. (2006). A cancer cell metalloprotease triad regulates the basement membrane transmigration program. Genes Dev *20*, 2673-2686.

Johnnidis JB, Harris MH, Wheeler RT, et al. (2008). Regulation of progenitor cell proliferation and granulocyte function by microRNA-223. Nature *451*, 1125-1129.

Krek A, Grün D, Poy MN, et al. (2005). Combinatorial microRNA target predictions. Nat Genet *37*, 495-500.

Kuwada SK and Li X. (2000). Integrin alpha5/beta1 mediates fibronectin-dependent epithelial cell proliferation through epidermal growth factor receptor activation. Mol Biol Cell *11*, 2485-2496.

Ma L, Teruya-Feldstein J, and Weinberg RA. (2007). Tumour invasion and metastasis initiated by microRNA-10b in breast cancer. Nature *449*, 682-688.

Pillé JY, Denoyelle C, Varet J, et al. (2005). Anti-RhoA and anti-RhoC siRNAs inhibit the proliferation and invasiveness of MDA-MB-231 breast cancer cells in vitro and in vivo. Mol Ther *11*, 267-274.

Rodriguez A, Vigorito E, Clare S, et al. (2007). Requirement of bic/microRNA-155 for normal immune function. Science *316*, 608-611.

Selbach M, Schwanhäusser B, Thierfelder N, et al. (2008). Widespread changes in protein synthesis induced by microRNAs. Nature *455*, 58-63.

Subauste MC, Von Herrath M, Benard V, et al. (2000). Rho family proteins modulate rapid apoptosis induced by cytotoxic T lymphocytes and Fas. J Biol Chem *275*, 9725-9733.

Surks HK, Richards CT, and Mendelsohn ME. (2003). Myosin phosphatase-Rho interacting protein. A new member of the myosin phosphatase complex that directly binds RhoA. J Biol Chem *27*, 51484-51493.

Thai TH, Calado DP, Casola S, et al. (2007). Regulation of germinal center response by microRNA-155. Science *316*, 604-608.

Valastyan S, Reinhardt F, Benaich N, et al. (2009). A pleiotropically acting microRNA, miR-31, inhibits breast cancer metastasis. Cell *137*, 1032-1046.

van Rooij E, Sutherland LB, Qi X, et al. (2007). Control of stress-dependent cardiac growth and gene expression by a microRNA. Science *316*, 575-579.

Ventura A and Jacks T. (2009). MicroRNAs and cancer: short RNAs go a long way. Cell *136*, 586-591.

Ventura A, Young AG, Winslow MM, et al. (2008). Targeted deletion reveals essential and overlapping functions of the miR-17 through 92 family of miRNA clusters. Cell *132*, 875-886.

Zhao Y, Ransom JF, Li A, et al. (2007). Dysregulation of cardiogenesis, cardiac conduction, and cell cycle in mice lacking miRNA-1-2. Cell *129*, 303-317.

Chapter 4

Concurrent Suppression of Integrin _5, Radixin, and RhoA Phenocopies the Effects of miR-31 on Metastasis

Scott Valastyan[1,2], Amelia Chang[1,2], Nathan Benaich[1,3], Ferenc Reinhardt[1], and Robert A. Weinberg[1,2,4]

[1]Whitehead Institute for Biomedical Research, Cambridge, MA 02142, USA
[2]Department of Biology, Massachusetts Institute of Technology, Cambridge, MA 02139, USA
[3]Department of Biology, Williams College, Williamstown, MA 01267, USA
[4]MIT Ludwig Center for Molecular Oncology, Cambridge, MA 02139, USA

This chapter is excerpted from the following publication (copyright permissions obtained):

<u>INTRODUCTION</u>

As discussed in Chapter One, metastases are responsible for 90% of human cancer deaths and arise via a complex, multi-step process termed the invasion-metastasis cascade (Fidler, 2003; Gupta and Massagué, 2006). In order to metastasize, cancer cells in a primary tumor must first acquire the capacity for motility, invade locally, intravasate into the systemic circulation, maintain viability during transit through the vasculature, extravasate into the parenchyma of a distant tissue, survive in this foreign microenvironment to form micrometastases, and finally re-initiate their proliferative program and establish macroscopic secondary tumors (metastatic colonization) (Fidler, 2003). Metastatic colonization is the rate-limiting step of the invasion-metastasis cascade, yet relatively few molecular mediators of this process have been identified (Gupta and Massagué, 2006).

MicroRNAs (miRNAs) are emerging as a class of critically important regulators of tumor metastasis. These evolutionarily conserved RNAs modulate gene expression at a post-transcriptional level via the pleiotropic suppression of sequence-complementary mRNA targets (Ambros, 2004; Bartel, 2004; Bartel, 2009). As indicated in Chapter One, a crucial role for miRNAs in tumor development has been firmly established by the identification of numerous miRNAs that function as *bona fide* oncogenes or tumor suppressor genes (Calin and Croce, 2006; Esquela-Kerscher and Slack, 2006; Sotiropoulou, 2009; Ventura and Jacks, 2009). Additionally, certain miRNAs have been more specifically implicated in the regulation of metastatic progression (Valastyan and Weinberg, 2009).

One such anti-metastatic miRNA is miR-31. As described in Chapter Two, I recently determined that miR-31 levels were inversely associated with the propensity for metastatic relapse in human breast carcinoma patients (Valastyan et al., 2009a). Moreover, miR-31

expression was both necessary and sufficient to inhibit metastasis in human breast cancer xenografts (Valastyan et al., 2009a). I attributed these effects to miR-31's capacity to intervene during at least three distinct steps of the invasion-metastasis cascade, doing so via the pleiotropic suppression of a cohort of pro-metastatic target genes (Valastyan et al., 2009a). Subsequently, as detailed in Chapter Three, I discovered that the anti-metastatic consequences of ectopic miR-31 expression could be entirely reversed by the concomitant overexpression of three downstream effectors of this miRNA – integrin _5 (ITGA5), radixin (RDX), and RhoA (Valastyan et al., 2009b).

Importantly, these earlier studies relied upon ectopic expression or overexpression of miR-31 and these target mRNAs, rather than modulation of the endogenous gene products. For this reason, I undertook to determine whether the concurrent suppression of the endogenous mRNAs encoding ITGA5, RDX, and RhoA was sufficient to phenocopy the impacts of ectopic miR-31 expression on metastasis. Success in this endeavor would indicate that these three proteins indeed function to promote metastasis and furthermore would implicate the pleiotropic suppression of ITGA5, RDX, and RhoA as a potential mechanism by which miR-31 antagonizes the metastatic phenotype.

<u>RESULTS</u>

Simultaneous Suppression of ITGA5, RDX, and RhoA Impairs Metastasis-Relevant Traits *in vitro*

I previously demonstrated that the metastatic potential of human breast cancer xenografts could be potently suppressed by the ectopic expression of miR-31, and that the concomitant re-expression of three downstream effectors of this miRNA – ITGA5, RDX, and RhoA – sufficed

to override the anti-metastatic actions of miR-31 (Valastyan et al., 2009a; Valastyan et al., 2009b). These prior analyses relied, however, upon overexpression of ITGA5, RDX, and RhoA via viral expression vectors, rather than on modulation of the endogenous mRNAs encoding these proteins. Consequently, I wished to determine whether the simultaneous downregulation of endogenous ITGA5, RDX, and RhoA levels could phenocopy the effects of miR-31 expression on metastasis.

To this end, I created otherwise-metastatic MDA-MB-231 human breast cancer cells ("231 cells") that concurrently expressed shRNAs targeting the endogenous mRNAs encoding ITGA5, RDX, and RhoA. Multiple sequence-independent hairpins were tested for their efficacy in suppressing the targeted molecules (Supplementary Figure 1 and data not shown). Importantly, cell lines generated upon sequential infection with several distinct combinations of shRNAs against these three proteins exhibited reductions in endogenous ITGA5, RDX, and RhoA levels reminiscent of the 50%-60% decreases in these three factors previously observed upon ectopic expression of miR-31 in 231 cells (Valastyan et al., 2009a). Accordingly, I focused my subsequent analyses on those cell lines that concomitantly displayed between two- and three-fold suppression of ITGA5, RDX, and RhoA.

Non-specific, deleterious effects have been observed in cells expressing large quantities of shRNA molecules, ostensibly due to competition for shared components of the miRNA biogenesis machinery that might impair, in turn, the actions of a broad spectrum of important but otherwise functionally unrelated endogenous cellular miRNAs (Grimm et al., 2006). Reassuringly, however, the processing of eight control miRNAs was unaffected in 231 cells simultaneously expressing ITGA5, RDX, and RhoA shRNAs (Supplementary Figure 2). Hence,

saturation of the miRNA biogenesis machinery was unlikely to have confounded my interpretations.

These shRNA-expressing 231 cells were first subjected to *in vitro* assays that gauge cell-biologic attributes required for metastasis. Coordinate suppression of ITGA5, RDX, and RhoA reduced invasion through an artificial extracellular matrix (Figure 1A), cell motility (Figure 1B), and resistance to anoikis-mediated cell death (Figure 1C) *in vitro*. Among the different combinations of sequence-independent hairpins against ITGA5, RDX, and RhoA, the magnitude of the observed biological response correlated with the extent of knockdown achieved, suggesting that these outcomes arose as specific consequences of reduced levels of the targeted proteins. Importantly, concomitant suppression of ITGA5, RDX, and RhoA failed to alter *in vitro* proliferation kinetics (Supplementary Figure 3), indicating the absence of significant cytostatic or cytotoxic effects due to the expression of these shRNAs. Together, these data confirmed that ITGA5, RDX, and RhoA control *in vitro* behaviors critical for the acquisition of metastatic competence.

Concomitant Suppression of ITGA5, RDX, and RhoA Phenocopies miR-31-Evoked Inhibition of Spontaneous Metastasis *in vivo*

While the preceding experiments demonstrated that the concurrent suppression of ITGA5, RDX, and RhoA impaired metastasis-relevant phenotypes in 231 cells *in vitro*, the consequences of concomitantly inhibiting these three proteins on the *in vivo* behavior of carcinoma cells remained unclear. Accordingly, I determined whether the simultaneous suppression of ITGA5, RDX, and RhoA impaired *in vivo* metastasis in a manner comparable to that triggered by ectopic miR-31 expression. In order to do so, I orthotopically implanted into the

mammary fat pads of mice 231 cells expressing either shRNAs against the mRNAs encoding

these three factors or, alternatively, a miR-31 expression vector. Consistent with my prior

findings (Valastyan et al., 2009a; Valastyan et al., 2009b), miR-31 enhanced primary mammary

tumor growth by 1.5-fold; in contrast, the combined shRNA-evoked suppression of ITGA5,

RDX, and RhoA failed to affect primary tumor size (Figure 2A).

After normalizing for differences in primary mammary tumor growth, miR-31-expressing

231 cells formed 95% fewer lung metastases than did controls in this assay; similarly, the

coordinate shRNA-conferred knockdown of ITGA5, RDX, and RhoA inhibited the incidence of

pulmonary metastatic lesions by 95% (Figure 2B). Cells concurrently expressing additional

combinations of shRNAs against alternative complementary sequences in the three targeted

mRNAs yielded identical results, implying that these effects were attributable specifically to the

ability of these shRNAs to reduce the levels of ITGA5, RDX, and RhoA (Supplementary Figure

4). Hence, the concomitant downregulation of endogenous ITGA5, RDX, and RhoA levels

closely phenocopied miR-31-imposed inhibition of metastasis in this xenograft assay.

Concurrent Knockdown of ITGA5, RDX, and RhoA Phenocopies the Influences of miR-31

on Local Invasion, Early Post-Intravasation Events, and Metastatic Colonization *in vivo*

Remaining unresolved, however, were the particular step(s) of the invasion-metastasis

cascade that were impaired due to the combined suppression of ITGA5, RDX, and RhoA in 231

cells. In my previous work, I observed that miR-31 impinges on three distinct steps of the

invasion-metastasis cascade *in vivo*: local invasion, one or more early post-intravasation events

(intraluminal viability, extravasation, and/or initial survival in distant tissues), and metastatic

colonization (Valastyan et al., 2009a; Valastyan et al., 2009b). Consequently, I evaluated

174

whether the coordinate shRNA-mediated suppression of ITGA5, RDX, and RhoA was sufficient to recapitulate one or more of miR-31's multiple effects on various discrete steps of the metastatic process.

To assess potential impacts on local invasion, I examined the histopathological appearance of orthotopically implanted primary mammary tumors. As before (Valastyan et al., 2009a; Valastyan et al., 2009b), control 231 cells formed invasive primary tumors, while miR-31 expression resulted in primary mammary tumors with a well-encapsulated phenotype (Figure 3A). Cells containing shRNAs directed against ITGA5, RDX, and RhoA formed non-invasive primary mammary tumors that were indistinguishable at a histopathological level from the tumors generated by miR-31-expressing cells (Figure 3A and Supplementary Figure 5A). Therefore, the concurrent suppression of ITGA5, RDX, and RhoA phenocopied the *in vivo* influences of miR-31 on local invasion.

Possible effects on early post-intravasation events were investigated by quantifying 231 cells in the lungs one day after intravenous injection via the tail vein. As anticipated (Valastyan et al., 2009a; Valastyan et al., 2009b), miR-31-expressing cells were five-fold impaired in terms of their ability to persist in the lungs at one day post-injection; cells with coordinately suppressed ITGA5, RDX, and RhoA levels owing to the simultaneous expression of shRNAs against these three mRNAs were also five-fold less prevalent than controls at this timepoint (Figure 3B and Supplementary Figure 5B). These outcomes were not attributable to differing abilities of the cells to become lodged initially in the lung microvasculature, as equal numbers of cells from each group were detected in the lungs 10 minutes after intravenous injection (Supplementary Figure 6). Instead, these observations indicated that the combined inhibition of ITGA5, RDX, and RhoA phenocopied the effects of miR-31 on early post-intravasation events in the lungs *in vivo*.

To evaluate putative effects on metastatic colonization, the sizes of subsequently arising lung metastases in intravenously injected mice were assessed at three months post-implantation. As expected (Valastyan et al., 2009a; Valastyan et al., 2009b), whereas control 231 cells generated robust macroscopic lung metastases, miR-31-expressing cells formed only small micrometastases (Figure 3C). Similarly, cells containing shRNAs concomitantly targeting ITGA5, RDX, and RhoA failed to spawn macroscopic metastases and generated only small micrometastases (Figure 3C and Supplementary Figure 5C). Hence, the simultaneous suppression of ITGA5, RDX, and RhoA phenocopied the *in vivo* consequences of miR-31 expression with respect to metastatic colonization.

Simultaneous Suppression of ITGA5, RDX, and RhoA Phenocopies miR-31-Mediated Inhibition of Experimental Metastasis *in vivo*

In this same intravenous injection assay, miR-31-expressing 231 cells formed 95% fewer lung metastases than did controls, while the concomitant shRNA-mediated suppression of ITGA5, RDX, and RhoA decreased the number of pulmonary metastatic lesions by 90% (Figure 4 and Supplementary Figure 7). Together, the preceding experiments indicated that the concurrent shRNA-mediated suppression of endogenous ITGA5, RDX, and RhoA levels was sufficient to phenocopy the full spectrum of miR-31's described influences on *in vivo* metastasis, including the effects of this miRNA on local invasion, early post-intravasation events, and metastatic colonization.

The Ability of Concomitant Suppression of ITGA5, RDX, and RhoA to Phenocopy the Influences of miR-31 on Metastasis-Relevant Traits is Not Confined to 231 Cells

It remained possible that the ability of concomitantly suppressed ITGA5, RDX, and RhoA to phenocopy miR-31's anti-malignant actions arose due to some peculiarity of 231 cells. To address this, I extended my analyses to SUM-159 human breast cancer cells. Like 231 cells, SUM-159 cells are highly aggressive *in vitro* and exhibit reduced invasiveness, motility, and anoikis resistance upon ectopic miR-31 expression (Valastyan et al., 2009a). I created SUM-159 cells that concurrently expressed shRNAs targeting the endogenous mRNAs encoding ITGA5, RDX, and RhoA, again utilizing multiple sequence-independent hairpins against an individual transcript (Supplementary Figure 8A). Of note, sequential infection with several distinct combinations of shRNAs against these three proteins resulted in reductions in endogenous ITGA5, RDX, and RhoA levels quite similar to the 50%-60% decreases in these three factors elicited by ectopic miR-31 expression in aggressive human breast cancer cells (Valastyan et al., 2009a). The simultaneous knockdown of ITGA5, RDX, and RhoA failed to alter the *in vitro* proliferative kinetics of SUM-159 cells (Supplementary Figure 8B), thus excluding potential confounding effects related to this parameter. Consistent with my observations in 231 cells, the concomitant suppression of ITGA5, RDX, and RhoA in SUM-159 cells impaired several *in vitro* surrogate markers of metastatic capacity, namely invasiveness through an artificial extracellular matrix (Supplementary Figure 8C), cell motility (Supplementary Figure 8D), and anoikis resistance (Supplementary Figure 8E). Thus, the ability of the simultaneous shRNA-conferred suppression of ITGA5, RDX, and RhoA to phenocopy the consequences of ectopic miR-31 expression on various cell-biologic attributes required for metastasis was not confined to 231 cells.

MATERIALS AND METHODS

Cell Culture, Plasmids, and Creation of Stable Cell Lines

GFP-labeled MDA-MB-231 cells were described (Valastyan et al., 2009a). SUM-159

cells were provided by S. Ethier, and cultured under conditions that I have delineated (Valastyan

et al., 2009a). miR-31 was expressed from pBABE-puro (Ma et al., 2007). Short hairpin RNAs

(shRNAs) targeting the mRNAs encoding Luciferase, ITGA5, RDX, or RhoA were expressed

from pLKO.1-puro (Open Biosystems); the sequences of these shRNAs hairpins are: shITGA5

#3, CCACTGTGGATCATCATCCTA; shITGA5 #4, CCTCAGGAACGAGTCAGAATT;

shITGA5 #5, CTCCTATATGTGACCAGAGTT; shRDX #3, GCCAGAGATGAAACCAAGAAA;

shRDX #4, GCAGACAATTAAAGCTCAGAA; shRDX #5, GCTAAATTCTTTCCTGAAGAT;

shRhoA #5, GAAAGCAGGTAGAGTTGGCTT. Stable expression of the indicated plasmids

was achieved via sequential retroviral or lentiviral transduction, followed by selection with

puromycin (Morgenstern and Land, 1990; Elenbaas et al., 2001). In the case of the Luciferase

shRNA hairpin, target cells were subjected to either a single complete infection protocol

("shLuc" cells) or, alternatively, to three sequential complete infection protocols ("shLuc +

shLuc + shLuc" cells); the latter strategy allowed me to obtain control cells containing

approximately the same total number of shRNA molecules as were present in the shITGA5 +

shRDX + shRhoA cells.

Invasion and Motility Assays

In the invasion assays, 1.0×10^5 cells were seeded in Matrigel-coated chambers with 8.0

_m pores (BD Biosciences); in the motility assays, 5.0×10^4 cells were plated atop uncoated

membranes with 8.0 _m pores (BD Biosciences). Cells were seeded in serum-free media, and

then were allowed to translocate toward complete growth media for 20 hours. Non-invaded or non-migrated cells were then physically removed by scraping. Successfully translocated cells were subsequently visualized using a Diff-Quick Staining Set (Dade) and manually counted under a light microscope.

Anoikis Assays

Anoikis resistance was measured by seeding 7.5×10^4 cells in 6-well ultra-low attachment plates (Corning). After 24 hours, cells were resuspended in 0.4% trypan blue (Sigma) and the proportion of viable cells was quantified using a hemocytometer.

Xenograft Studies

All animal studies complied with protocols approved by the MIT Committee on Animal Care. Age-matched NOD/SCID mice (propagated on-site) were employed in all xenograft experiments. For spontaneous metastasis assays, female mice were subjected to bilateral orthotopic injections into the mammary fat pads with 1.0×10^6 tumor cells resuspended in 1:2 Matrigel (BD Biosciences) plus normal growth media. For experimental metastasis assays, male mice were intravenously injected with 5.0×10^5 tumor cells (resuspended in PBS) via the tail vein. Lung metastasis was quantified at the indicated timepoints using a fluorescent dissecting microscope; these analyses were performed within three hours of specimen isolation. Tumor and lung histology was assessed by staining paraffin-embedded tissue sections with hematoxylin and eosin (H&E). In my studies, metastatic foci less than 50 _m in average diameter were classified as micrometastases; in contrast, macroscopic metastases were defined as metastatic lesions greater than 50 _m in average diameter.

Statistical Analyses

Data are presented as mean ± SEM from a representative experiment; each assay was independently repeated at least three times. Student's t-test was utilized for comparisons between groups, with $P < 0.05$ considered statistically significant.

Real Time RT-PCR

Total RNA, including small RNAs, was isolated with a *mir*Vana MicroRNA Isolation Kit (Ambion). RT-PCR-based detection of mature miRNAs and the 5S rRNA was achieved via utilization of a *mir*Vana MicroRNA Detection Kit and gene-specific primer sets (Ambion). For detection of GAPDH, ITGA5, RDX, and RhoA transcript levels, cDNA was prepared from 500 ng of total RNA using the SuperScript III First-Strand Synthesis System (Invitrogen), and subsequently quantified by SYBR Green real time RT-PCR (Applied Biosystems) using oligonucleotides that I have described previously (Valastyan et al., 2009b).

Immunoblotting

Cell lysates were resolved by NuPAGE gel electrophoresis (Invitrogen), transferred to a PVDF membrane, and probed with antibodies recognizing _-actin (Santa Cruz), ITGA5 (Santa Cruz), RDX (Cell Signaling), or RhoA (Abcam).

Measurements of *in vitro* Cell Proliferation

Unless otherwise indicated, cellular proliferation was evaluated by seeding 1.0×10^5 cells per well in 6-well plates. Total cell number was assessed every two to three days by trypsinization and manual counting with a hemocytometer. Alternatively, proliferative kinetics

were measured by seeding 5.0×10^2 cells per well in 96-well plates and then employing a CellTiter96 AQ$_{ueous}$ One Solution MTS Cell Proliferation Assay (Promega); cells were incubated with the MTS reagent for 1.5 hours, then total cell number was quantitated by measuring absorbance at 492 nm on a 96-well plate reader.

Oligonucleotide Sequences

Oligonucleotides employed in this study were: GAPDH RT-PCR, TCACCAGGGCTGCTTTTAAC and GACAAGCTTCCCGTTCTCAG; ITGA5 RT-PCR, AACTCATCATGGCCAGTGAGGGTAAGGGT and ATCCTTAATGGCTCAGACATTCGATCCCTCTACAACT; RDX RT-PCR, GAATCAGGAGCAGCTAGCAGCAGAACTT and TTGGTCTTTTCCAAGTCTTCCTGGGCTGCA; RhoA RT-PCR, AGGTGGATGGAAAGCAGGTAGAGTTGGCT and AGGATGATGGGCACGTTGGGACAGA.
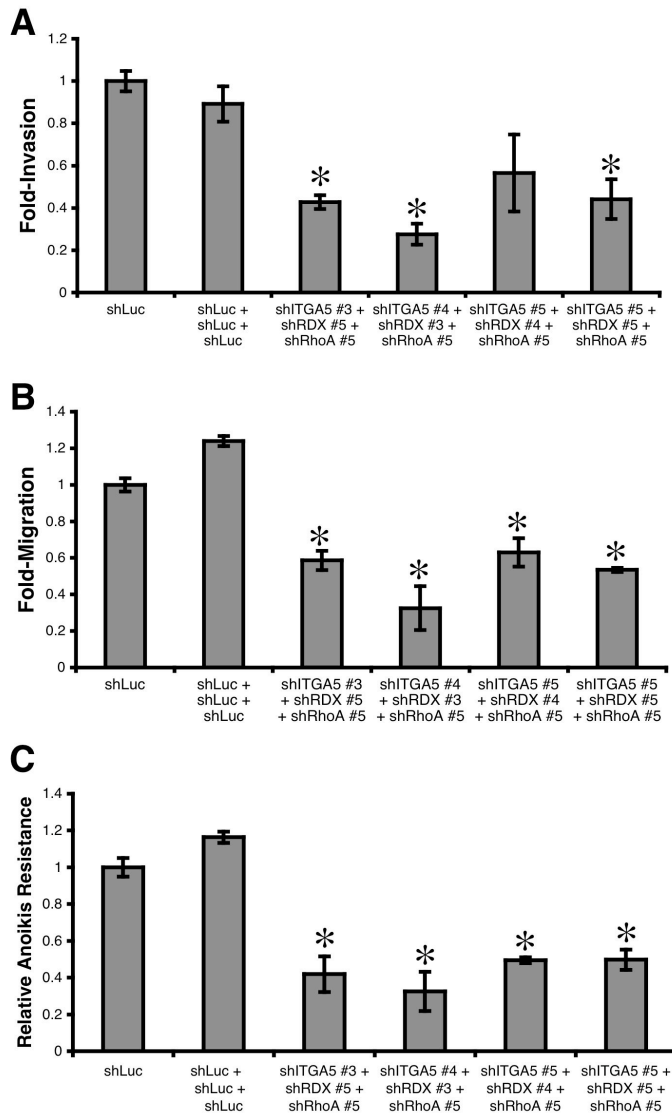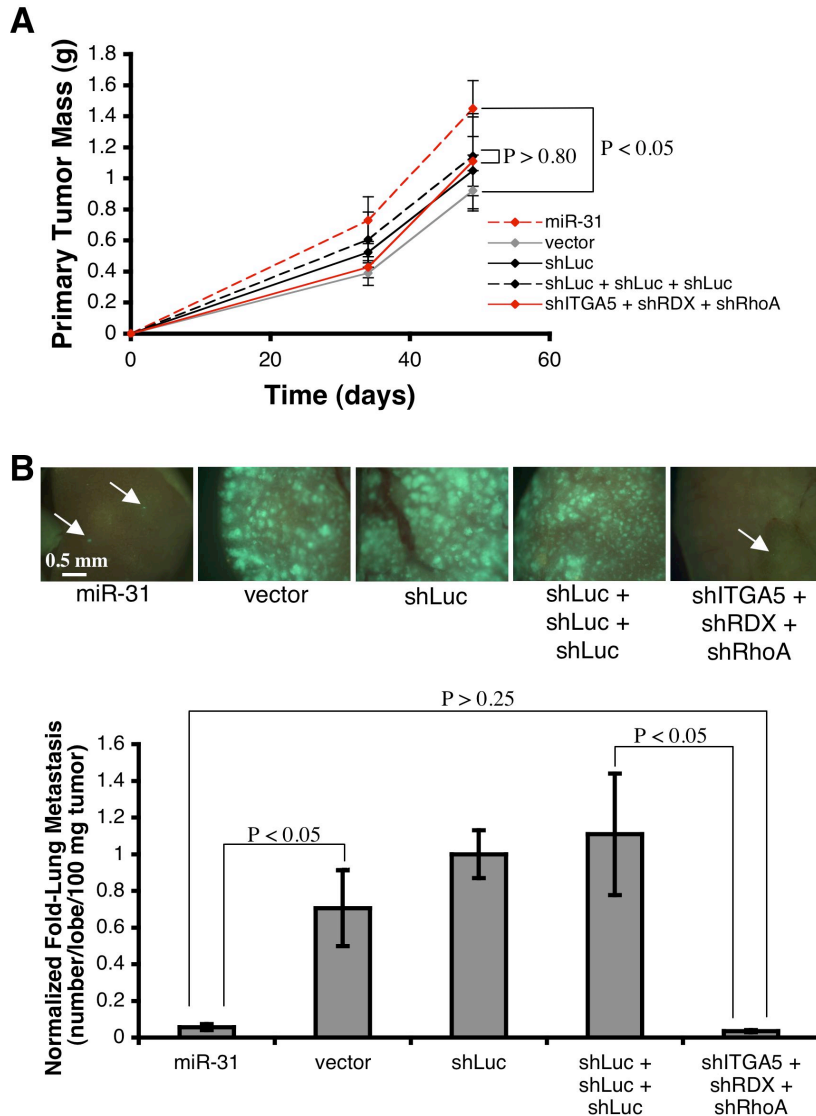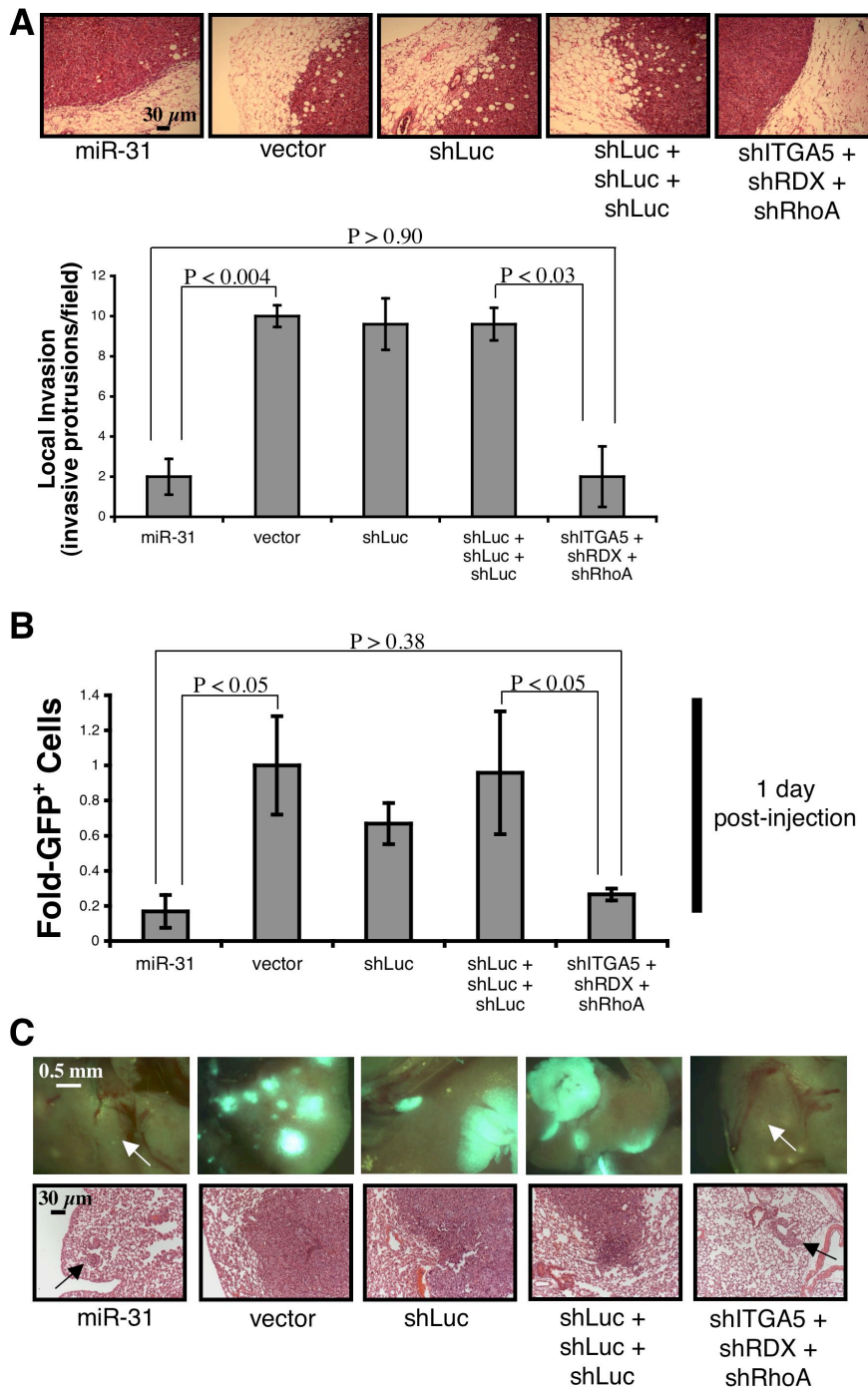
Figure 1

Figure 1. Simultaneous Suppression of ITGA5, RDX, and RhoA Impairs Metastasis-Relevant Traits *in vitro*. (A) Invasive capacity of 231 cells through Matrigel in a Boyden chamber transwell assay. n = 3. **(B)** Transwell motility assays employing 231 cells. n = 3. **(C)** Sensitivity of 231 cells to anoikis-mediated cell death after 24 hours of suspension culture. n = 3. Luc = Luciferase. Asterisks: P <0.05 relative to shLuc + shLuc + shLuc. Data are presented as mean ± SEM from a representative experiment; each assay was independently repeated at least three times.

Figure 2. Concomitant Suppression of ITGA5, RDX, and RhoA Phenocopies miR-31-

Evoked Inhibition of Spontaneous Metastasis *in vivo*. (A) Primary mammary tumor growth

kinetics upon orthotopic implantation of 231 cells. The experiment was terminated after seven

weeks due to primary tumor burden. n = 4. **(B)** Fluorescent images of murine lungs to visualize

231 cells 49 days after orthotopic injection (top panels). Quantification of metastatic burden

(bottom panel). Arrows: micrometastases. n = 4. Luc = Luciferase. shRNAs utilized: shITGA5

#5, shRDX #5, and shRhoA #5. Data are presented as mean ± SEM from a representative

experiment; each assay was independently repeated three times.

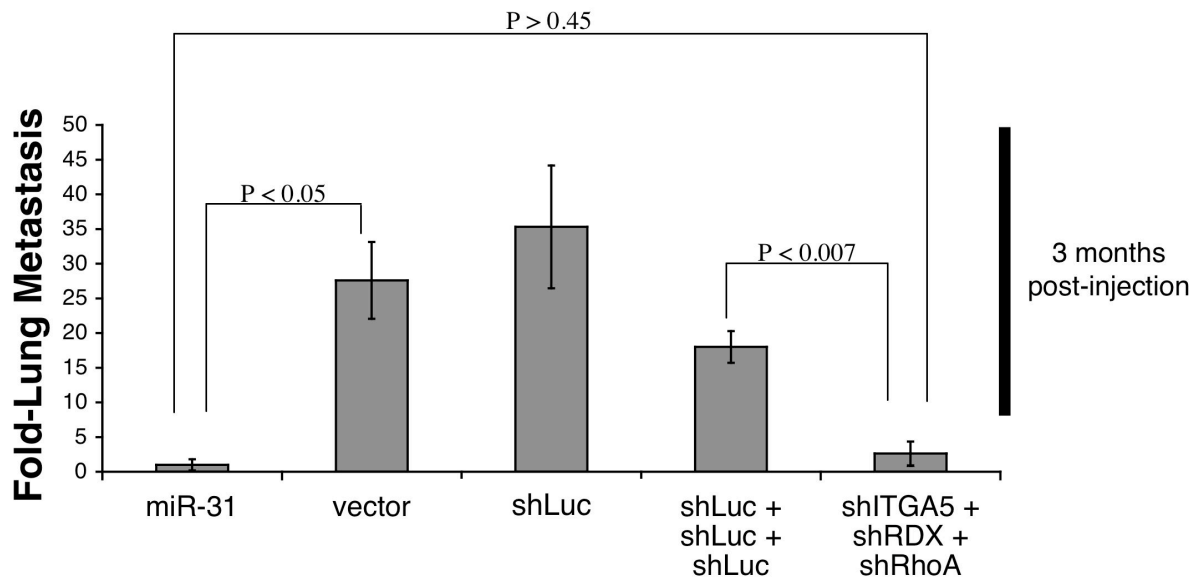Figure 3

Figure 3. Concurrent Knockdown of ITGA5, RDX, and RhoA Phenocopies the Influences

of miR-31 on Local Invasion, Early Post-Intravasation Events, and Metastatic Colonization

***in vivo*. (A)** H&E staining of 231 cell primary mammary tumors 34 days after orthotopic

implantation (top panels). Quantification of local invasion (bottom panel). n = 4. **(B)** Prevalence

of 231 cells in the lungs one day after intravenous introduction. n = 4. **(C)** Fluorescent images of

murine lungs to visualize 231 cells 84 days after tail vein injection (top panels). H&E staining of

lungs from animals implanted with the indicated tumor cells (bottom panels). Arrows:

micrometastases. n = 5. Luc = Luciferase. shRNAs utilized: shITGA5 #5, shRDX #5, and

shRhoA #5. Data are presented as mean ± SEM from a representative experiment; each assay

was independently repeated three times.
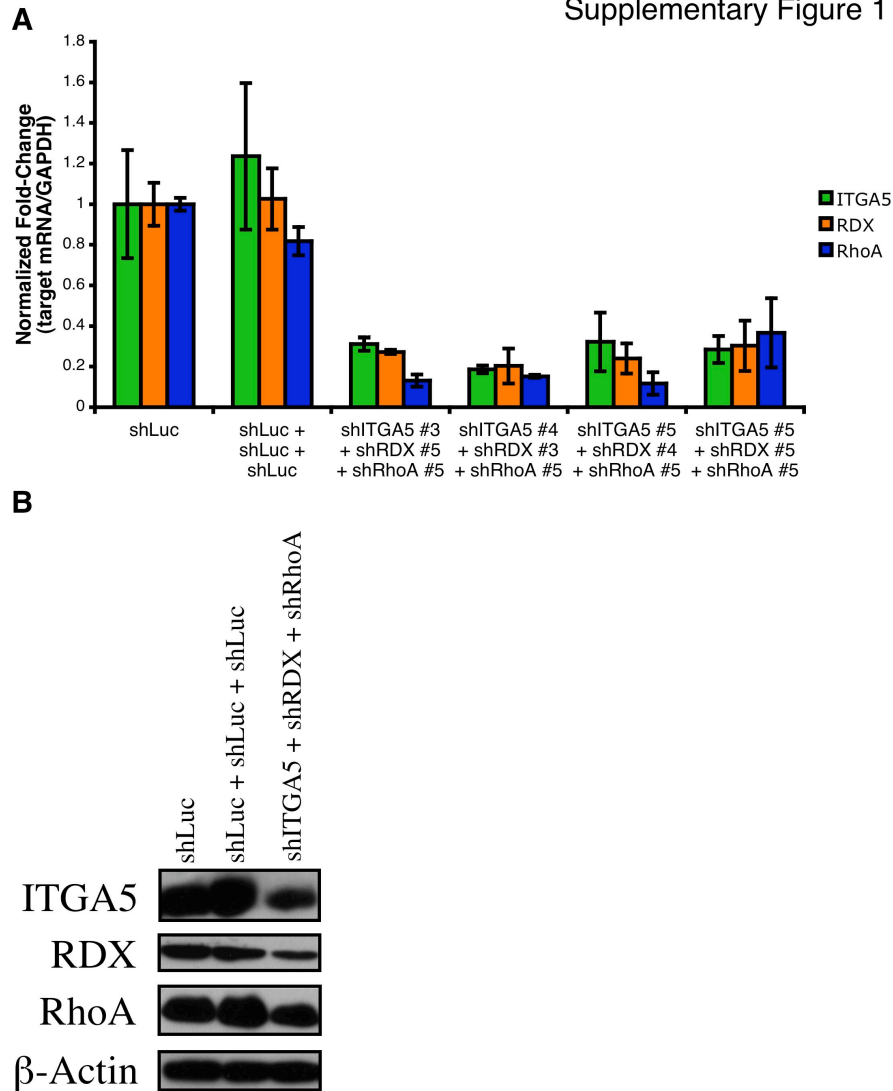
Figure 4

Figure 4. Simultaneous Suppression of ITGA5, RDX, and RhoA Phenocopies miR-31-Mediated Inhibition of Experimental Metastasis *in vivo*. Lung metastatic burden 84 days subsequent to intravenous injection of the indicated 231 cells. n = 5. Luc = Luciferase. shRNAs utilized: shITGA5 #5, shRDX #5, and shRhoA #5. Data are presented as mean ± SEM from a representative experiment; this assay was independently repeated three times.
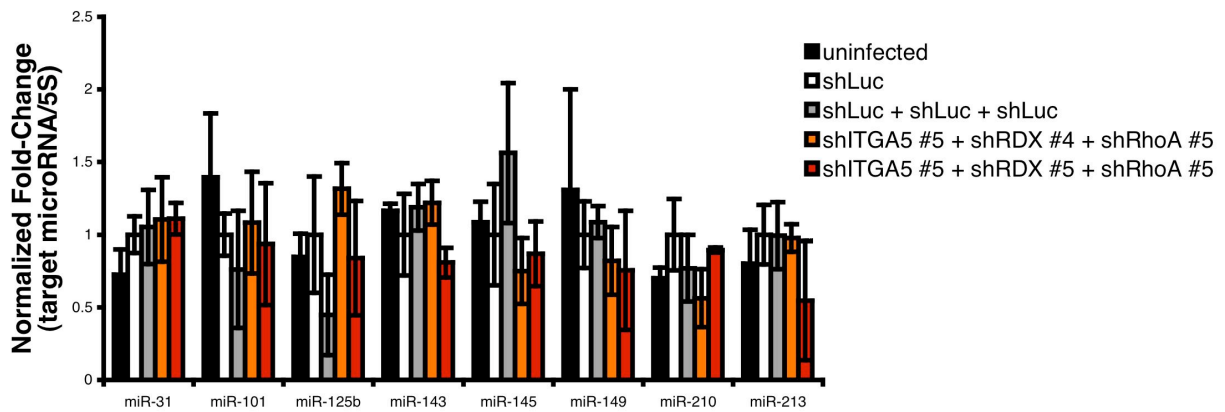
SUPPLEMENTARY FIGURES

Supplementary Figure 1. shRNA-Mediated Concurrent Suppression of ITGA5, RDX, and RhoA. (A) Real time RT-PCR for integrin _5 (ITGA5), radixin (RDX), and RhoA in the indicated MDA-MB-231 (231) cells. GAPDH was a loading control. n = 3. **(B)** Immunoblots for endogenous ITGA5, RDX, and RhoA in 231 cells infected as denoted. _-actin was a loading control. Short hairpin RNAs (shRNAs) utilized: shITGA5 #5, shRDX #5, and shRhoA #5. Luc = Luciferase. Data are presented as mean ± SEM from a representative experiment; each assay was independently repeated three times.
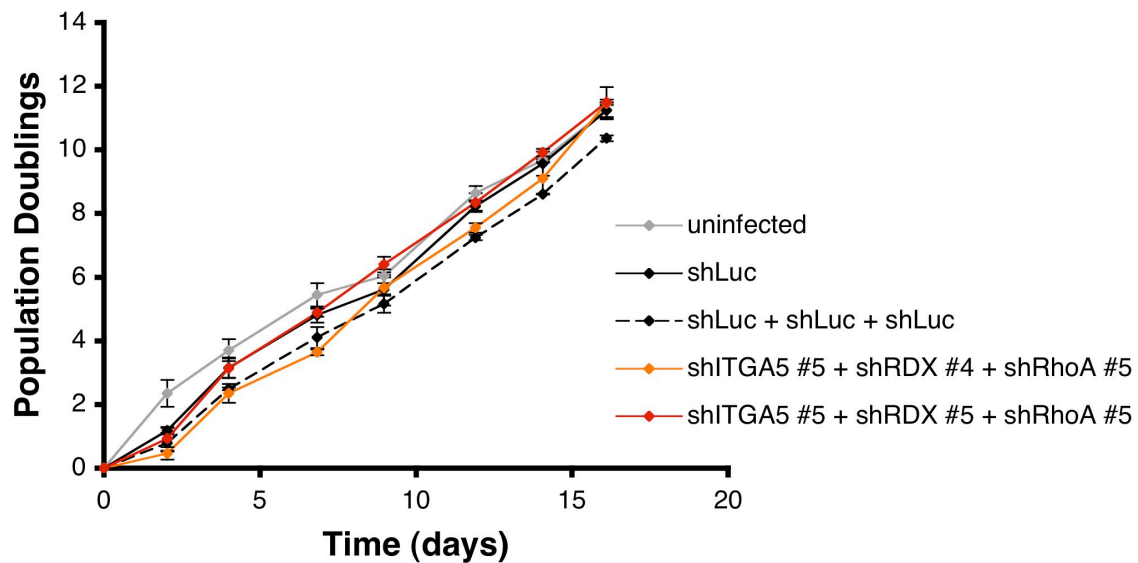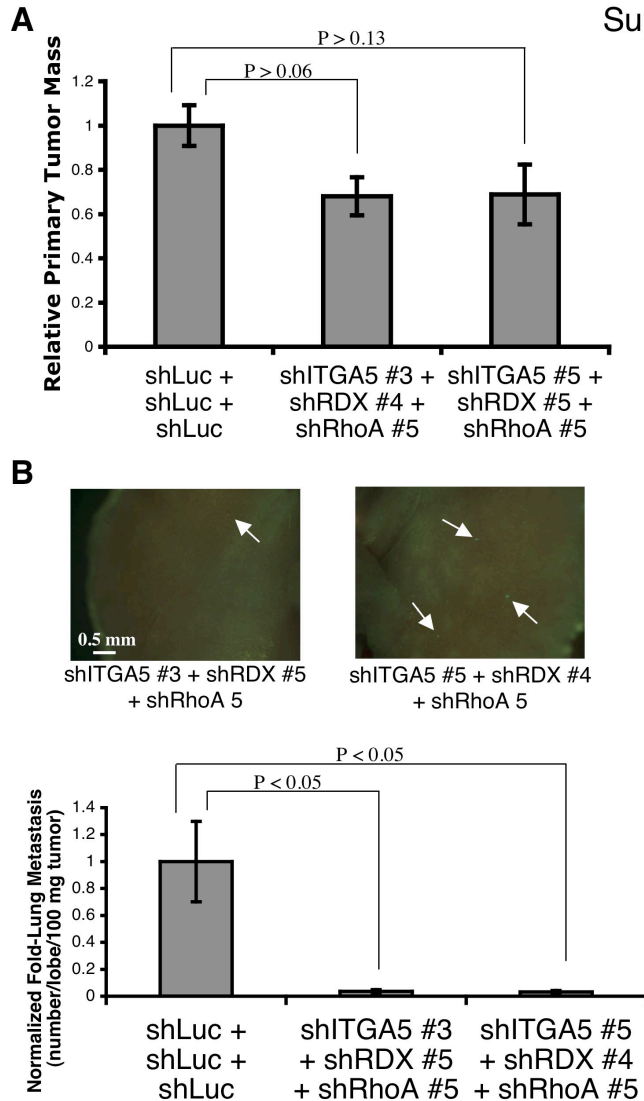
Supplementary Figure 2. shRNA Expression Does Not Interfere With MicroRNA

Biogenesis. Real time RT-PCR analysis of various mature microRNAs in the indicated 231 cells.

5S rRNA was a loading control. n = 3. Luc = Luciferase. All P-values are >0.12 relative to shLuc

+ shLuc + shLuc. Data are presented as mean ± SEM from a representative experiment; this

assay was independently repeated three times.

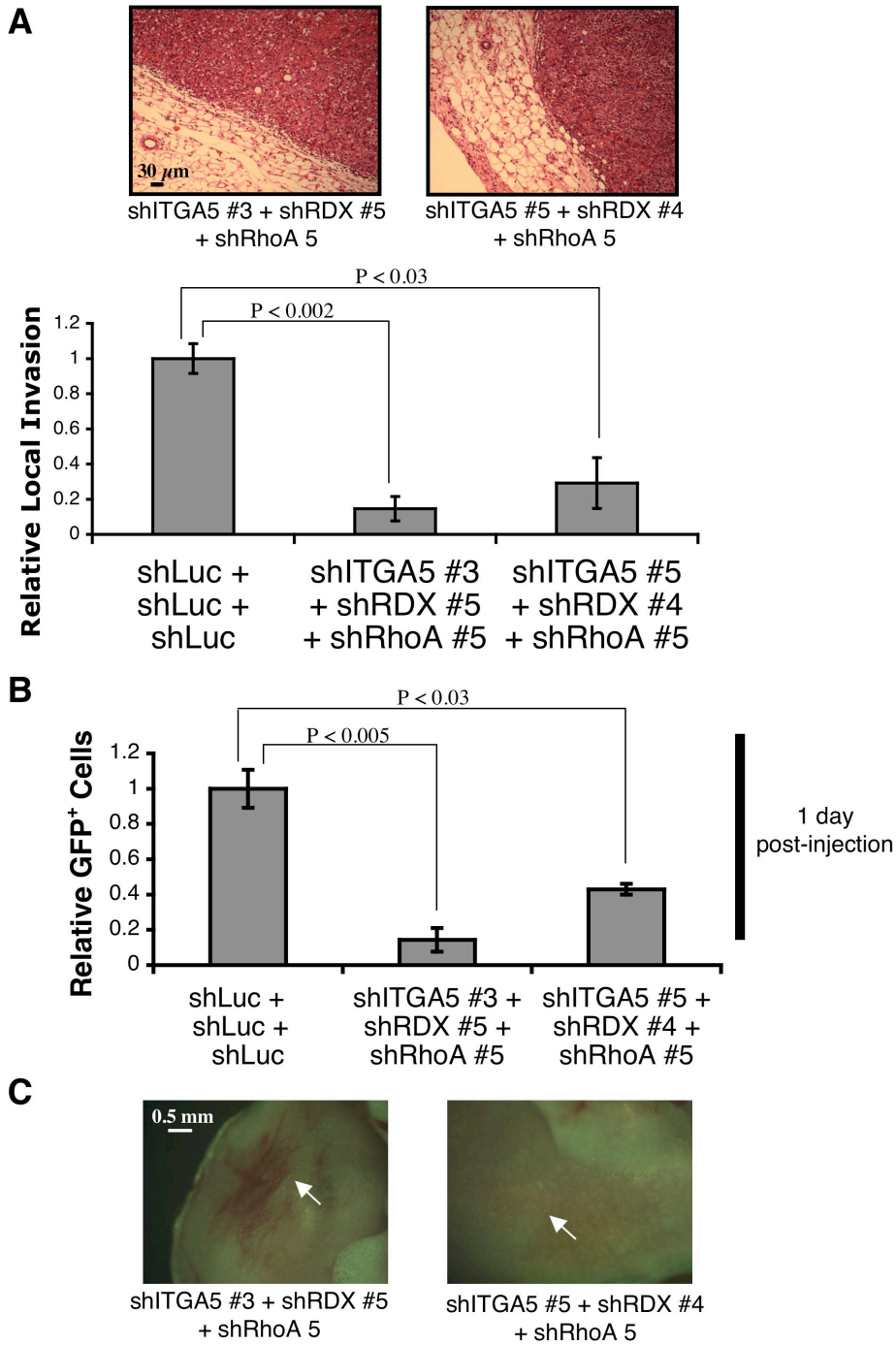**Supplementary Figure 3. Simultaneous Suppression of ITGA5, RDX, and RhoA Does Not Affect Proliferative Kinetics *in vitro*.** *In vitro* proliferation rates of the indicated 231 cells. n = 3. Luc = Luciferase. No statistically significant differences were observed relative to shLuc + shLuc + shLuc. Data are presented as mean ± SEM from a representative experiment; this assay was independently repeated three times.

A

Relative Primary Tumor Mass

P > 0.13

P > 0.06

shLuc + shLuc + shLuc

shITGA5 #3 + shRDX #4 + shRhoA #5

shITGA5 #5 + shRDX #5 + shRhoA #5

B

0.5 mm

shITGA5 #3 + shRDX #5 + shRhoA 5

shITGA5 #5 + shRDX #4 + shRhoA 5

Normalized Fold-Lung Metastasis (number/lobe/100 mg tumor)

P < 0.05

P < 0.05

shLuc + shLuc + shLuc

shITGA5 #3 + shRDX #5 + shRhoA #5

shITGA5 #5 + shRDX #4 + shRhoA #5

Supplementary Figure 4. Concomitant Suppression of ITGA5, RDX, and RhoA Phenocopies miR-31-Evoked Inhibition of Spontaneous Metastasis *in vivo*. (A) Relative primary tumor mass 49 days after orthotopic implantation of the indicated 231 cells. The assay was terminated after seven weeks due to primary tumor burden. n = 4. **(B)** Fluorescent images of murine lungs to visualize 231 cells 49 days after orthotopic injection (top panels). Quantification of metastatic burden (bottom panel). Arrows: micrometastases. n = 4. Luc = Luciferase. Data are presented as mean ± SEM from a representative experiment; each assay was independently repeated three times.

A

shITGA5 #3 + shRDX #5
+ shRhoA 5

shITGA5 #5 + shRDX #4
+ shRhoA 5

B

1 day
post-injection

C

shITGA5 #3 + shRDX #5
+ shRhoA 5

shITGA5 #5 + shRDX #4
+ shRhoA 5

Supplementary Figure 5. Simultaneous Knockdown of ITGA5, RDX, and RhoA

Phenocopies the Influences of miR-31 on Local Invasion, Early Post-Intravasation Events,

and Metastatic Colonization *in vivo*. (A) Hematoxylin and eosin staining of 231 cell primary

mammary tumors 34 days after orthotopic implantation (top panels). Quantification of local invasion (bottom panel). n = 5. **(B)** Prevalence of the indicated 231 cells in the lungs one day after intravenous introduction. n = 4. **(C)** Fluorescent images of murine lungs to visualize 231 cells 84 days after tail vein injection. Arrows: micrometastases. n = 5. Luc = Luciferase. Data are presented as mean ± SEM from a representative experiment; each assay was independently repeated three times.
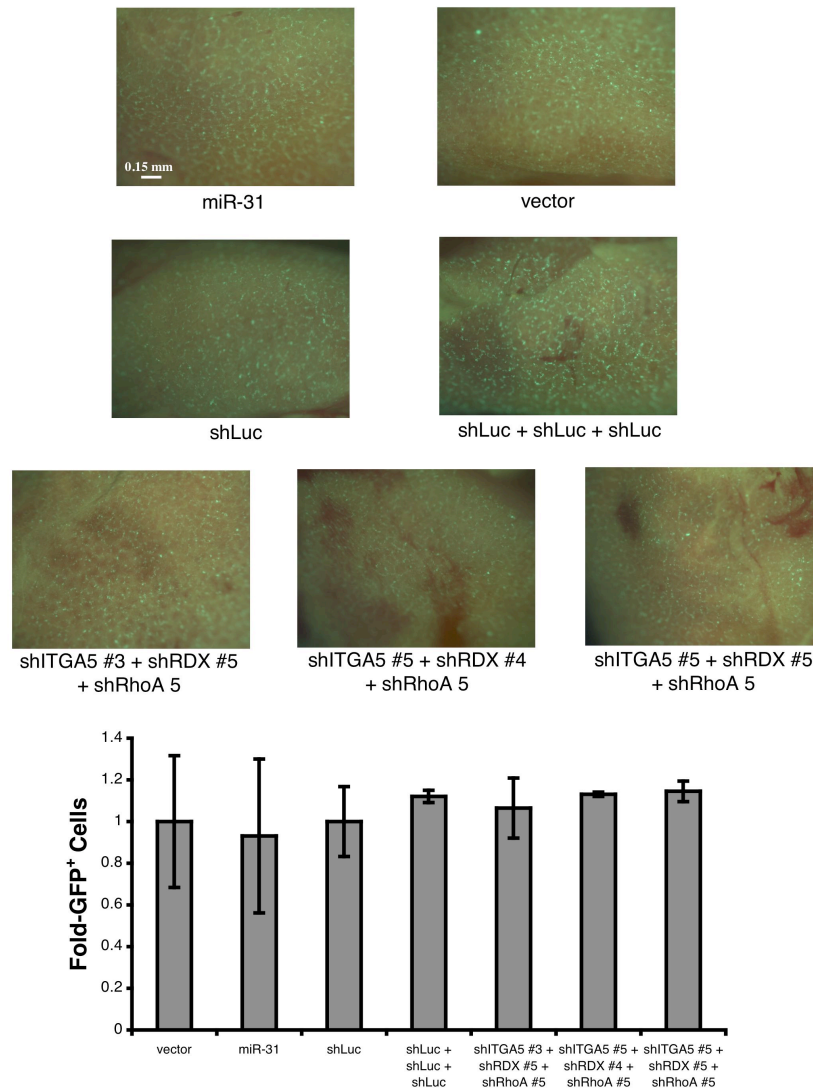
Supplementary Figure 6. Coordinate Suppression of ITGA5, RDX, and RhoA Fails to Affect the Initial Vascular Lodging of Intravenously Injected Cells *in vivo*. Fluorescent images of murine lungs to visualize the indicated 231 cells 10 minutes subsequent to tail vein injection (top panels). Quantification of the relative prevalence of these cells in the lungs (bottom panel). n = 3. Luc = Luciferase. All P-values are >0.77 relative to shLuc + shLuc + shLuc. Data are presented as mean ± SEM from a representative experiment; this assay was independently repeated three times.
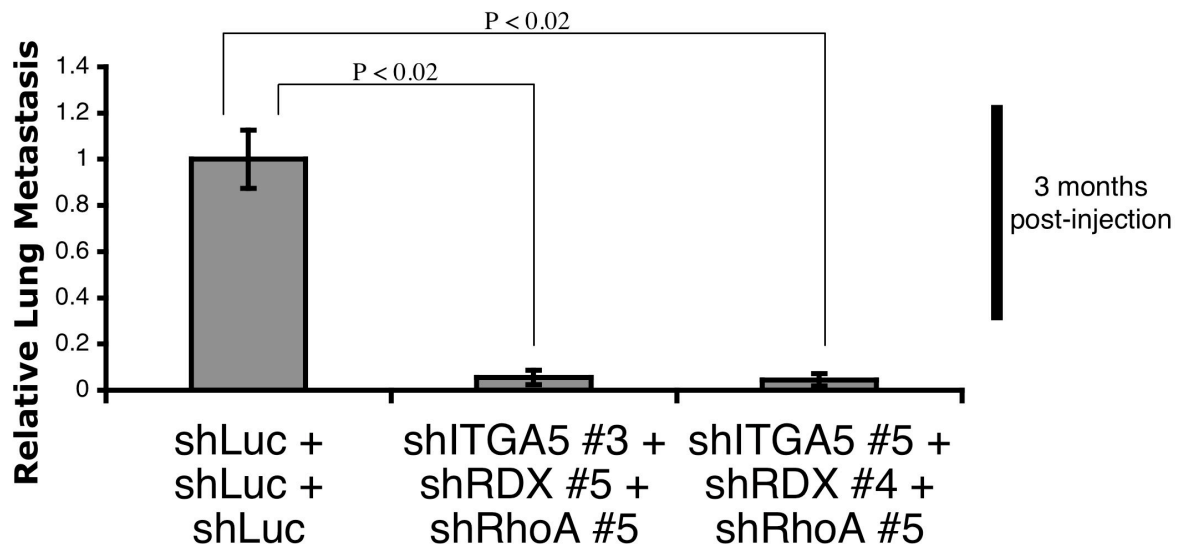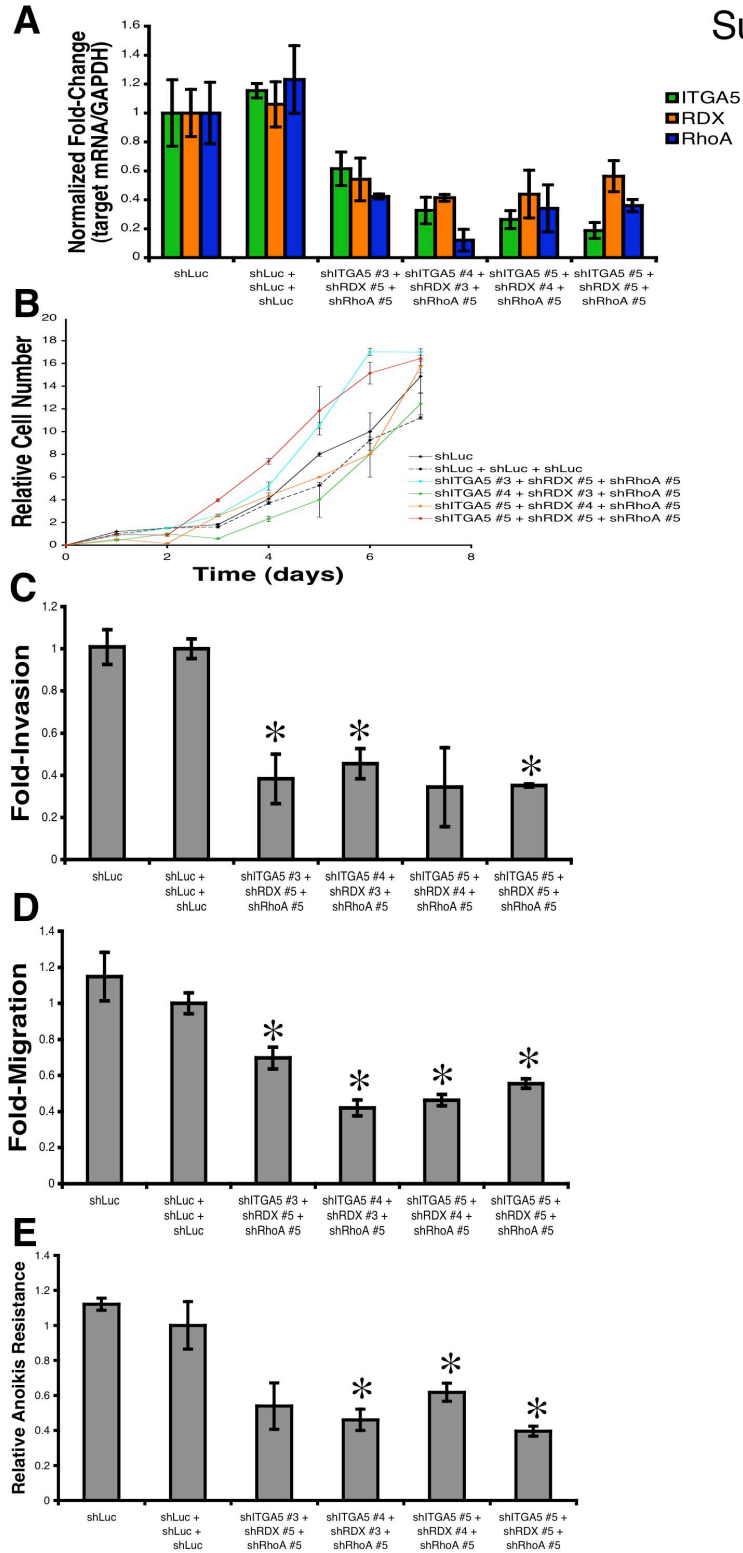
Supplementary Figure 7. Concurrent Suppression of ITGA5, RDX, and RhoA Phenocopies miR-31-Mediated Inhibition of Experimental Metastasis *in vivo*. Lung metastatic burden 84 days subsequent to intravenous injection. n = 5. Luc = Luciferase. Data are presented as mean ± SEM from a representative experiment; this assay was independently repeated three times.

Supplementary Figure 8. Simultaneous Suppression of ITGA5, RDX, and RhoA Impairs

Metastasis-Relevant Traits in SUM-159 Cells *in vitro*. (A) Real time RT-PCR for ITGA5,

RDX, and RhoA in the indicated SUM-159 cells. GAPDH was a loading control. n = 3. **(B)** *In vitro* proliferation of SUM-159 cells, as measured by an MTS assay. n = 3. **(C)** Invasive capacity of SUM-159 cells through Matrigel in a Boyden chamber transwell assay. n = 3. **(D)** Transwell motility assays employing SUM-159 cells. n = 3. **(E)** Sensitivity of SUM-159 cells to anoikis-mediated cell death after 24 hours of suspension culture. n = 3. Luc = Luciferase. Asterisks: P <0.05 relative to shLuc + shLuc + shLuc. Data are presented as mean ± SEM from a representative experiment; each assay was independently repeated at least three times.

ACKNOWLEDGMENTS

REFERENCES

Ambros V. (2004). The functions of animal microRNAs. Nature *431*, 350-355.

Bartel DP. (2004). MicroRNAs: Genomics, biogenesis, mechanism, and function. Cell *116*, 281-297.

Bartel DP. (2009). MicroRNAs: target recognition and regulatory functions. Cell *136*, 215-233.

Calin GA and Croce CM. (2006). MicroRNA signatures in human cancers. Nat Rev Cancer *6*, 857-866.

Elenbaas B, Spirio L, Koerner F, et al. (2001). Human breast cancer cells generated by oncogenic transformation of primary mammary epithelial cells. Genes Dev *15*, 50-65.

Esquela-Kerscher A, Slack FJ. (2006). Oncomirs - microRNAs with a role in cancer. Nat Rev Cancer *6*, 259-269.

Fidler IJ. (2003). The pathogenesis of cancer metastasis: the 'seed and soil' hypothesis revisited. Nat Rev Cancer *3*, 453-458.

Grimm D, Streetz KL, Jopling CL, et al. (2006). Fatality in mice due to oversaturation of cellular microRNA/short hairpin RNA pathways. Nature *441*, 537-41.

Gupta GP and Massagué J. (2006). Cancer metastasis: building a framework. Cell *127*, 679-695.

Ma L, Teruya-Feldstein J, and Weinberg RA. (2007). Tumour invasion and metastasis initiated by microRNA-10b in breast cancer. Nature *449*, 682-688.

Morgenstern JP and Land H. (1990). Advanced mammalian gene transfer: high titre retroviral vectors with multiple drug selection markers and a complementary helper-free packaging cell line. Nucleic Acids Res *18*, 3587-3596.

Sotiropoulou G, Pampalakis G, Lianidou E, and Mourelatos Z. (2009). Emerging roles of microRNAs as molecular switches in the integrated circuit of the cancer cell. RNA *15*, 1443-1461.

Valastyan S, Benaich N, Chang A, et al. (2009b). Concomitant suppression of three target genes can explain the impact of a microRNA on metastasis. Genes Dev *23*, 2592-2597.

Valastyan S, Reinhardt F, Benaich N, et al. (2009a). A pleiotropically acting microRNA, miR-31, inhibits breast cancer metastasis. Cell *137*, 1032-1046.

Valastyan S and Weinberg RA. (2009). MicroRNAs: crucial multi-tasking components in the complex circuitry of tumor metastasis. Cell Cycle *8*, 3506-3512.

Ventura A and Jacks T. (2009). MicroRNAs and cancer: short RNAs go a long way. Cell *136*, 586-591.

Chapter 5

Restoration of miR-31 Function in Already-Established Metastases Elicits Metastatic Regression *in vivo*

Scott Valastyan[1,2], Amelia Chang[1,2], Ferenc Reinhardt[1], Nathan Benaich[1,3], and Robert A. Weinberg[1,2,4]

[1]Whitehead Institute for Biomedical Research, Cambridge, MA 02142, USA
[2]Department of Biology, Massachusetts Institute of Technology, Cambridge, MA 02139, USA
[3]Department of Biology, Williams College, Williamstown, MA 01267, USA
[4]MIT Ludwig Center for Molecular Oncology, Cambridge, MA 02139, USA

A. Chang is an MIT undergraduate who assisted with several experiments. F. Reinhardt provided technical assistance for the mouse studies. N. Benaich is a Williams College summer student who assisted with several experiments. R.A. Weinberg supervised the research and assisted with the writing of the manuscript. All other experiments, data analysis, and writing were carried out by the thesis author, S. Valastyan.

INTRODUCTION

Distant metastases, rather than the primary tumors from which these malignant lesions originate, are responsible for greater than 90% of human cancer-associated mortality (Fidler, 2003; Gupta and Massagué, 2006). Consequently, as was discussed previously in Chapter One, our ability to effectively manage and treat human neoplasias is dependent on our capacity to either prevent or reverse the process of metastasis.

It has been widely believed that agents that effectively target any step of the invasion-metastasis cascade – the complex process whereby tumor cells disseminate from their primary site of growth, travel to a distant organ, and then survive and thrive within an ectopic microenvironment – should be capable of conferring measurable therapeutic responses in human cancer patients with advanced disease (Fidler, 2003; Gupta and Massagué, 2006). However, existing clinical data reveal little anti-metastatic benefit upon the administration of compounds designed to block the initial escape of neoplastic cells from primary tumors (Coussens et al., 2002; Steeg, 2006; Smith and Theodorescu, 2009). This finding can be rationalized by the observation that many cancer patients already harbor significant numbers of disseminated tumor cells in their bloodstream, bone marrow, and distant organ sites when they initially present with their disease (Nagrath et al., 2007; Hüsemann et al., 2008; Pantel et al., 2008); hence, the putative precursor cells of overt metastases can disseminate relatively early during the course of tumor progression. Consequently, it is now increasingly appreciated that effective anti-metastatic therapeutics must be capable of impairing the survival and proliferation of already-disseminated tumor cells. Unfortunately, few examples of compounds exemplifying these attributes have been identified (Steeg, 2006; Smith and Theodorescu, 2009). Instead, many anti-metastatic agents currently in pre-clinical or clinical testing impede the initial dissemination of neoplastic cells

without influencing the behavior of already-seeded metastases (Coussens et al., 2002; Steeg, 2006; Smith and Theodorescu, 2009; Ma et al., 2010).

As described in Chapter One, microRNAs (miRNAs) have recently emerged as crucial regulators of a variety of physiologic and pathologic processes (Bartel, 2009), including carcinoma development and subsequent metastatic progression (Ventura and Jacks, 2009; Valastyan and Weinberg, 2009). As I have outlined in Chapter Two and Chapter Three, miR-31 is a pleiotropically acting miRNA that functions as a potent suppressor of breast cancer metastasis without exerting inhibitory influences on primary tumor growth (Valastyan et al., 2009a; Valastyan et al., 2009b). Data presented in Chapter Two and Chapter Three indicate that the anti-metastatic activities of miR-31 are attributable to its ability – when constitutively expressed – to impair at least three distinct steps of the invasion-metastasis cascade: local invasion, one or more early post-intravasation events (intraluminal viability, extravasation, and/or initial survival in the parenchyma of a distant tissue), and metastatic colonization (Valastyan et al., 2009a; Valastyan et al., 2009b). Thus, constitutive miR-31 expression impeded the post-intravasation survival and proliferation of disseminated tumor cells. These prior findings – when coupled with the clinical data concerning requirements for effective anti-metastatic therapeutic strategies enumerated above – prompted me to investigate whether the temporally controlled, acute re-activation of miR-31 in already-established metastases might elicit anti-metastatic therapeutic responses *in vivo*.

RESULTS

Re-Activation of miR-31 Triggers the Regression of Already-Established Experimental Metastases *in vivo*

In order to determine the consequences of acutely restoring miR-31 function, I utilized a doxycycline (dox)-inducible miR-31 expression vector system (Supplementary Figure 1A). As anticipated (Valastyan et al., 2009a), when these vectors were introduced into otherwise-metastatic MDA-MB-231 human breast cancer cells ("231 cells") – which are essentially devoid of endogenous miR-31 expression (Valastyan et al., 2009a) – I observed dox-dependent inhibition of several *in vitro* surrogate markers of metastatic proficiency (invasion through an artificial extracellular matrix, cell motility, and resistance to anoikis-mediated cell death) (Supplementary Figures 1B-1D). In contrast, acute induction of miR-31 expression failed to alter the *in vitro* proliferative kinetics of 231 cells (Supplementary Figure 1E). These findings established that my dox-inducible system closely recapitulated the previously observed influences of constitutive miR-31 expression on malignant cellular behaviors.

I next exploited my ability to precisely control the timing of miR-31 re-expression in carcinoma cells to gauge the impact of restoring miR-31 function in already-disseminated 231 cells at various timepoints subsequent to their implantation *in vivo*. To this end, I intravenously injected these cells into mice and then re-activated miR-31 at various intervals post-implantation via dox administration. More specifically, I re-expressed miR-31 either (1) at no point during the study, (2) for the entire duration of the experiment, (3) only after the formation of small micrometastases at one month following implantation, (4) subsequent to the creation of moderately sized macroscopic metastases at two months after injection, or (5) only following the establishment of very large macroscopic metastases at three months post-implantation (Figure

1A). I then assayed the effects of miR-31-based therapeutic intervention on lung metastatic burden.

Consistent with my prior findings (Valastyan et al., 2009a), in the absence of miR-31 expression, the implanted 231 cells formed numerous robustly growing macroscopic metastases within three months of their intravenous introduction; also anticipated was the observation that persistent expression of miR-31 for the entire duration of the assay substantially impaired both the overall number of pulmonary metastases and their metastatic colonization efficiency (i.e., the proportion of disseminated metastatic cells that were capable of re-initiating their proliferative program in order to form macroscopic malignant lesions) (Figures 1B-1D). These differences in metastatic potential were not attributable to a failure of the dox-treated cells to become lodged initially in the lung microvasculature, as equal numbers of cells from each group were detected in the lungs 10 minutes subsequent to intravenous injection (Supplementary Figure 2).

Of interest, I discovered that if miR-31 was not expressed for the first month after intravenous implantation in order to permit the formation of small micrometastases by the 231 cells – but was then re-introduced for the following two months of the experiment – strong anti-metastatic responses were still evoked (Figures 1B-1D). I also evaluated the consequences of re-activating miR-31 in already-robustly growing macroscopic metastases; quite remarkably, even when miR-31 was expressed for only the final seven days of a three-month xenograft assay, a significant reduction was observed in both the total number of metastatic foci and the relative prevalence of macroscopic metastases among these pulmonary lesions (Figures 1B-1D). Taken together, these findings suggested that an intervention approach involving the re-activation of miR-31 in already-established metastases sufficed to elicit anti-metastatic therapeutic responses *in vivo*.

Acute Re-Expression of miR-31 Reverses the Invasiveness of Primary Mammary Tumors and Elicits the Regression of Already-Established Spontaneous Metastases *in vivo*

The intravenous injection strategy utilized above affords a means by which to compare post-extravasation proliferation kinetics due to the synchronous nature of initial dissemination in this assay. However, this approach does not recapitulate the full sequence of events required for *de novo* metastasis formation *in vivo*, because it circumvents the initial steps of local invasion and intravasation (Fidler, 2003; Gupta and Massagué, 2006). Accordingly, in order to measure the effects of the temporally controlled re-activation of miR-31 on the entirety of the invasion-metastasis cascade, I next implanted the dox-inducible miR-31-expressing cells orthotopically into the mammary fat pads of mice. The expression of this miRNA was then restored at defined intervals subsequent to implantation.

In particular, miR-31 was re-expressed either (1) at no point during the experiment, (2) for the entire course of the study, (3) only after a relatively modest number of metastatic cells had already reached the lungs at one month post-injection, (4) subsequent to the formation of a large number of pulmonary metastases at six weeks after implantation, or (5) only following the establishment of a near-saturating metastatic burden in the lungs at two months subsequent to injection (Figure 2A). Importantly, at all three of the timepoints selected for intervention, the implanted carcinoma cells had already formed primary mammary tumors that displayed extensive histopathological evidence of local stromal invasion (Valastyan et al., 2009a). The consequences of miR-31-dependent therapeutic intervention on both primary mammary tumor development and subsequent metastatic progression were then assessed.

Re-activation of miR-31 at any of the assayed timepoints failed to alter the growth kinetics of 231 cell primary mammary tumors (Figure 2B). The absence of an effect on primary

tumor size did not arise due to a failure in the dox-mediated upregulation of miR-31 in these orthotopically implanted cells (Supplementary Figure 3). Moreover, the miR-31 molecules produced upon dox-controlled induction were indeed functionally active, as gauged by their ability to suppress endogenous levels of the known (Valastyan et al., 2009a; Valastyan et al., 2009b) miR-31 downstream target genes integrin _5 (ITGA5), radixin (RDX), and RhoA *in vivo* (Supplementary Figure 4). Notably, together these observations indicated that acute re-expression of miR-31 did not elicit general cytostatic or cytotoxic responses in carcinoma cells growing *in vivo*; stated differently, the effects of miR-31 re-activation on already-established metastases – as described above and again below – could not be ascribed to generic, context-independent anti-proliferative or pro-apoptotic influences.

Despite the lack of significant changes in their overall sizes, histological examination of these 231 cell primary mammary tumors revealed stark differences upon the acute re-introduction of miR-31. Consistent with my prior observations (Valastyan et al., 2009a), control cells yielded primary mammary tumors that demonstrated clear histopathological evidence of invasion into the surrounding stroma; in contrast, those primary tumors formed by cells that expressed miR-31 for the entire duration of the experiment had a well-encapsulated appearance and were largely non-invasive (Figures 2C and 2D). Interestingly, if miR-31 was not expressed for the first month of the experiment in order to allow for the formation of poorly encapsulated primary mammary tumors – but was then re-activated for the remainder of the study – the histopathological appearance of these primary tumors was converted from an invasive phenotype to a largely non-invasive phenotype (Figures 2C and 2D). Similarly, reversal of the invasive histological presentation of 231 cell primary mammary tumors was observed when miR-31 was re-expressed beginning at six weeks post-implantation (Figures 2C and 2D). In contrast,

however, I found no discernible change in primary mammary tumor histology when miR-31 was re-expressed for only the final seven days of a two-month xenograft experiment (Figures 2C and 2D). Taken together, these data revealed that acute re-activation of miR-31 in already-established primary mammary tumors was capable of reversing their invasiveness *in vivo*.

In this same orthotopic injection experiment, I also determined the effects of acutely re-expressing miR-31 on the formation of distant metastases. In these studies, systemic administration of dox to the animals resulted in the induction of miR-31 expression in implanted carcinoma cells present at both their initial site of injection in the mammary fat pads and in those tumors cells that had already disseminated to distant organ sites. For this reason – in contrast to the situation encountered in my intravenous implantation assays – it is likely that any anti-metastatic therapeutic responses observed in this orthotopic injection strategy reflect a combination of the influences of re-introduced miR-31 on the initial escape of neoplastic cells from primary mammary tumors and the ability of this miRNA to affect the fate of already-disseminated tumor cells.

As anticipated (Valastyan et al., 2009a), in the absence of miR-31 expression, the 231 cells formed large numbers of pulmonary metastases within two months of orthotopic implantation; also expected was my finding that metastasis was strongly impaired when miR-31 was expressed for the entire duration of the assay (Figures 2E and 2F). Notably, if miR-31 was not expressed for the first month of the experiment – thereby permitting the establishment of pulmonary micrometastases – but was then re-activated for the remaining one month of the assay, a substantial reduction in metastasis formation was observed (Figures 2E and 2F). In contrast, however, re-expression of miR-31 only at later timepoints failed to diminish the number of pulmonary metastatic foci in a statistically significant manner (Figures 2E and 2F).

Consequently, these data indicated that acute re-activation of miR-31 in already-established primary tumors and distant metastases was sufficient to evoke anti-metastatic therapeutic benefits *in vivo*, with these effects occurring in the absence of potentially confounding influences on the proliferation and survival of the corresponding primary mammary tumors.

Re-Activation of miR-31 Triggers Cell Cycle Arrest and Apoptosis in Already-Established Metastases *in vivo*

I next undertook to determine the cellular mechanisms underlying the anti-metastatic therapeutic responses observed upon acute re-expression of miR-31. To do so, I performed immunohistochemical staining on tissue sections derived from animals bearing the dox-inducible 231 cells for established markers of neo-vascularization, cell cycle progression, and apoptotic cell death. Re-activation of miR-31 failed to impact vascular density within the pulmonary metastases (Supplementary Figure 5). However, regardless of the timepoint at which miR-31 expression was induced, restoring the function of this miRNA diminished the proportion of disseminated tumor cells in the lungs that were actively dividing (Figures 3A and 3B). Moreover, an increased rate of apoptosis was elicited when miR-31 was re-activated specifically in already-macroscopic metastases (Figures 3C and 3D). Importantly, these anti-proliferative and pro-apoptotic responses were not attributable to general cytostatic or cytotoxic influences stemming from acute miR-31 expression, since re-activation of miR-31 in 231 cell primary mammary tumors failed to impair either cell cycle progression or cell viability (Figures 3E and 3F); in fact, miR-31 re-expression enhanced the proportion of cells in these primary mammary tumors that were actively dividing, in consonance with my previous findings (Valastyan et al., 2009a). Collectively, these observations revealed that miR-31 was capable of utilizing multiple distinct

cellular mechanisms to antagonize the metastatic outgrowth of already-disseminated tumor cells *in vivo*; additionally, these therapeutic responses arose specifically within the context of the foreign microenvironment afforded by a metastatic locus.

Given the striking reductions in total metastatic burden observed upon miR-31 re-activation, I was surprised by the relatively modest effects on cell cycle arrest and apoptosis triggered by miR-31 re-expression. I reasoned that this might derive from impaired dox-dependent activation of miR-31 in the remaining – ostensibly unaffected – metastatic foci. To address this possibility, I attempted to detect dox-refractory subpopulations within dox-treated tumor cells by performing *in situ* hybridizations for miR-31 in tissue sections prepared from animals bearing the dox-inducible 231 cells. Indeed, disseminated tumor cells in the lungs that had been exposed to dox for one month or longer were greatly impaired in their ability to properly induce miR-31 expression in response to dox administration (Figures 3G and 3H). Moreover, when the proportion of cells that expressed miR-31 in response to dox treatment was compared between animal-matched primary mammary tumors and pulmonary metastases, I found that a lower percentage of cells in the distant metastases appropriately induced miR-31 in response to dox treatment relative to the dox-dependent re-expression that occurred in the primary breast tumors from which these malignant lesions were initially spawned (Supplementary Figure 6). Thus, it appeared that a substantial fraction of the residual pulmonary metastases present in the lungs of animals bearing the dox-inducible miR-31-expressing cells achieved a selective advantage by losing their ability to properly re-activate miR-31 in response to dox treatment. Additionally, the presence of a significant dox-unresponsive subpopulation provided a plausible rationale for the observed only partial induction of cell cycle arrest and apoptosis upon the administration of dox.

Acute Restoration of Endogenous miR-31 Function Prevents the Outgrowth of Already-Established Experimental Metastases and Reduces Overall Metastatic Burden *in vivo*

It remained possible that the observed anti-metastatic therapeutic benefits resulting from acute miR-31 re-expression arose due to some peculiarity of either 231 cells or my miR-31 ectopic expression strategy. To address these possibilities, I evaluated the consequences of acutely restoring endogenous miR-31 function in an appropriate independent cell line; this was achieved by creating a dox-repressible modified miR-31 miRNA sponge vector system. miRNA sponges function as competitive inhibitors of miRNA activity by sequestering miRNAs, thereby diverting them from their endogenous mRNA targets (Ebert et al., 2007; Valastyan et al., 2009a). The dox-repressible miR-31 sponge system was introduced into otherwise-non-metastatic MCF7-Ras human breast cancer cells – a cell line that expresses endogenous miR-31 and in which constitutive miR-31 sponge expression confers metastatic competence (Valastyan et al., 2009a). Indeed, miR-31 activity was impaired specifically in the absence of dox treatment (Supplementary Figure 7A). As anticipated (Valastyan et al., 2009a), this inhibition of endogenous miR-31 function enhanced various *in vitro* surrogate markers of metastatic capacity (invasion, motility, and anoikis resistance) without impacting the proliferative rates of these cells *in vitro* (Supplementary Figures 7B-7E).

Moreover, when these dox-repressible miR-31 sponge-expressing MCF7-Ras cells were injected intravenously into mice, acute restoration of endogenous miR-31 function in already-established micrometastases both reduced the total number of metastatic foci and prevented the successful outgrowth of remaining lesions into large macroscopic metastases (Figure 4). These influences were not attributable to differing abilities of these various cells to lodge initially in the lung microvasculature (Supplementary Figure 8). Robust repression of the miR-31 sponge

persisted for the entire duration of the assay in a dox-dependent manner (Supplementary Figure 9). Assessed collectively, these findings revealed that the anti-metastatic therapeutic responses observed upon acute restoration of miR-31 function in already-seeded metastases did not arise solely in 231 cells, nor were these effects confined to approaches in which miR-31 was ectopically re-expressed.

MATERIALS AND METHODS

Plasmid Construction

The reverse tetracycline-controlled transactivator (rtTA) was expressed from the FUdeltaGW lentiviral vector (Maherali et al., 2008), while the lentiviral vector pTK365 carried the tetracycline-controlled transactivator (tTA) (Haack et al., 2004). miR-31 and the miRNA sponge constructs were expressed from the pTK380 lentiviral vector (Haack et al., 2004). The pISO firefly luciferase normalization control plasmid and the pIS1 *Renilla* luciferase reporter containing a synthetic miR-31 binding site motif in its 3' UTR have been described previously (Valastyan et al., 2009a).

Cell Culture and Reagents

GFP-labeled 231 cells and MCF7-Ras cells have been described (Valastyan et al., 2009a). Stable expression of the indicated plasmids was achieved via lentiviral transduction (Valastyan et al., 2009b). 1.0 _g/mL dox (Sigma) was provided directly in the culture medium for *in vitro* studies; in the *in vivo* analyses, dox was added to sucrose-supplemented (10 mg/mL) drinking water at a final concentration of 2.0 mg/mL.

Xenograft Studies

All animal studies complied with protocols approved by the MIT Committee on Animal Care. NOD/SCID mice (propagated on-site) were employed in all xenograft experiments. For spontaneous metastasis assays, female mice were subjected to bilateral orthotopic injections into the mammary fat pads with 1.0×10^6 tumor cells resuspended in 1:2 Matrigel (BD Biosciences) plus normal growth media. For experimental metastasis assays, male mice were intravenously injected with 5.0×10^5 tumor cells (resuspended in PBS) via the tail vein. Where indicated, cells were pre-treated with 1.0 _g/mL dox 72 hours prior to injection. Lung metastasis was quantified at the indicated timepoints using a fluorescent dissecting microscope; these analyses were performed within three hours of specimen isolation.

Immunohistochemistry

Tumor and lung histology was assessed by staining paraffin-embedded tissue sections with hematoxylin and eosin (H&E). Detection of CD31 (Cell Signaling), cleaved-caspase3 (Cell Signaling), and phosphorylated-histone H3 (phospho-H3) (Cell Signaling) was performed on 10 _m sections using the indicated antibodies, Vectastain Elite ABC kits (Vector), and ImmPACT DAB Substrate (Vector).

miRNA *in situ* Hybridization

miRNA expression was assessed from paraffin-embedded tissue sections using a protocol adapted from Silahtaroglu (Silahtaroglu et al., 2007). Briefly, after a four hour pre-hybridization, 5' FITC-labeled miRCURY LNA probes targeting miR-31 (Exiqon) were hybridized to proteinase K-treated 10 _m sections at 55°C for 12 hours. Slides were then incubated with anti-

FITC-HRP (PerkinElmer), and the resulting signal was intensified via utilization of the TSA Plus Fluorescein System (PerkinElmer).

Statistical Analyses

Data are presented as mean ± s.e.m. Student's t-test was utilized for all comparisons, with $P < 0.05$ considered statistically significant.

Real Time RT-PCR

Total RNA, including small RNAs, was extracted from the indicated cells or homogenized primary mammary tumor tissue xenografts with a *mir*Vana MicroRNA Isolation Kit (Ambion). RT-PCR-based detection of mature miR-31 and the U6 snRNA was achieved via use of Taqman MicroRNA Assays (Applied Biosystems). For detection of the levels of GAPDH, ITGA5, RDX, RhoA, and the dox-repressible miRNA sponge transcripts, cDNA was prepared from 500 ng of total RNA using the SuperScript III First-Strand Synthesis System (Invitrogen), and then quantitated by SYBR Green real time RT-PCR (Applied Biosystems).

Invasion and Motility Assays

For invasion assays, 1.0×10^5 cells were seeded in a Matrigel-coated chamber with 8.0 _m pores (BD Biosciences); for motility assays, 5.0×10^4 cells were plated on top of uncoated membranes with 8.0 _m pores (BD Biosciences). Cells were seeded in serum-free media, and translocated toward complete growth media for 20 hours. Where indicated, cells were pre-treated with 1.0 _g/mL dox 48 hours prior to initiating the experiment.

Anoikis Assays

Anoikis resistance was evaluated by seeding 7.5×10^4 cells in ultra-low attachment plates (Corning). After 24 hours of anchorage-independent culture, cells were resuspended in 0.4% trypan blue (Sigma) and cell viability was assessed via manual counting with a hemocytometer. Where indicated, cells were pre-treated with 1.0 _g/mL dox 48 hours prior to initiating the experiment.

Measurements of *in vitro* Cell Proliferation

Proliferative kinetics were assayed by seeding 1.0×10^3 cells per well in 96-well plates and utilizing a CellTiter96 AQ$_{ueous}$ One Solution MTS Cell Proliferation Assay (Promega). Cells were incubated with the MTS reagent for 1.5 hours, and then total cell number was quantitated by measuring absorbance at 492 nm on a 96-well plate reader. Where indicated, cells were pre-treated with 1.0 _g/mL dox 48 hours prior to initiating the experiment; these cells were then re-treated with dox on day four of the assay.
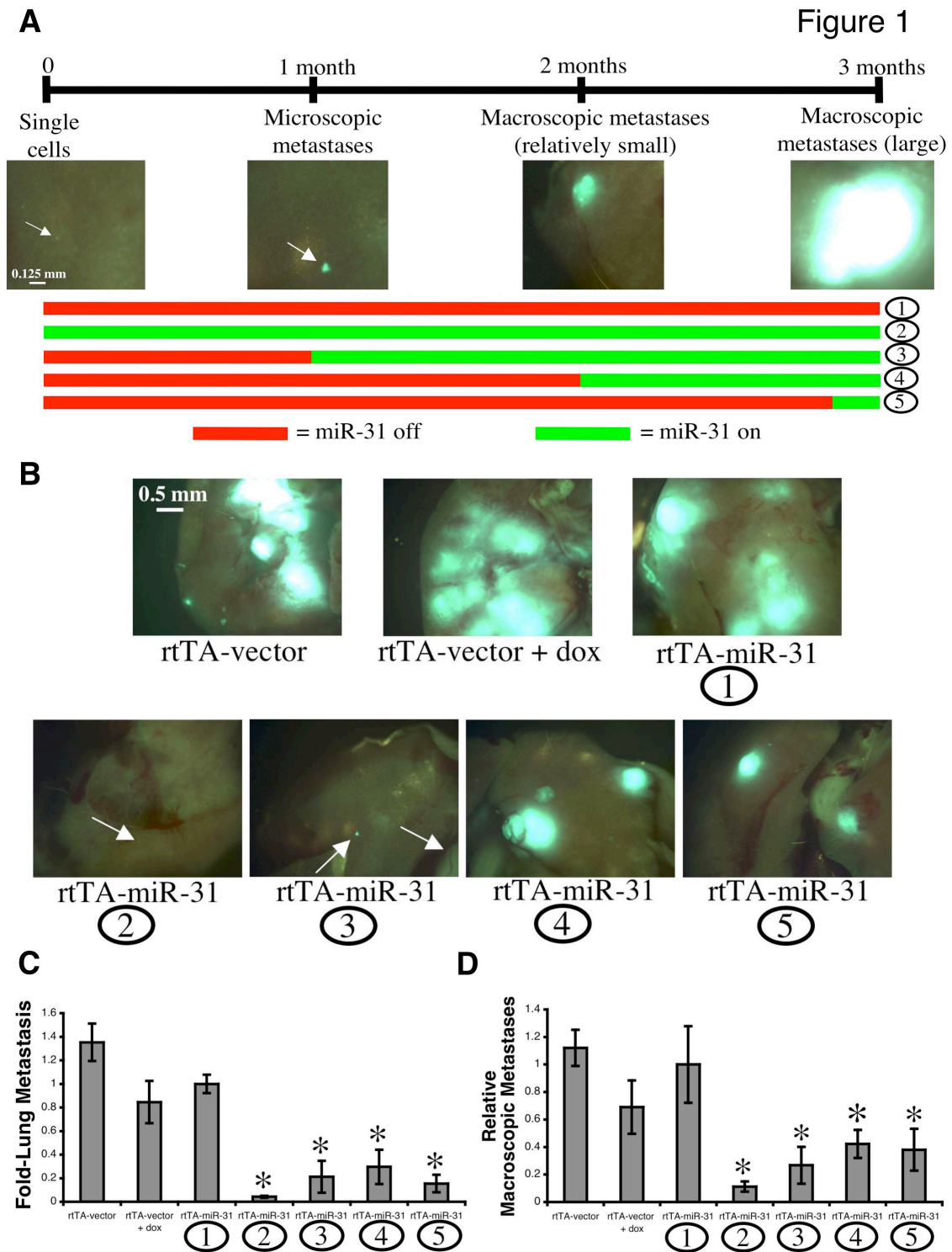
Luciferase Reporter Gene Assays

5.0×10^4 cells were co-transfected with 50 ng of a miR-31 binding motif-containing pIS1 *Renilla* luciferase construct and 50 ng of a pIS0 firefly luciferase normalization control using Fugene6 (Roche). Lysates were collected 24 hours post-transfection, and *Renilla* and firefly luciferase activities were measured with a Dual-Luciferase Reporter System (Promega). Where indicated, cells were pre-treated with 1.0 _g/mL dox 48 hours prior to initiating the experiment.

Oligonucleotide Sequences

Oligonucleotides employed in this study were: Subcloning miRNA sponges to the dox-repressible vector, TTGGTACCGAGCTCGGATCCAC and AATGGTGTGTCGACTAGAAGGCACAGTCGAGGCTGATCAG; Subcloning miR-31 to the dox-inducible vector, TTGGTTTCCAGGATCCACAATACATAGCAGGACAGGAAGTAAGGAAGGTG and TTGGTTTCCAGTCGACCATCTTCAAAAGCGGACACTCTAAGGAAGACTATGTTG; GAPDH RT-PCR, TCACCAGGGCTGCTTTTAAC and GACAAGCTTCCCGTTCTCAG; ITGA5 RT-PCR, AACTCATCATGGCCAGTGAGGGTAAGGGT and ATCCTTAATGGCTCAGACATTCGATCCCTCTACAACT; RDX RT-PCR, GAATCAGGAGCAGCTAGCAGCAGAACTT and TTGGTCTTTTCCAAGTCTTCCTGGGCTGCA; RhoA RT-PCR, AGGTGGATGGAAAGCAGGTAGAGTTGGCT and AGGATGATGGGCACGTTGGGACAGA; miRNA sponge vector RT-PCR, ATCCACCGGTCGCCACCATGGTGAGCAA and TGGTGCAGATGAACTTCAGGGTCAGCTT.

A

Figure 1

0   1 month   2 months   3 months

Single cells

Microscopic metastases

Macroscopic metastases (relatively small)

Macroscopic metastases (large)

0.125 mm

①
②
③
④
⑤

= miR-31 off   = miR-31 on

B

0.5 mm

rtTA-vector   rtTA-vector + dox   rtTA-miR-31 ①

rtTA-miR-31 ②   rtTA-miR-31 ③   rtTA-miR-31 ④   rtTA-miR-31 ⑤

C

Fold-Lung Metastasis

rtTA-vector   rtTA-vector + dox   rtTA-miR-31 ①   rtTA-miR-31 ②   rtTA-miR-31 ③   rtTA-miR-31 ④   rtTA-miR-31 ⑤

D

Relative Macroscopic Metastases

rtTA-vector   rtTA-vector + dox   rtTA-miR-31 ①   rtTA-miR-31 ②   rtTA-miR-31 ③   rtTA-miR-31 ④   rtTA-miR-31 ⑤

Figure 1. Acute Re-Activation of miR-31 Triggers the Regression of Already-Established Experimental Metastases *in vivo*. (A) Schematic depicting the dox-mediated intervention

strategy for miR-31 re-expression upon intravenous injection of 5.0 x 10^5 of the indicated GFP-labeled 231 cells. Images document the normal progression of control cells in this assay. **(B)** Fluorescent images of murine lungs to visualize 231 cells 88 days after intravenous implantation. **(C)** Quantification of total metastatic burden in the lungs 88 days following intravenous injection. n = 5. **(D)** Quantification of the prevalence of macroscopic metastases in the lungs 88 days subsequent to intravenous introduction. n = 5. Arrows: micrometastases. Asterisks: P <0.05 relative to rtTA-miR-31 cells (no dox treatment). Data are presented as mean ± s.e.m.
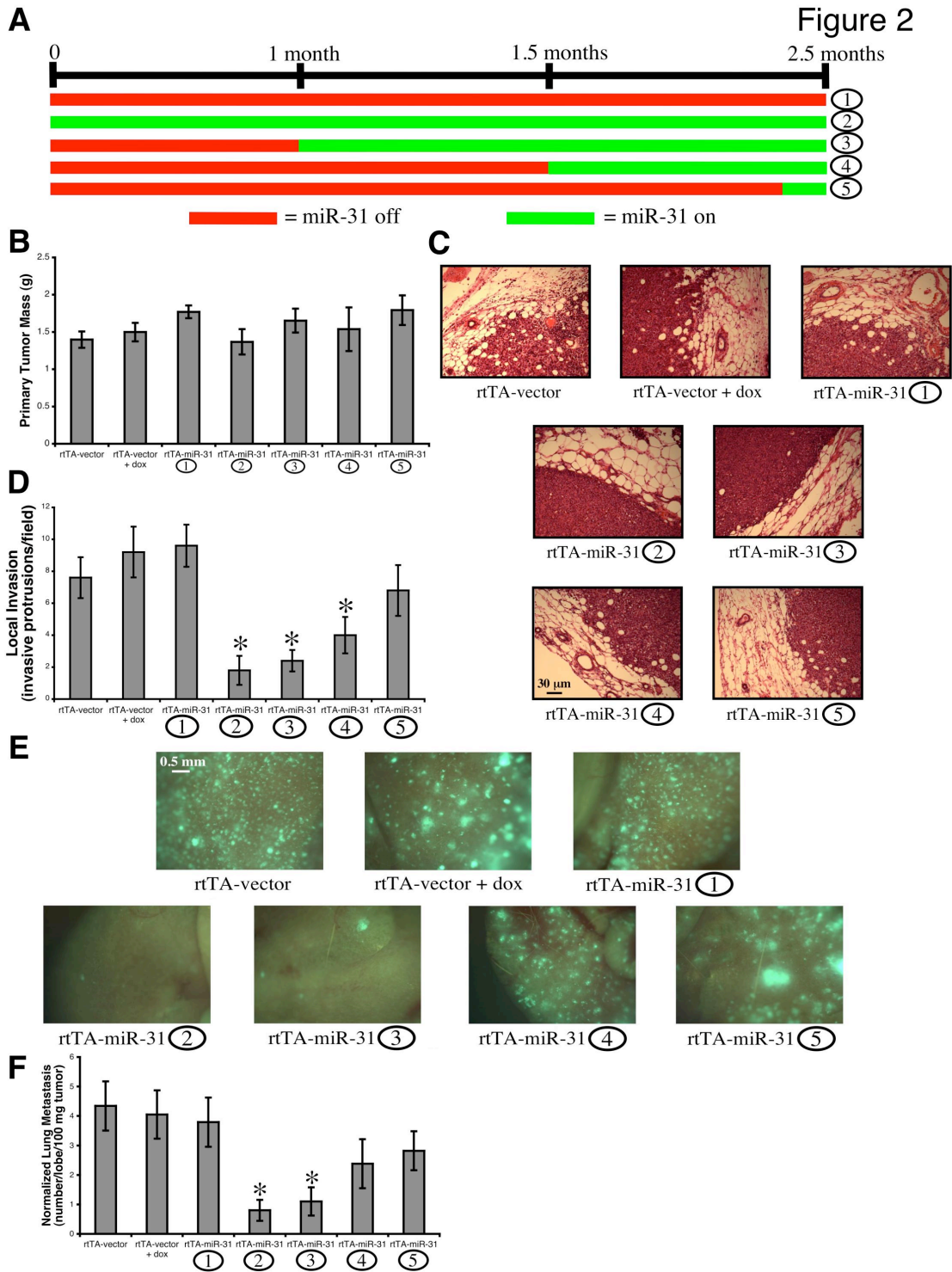
Figure 2. Acute Re-Expression of miR-31 Reverses the Invasiveness of Primary Mammary Tumors and Elicits the Regression of Already-Established Spontaneous Metastases *in vivo*.

(A) Overview of the dox-controlled intervention strategy for miR-31 re-expression upon

219

orthotopic implantation of 1.0 x 10^6 of the indicated GFP-labeled 231 cells. **(B)** Masses of 231

cell primary mammary tumors 56 days subsequent to injection. **(C)** H&E staining of primary

mammary tumors 56 days after orthotopic implantation. **(D)** Quantification of primary mammary

tumor local invasion 56 days following orthotopic injection. n = 5. **(E)** Fluorescent images of

murine lungs to visualize disseminated 231 cells 56 days after orthotopic implantation. **(F)**

Quantification of total metastatic burden in the lungs 56 days after orthotopic injection. n = 5.

Asterisks: P <0.04 relative to rtTA-miR-31 cells (no dox treatment). Data are presented as mean

± s.e.m.
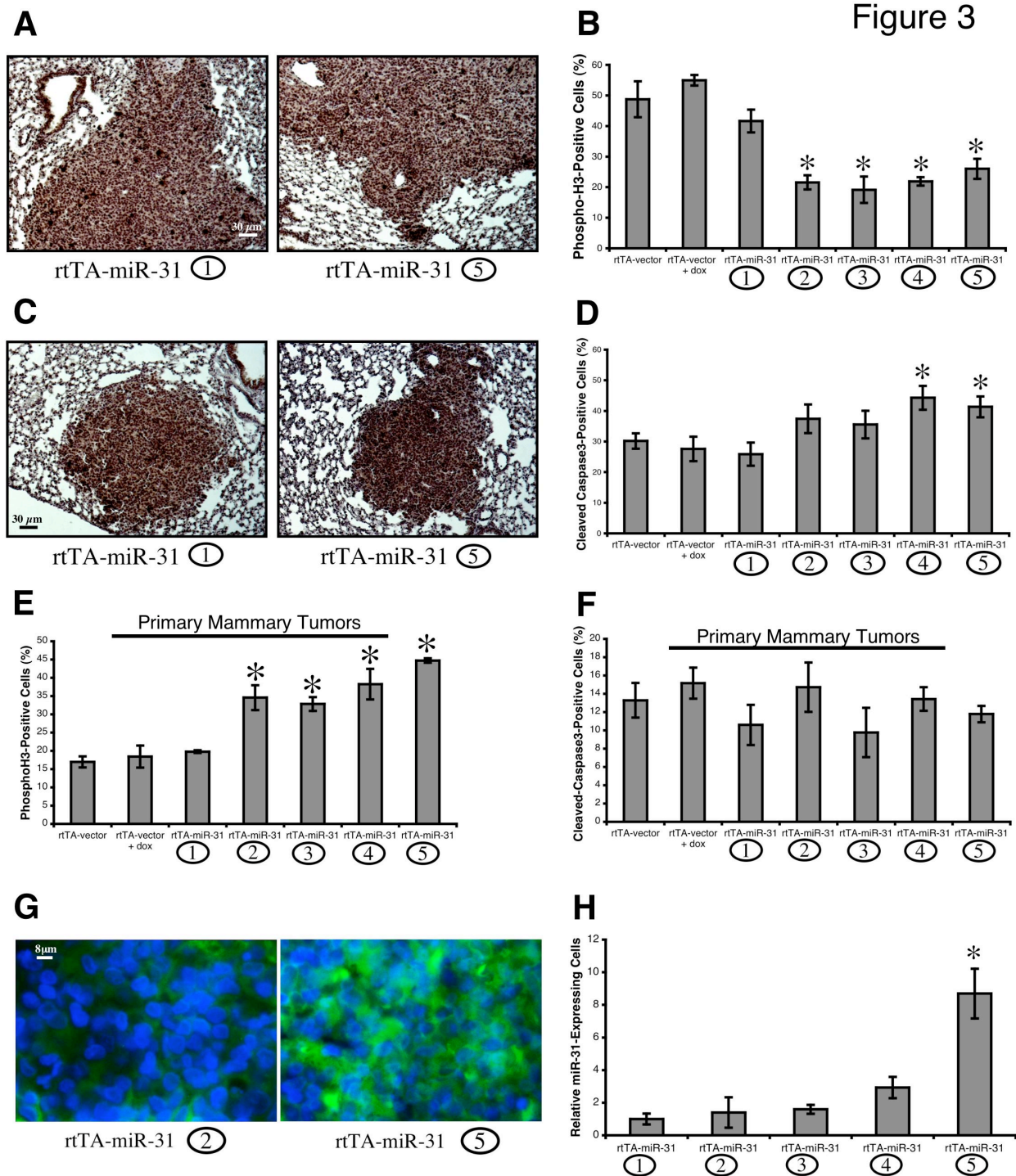
Figure 3. Acute Restoration of miR-31 Function in Already-Established Metastases Leads to Metastasis-Specific Cell Cycle Arrest and Apoptosis *in vivo*. (A) 231 cell lung metastases 88 days after intravenous injection, immunohistochemically stained for phospho-H3. **(B)**

Quantification of phospho-H3 staining in pulmonary metastases 88 days post-intravenous

implantation. n = 5. **(C)** 231 cell lung metastases 88 days subsequent to intravenous injection,

immunohistochemically stained for cleaved-caspase3. **(D)** Quantification of cleaved-caspase3

staining in pulmonary metastases 88 days following intravenous introduction. n = 5. **(E)**

Quantification of phospho-H3 immunohistochemical staining in 231 cell primary mammary

tumors at 56 days post-orthotopic injection. n = 5. **(F)** Quantification of cleaved-caspase3

immunohistochemical staining in 231 cell primary mammary tumors 56 days subsequent to

orthotopic implantation. n = 5. **(G)** *In situ* hybridizations for miR-31 (green) in lung metastases

formed by intravenously injected 231 cells 88 days following implantation. DAPI counterstain

(blue). **(H)** Quantification of miR-31 staining in pulmonary metastases 88 days after intravenous

injection. n = 5. Asterisks: P <0.03 relative to rtTA-miR-31 cells (no dox treatment). Data are

presented as mean ± s.e.m.
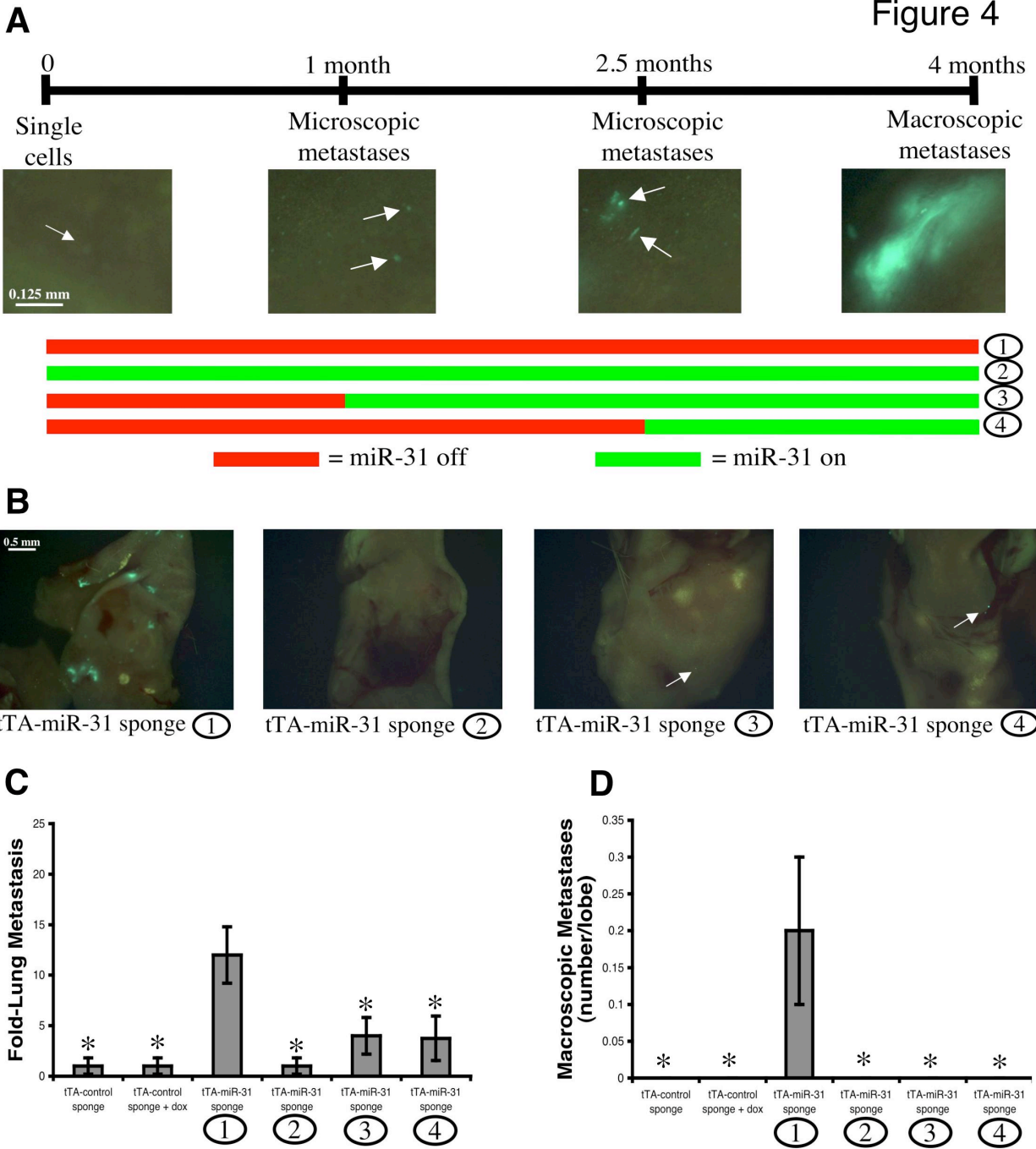
Figure 4. Acute Restoration of Endogenous miR-31 Function Prevents the Outgrowth of Already-Established Experimental Metastases and Reduces Overall Metastatic Burden *in vivo*. (A) Schematic depicting the dox-mediated intervention strategy for the re-activation of endogenous miR-31 function – achieved via repression of a modified miR-31 miRNA sponge –

upon intravenous injection of 5.0 x 10^5 of the indicated GFP-labeled MCF7-Ras cells. Images

document the normal progression of MCF7-Ras cells expressing a miR-31 sponge for the entire

duration of this assay. **(B)** Fluorescent images of murine lungs to visualize MCF7-Ras cells 117

days after intravenous implantation. **(C)** Quantification of total metastatic burden in the lungs

117 days following intravenous injection. n = 5. **(D)** Quantification of the prevalence of

macroscopic metastases in the lungs 117 days subsequent to intravenous introduction. n = 5.

Arrows: micrometastases. Asterisks: P <0.03 relative to tTA-miR-31 sponge cells (no dox

treatment). Data are presented as mean ± s.e.m.

SUPPLEMENTARY FIGURES
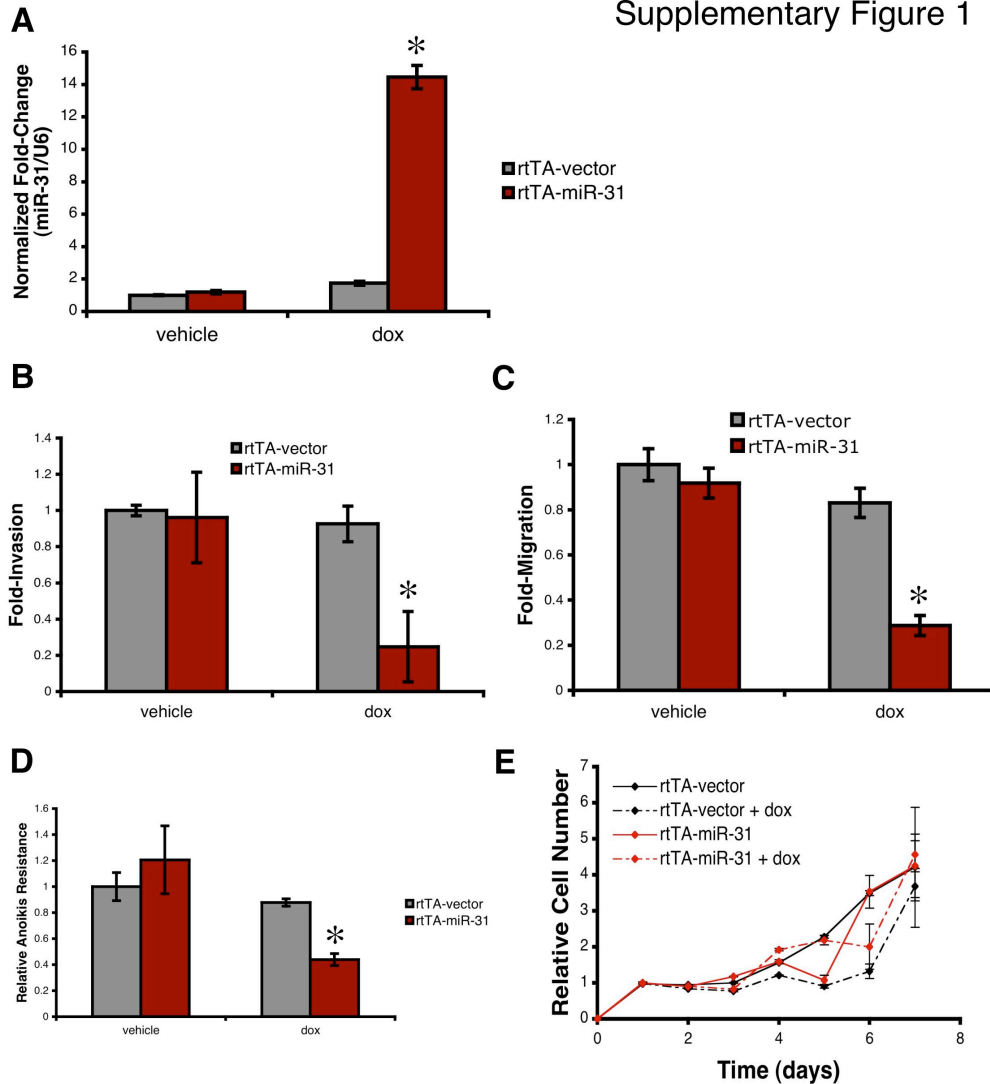
Supplementary Figure 1. The Temporally Controlled Re-Activation of miR-31 Impairs Metastasis-Relevant Traits *in vitro*. (A) Real time RT-PCR for miR-31 in the indicated 231 cells. The U6 snRNA was a loading control. n = 3. **(B)** Invasion assays using the indicated 231 cells. n = 3. **(C)** Motility assays employing 231 cells infected as denoted. n = 3. **(D)** Anoikis assays with the indicated 231 cells. n =3. **(E)** Proliferation of the indicated 231 cells *in vitro*. n = 3. Asterisks: P <0.03 relative to rtTA-miR-31 cells (no dox treatment). Data are presented as mean ± s.e.m.

A

| rtTA-vector | rtTA-vector + dox | rtTA-miR-31 | rtTA-miR-31 + dox |

B

10 minutes
post-injection
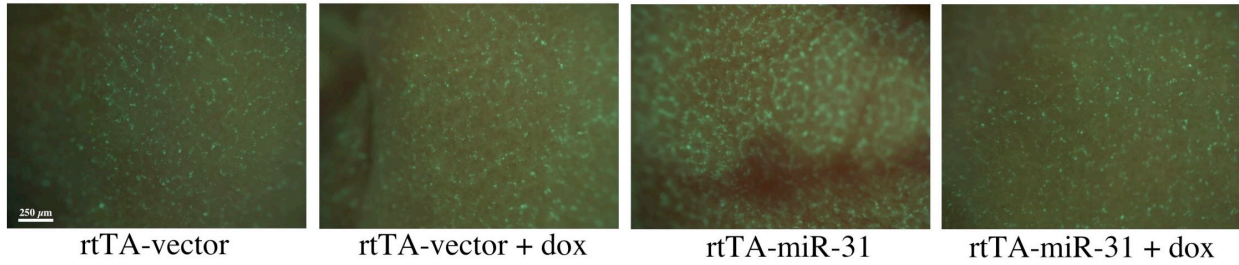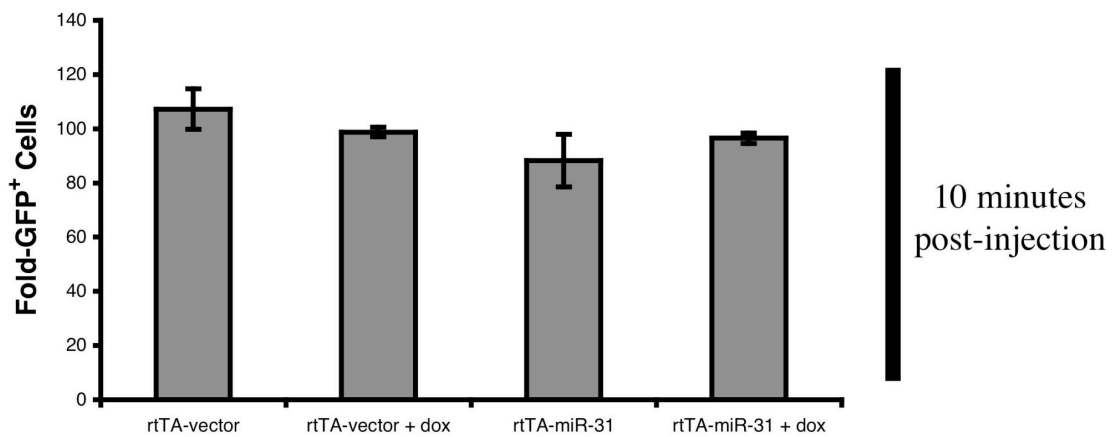
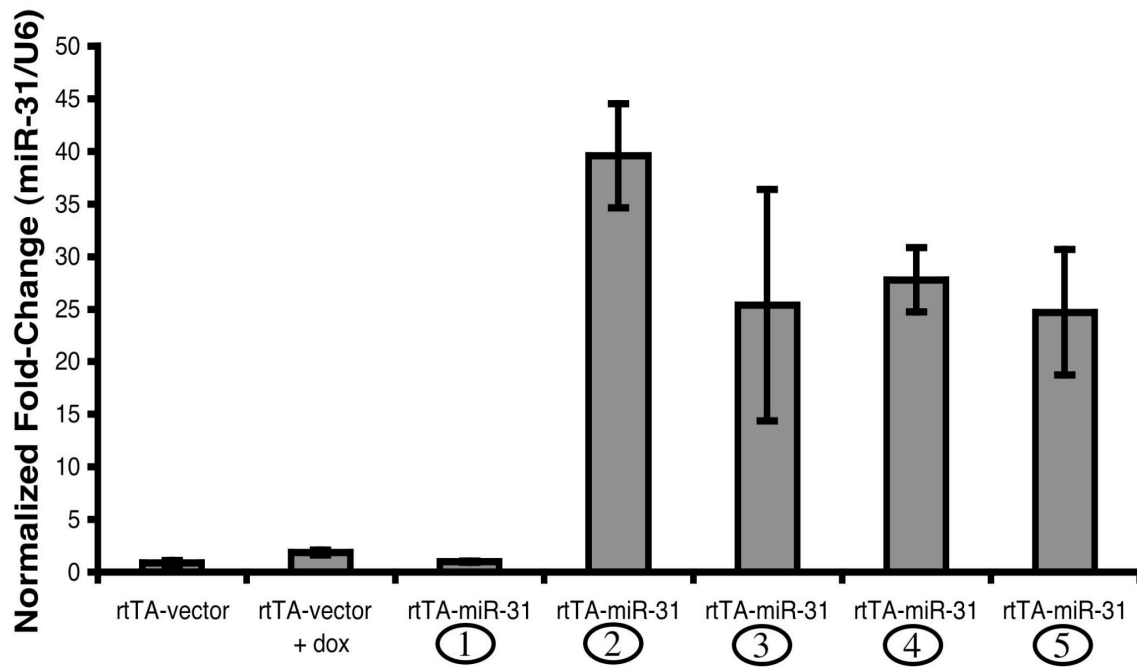**Supplementary Figure 2. miR-31 Expression and Doxycycline Treatment Fail to Affect the Initial Vascular Lodging of Intravenously Injected MDA-MB-231 Cells *in vivo*. (A)** Fluorescent images of murine lungs to visualize GFP-labeled 231 cells 10 minutes subsequent to intravenous injection. **(B)** Quantification of the relative prevalence of these cells in the lungs. n = 2. All P-values are >0.35 relative to rtTA-miR-31 cells (no dox treatment). Data are presented as mean ± s.e.m.
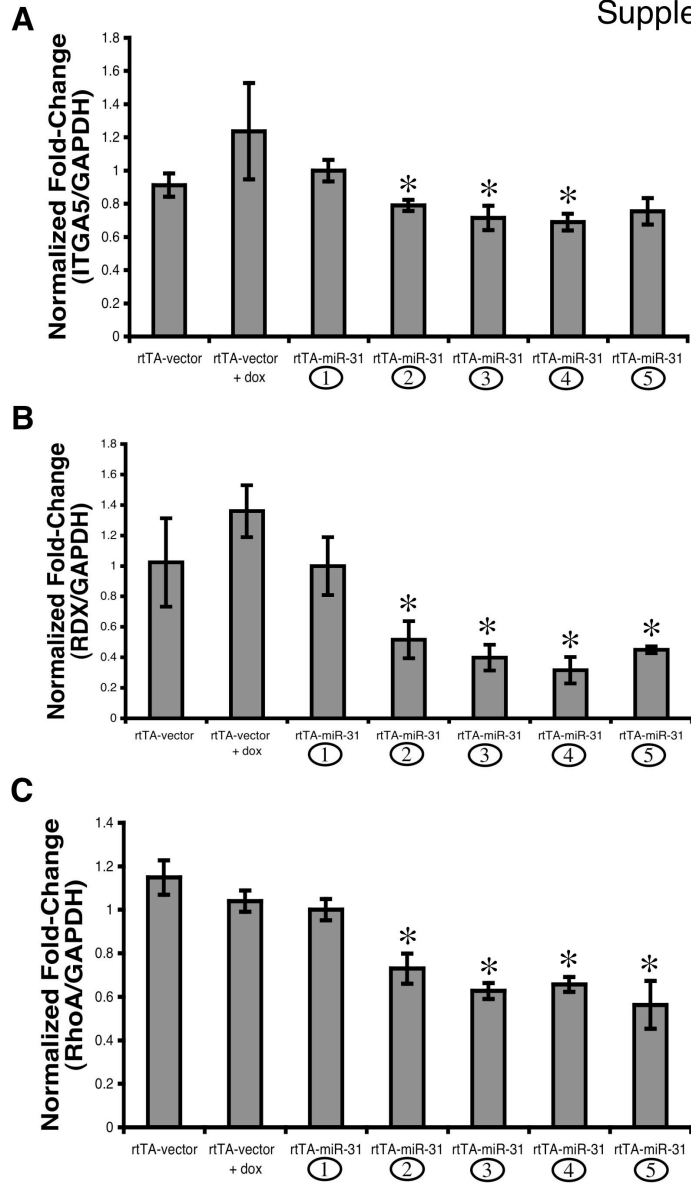
Supplementary Figure 3. miR-31 Expression is Successfully Induced in Response to Doxycycline Treatment *in vivo*. Real time RT-PCR for miR-31 in orthotopically implanted primary mammary tumors derived from the indicated 231 cells. The U6 snRNA was a loading control. n = 3. Data are presented as mean ± s.e.m.

Supplementary Figure 4. Endogenous Integrin _5, Radixin, and RhoA Expression is Suppressed Upon Doxycycline-Mediated Re-Activation of miR-31 *in vivo*. (A) Real time RT-PCR for ITGA5 in primary mammary tumors formed by the indicated 231 cells. GAPDH was a loading control. n = 3. **(B)** Real time RT-PCR for RDX in 231 cell primary mammary tumors. GAPDH was a loading control. n = 3. **(C)** Real time RT-PCR for RhoA in primary mammary tumors derived from the indicated 231 cells. GAPDH was a loading control. n = 3. Asterisks: P <0.03 relative to rtTA-miR-31 cells (no dox treatment). Data are presented as mean ± s.e.m.

A

rtTA-miR-31 ①   rtTA-miR-31 ③

B
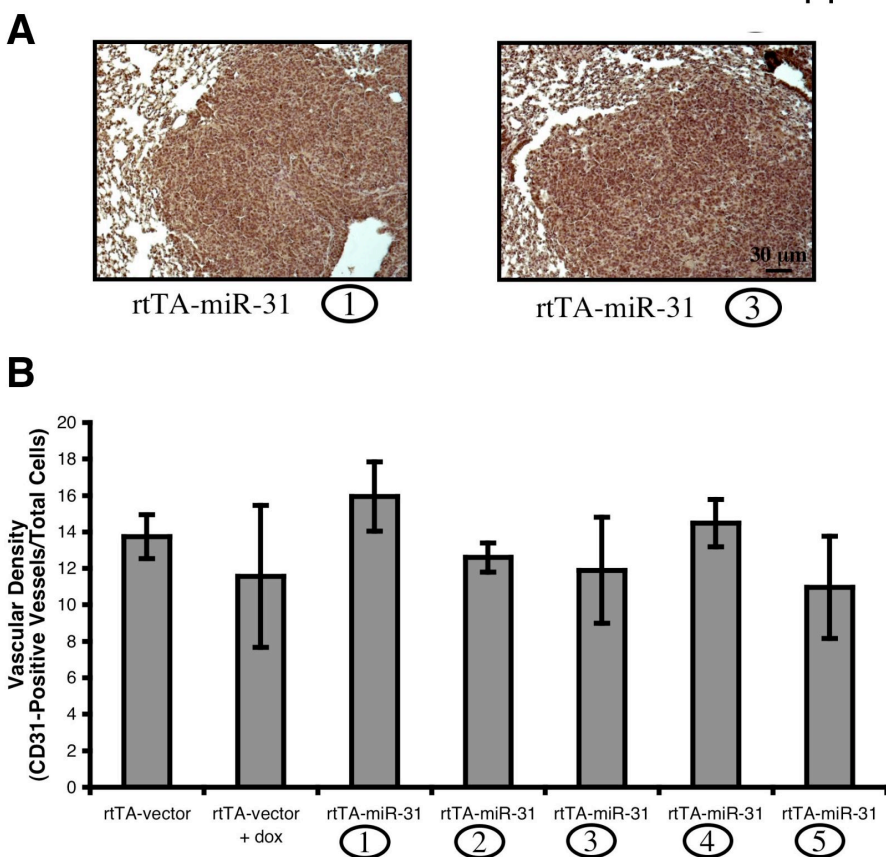
**Supplementary Figure 5. Acute Re-Introduction of miR-31 Fails to Impact Vascular Density Within Already-Established Metastases *in vivo*. (A)** 231 cell lung metastases 88 days after intravenous injection, immunohistochemically stained for CD31. **(B)** Quantification of CD31 staining 88 days following intravenous implantation. n = 5. All P-values are >0.30 relative to rtTA-miR-31 cells (no dox treatment). Data are presented as mean ± s.e.m.

A

Primary tumor, rtTA-miR-31 (5)   Lung metastasis, rtTA-miR-31 (5)

B
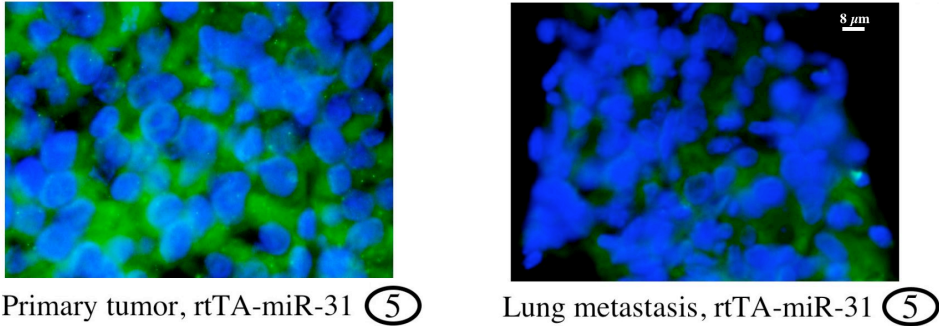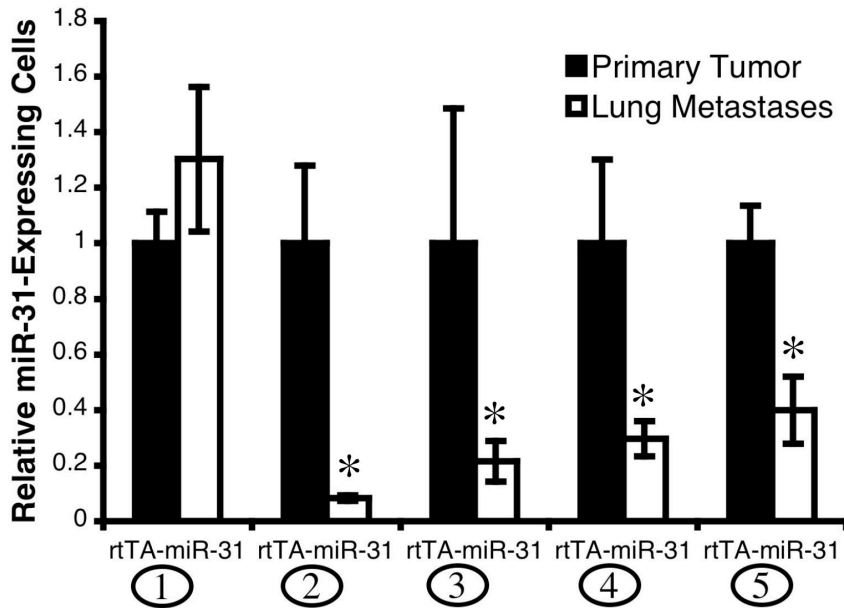
Supplementary Figure 6. Selective Loss of Proper miR-31 Induction in Response to Doxycycline Treatment in Pulmonary Metastases *in vivo*. (A) *In situ* hybridizations for miR-31 (green) in animal-matched primary mammary tumors and lung metastases formed by orthotopically injected 231 cells 56 days following implantation. DAPI counterstain (blue). **(B)** Quantification of miR-31 staining in animal-matched primary mammary tumors and lung metastases at 56 days post-injection. n = 5. Asterisks: P <0.02 relative to the corresponding primary tumor. Data are presented as mean ± s.e.m.
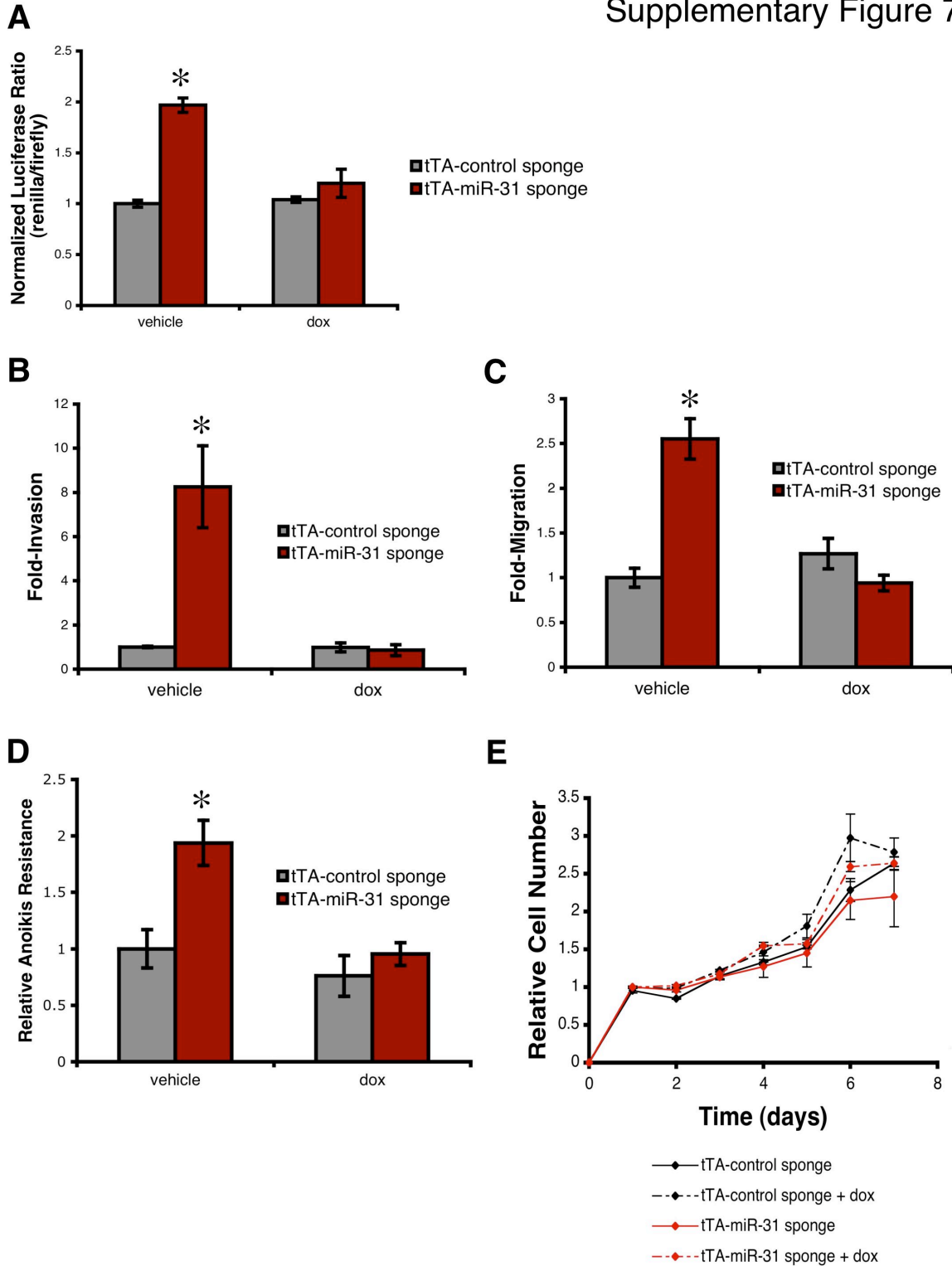
Supplementary Figure 7. The Temporally Controlled Re-Activation of Endogenous miR-31

Function Impairs Metastasis-Relevant Traits *in vitro*. (A) Luciferase activity in the indicated

MCF7-Ras cells 24 hours after transfection of a reporter construct driven by a miR-31 3' UTR binding site motif. n = 3. **(B)** Invasion assays using the indicated MCF7-Ras cells. n = 3. **(C)** Motility assays employing MCF7-Ras cells infected as denoted. n = 3. **(D)** Anoikis assays with the indicated MCF7-Ras cells. n =3. **(E)** Proliferation of the indicated MCF7-Ras cells *in vitro*. n = 3. Asterisks: P <0.02 relative to tTA-miR-31 sponge cells treated with dox. Data are presented as mean ± s.e.m.

A

| tTA-control sponge | tTA-control sponge + dox | tTA-miR-31 sponge | tTA-miR-31 sponge + dox |

B
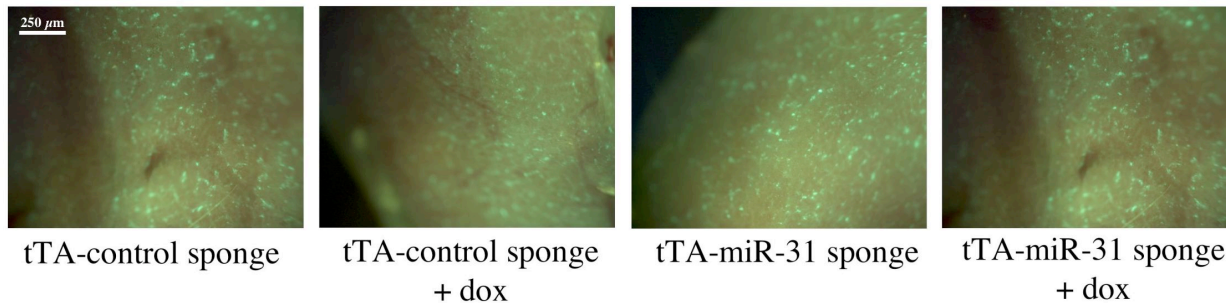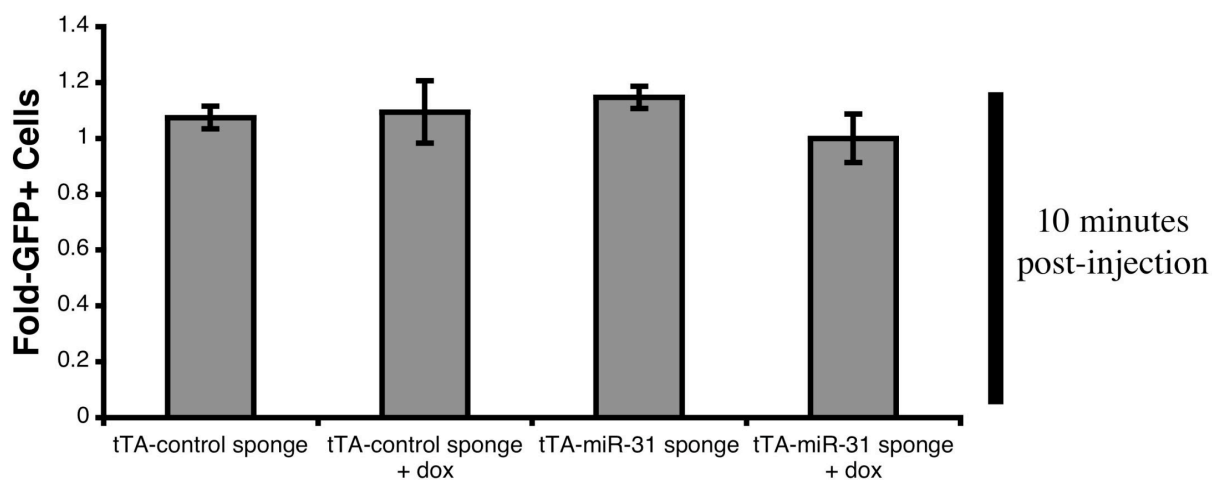
Supplementary Figure 8. miR-31 Sponge Expression and Doxycycline Treatment Do Not Affect the Initial Vascular Lodging of Intravenously Injected MCF7-Ras Cells *in vivo*. (A) Fluorescent images of murine lungs to visualize GFP-labeled MCF7-Ras cells 10 minutes subsequent to intravenous injection. **(B)** Quantification of the relative prevalence of these cells in the lungs. n = 2. All P-values are >0.35 relative to dox-treated tTA-miR-31 sponge cells. Data are presented as mean ± s.e.m.
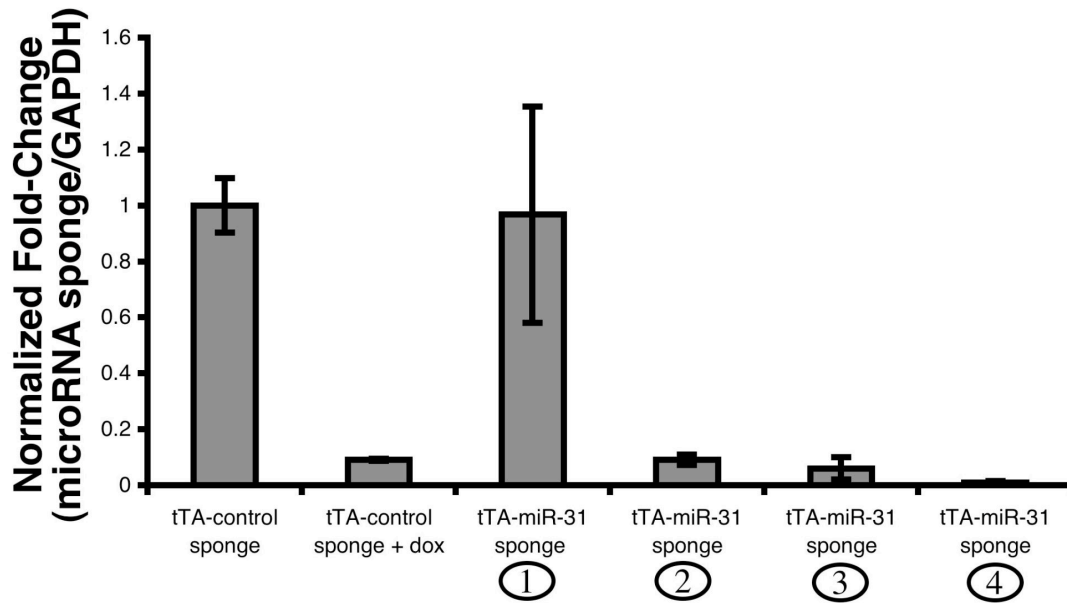
Supplementary Figure 9. MicroRNA Sponge Expression is Successfully Repressed in Response to Doxycycline Treatment *in vivo*. Real time RT-PCR for miRNA sponge expression in primary mammary tumors derived from the indicated MCF7-Ras cells. GAPDH was a loading control. n = 3. Data are presented as mean ± s.e.m.

ACKNOWLEDGMENTS

REFERENCES

Bartel DP. (2009). MicroRNAs: target recognition and regulatory functions. Cell *136*, 215-233.

Coussens LM, Fingleton B, and Matrisian LM. (2002). Matrix metalloproteinase inhibitors and cancer: trials and tribulations. Science *295*, 2387-2392.

Ebert MS, Neilson JR, and Sharp PA. (2007). MicroRNA sponges: competitive inhibitors of small RNAs in mammalian cells. Nat Methods *4*, 721-726.

Fidler IJ. (2003). The pathogenesis of cancer metastasis: the 'seed and soil' hypothesis revisited. Nat Rev Cancer *3*, 453-458.

Gupta GP and Massagué J. (2006). Cancer metastasis: building a framework. Cell *127*, 679-695.

Haack K, Cockrell AS, Ma H, et al. (2004). Transactivator and structurally optimized inducible lentiviral vectors. Mol Ther *10*, 585-596.

Hüsemann Y, Geigl JB, Schubert F, et al. (2008). Systemic spread is an early step in breast cancer. Cancer Cell *13*, 58-68.

Ma L, Reinhardt F, Pan E, et al. (2010). Therapeutic silencing of miR-10b inhibits metastasis in a mouse mammary tumor model. Nat Biotechnol *28*, 341-347.

Maherali N, Ahfeldt T, Rigamonti A, et al. (2008). A high-efficiency system for the generation and study of human induced pluripotent stem cells. Cell Stem Cell *3*, 340-345.

Nagrath S, Sequist LV, Maheswaran S, et al. (2007). Isolation of rare circulating tumour cells in cancer patients by microchip technology. Nature *450*, 1235-1239.

Pantel K, Brakenhoff RH, and Brandt B. (2008). Detection, clinical relevance and specific biological properties of disseminating tumour cells. Nat Rev Cancer *8*, 329-340.

Silahtaroglu AN, Nolting D, Dyrskjøt L, et al. (2007). Detection of microRNAs in frozen tissue sections by fluorescence in situ hybridization using LNA probes and tyramide signal amplification. Nat Protoc *2*, 2520-2528.

Smith SC and Theodorescu D. (2009). Learning therapeutic lessons from metastasis suppressor proteins. Nat Rev Cancer *9*, 253-264.

Steeg PS. (2006). Tumor metastasis: mechanistic insights and clinical challenges. Nat Med *12*, 895-904.

Valastyan S, Benaich N, Chang A, et al. (2009b). Concomitant suppression of three target genes can explain the impact of a microRNA on metastasis. Genes Dev *23*, 2592-2597.

Valastyan S, Reinhardt F, Benaich N, et al. (2009a). A pleiotropically acting microRNA, miR-31, inhibits breast cancer metastasis. Cell *137*, 1032-1046.

Valastyan S and Weinberg RA. (2009). MicroRNAs: crucial multi-tasking components in the complex circuitry of tumor metastasis. Cell Cycle *8*, 3506-3512.

Ventura A and Jacks T. (2009). MicroRNAs and cancer: short RNAs go a long way. Cell *136*, 586-591.

Chapter 6

An Experimental System for the Unbiased Discovery of Genes Relevant for Breast Cancer Metastasis

Scott Valastyan[1,2], Amelia Chang[1,2], Nathan Benaich[1,3], Ferenc Reinhardt[1], and Robert A. Weinberg[1,2,4]

[1]Whitehead Institute for Biomedical Research, Cambridge, MA 02142, USA
[2]Department of Biology, Massachusetts Institute of Technology, Cambridge, MA 02139, USA
[3]Department of Biology, Williams College, Williamstown, MA 01267, USA
[4]MIT Ludwig Center for Molecular Oncology, Cambridge, MA 02139, USA

INTRODUCTION

As described in Chapter One, metastases are responsible for 90% of human cancer-associated mortality (Fidler, 2003; Gupta and Massagué, 2006). These malignant growths arise through the completion of a series of ordered events, whereby cancer cells that were initially confined within a primary tumor become motile, invade through their surrounding extracellular matrix, intravasate into the lumen of a blood vessel, survive during transit through the systemic circulation, arrest at a distant organ site, extravasate into the parenchyma of that secondary locus, adapt to survive within this foreign microenvironment to form micrometastases, and finally succeed in colonizing the metastatic site in order to generate clinically detectable macroscopic metastases (Fidler, 2003; Gupta and Massagué, 2006).

Over the last decade, much attention has been devoted to elucidating molecular regulators of metastatic progression – a point that was initially discussed in Chapter One. In fact, a number of genomics-based approaches have recently been undertaken in an endeavor to enumerate novel regulators of the invasion-metastasis cascade (Clark et al., 2000; van't Veer et al., 2002; Ramaswamy et al., 2003; Kang et al., 2003; Minn et al., 2005a; Bos et al., 2009). While these studies have identified interesting candidate regulators of the metastatic process – some of which appear to hold promise as clinically useful prognostic biomarkers for aggressive disease (Gupta and Massagué, 2006) – our knowledge of the molecular circuitry that governs metastasis still remains fragmentary. Accordingly, alternative approaches that serve to elucidate previously unappreciated molecular mediators of metastasis are required in order to more fully comprehend the complex etiology of metastatic disease.

Past strategies for identifying novel genetic determinants of metastatic propensity have largely centered upon either serial *in vivo* selection for highly metastatic variants in experimental

animal models followed by gene expression profiling of the selected variant populations (Clark et al., 2000; Kang et al., 2003; Minn et al., 2005a; Bos et al., 2009) or, alternatively, gene expression profiling of clinical human tumor specimens (van't Veer et al., 2002; Ramaswamy et al., 2003). One severe limitation of these prior approaches stems from the fact that these strategies fail to preserve and assay the extensive – and functionally critical (Gupta and Massagué, 2006) – heterogeneity that is intrinsically present within tumor cell populations. Stated differently, because these strategies either (1) eliminate potentially important genetic diversity through serial *in vivo* selection and/or (2) are constrained by their ability to measure only the genetic makeup of the few most prevalent clones present within a much more substantially heterogeneous cell population, they have almost certainly failed to identify numerous critically important metastasis-regulatory factors.

In response to the shortcomings of these past approaches, I outline here a novel alternative strategy for the elucidation of key modulators of metastatic progression. More specifically, I describe an experimental system that can be deployed to implicate genetic factors that contribute to various aspects of metastatic progression in an unbiased manner. Importantly, this novel experimental tool is capable of both maintaining and investigating the profound phenotypic heterogeneity and genetic diversity that pre-exists within tumor cell populations, thus providing a means by which to identify multiple distinct combinations of genetic alterations that succeed in driving a common cell-biologic phenotype – including genomic changes that arise only in relatively rare sub-populations.

RESULTS

Single-Cell Clones Derived from the Parental Bulk Population of MDA-MB-231 Cells

Display Extensive Functional Heterogeneity and Genetic Diversity

MDA-MB-231 cells ("231 cells") are an established line of human breast carcinoma cells that were isolated from the pleural effusion of a patient afflicted with widespread metastatic disease (Cailleau et al., 1978). 231 cells are known to possess a strong capacity to form primary tumors when grown as xenografts in mice; moreover, these implanted primary tumors efficiently seed distant metastases (Kang et al., 2003; Minn et al., 2005a; Minn et al., 2005b; Bos et al., 2009). Importantly, the work of others has demonstrated that the bulk 231 cell population is comprised of a rich assemblage of functionally distinct sub-clones (Kang et al., 2003; Minn et al., 2005b). Additionally, these different sub-populations have been shown to possess at least some degree of genetic diversity, as the expression levels of several genes of interest were retrospectively found to differ between various functionally distinct clones (Kang et al., 2003; Minn et al., 2005b). I therefore hypothesized that widespread genomic differences might exist between the various 231 cell sub-clones, and also that these genetic differences might dictate the observed phenotypic heterogeneity of the sub-clones. Consequently, I reasoned that detailed study of these genetically and functionally diverse clones might afford a means by which to implicate previously unappreciated modulators of biological processes of interest in an unbiased manner.

Accordingly, in order to establish an experimental system capable of identifying novel regulators of metastasis-relevant phenotypes, I isolated 30 single-cell clones (SCCs) from a parental bulk population of green fluorescent protein (GFP)-labeled 231 cells. Because a relatively large number of SCCs were obtained, I postulated that my collection of SCCs

contained representatives from a number of the distinct sub-populations that pre-exist within the parental bulk 231 cell line. Of note, these might include functionally interesting, yet rare, sub-populations whose genetic makeup would be entirely masked by the genomic attributes of more prevalent clones when traditional bulk analyses (e.g., microarray expression profiling) were conducted using the heterogeneous parental 231 cell population. Hence, by isolating a large number of SCCs from this initially heterogeneous cell line, I was able to obtain a diverse array of SCCs whose individual genetic constitutions could subsequently be interrogated and whose individual functional attributes were perhaps likely to vary widely.

Indeed, these 30 SCCs exhibited extensive morphological diversity, even when grown under standard culture conditions (data not shown). Moreover, the 30 SCCs were found to possess a wide range of capacities for *in vitro* cell proliferation, *in vivo* primary tumor growth, *in vitro* cell motility, and *in vivo* metastasis formation (Figure 1). As expected, the majority of the various SCCs proliferated at the same rate as the parental bulk 231 cell population *in vitro* (Figure 1B), thus providing a rationale for how a number of genetically distinct sub-populations can be stably maintained within these cultures. However, the proliferative kinetics of 10 of the SCCs were significantly slower than the doubling rate of the parental bulk 231 cell population (Figure 1B), perhaps suggesting that these isolates were likely to have been generated *de novo* and persist only transiently in 231 cell cultures. Alternatively, selective pressures may exist that operate to ensure the continuous presence of these slow-proliferating clones.

Another surprising observation stemmed from the finding that 22 of the 30 isolated SCCs were more weakly tumorigenic *in vivo* than was the parental bulk 231 cell population, while only one of the SCCs formed significantly larger tumors than parental bulk 231 cells (Figure 1C). These findings could be interpreted as being consistent with the notion that only a minority of the

243

cells present in an initial tumor cell population have a robust capacity to seed new tumors – in consonance with the "tumor-initiating cell" hypothesis (Brabletz et al., 2005; Rosen and Jordan, 2009). Alternatively, these data might simply indicate that extensive intercellular heterogeneity is an important pre-requisite for tumor formation.

Additionally, the 30 SCCs displayed extensive phenotypic variability in terms of their *in vitro* cell motility (Figure 1D) and *in vivo* metastatic capacity (Figure 1E). In fact, four SCCs were found to be significantly more motile than the parental bulk 231 cells, while three SCCs possessed impaired migratory capacity relative to that of the parental bulk 231 cell population (Figure 1D). Analogously, five SCCs displayed heightened *in vivo* metastatic propensity, while four SCCs were significantly less competent to seed metastases, relative to the parental bulk 231 cell population. Assessed collectively, the preceding observations revealed that my collection of 30 SCCs exhibited an extensive range of functional diversity.

I investigated whether the observed phenotypic heterogeneity between the SCCs might be accompanied by substantial genetic differences at a genome-wide level. Accordingly, I performed microarray gene expression profiling on those 13 SCCs that displayed significant phenotypic differences (SCC-2, SCC-4, SCC-5, SCC-7, SCC-12, SCC-13, SCC-18, SCC-19, SCC-20, SCC-21, SCC-23, SCC-27, and SCC-29). Indeed, while evidence of their common ancestry from a single human tumor was evident, I observed numerous differences between the global mRNA expression profiles of these various SCCs (data not shown). Hence, when taken together, these data revealed that the widespread genetic and functional diversity that existed among the various clones present in this initial heterogeneous tumor cell population was maintained and subsequently assayed by deriving a large number of SCCs from the parental bulk population of 231 cells and then performing parallel functional and genomic analyses.

The SCC Experimental System Can be Utilized to Identify Novel Regulators of Metastasis-Relevant Processes *in vitro*

Because the acquisition of a motile phenotype is a critical pre-requisite for metastasis formation that can be accurately modeled *in vitro* (Gupta and Massagué, 2006), I asked whether the SCC system might be capable of implicating certain genetic factors as novel regulators of *in vitro* cell motility. Accordingly, I utilized data obtained from the functional assays and microarray expression profiling described above to compile a roster of genes whose expression levels were significantly correlated with migratory potential across the seven SCCs displaying either weakly motile behavior (SCC-7, SCC-19, and SCC-29) or strongly motile behavior (SCC-2, SCC-4, SCC-13, and SCC-18) (Figure 1D). These different SCCs displayed a >40-fold overall range in motility *in vitro* (Figure 1D). From these analyses, I identified 88 genes whose levels were significantly associated with this parameter (data not shown). Collectively, these findings indicated that the SCC system can indeed be used to enumerate candidate regulators of a metastasis-relevant process.

A subset of 12 of these 88 identified differentially expressed genes was selected for further study on the basis of (1) the lack of previous reports concerning their potential role in cell migration and (2) the magnitude of their differential expression between the weak-motility and high-motility SCCs (Figure 2A and data not shown). Of these 12 genes, the differential expression patterns observed on the microarrays were indeed verified by independent RT-PCR-based analyses in the cases of eight of the 12 candidates: a disintegrin-like and metalloproteinase with thrombospondin type 1 motif 12 (ADAMTS12), DEAD box protein 4 (DDX4), forkhead-related transcription factor F2 (FOXF2), phosphatase and actin regulator 2 (PHACTR2), plexin

C1 (PLXNC1), RhoJ, transcription factor EC-like (TFEC), and zinc finger matrin type 4 (ZMAT4) (Figures 2B-2I).

Among these eight independently confirmed, differentially expressed candidates, RhoJ – a cdc42-like small GTPase with no described role in cancer (Jaffe and Hall, 2005; Heasman and Ridley, 2008) – was of particular interest, given its >90% downregulation in all four of the high-motility SCCs (SCC-2, SCC-4, SCC-13, and SCC-18) (Figure 2G). In contrast, RhoJ levels in two of the three low-motility SCCs (SCC-19 and SCC-29) were comparable to those expressed by the parental bulk population of 231 cells, while the levels of RhoJ were modestly downregulated in the third low-motility SCC (SCC-7) relative to the parental bulk population of 231 cells (Figure 2G). Thus, RhoJ expression levels were inversely associated with migratory capacity.

In light of this strong correlation, I hypothesized that RhoJ might play a functional role in impeding cell motility. Therefore, I investigated the consequences of perturbing RhoJ expression levels. To this end, I infected otherwise-weakly motile SCCs with short hairpin RNAs (shRNAs) against RhoJ. More specifically, two distinct lines of low-motility SCCs (SCC-19 and SCC-29) were individually infected with five sequence-independent hairpins targeting alternative complementary sequences located within the RhoJ transcript; most of these shRNAs succeeded in reducing endogenous RhoJ expression levels by >70% (Supplementary Figure 1). When cells containing the various RhoJ shRNAs were subjected to *in vitro* motility assays, I found that RhoJ knockdown enhanced the migratory capacity of these otherwise-weakly motile SCCs between approximately two-fold and five-fold (Figures 3A and 3B). In fact, the magnitude of the observed biological response was correlated with the extent of RhoJ knockdown achieved by the introduced shRNAs, suggesting that these effects on cell migration were specifically attributable

to diminished RhoJ expression; moreover, the only RhoJ-targeting hairpins that did not enhance motility were those that failed to successfully downregulate RhoJ levels. Taken together, these findings indicated that RhoJ expression is necessary to prevent the acquisition of a motile phenotype.

To further extend these observations, I ectopically expressed RhoJ in each of the four otherwise-highly motile SCCs (Supplementary Figure 2). In the cases of two of these four SCCs (SCC-4 and SCC-18), ectopic RhoJ expression impaired *in vitro* motility by >75% (Figure 3C). In contrast, however, RhoJ expression failed to diminish the migratory capacity of the other two high-motility SCCs (SCC-2 and SCC-13) (Figure 3C). These data therefore suggested that RhoJ expression is sufficient to impede cell motility in certain otherwise-aggressive breast cancer cells, but that alternative lines of high-motility breast cancer cells are impervious to the influences of ectopically expressed RhoJ and thus might modulate their motile behaviors via RhoJ-independent pathways. In fact, these observations provided empirical support for one of the stated goals of the SCC experimental system: namely, that this system would be capable of identifying multiple alternative genetic pathways that each were capable of fostering the same ultimate phenotypic output – instead of simply selecting for a single combination of genetic insults that drive that phenotype, as is typically accomplished by previously described approaches (Clark et al., 2000; Kang et al., 2003; Minn et al., 2005a; Bos et al., 2009).

Assessed collectively, these observations supported the notion that RhoJ can function to inhibit the *in vitro* motility of breast carcinoma cells. Moreover, the identification of RhoJ as a *bona fide* regulator of cell motility provided a proof-of-concept concerning the viability and utility of the SCC experimental system as a tool for the identification of novel regulators of metastasis-relevant processes of interest.

The SCC Experimental System Can be Utilized to Identify Candidate Novel Regulators of Metastatic Capacity *in vivo*

Encouraged by the successful identification of a previously unappreciated modulator of *in vitro* cell motility via deployment of the SCC system, I attempted to utilize this experimental tool to elucidate novel regulators of *in vivo* metastatic capacity. Upon sub-cutaneous implantation, the 30 SCCs displayed a >110-fold range in *in vivo* metastatic potential (Figure 1E). Among the 30 SCCs, four possessed weak metastatic abilities (SCC-4, SCC-18, SCC-19, and SCC-21) and five had a high proclivity to form metastases (SCC-5, SCC-12, SCC-20, SCC-23, and SCC-27), as compared to the parental bulk 231 cell population (Figure 1E). Microarray expression profiling succeeded in identifying a cohort of 314 differentially expressed genes whose levels were significantly correlated with the demonstrated metastatic abilities of these SCCs (data not shown). Thus, the SCC experimental system was capable of identifying candidate regulators of *in vivo* metastatic ability.

I focused on a subset of these candidates for follow-up analyses. This group of 35 genes was highlighted due to (1) the lack of previous reports concerning their potential role in metastasis and (2) the magnitude of their differential expression between the weakly metastatic and highly metastatic SCCs (Figure 4A and data not shown). From this group of candidate genes, independent RT-PCR analyses indeed verified the expression level changes observed in the initial microarray studies for 15 of these potential modulators of *in vivo* metastasis (Figures 4B-4P).

More specifically, CD33, cystatin F (CST7), interleukin 7 (IL7), leucine rich repeat and coiled-coil domain containing 1 (LRRCC1), matrix metallopeptidase 12 (MMP12), paraneoplastic antigen MA2 (PNMA2), PR domain containing 16 (PRDM16), syndecan 2

(SDC2), spectrin repeat containing nuclear envelope 1 (SYNE1), synaptotagmin-like 5 (SYTL5), tektin 1 (TEKT1), transmembrane protein 200A (TMEM200A), transmembrane phosphoinositide 3-phosphatase and tensin homolog 2 (TPTE2), testis-specific transcript Y-linked 15 (TTTY15), and Unc5B exhibited expression level changes that were associated with the known differential metastatic abilities of these nine SCCs (Figures 4B-4P). Hence, the SCC experimental system has implicated these gene products as possible regulators of *in vivo* metastatic capacity. Detailed investigation of the functional relevance of these various candidates for the process of *in vivo* tumor metastasis represents a topic of ongoing study and awaits definitive resolution.

MATERIALS AND METHODS

Cell Culture and Plasmid Construction

GFP-labeled 231 cells have been described (Valastyan et al., 2009a). shRNAs targeting the mRNA encoding RhoJ were expressed from the lentiviral vector pLKO.1-puro (Open Biosystems). The RhoJ cDNA was expressed from the pBABE-puro retroviral vector (Morgenstern and Land, 1990). Stable expression of the indicated plasmids was achieved via lentiviral or retroviral transduction, followed by selection with puromycin (Morgenstern and Land, 1990; Elenbaas et al., 2001; Valastyan et al., 2009b).

Measurements of *in vitro* Cell Proliferation

Proliferative kinetics were assayed by seeding 1.0×10^3 cells per well in 96-well plates and utilizing a CellTiter96 AQ$_{ueous}$ One Solution MTS Cell Proliferation Assay (Promega).

Subsequently, cells were incubated with the MTS reagent for 1.5 hours, and then total cell number was quantitated by measuring absorbance at 492 nm on a 96-well plate reader.

in vitro Motility Assays

For motility assays, 5.0×10^4 cells were plated atop uncoated membranes with 8.0 _m pores (BD Biosciences). Cells were seeded in serum-free media, and translocated toward complete growth media for 20 hours. Non-migrated cells were then physically removed by scraping. Successfully translocated cells were subsequently visualized using a Diff-Quick Staining Set (Dade) and manually counted under a light microscope.

Xenograft Studies

All animal studies complied with protocols approved by the MIT Committee on Animal Care. Male NOD/SCID mice (propagated on-site) were employed in the xenograft experiments. Mice were subjected to bilateral sub-cutaneous injections with 1.0×10^6 tumor cells resuspended in 1:2 Matrigel (BD Biosciences) plus normal growth media. Lung metastasis was subsequently quantified at the indicated timepoints using a fluorescent dissecting microscope; these analyses were performed within three hours of specimen isolation.

Microarray Gene Expression Profiling

Microarray analyses were conducted using 4x44k human whole-genome multiplex cDNA expression arrays (Agilent). Cy3-labeled cRNA was hybridized to individual microarrays, and raw intensity values were measured with an Agilent DNA microarray scanner at 532 nm. One-

color chip-normalized intensity readings for each of the assayed SCCs were then converted to fold-change values relative to the parental bulk 231 cell population.

Statistical Analyses

Data are presented as mean ± s.e.m. Student's t-test was utilized for all comparisons, with P <0.05 considered statistically significant.

Real Time RT-PCR

Total RNA was extracted from the indicated cells with a *mir*Vana MicroRNA Isolation Kit (Ambion). For detection of the levels of the indicated transcripts, cDNA was prepared from 500 ng of total RNA using the SuperScript III First-Strand Synthesis System (Invitrogen), and then quantitated by SYBR Green real time RT-PCR (Applied Biosystems).

Oligonucleotide Sequences

Oligonucleotides employed in this study were: ADAMTS12 RT-PCR, CAAGAGTGACCTCAATCCTGTTCATCACG and ATGTCTGCCCACAGGCTCACAGTCAT; CD33 RT-PCR, GTTCCACAGAACCCAACAACTGGTATCTTTC and TGACCCTGTGGTAGGGTGGGTGTCATT; CST7 RT-PCR, ACTCTGCTGGCCTTCTGCTGCCTGGTCTTGA and TATCTGAACTAGGGCCCTTGTGATGCGGGA; DDX4 RT-PCR, AGTGGCACAGGTAATGGTGATACTTCTCA and AGATGGAGTCCTCATCCTCAGGTGGA; FOXF2 RT-PCR, TCATCGTCATGGCCATCCAGAGCTC and CTCCTCGAACATGAACTCGCTGGC; GAPDH RT-PCR, TCACCAGGGCTGCTTTTAAC and GACAAGCTTCCCGTTCTCAG; IL7 RT-PCR, CTGATCCTTGTTCTGTTGCCAGTAGCATCA and GTGGAGATCAAAATCACCAGTGCTATTCA; LRRCC1 RT-PCR, ACCAAAGTCACTCAGAAGACAACACTTACCAG and GTTTGTGAACCATAACTTCGAGTTGTCCT; MMP12 RT-PCR,

TGACATACGTGGCATTCAGTCCCTGTAT and CTGGCTTCAATTTCATAAGCAGCTTCAATGCCA; PHACTR2 RT-PCR,

CACAGCGATGGTAAGAGACACCGT and CAAGTCTTTGAGGAATCCACATCAGGAGGT; PLXNC1 RT-PCR,

CTTGATCCATTCCGACCTGACATCCGT and GAATTCTCCTCACCTCTTTCCCAGCTGTTAG; PNMA2 RT-PCR,

TGTGACTGTCTTTGAGTGACCTAGTCTGGGAC and TATCCCCGTAACCATCAGTGACTTCTGCTCA; PRDM16 RT-PCR,

CACCTCAAGAAGCACGAGCACGAGAACGCA and ACACTGGGCACTGCCGTCCACGATCTGCATGT; RhoJ RT-PCR,

ACACTTGCTCGGACTGTATGACACCG and TGCGAGCTTCACACCATGCTC; SDC2 RT-PCR,

GACGCTGAATATACAGAACAAGATACCTGCTCAG and AGGTCATAGCTTCCTTCATCCTTCTTTCTC; SYNE1 RT-PCR,

TCTCCATCAATCTCTGCAGCCCTGAGTTCA and TACTCTGAGTTGGGATTCCAACAGCTCATG; SYTL5 RT-PCR,

TGTTCTCGGCACTGATGTTGTCCGACAGTC and TGTTGACCGTCTAAGTCCAAGCTATAGCTC; TEKT1 RT-PCR,

AGACCACAAGAAAATCTCAAAGCGATGTG and TGCACCAGGTCAATGCCAATGCGCTTCT; TFEC RT-PCR,

AGCAGCAACTTGGTGGTGTACTACTGG and CAATGGAGAAAGGCAATGACCACCTG; TMEM200A RT-PCR,

GAATGAAGGCGGTGTGGTGGTTCGCTTCT and CTTAGCGTGTGAATGTCAATGACTGTGGA; TPTE2 RT-PCR,

ATGACGGTCCACCTCTGTATGATGATGTGA and GCCAAAAAGTATCTCCACAGCAAATTCTGG; TTTY15 RT-PCR,

CAAGTTAGAAACTGTTCAGGGCCAACTTACCT and GTATGTTGGTTCAGTCTAGAAAGGCAGGGA; Unc5B RT-PCR,

ACGCTGCTCGACTCTAAGAACTGCACAGAT and CAGCAGATGAGTCAGTGATGTCTGTGTCGA; ZMAT4 RT-PCR,

CTGAAAGGATCTAAACACCAGACCAACCTG and GGATAGAGGTGGTTTACATCACACTCATTGAGG; Subcloning RhoJ

to pBABEpuro, TTGGTTTCCAGGATCCATGAACTGCAAAGAGGGAACTGACAGCAG and
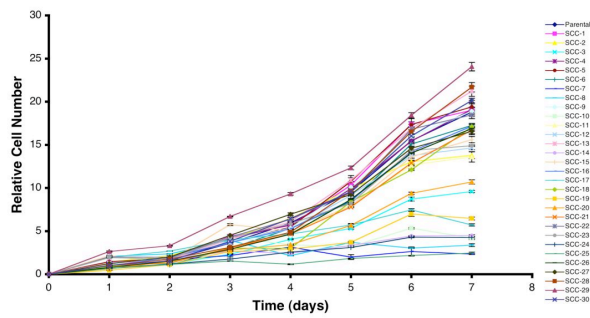
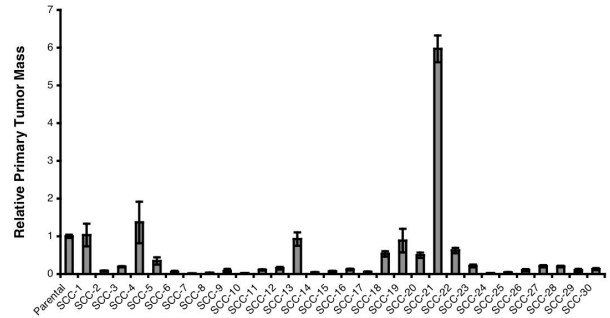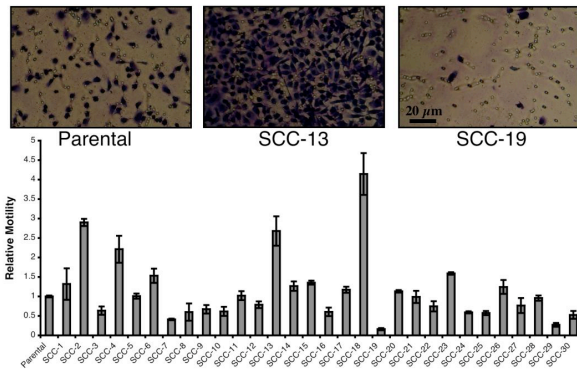TTGGTTTCCAGAATTCTCAGATAATTGAACAGCAGCTGTGACCCTCAG.

FIGURES

Figure 1

Figure 1. Single-Cell Clones Derived from the Parental Bulk Population of MDA-MB-231 Cells Display Extensive Functional Heterogeneity. (A) Summary of the functional diversity that exists among the 30 isolated MDA-MB-231 (231) cell single-cell clones (SCCs). **(B)**

Proliferative kinetics of the 30 SCCs *in vitro*. n =3. **(C)** Primary tumor sizes 60 days after sub-

cutaneous implantation of the 30 SCCs *in vivo*. n = 4. **(D)** Images of successfully migrated cells

20 hours after seeding *in vitro* for the indicated SCCs (top panels). Quantification of *in vitro*

motility for the 30 SCCs (bottom panel). n = 3. **(E)** Fluorescent images of murine lungs to

visualize the indicated SCCs 60 days after sub-cutaneous injection *in vivo* (top panels).

Quantification of *in vivo* metastatic burden for the 30 SCCs (bottom panel). n = 4. Data are

presented as mean ± s.e.m.

Figure 2

A

	SCC-2	SCC-4	SCC-7	SCC-13	SCC-18	SCC-19	SCC-29
ADAMTS12	2.504406124	0.084266971	8.659962447	2.23860455	1.26043359	2.31744249	51.8288581
DDX4	0.459741485	3.829914199	2.381312502	2.54587081	10.7837599	0.7448607	0.94635201
FOXF2	0.941717056	0.697589656	1.483969125	2.06383927	0.98298548	0.11999164	0.03360482
PHACTR2	0.201145279	0.159490391	1.000977103	0.14693329	0.4978471	0.66327651	8.54612457
PLXNC1	0.611730093	0.441826587	0.259125541	0.49318332	0.81303311	0.42342372	0.00271917
RHOJ	0.068615484	0.02771778	0.15073634	0.03568756	0.05619552	0.21426335	0.24835483
TFEC	1.920393576	2.197108901	40.18464337	0.19556188	18.9719486	31.242163	8.41278729
ZMAT4	0.552673641	0.416573387	0.422334644	0.52305441	1.02728359	9.6794507	2.35650635
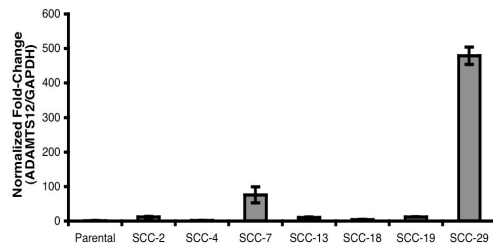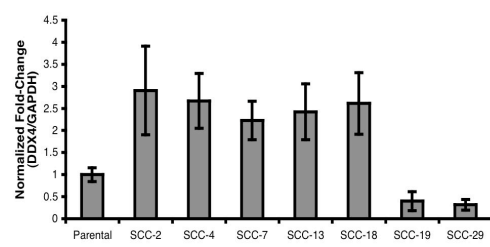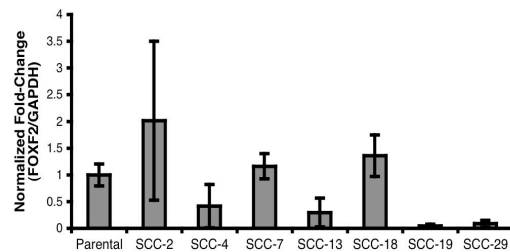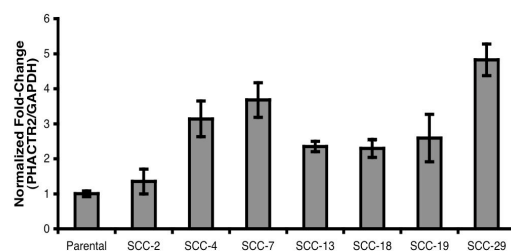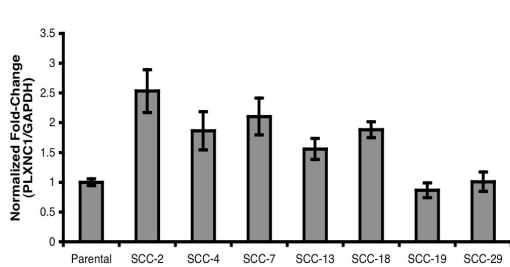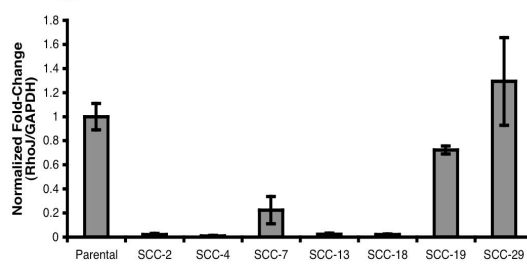
Figure 2. The SCC Experimental System Can be Utilized to Identify Novel Candidate Regulators of Metastasis-Relevant Processes *in vitro*. **(A)** Microarray expression profiling data

for eight selected candidate genes from the seven SCCs that displayed either high-motility

(green) or low-motility (red) phenotypes *in vitro*. Fold-change values are presented relative to the

parental bulk 231 cell population. **(B)** Real time RT-PCR for ADAMTS12 in the indicated SCCs.

GAPDH was a loading control. n = 3. **(C)** DDX4 levels in the indicated SCCs, as gauged by real

time RT-PCR. GAPDH was a loading control. n = 3. **(D)** Real time RT-PCR for FOXF2 in the

indicated SCCs. GAPDH was a loading control. n = 3. **(E)** PHACTR2 levels in the indicated

SCCs, as gauged by real time RT-PCR. GAPDH was a loading control. n = 3. **(F)** Real time RT-

PCR for PLXNC1 in the indicated SCCs. GAPDH was a loading control. n = 3. **(G)** RhoJ levels

in the indicated SCCs, as gauged by real time RT-PCR. GAPDH was a loading control. n = 3.

(H) Real time RT-PCR for TFEC in the indicated SCCs. GAPDH was a loading control. n = 3.

(I) ZMAT4 levels in the indicated SCCs, as gauged by real time RT-PCR. GAPDH was a

loading control. n = 3. Data are presented as mean ± s.e.m.

Figure 3

A

SCC-19

B

SCC-29

C
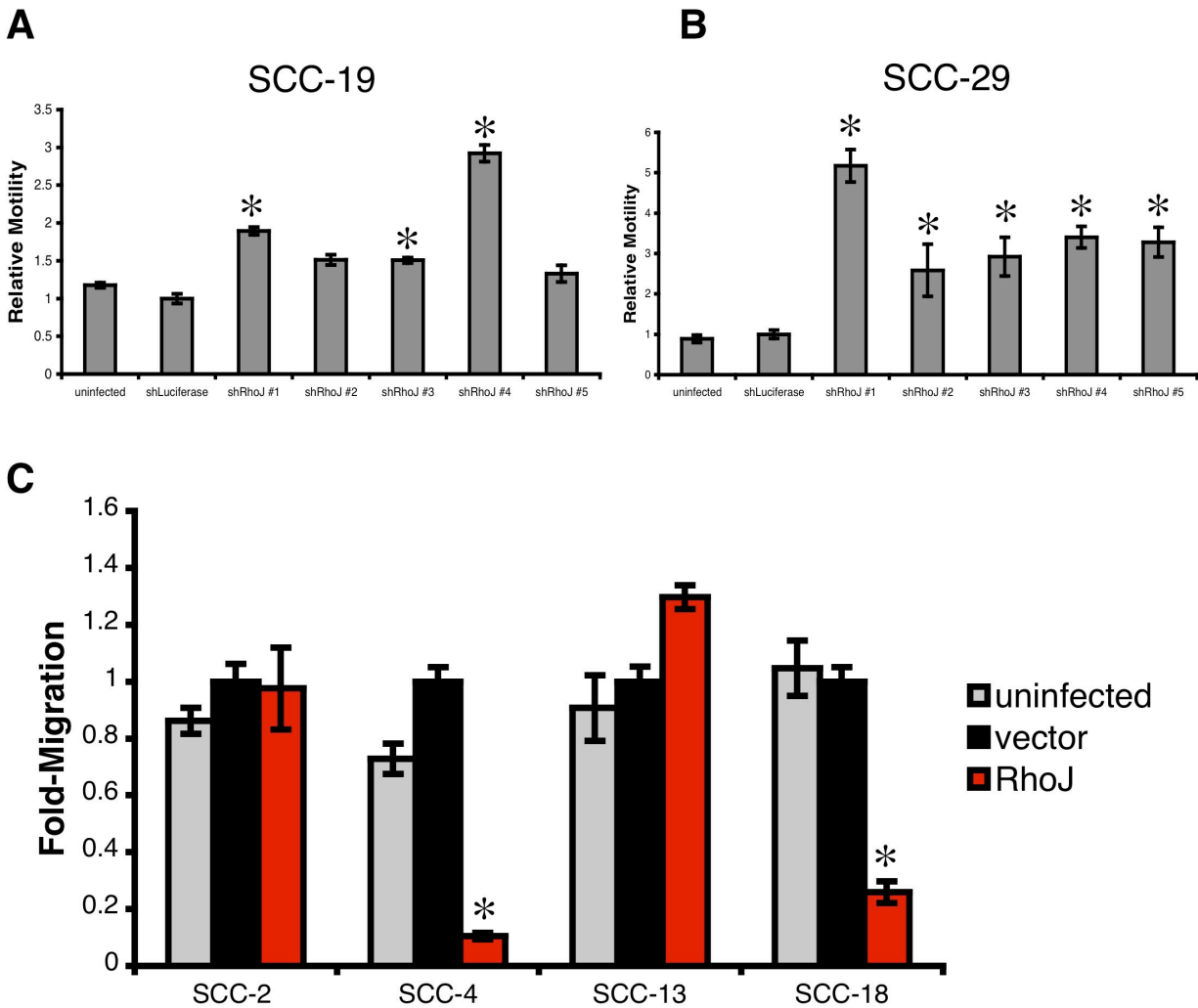
Figure 3. RhoJ Expression Can be Both Necessary and Sufficient to Impair Cell Motility *in*

***vitro*. (A)** Migration assays utilizing the indicated SCCs. n =3. Asterisks: P <0.05 relative to

shLuciferase cells. **(B)** Migration assays employing SCCs infected as denoted. n =3. Asterisks: P

<0.05 relative to shLuciferase cells. **(C)** Migration assays utilizing the indicated SCCs. n =3.

Asterisks: P <0.02 relative to vector control cells. Data are presented as mean ± s.e.m.

Figure 4

A

	SCC-4	SCC-5	SCC-12	SCC-18	SCC-19	SCC-20	SCC-21	SCC-23	SCC-27
CD33	0.09577565	2.47742116	0.67502994	0.07136415	0.05240543	0.26567272	0.05322228	1.52483193	0.27418708
CST7	0.10254001	6.86599686	5.08984533	0.2565456	0.23307634	0.44565473	0.10391844	60.2047719	5.98989066
IL7	0.04898063	0.61800258	0.10820351	0.11663001	0.14258854	1.43781996	0.21806212	0.80881855	0.76046706
LRRCC1	1.03852527	0.09045288	0.16024699	0.72913308	0.48177919	0.06712493	0.85452545	0.1281808	0.08742004
MMP12	0.17669969	7.22384572	2.32685605	0.19409138	2.2508314	0.68820798	0.39046811	15.5490657	1.7384798
PNMA2	12.9738779	3.98012755	3.82825106	15.467345	4.0797543	1.25651854	5.18357022	0.51639334	2.02776378
PRDM16	0.1339851	0.00115675	1.33022998	0.16330297	0.02979971	0.67686255	0.08312482	0.34306888	0.4716069
SDC2	0.04019128	0.54325897	0.65405602	0.10670473	0.14887486	0.08407196	0.08104571	0.9652067	0.55522438
SYNE1	5.55009529	3.36417633	3.78846507	15.0529394	16.3043783	1.84869436	14.2284736	1.70837759	1.94761373
SYTL5	0.004843	0.3594043	0.36392209	0.00048352	0.00849356	1.48289743	0.00452022	0.462944	0.04918411
TEKT1	8.49407897	0.9937864	2.7211569	45.0612165	121.783276	1.89385609	0.6843211	1.94664704	0.19775116
TMEM200A	1.14599327	0.26490689	0.03032801	1.3620539	4.14157608	0.90288105	0.02870948	0.04167773	0.23899456
TPTE2	0.03172785	1.11602784	0.06470059	0.06290106	0.00903925	1.44629974	0.02828172	0.09580902	0.07730346
TTTY15	18.8382615	1.46460224	15.5832646	247.897426	48.3139488	1.5550178	51.9074868	1.46276059	0.55936675
UNC5B	0.01899176	0.92972875	1.10747899	0.02510206	0.00709187	1.09057269	0.01898847	1.18229542	1.11206956
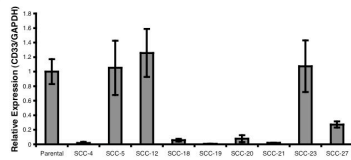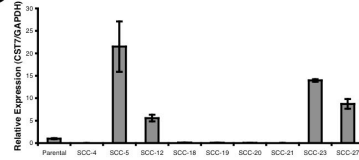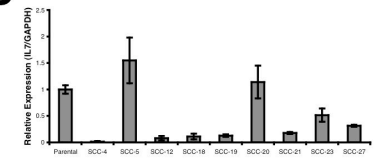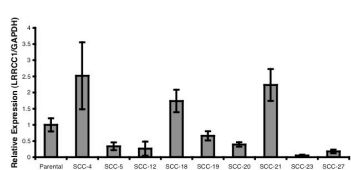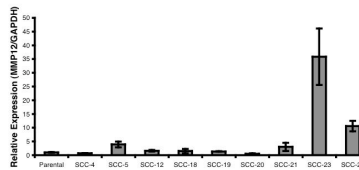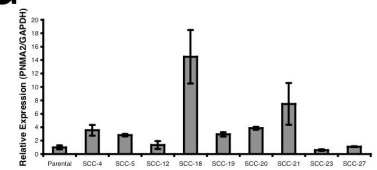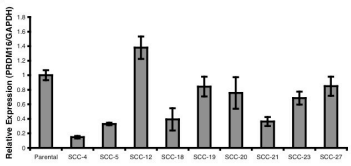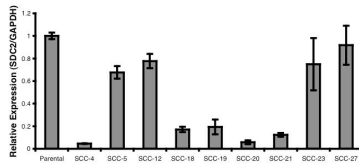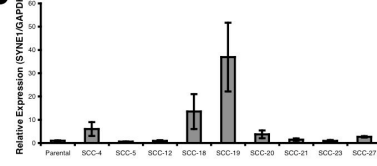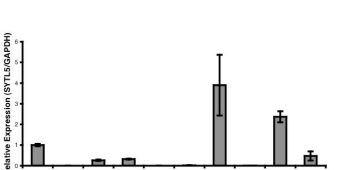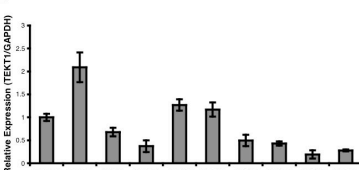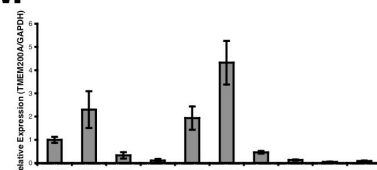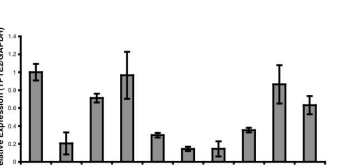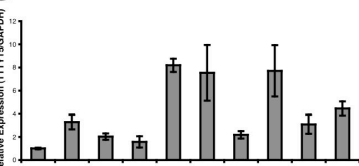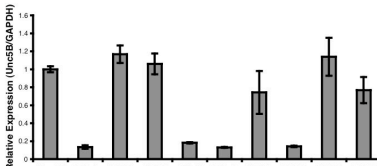
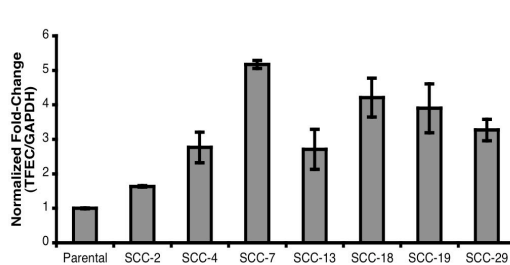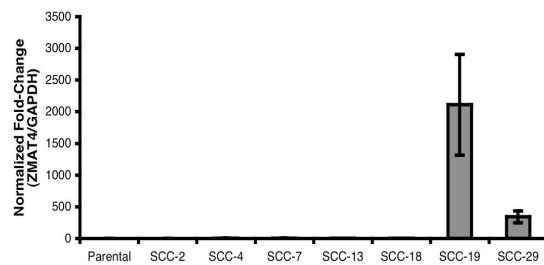**Figure 4. The SCC Experimental System Can be Utilized to Identify Novel Candidate Regulators of Metastatic Capacity *in vivo*. (A)** Microarray expression profiling data for 15

selected candidate genes from the nine SCCs that displayed either highly metastatic (green) or weakly metastatic (red) phenotypes *in vivo*. Fold-change values are presented relative to the parental bulk 231 cell population. **(B)** Real time RT-PCR for CD33 in the indicated SCCs. GAPDH was a loading control. n = 3. **(C)** CST7 levels in the indicated SCCs, as gauged by real time RT-PCR. GAPDH was a loading control. n = 3. **(D)** Real time RT-PCR for IL7 in the indicated SCCs. GAPDH was a loading control. n = 3. **(E)** LRRCC1 levels in the indicated SCCs, as gauged by real time RT-PCR. GAPDH was a loading control. n = 3. **(F)** Real time RT-PCR for MMP12 in the indicated SCCs. GAPDH was a loading control. n = 3. **(G)** PNMA2 levels in the indicated SCCs, as gauged by real time RT-PCR. GAPDH was a loading control. n = 3. **(H)** Real time RT-PCR for PRDM16 in the indicated SCCs. GAPDH was a loading control. n = 3. **(I)** SDC2 levels in the indicated SCCs, as gauged by real time RT-PCR. GAPDH was a loading control. n = 3. **(J)** Real time RT-PCR for SYNE1 in the indicated SCCs. GAPDH was a loading control. n = 3. **(K)** SYTL5 levels in the indicated SCCs, as gauged by real time RT-PCR. GAPDH was a loading control. n = 3. **(L)** Real time RT-PCR for TEKT1 in the indicated SCCs. GAPDH was a loading control. n = 3. **(M)** TMEM200A levels in the indicated SCCs, as gauged by real time RT-PCR. GAPDH was a loading control. n = 3. **(N)** Real time RT-PCR for TPTE2 in the indicated SCCs. GAPDH was a loading control. n = 3. **(O)** TTTY15 levels in the indicated SCCs, as gauged by real time RT-PCR. GAPDH was a loading control. n = 3. **(P)** Real time RT-PCR for Unc5B in the indicated SCCs. GAPDH was a loading control. n = 3. Data are presented as mean ± s.e.m.

Supplementary Figure 1

A

B
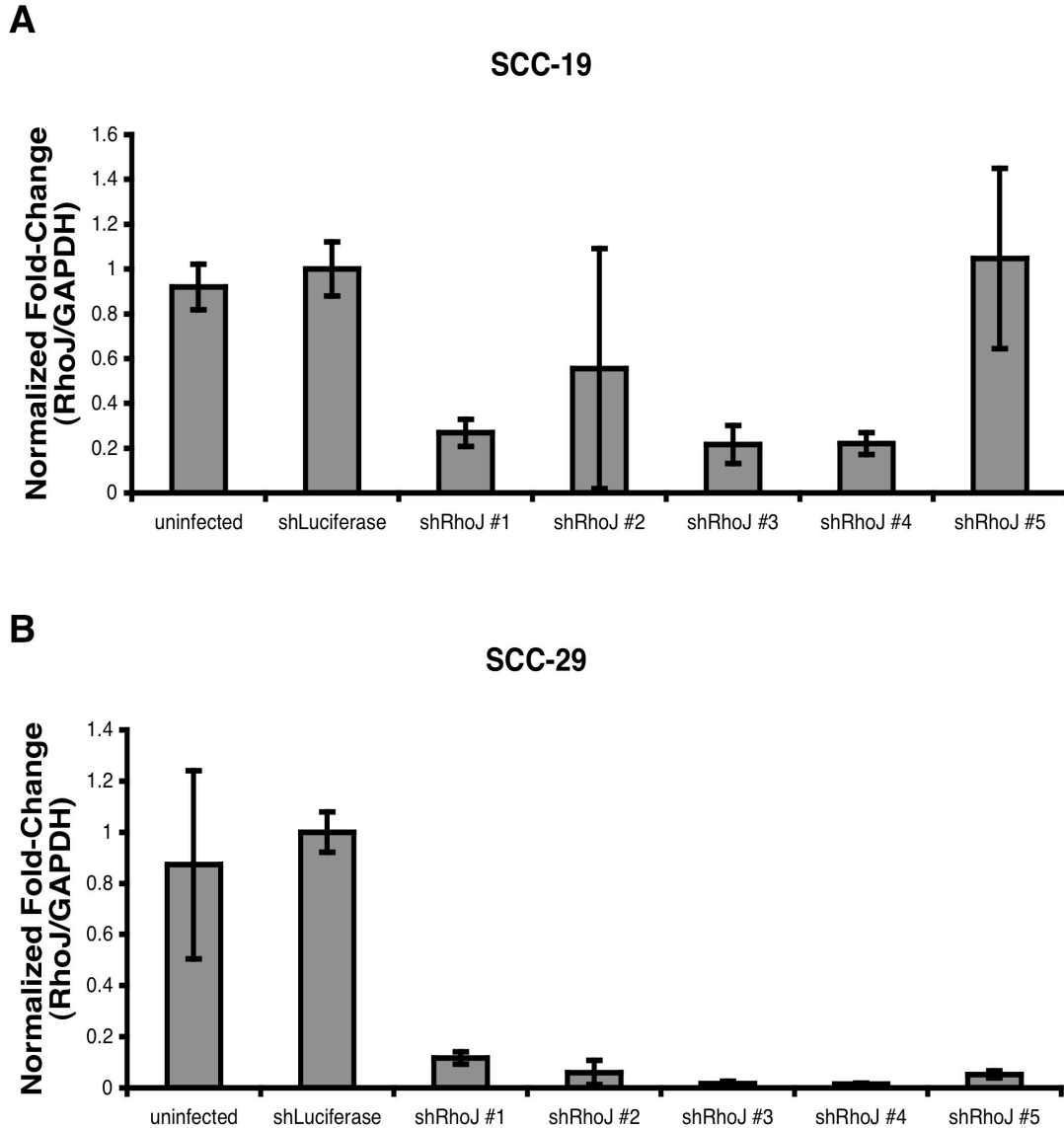
Supplementary Figure 1. Quantification of the Extent of Knockdown Achieved Upon Transduction of RhoJ-Targeting shRNAs. (A) Real time RT-PCR analysis for RhoJ in the indicated single-cell clones (SCCs). GAPDH was a loading control. n = 3. **(B)** RhoJ expression levels in the indicated SCCs, as gauged by RT-PCR. GAPDH was a loading control. n = 3. Data are presented as mean ± s.e.m.

A

SCC-2

B

SCC-4

C

SCC-13

D

SCC-18
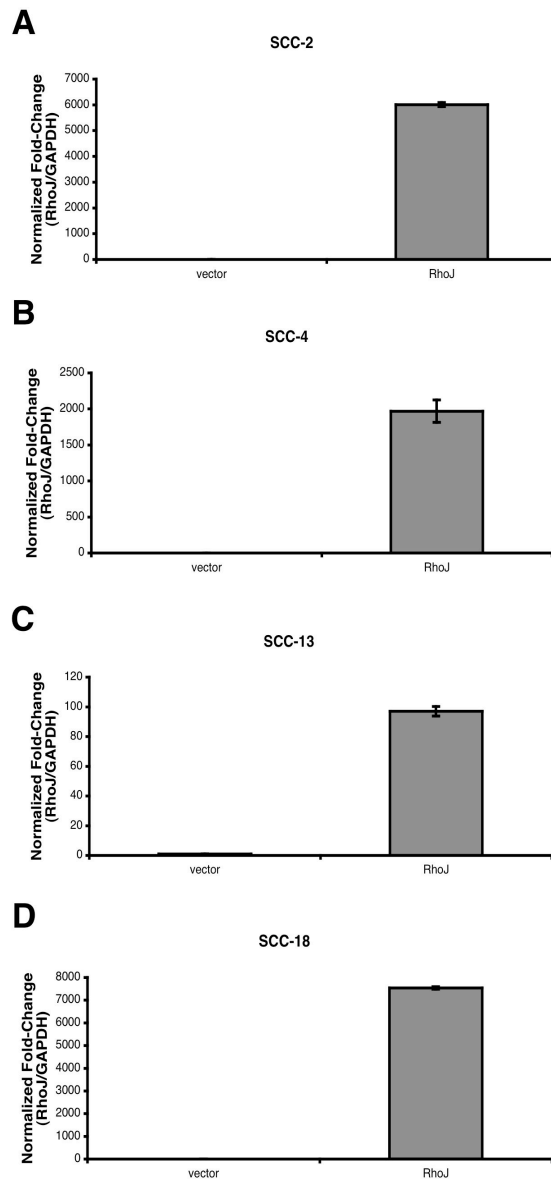
Supplementary Figure 2. Quantification of Total RhoJ Levels in Cells Infected with a RhoJ-Encoding cDNA. (A) Real time RT-PCR analysis for RhoJ in the indicated SCC. GAPDH was a loading control. n = 3. **(B)** RhoJ expression levels in the indicated SCC, as gauged by RT-PCR. GAPDH was a loading control. n = 3. **(C)** Real time RT-PCR analysis for RhoJ in the indicated SCC. GAPDH was a loading control. n = 3. **(D)** RhoJ expression levels in the indicated SCC, as gauged by RT-PCR. GAPDH was a loading control. n = 3. Data are presented as mean ± s.e.m.

ACKNOWLEDGMENTS

REFERENCES

Bos PD, Zhang XH, Nadal C, et al. (2009). Genes that mediate breast cancer metastasis to the brain. Nature *459*,1005-1009.

Brabletz T, Jung A, Spaderna S, Hlubek F, and Kirchner T. (2005). Migrating cancer stem cells – an integrated concept of malignant tumour progression. Nat Rev Cancer *5*, 744-749.

Cailleau R, Olive M, and Cruciger QV. (1978). Long-term human breast carcinoma cell lines of metastatic origin: preliminary characterization. In Vitro *14*, 911-915.

Clark EA, Golub TR, Lander ES, and Hynes RO. (2000). Genomic analysis of metastasis reveals an essential role for RhoC. Nature *406*, 532-535.

Elenbaas B, Spirio L, Koerner F, et al. (2001). Human breast cancer cells generated by oncogenic transformation of primary mammary epithelial cells. Genes Dev *15*, 50-65.

Fidler IJ. (2003). The pathogenesis of cancer metastasis: the 'seed and soil' hypothesis revisited. Nat Rev Cancer *3*, 453-458.

Gupta GP and Massagué J. (2006). Cancer metastasis: building a framework. Cell *127*, 679-695.

Heasman SJ and Ridley AJ. (2008). Mammalian Rho GTPases: new insights into their functions from in vivo studies. Nat Rev Mol Cell Biol *9*, 690-701.

Jaffe AB and Hall A. (2005). Rho GTPases: biochemistry and biology. Annu Rev Cell Dev Biol *21*, 247-269.

Kang Y, Siegel PM, Shu W, et al. (2003). A multigenic program mediating breast cancer metastasis to bone. Cancer Cell *3*,537-549.

Minn AJ, Gupta GP, Siegel PM, et al. (2005a). Genes that mediate breast cancer metastasis to lung. Nature *436*, 518-524.

Minn AJ, Kang Y, Serganova I, et al (2005b). Distinct organ-specific metastatic potential of individual breast cancer cells and primary tumors. J Clin Invest *115*, 44-55.

Morgenstern JP and Land H. (1990). Advanced mammalian gene transfer: high titre retroviral vectors with multiple drug selection markers and a complementary helper-free packaging cell line. Nucleic Acids Res *18*, 3587-3596.

Ramaswamy S, Ross KN, Lander ES, and Golub TR. (2003). A molecular signature of metastasis in primary solid tumors. Nat Genet *33*, 49-54.

Rosen JM and Jordan CT. (2009). The increasing complexity of the cancer stem cell paradigm. Science *324*, 1670-1673.

Valastyan S, Benaich N, Chang A, et al. (2009b). Concomitant suppression of three target genes can explain the impact of a microRNA on metastasis. Genes Dev *23*, 2592-2597.

Valastyan S, Reinhardt F, Benaich N, et al. (2009a). A pleiotropically acting microRNA, miR-31, inhibits breast cancer metastasis. Cell *137*, 1032-1046.

van't Veer, Dai H, van de Vijver MJ, et al. (2002). Gene expression profiling predicts clinical outcome of breast cancer. Nature *415*, 530-536.

Chapter 7

Conclusions and Future Directions

Portions of this chapter are excerpted from the following publications (copyright permissions obtained):

1. Valastyan S, Reinhardt F, Benaich N, Calogrias D, Szász AM, Wang ZC, Brock JE, Richardson AL, and Weinberg RA. (2009). A pleiotropically acting microRNA, miR-31, inhibits breast cancer metastasis. Cell *137*, 1032-1046.

2. Valastyan S and Weinberg RA. (2009). MicroRNAs: crucial multi-tasking components in the complex circuitry of tumor metastasis. Cell Cycle *8*, 3506-3512.

3. Valastyan S, Benaich N, Chang A, Reinhardt F, and Weinberg RA. (2009). Concomitant suppression of three target genes can explain the impact of a microRNA on metastasis. Genes Dev *23*, 2592-2597.

4. Valastyan S and Weinberg RA. (2010). miR-31: a crucial overseer of tumor metastasis and other emerging roles. Cell Cycle. In press.

5. Valastyan S, Chang A, Benaich N, Reinhardt F, and Weinberg RA. (2010). Concurrent suppression of integrin _5, radixin, and RhoA phenocopies the effects of miR-31 on metastasis. Cancer Res. In press.

This thesis has focused on defining genetic events that drive the complex cell-biologic processes that underlie metastatic progression in human breast carcinoma cells. To this end, two independent lines of study were conducted. First, I succeeded in identifying a human microRNA (miRNA) that regulated tumor metastasis and subsequently investigated the mechanistic underpinnings of these phenotypic influences. I was able to accomplish this by creating various novel cell line models that perturbed the functional levels of miR-31 and/or certain downstream effectors of this miRNA. Second, I developed a novel experimental system capable of elucidating molecular regulators of metastasis in an unbiased fashion; this tool was utilized to uncover previously unexplored genes of possible relevance to metastatic progression. In order to do so, I devised a genomics-based approach that preserved and assayed the intrinsic genetic diversity and functional heterogeneity that pre-exists within tumor cell populations. In this chapter, I will discuss the implications of my work for the larger field of cancer research and I will consider potential future directions that stem from my previous observations.

miR-31 Functions as a Negative Regulator of Breast Cancer Metastasis

Experiments described in Chapter Two revealed that expression of the human miRNA miR-31 is both necessary and sufficient to inhibit breast cancer metastasis. In humans, miR-31 is encoded by a single genomic locus and is normally expressed in a variety of tissues and cell types (Grimson et al., 2007; Landgraf et al., 2007). Additionally, miR-31 is the only member of a broadly conserved miRNA "seed family" that is present in vertebrates and *Drosophila* (i.e., miR-31 is the only known miRNA possessing a particular eight nucleotide motif that acts as the major determinant of miRNA targeting specificity) (Grimson et al., 2007).

Of interest, in Chapter Two, I demonstrated that miR-31 is endowed with the ability to concomitantly inhibit several distinct steps of the invasion-metastasis cascade. More specifically, miR-31 impedes local invasion, one or more early post-intravasation events (intraluminal viability, extravasation, and/or initial survival in the lung parenchyma), and metastatic colonization. Remaining unresolved by these analyses, however, is a detailed understanding of the particular early post-intravasation event(s) affected by the biological actions of miR-31. Accordingly, one potential future direction for this work involves dissecting this observed effect in greater detail. Experimentally, this could be accomplished by intravenously injecting fluorescently labeled tumor cells into mice, waiting for a relatively short period of time (between one and three days), intravenously injecting the mice with rhodamine-conjugated lectin to stain the pulmonary vasculature, and then assessing whether the labeled tumor cells were still located intraluminally or had instead extravasated into the lung parenchyma (Gupta et al., 2007).

At the time of this study, only a limited number of miRNAs with pro- (miR-10b, -21, and -373/520c) or anti-metastatic (miR-34b/c, -126, -148a, -206, and -335) functions had been identified (Ma et al., 2007; Huang et al., 2008; Tavazoie et al., 2008; Asangani et al., 2008; Zhu et al., 2008; Lujambio et al., 2008). However, the contributions of miR-10b, miR-21, and miR-373/520c specifically to metastasis-promotion are not easily discerned due to their mitogenic and/or anti-apoptotic roles (Voorhoeve et al., 2006; Ma et al., 2007; Si et al., 2007). Similarly, the anti-metastatic miRNAs miR-34b/c, miR-126, and miR-148a impair primary tumor growth (Lujambio et al., 2008; Tavazoie et al., 2008), while miR-206 and miR-335 inhibit proliferation or promote apoptosis (Sathyan et al., 2007; Kondo et al., 2008), again obscuring their precise roles in metastasis. In contrast, miR-31 obstructs metastasis without exerting confounding

influences on primary tumor development. As such, *mir-31* might aptly be categorized as a "metastasis suppressor gene" (Steeg, 2003).

Previous studies described effects of specific miRNAs only on an early stage of the invasion-metastasis cascade – local invasion. In contrast, the work described in Chapter Two demonstrated that miRNAs can also influence subsequent steps of metastasis and that an individual miRNA can intervene at multiple distinct stages of the invasion-metastasis cascade. Notably, miR-31 suppresses metastatic colonization – the final and rate-limiting step of metastasis (Fidler, 2003; Gupta and Massagué, 2006). Because clinical observations link colonization efficiency with ultimate disease outcome in human carcinoma patients (Fidler, 2003; Gupta and Massagué, 2006), miR-31's ability to impede metastatic colonization may be quite significant.

Of additional interest, in Chapter Two, I found that loss of miR-31 activity enhances invasiveness, motility, and anoikis resistance in primary normal human mammary epithelial cells. Hence, inactivation of miR-31 in a normal epithelial cell may facilitate its dissemination even prior to its transformation to a fully neoplastic state. This suggests one possible mechanism by which the invasion-metastasis cascade could be initiated very early during the course of primary tumor progression, a phenomenon that has recently been observed in clinical breast tumors (Hüsemann et al., 2008).

All of my studies were conducted using breast cancer cells. Therefore, the functional ramifications of miR-31 expression for metastatic progression in carcinoma cells originating from other tissue types remain unclear. This represents an important question to investigate moving forward, as these analyses will reveal whether miR-31 downregulation is a common

event that causatively drives metastatic progression across a variety of carcinoma types or, alternatively, if the anti-metastatic roles of miR-31 are more tissue-specific.

My analyses relied on established human cell lines and xenograft studies, approaches that cannot fully simulate clinical carcinomas. For example, cell lines accumulate genetic changes in culture, while xenografts fail to recapitulate species-specific interactions between tumor cells and their stroma. However, the consistency of my results upon use of multiple independent cell lines (including a single-cell-derived population), the convergence of my gain- and loss-of-function findings, and my correlative studies in human breast cancer patients and murine mammary tumor cell lines argue against major confounding influences stemming from my experimental models.

Collectively, the findings of the studies presented in Chapter Two carry significant implications regarding our understanding of the pathogenesis of high-grade malignancies. My data suggest that the loss of a single gene product can facilitate the completion of multiple distinct steps of the invasion-metastasis cascade; this pleiotropic action may help to explain how tumor cells can accumulate enough genetic and epigenetic aberrations over the course of a human lifespan to overcome the numerous barriers that normally operate to prevent metastasis. Moreover, because distant metastases are responsible for patient mortality in the vast majority of human carcinomas, miR-31's ability to impede metastasis may prove to be clinically useful in the development of diagnostic, prognostic, and/or therapeutic reagents.

Correlations Between miR-31 Levels and Disease Progression in Human Tumors

In Chapter Two, I documented an inverse association between miR-31 levels in primary human breast tumors and the propensity for these patients to suffer from metastatic relapse. Of note, in contrast to existing clinically utilized biomarkers for breast cancer (Desmedt et al.,

2008), the inverse correlation between miR-31 levels and the tendency for disease relapse operated independently of both the grade and molecular subtype of the primary tumor. In this respect, miR-31 may stand apart from the great majority of biomarkers that are currently utilized prognostically for this disease. Additionally, my prior investigations in Chapter Two concerning miR-31 expression in patient-matched primary tumors and distant metastases revealed that selective pressures may operate that act to diminish the prevalence of miR-31-expressing cells during the course of metastatic progression.

Concordant with my own observations was a recent report indicating that reduced miR-31 expression is a hallmark of the acquisition of an invasive phenotype in clinical bladder cancers (Wszolek et al., 2009). Similarly, microarray expression profiling of clinical breast tumors revealed reduced miR-31 in luminal B (relative to luminal A), basal-like, and HER2^{+} tumors (Mattie et al., 2006; Blenkiron et al., 2007) – patterns of reduction that correlate with aggressive disease (Sørlie et al., 2001).

miR-31 expression has also been found to be attenuated in human carcinomas of the breast (Calin et al., 2004; Zhang et al., 2006; Yan et al., 2008), prostate (Schaefer et al., 2010), ovary (Creighton et al., 2010), and stomach (Guo et al., 2009; Zhang et al., 2009). Indeed, homozygous loss of the miR-31-encoding genomic locus has been described in human urothelial carcinomas (Veerla et al., 2009) and acute lymphoblastic leukemias (Usvasalo et al., 2010). Paradoxically, upregulation of miR-31 in human colorectal (Bandrés et al., 2006; Motoyama et al., 2009), liver (Wong QW et al., 2008), and head-and-neck tumors (Liu et al., 2009; Liu et al., 2010), as well as squamous cell carcinomas of the tongue (Wong TS et al., 2008), has also been observed. Importantly, none of these studies stratified their patient cohorts based on metastasis status.

In light of these diverse clinical findings, it is plausible that downregulation of miR-31 is associated with malignant progression in a variety of types of human neoplasias; however, at present, I cannot exclude a more tissue-specific anti-malignant role for this miRNA, potentially arising due to restricted expression patterns of certain functionally relevant downstream effectors of miR-31 in carcinoma cells originating from different tissues. One important subject for future investigation will involve deciphering whether miR-31 expression levels in primary tumors are associated with the propensity for metastasis formation in carcinomas arising in epithelial tissues other than the breast. In these studies, it will be critical to carefully case-control patient cohorts with respect to potentially confounding variables that are known to correlate with metastatic propensity, including lymph node status and tumor grade (Desmedt et al., 2008).

Ectopic miR-31 Expression Enhances Primary Mammary Tumor Growth

An unexpected finding from my analyses presented in Chapter Two stems from the observation that – despite miR-31's metastasis-suppressing roles – ectopic expression of this miRNA enhanced primary mammary tumor growth in orthotopic implantation xenograft assays. One possible interpretation of this result would be that the high levels of ectopic expression achieved with my viral delivery system are not physiologically relevant and that this phenotype may represent an artifact of high-level overexpression. However, data presented in Chapter Two indicated that the retrovirus-mediated ectopic expression of miR-31 in aggressive human breast cancer cells achieved a level of mature miR-31 that was quite comparable to the endogenous levels of this miRNA expressed by primary normal human mammary epithelial cells.

It is therefore plausible that miR-31's capacity to promote primary mammary tumor growth does not represent an overexpression artifact. Consequently, an oncogenic role for this

metastasis-suppressing miRNA cannot be formally excluded. Such duality of action is not unprecedented (Massagué, 2008) and is consistent with notions that metastasis- and tumorigenesis-enabling attributes can be biologically distinct and acquired via independent selective pressures during distinct stages of malignant progression. Mechanistically, findings detailed in Chapter Three indicated that the capacity of miR-31 to enhance primary tumor growth operates independently of the protein machinery deployed by miR-31 to mediate its anti-metastatic activities.

The recent work of others may provide insight regarding miR-31's capacity to promote primary tumor growth. It was reported that miR-31 increased the oncogenic potential of head-and-neck squamous cell carcinoma cell lines *in vitro* and also slightly augmented their ability to form primary tumors *in vivo* (Liu et al., 2010). The authors also discovered that miR-31 directly targeted FIH, a negative modulator of hypoxia-inducible factor (HIF) signaling under normoxic conditions (Liu et al., 2010). Thus, miR-31 fostered ectopic HIF-mediated signaling even under conditions devoid of oxygen deprivation. Given the well-described roles of HIF in pro-survival and hyper-proliferative signaling (Semenza, 2003), it is possible that miR-31-evoked stimulation of primary tumor growth *in vivo* may one day be traced to the ability of this miRNA to activate HIF-dependent tumor-promoting signaling circuitry.

In contrast, an independent global miRNA expression profiling study discovered that miR-31 was the most strongly downregulated miRNA in serous ovarian tumors (Creighton et al., 2010). Functional analyses subsequently demonstrated that miR-31 expression inhibited proliferation and promoted apoptosis in ovarian tumor cells; interestingly, these tumor-suppressing effects were observable only in cell lines with a dysfunctional p53 signaling pathway (Creighton et al., 2010). This relationship between miR-31-dependent cell cycle arrest

or apoptosis and defective p53-mediated signaling also applied to osteosarcoma and pancreatic carcinoma cell lines (Creighton et al., 2010). At a mechanistic level, the authors attributed these anti-tumorigenic functions to miR-31's capacity to directly target the E2F2 cell cycle regulator (Creighton et al., 2010). This supposition was consistent with the p53 status-dependence of these responses, as high-level E2F2 activity typically leads to p14^{ARF}-evoked upregulation of p53-mediated apoptosis in cells possessing an intact p53 pathway; in contrast, E2F2 readily promotes cell cycle progression in a p53-deficient cellular context (Sherr and McCormick, 2002). Although not investigated in this report, it will be important for future work to determine whether miR-31 impacts the *in vivo* behavior of ovarian carcinoma cell lines grown as tumor xenografts, as well as the p53 status-dependence of these putative effects.

When taken together, these studies indicate that miR-31 may exert multiple cancer-relevant functions in different tissue types and genetic contexts. This initially perplexing observation has also been documented for a number of other miRNAs that critically regulate tumor biology, including the let-7 (Brueckner et al., 2007; Kumar et al., 2008) and miR-200 (Dykxhoorn et al., 2009; Wellner et al., 2009) seed families. I speculate that many of these differences arise as a consequence of differential expression patterns of the repertoire of miR-31 target genes in distinct tissue types, although direct validation of this model awaits future studies.

Concomitant Suppression of Integrin 5, Radixin, and RhoA Can Explain the Impact of miR-31 on Breast Cancer Metastasis

Work presented in Chapters Two, Three, and Four investigated the molecular mechanisms underlying miR-31-imposed metastasis suppression. In Chapter Two, I identified frizzled3 (Fzd3), integrin _5 (ITGA5), matrix metallopeptidase 16 (MMP16), myosin

phosphatase-Rho interacting protein (M-RIP), radixin (RDX), and RhoA as direct downstream effectors of miR-31 and discovered that modulation of the levels of ITGA5, RDX, and RhoA (but not Frzd3, MMP16, or M-RIP) affected miR-31-evoked inhibition of a variety of *in vitro* surrogate markers of metastatic capacity. In Chapter Three, I found that the concurrent re-expression of ITGA5, RDX, and RhoA was sufficient to override the full spectrum of miR-31's described influences on metastasis *in vivo*. Finally, in Chapter Four, I extended these prior observations by determining that the simultaneous short hairpin RNA (shRNA)-mediated suppression of ITGA5, RDX, and RhoA sufficed to closely phenocopy the pleiotropic actions of miR-31 on *in vivo* metastasis. Assessed collectively, these studies revealed that miR-31's ability to antagonize metastasis is likely to be intimately associated with the capacity of this miRNA to concomitantly downregulate the expression levels of ITGA5, RDX, and RhoA. Perhaps surprisingly, my data further indicated that even a relatively modest change in the levels of ITGA5, RDX, and RhoA can profoundly impact the metastatic potential of human mammary carcinoma cells *in vivo*.

In consonance with these findings, others have previously described positive associations between elevated levels of ITGA5, members of the RDX family, or RhoA in carcinoma cells and disease progression in human tumors (Sahai and Marshall, 2002; McClatchey, 2003; Sanchez-Carbayo et al., 2006). One question that remains unanswered concerns whether the elevated levels of ITGA5, RDX, and RhoA encountered in patient tumor specimens arise as a direct consequence of decreased miR-31 function or, alternatively, through unrelated regulatory mechanisms. In the future, it would be worthwhile to address this issue by simultaneously analyzing the expression levels of miR-31, ITGA5, RDX, and RhoA in the same human tumors.

Notably, the concomitant suppression of ITGA5, RDX, and RhoA impedes not only the initial escape of neoplastic cells from a primary tumor, but also the ability of already-disseminated cancer cells to thrive at distant organ sites. In light of the fact that significant numbers of disseminated tumor cells are frequently already present in the systemic circulation, bone marrow, and/or distant organs of human carcinoma patients even at early stages of disease progression (Nagrath et al., 2007; Hüsemann et al., 2008), ITGA5, RDX, and RhoA may represent attractive therapeutic targets owing to their actions in metastasis-promotion at secondary organ sites. In particular, the capabilities of these proteins to alter metastatic colonization efficiency may be quite significant, as completion of this rate-limiting step of the invasion-metastasis cascade is believed to dictate disease outcome in many human cancers (Fidler, 2003; Gupta and Massagué, 2006).

Collectively, the findings of Chapters Three and Four suggested that a miRNA's effects on a given phenotype can be explained by its ability to suppress a relatively modest number of downstream targets. In the present case, the relevant effectors comprise only a small percentage of the total roster of mRNAs targeted by the miRNA under investigation. My observations are confined to a single miRNA and a single biological endpoint; accordingly, the extent to which this phenomenon is generalizable awaits future investigation. Nevertheless, several recent studies describe strong, but partial, effects on miRNA-mediated phenotypes by modulating individual target genes of miRNAs of interest (Xiao et al., 2007; Ma et al., 2007; Yu et al., 2007; Kumar et al. 2008). Such reports suggest the existence of other similarly organized miRNA response networks, in which a miRNA's impact on a biological process can be attributed to its ability to inhibit only a small sub-fraction of its mRNA targets.

miR-31 is predicted to regulate >200 mRNAs (Krek et al., 2005; Grimson et al., 2007). The findings of Chapters Three and Four, which indicated that miR-31's anti-metastatic effects can derive largely – if not entirely – from the ability of this miRNA to suppress a cohort of only three downstream target genes, are therefore quite surprising. Nonetheless, my data do not preclude the existence of still-uncharacterized miR-31 target genes that impinge upon the metastatic process in a manner that is functionally masked by the consequences of altering ITGA5, RDX, or RhoA levels. Also, it is possible that one or more *bona fide* targets of miR-31 that have relevance to the process of metastasis fail to be significantly downregulated by this miRNA in my breast cancer cell lines. Finally, my observation that the simultaneous suppression of ITGA5, RDX, and RhoA fails to recapitulate miR-31's ability to enhance primary mammary tumor growth suggests that additional miR-31 downstream effectors can mediate miR-31-dependent influences on the *in vivo* behavior of carcinoma cells that are mechanistically unrelated to metastasis.

One area that remains largely unexplored concerns the elucidation of additional functionally relevant direct downstream effectors of miR-31-imposed metastasis suppression. The work of others has implicated E2F2 and FIH as miR-31 target genes of putative relevance to neoplastic progression in ovarian carcinoma and head-and-neck squamous cell carcinoma, respectively (Creighton et al., 2010; Liu et al., 2010); however, the contributions of miR-31-mediated suppression of these two mRNAs to breast cancer progression remain unresolved. Moreover, while my *in vitro* analyses and *in vivo* findings upon intravenous injection suggested that miR-31-evoked modulation of Fzd3, MMP16, and M-RIP levels did not alter malignant behaviors, my preliminary data suggest that restored expression of Fzd3 or MMP16 may partially reverse miR-31-imposed metastasis suppression upon orthotopic implantation (data not

shown). Similarly, my preliminary data reveal that shRNA-mediated suppression of Fzd3 or MMP16 appears to impair the metastatic potential of orthotopically implanted otherwise-aggressive human breast cancer cells (data not shown). These preliminary observations merit future attention, as will deciphering the extent to which the metastasis-relevant functions of Fzd3 and MMP16 overlap with those of ITGA5, RDX, and RhoA.

Finally, in order to identify novel downstream effectors of miR-31 in an unbiased manner, I have performed microarray gene expression profiling on metastatic human breast cancer cells transduced with either a miR-31 expression vector or a control vector; these analyses revealed changes in the levels of a large number of mRNAs (data not shown). In the future, it will be essential to validate these microarray data by RT-PCR, as well as determine whether verified mRNA level changes reflect direct targeting of the transcript by miR-31 or instead an indirect effect of ectopic miR-31 expression. To this end, computational approaches and reporter gene assays utilizing mutagenized 3' untranslated region (UTR)-driven luciferase constructs will prove invaluable.

Whereas the individual re-expression of ITGA5, RDX, or RhoA largely reversed certain miR-31-imposed metastasis-relevant defects *in vitro*, individual restoration of ITGA5, RDX, or RhoA levels only partially rescued miR-31's effects on metastasis *in vivo*. This underscores the fact that available *in vitro* assays inadequately model the fully complexity of *in vivo* metastasis; caution must therefore be exercised when deploying these techniques, particularly in the absence of parallel *in vivo* analyses.

In summary, the data presented in Chapters Two, Three, and Four indicated that miR-31 sits atop ITGA5-, RDX-, and RhoA-containing regulatory pathways that affect multiple steps of the metastatic process, altering both the capacity of cancer cells to exit from a primary tumor and

the ability of already-disseminated neoplastic cells to survive and thrive in the foreign microenvironment afforded by the site of metastasis. As such, miR-31's pleiotropic anti-metastatic capabilities appear to position this miRNA as a critical safeguard against the acquisition of metastatic competence.

Therapeutic Potential of miR-31 Mimetics for the Remediation of Metastatic Disease

The data delineated in Chapter Five demonstrated that the temporally controlled re-activation of miR-31 in already-established metastases leads to marked regression of those malignant lesions; in contrast, acute re-expression of miR-31 in primary mammary tumors does not elicit cytostatic or cytotoxic responses. Recently, several laboratories have described effective methodologies for the *in vivo* delivery of either direct miRNA mimetics or miRNA-encoding genetic elements in murine model systems (Kota et al., 2009; Takeshita et al., 2010; Trang et al., 2010). These technological advances, when coupled with the findings presented in Chapter Five, provide a strong impetus for further evaluation of the safety and efficacy of miR-31-based therapeutic agents.

The majority of anti-cancer drugs in pre-clinical or clinical testing are designed to reduce primary tumor burden; moreover, most therapeutics intended for the remediation of metastatic disease block the initial dissemination of tumor cells but fail to affect the proliferation and survival of already-established metastases (Coussens et al., 2002; Steeg, 2006; Smith and Theodorescu, 2009; Ma et al., 2010). Because carcinoma patients frequently already harbor numerous disseminated tumor cells at the time of initial diagnosis and greater than 90% of human cancer mortality is attributable to distant metastases (Fidler, 2003; Gupta and Massagué, 2006; Nagrath et al., 2007; Hüsemann et al., 2008; Pantel et al., 2008), existing therapeutic

strategies are unlikely to satisfactorily address the principal cause of cancer-associated deaths. However, my observations in Chapter Five raise the possibility that intervention approaches centered upon restoring miR-31 functional activity may prove useful for combating metastatic disease in certain human carcinomas.

At present, I am undertaking several lines of investigation to address the major unresolved questions stemming from the data presented in Chapter Five. First, although acute miR-31 re-activation was found to trigger metastasis-specific cell cycle arrest and apoptosis, the downstream effector(s) of miR-31 responsible for mediating these phenotypic outcomes remained unexplored. In an endeavor to implicate specific miR-31 target genes as the key effectors of miR-31-evoked metastatic regression, I have created the 16 potential combinations of MDA-MB-231 metastatic human breast cancer cells ("231 cells") expressing either doxycycline (dox)-inducible miR-31 or control vector, plus constitutive ITGA5, RDX, and/or RhoA (data not shown). These cells have now been implanted into mice either orthotopically or intravenously in metastasis intervention assays similar to those outlined in Chapter Five. Given the vital roles of ITGA5, RDX, and RhoA downstream of miR-31 during breast cancer metastasis demonstrated in Chapters Three and Four – including the effects of ITGA5, RDX, and RhoA on the post-intravasation proliferation and survival of disseminated tumor cells – it is reasonable to hypothesize that one or more of these effector molecules will prove to be a critical target for the metastatic regression elicited by acute re-introduction of miR-31. However, it is also plausible that miR-31's capacity to elicit anti-metastatic therapeutic responses when re-activated in already-established metastases is mechanistically independent from its ability to control the expression levels of ITGA5, RDX, and/or RhoA. Should this prove to be the case,

additional miR-31 target genes must be assayed in the future for their respective abilities to reverse miR-31-dependent metastatic regression.

To further extend the work described in Chapter Five, I have also forged a collaboration with Thomas Andl of Vanderbilt University. A dox-inducible miR-31 transgenic mouse has been created (data not shown). In the future, it will be possible to cross this dox-inducible miR-31 mouse with established transgenic mammary carcinoma models – such as Mouse Mammary Tumor Virus (MMTV)-Neu and Polyoma Middle T (PyMT) mice (Muller et al., 1988; Maglione et al., 2001) – in order to perform metastasis intervention experiments analogous to those detailed in Chapter Five, but now in well-defined genetic models of breast cancer progression. As will be described in greater detail below, I am also in the process of generating Cre-loxP conditional miR-31-deficient mice that might similarly prove useful for dissecting the consequences of acutely perturbing miR-31 function in already-established metastases generated by genetic mouse models of breast cancer.

Together, these ongoing studies are anticipated to provide a more detailed understanding regarding the therapeutic potential for miR-31 mimetics in preventing and reversing metastatic progression. If the more sophisticated model systems described in the preceding paragraphs confirm the efficacy of miR-31 re-introduction as a form of anti-metastatic intervention, it is possible that future work will need to address the anti-metastatic activities of miR-31-based therapeutic agents in more rigorously structured pre-clinical and clinical trials.

What are the Upstream Signaling Events that Control miR-31 Expression Levels?

This thesis has focused largely on defining the biological consequences of altered miR-31 functional activity, as well as the efferent downstream mechanisms by which miR-31 elicits

these phenotypic responses. In contrast, Chapters Two, Three, Four, and Five provide little

insight regarding the afferent upstream stimuli that serve to control miR-31 expression levels. In

fact, I have previously attempted to implicate a number of candidate signaling pathways in the

regulation of endogenous miR-31 expression levels in both metastatic human breast cancer cells

and primary normal human mammary epithelial cells. My results, however, indicate that

exogenously supplied bone morphogenetic protein-2 (BMP-2), epidermal growth factor (EGF),

fibroblast growth factor (FGF), hepatocyte growth factor (HGF), insulin-like growth factor

(IGF), keratinocyte growth factor (KGF), platelet-derived growth factor (PDGF), transforming

growth factor _ (TGF_), or tumor necrosis factor (TNF) failed to affect miR-31 expression levels

in both of these cell types (data not shown). Similarly, pharmacological and genetic inhibition of

these pathways did not affect miR-31 expression in metastatic human breast cancer cells or

primary normal human mammary epithelial cells (data not shown). It has previously been

reported that endogenous miR-31 expression levels can be enhanced by TNF or BMP-2

treatment of endothelial cells and mesenchymal stem cells, respectively (Suárez et al., 2010; Sun

et al., 2009); however, my data suggest that these regulatory circuits do not operate in breast

epithelial cells. Instead, it appears plausible that miR-31 expression is regulated in an intricate

lineage- and cell type-dependent manner.

Given the important role of the epithelial-mesenchymal transition (EMT) in regulating

metastatic progression (Thiery, 2002; Polyak and Weinberg, 2009), I hypothesized that miR-31

levels might be controlled by the actions of one or more transcription factors known to induce an

EMT; however, I found that endogenous miR-31 expression in untransformed human mammary

epithelial cells was unaltered by ectopic expression of the EMT-inducing transcription factors

Snail, Twist, and Zeb1, as well as the EMT-inducing shRNA-conferred suppression of E-

cadherin (data not shown). Hence, the introduction of various EMT-provoking genetic alterations does not seem to elicit changes in endogenous miR-31 expression levels.

I have also examined the possibility that miR-31 might be epigenetically silenced in metastatic human breast cancer cells. While miR-31 expression remained unchanged upon treatment with a DNA methyltransferase inhibitor, endogenous miR-31 levels were dramatically increased when metastatic 231 cells were cultured in the presence of a histone deacetylase (HDAC) inhibitor (data not shown). In contrast, miR-31 expression in SUM-159 cells – another line of aggressive human breast cancer cells – was unaffected by treatment with this same HDAC inhibitor (data not shown). Taken together, these findings indicate that although miR-31 is epigenetically silenced in certain metastatic human breast cancer cell lines, the expression of this miRNA is downregulated by alternative mechanisms in other aggressive human breast cancer cell lines.

Because of the very limited success of the above-mentioned candidate-based approaches designed to uncover miR-31-regulating signals, I am also currently attempting to identify upstream transcriptional modulators of miR-31 expression in both metastatic human breast carcinoma cells and primary normal human mammary epithelial cells in an unbiased manner. One approach that I am deploying to achieve this goal involves deriving cell lines in which a luciferase reporter gene has been knocked in to the endogenous miR-31 locus (data not shown). These cells will then be used for high-throughput screening to uncover both shRNA hairpins and small molecules that impact reporter gene activity driven by the endogenous miR-31 promoter. It is anticipated that these analyses will yield insight regarding upstream stimuli – both genetic and epigenetic in nature – that act to dictate miR-31 expression levels. In light of the findings presented in Chapters Two, Three, Four, and Five, some of these miR-31-controlling proteins

and small molecules may merit further investigation concerning their potential prognostic and/or therapeutic utility in the diagnosis and/or remediation of metastatic disease.

Relevant to this proposed high-throughput reporter-based screening strategy is the recent demonstration that reduced mature miR-31 levels in certain cancer cell lines may arise due to the defective post-transcriptional processing of the miR-31 RNA precursor rather than transcriptional repression of the miR-31 gene itself (Lee et al., 2008). More specifically, while miR-31 precursor RNA was detected in a variety of tumor cell lines, levels of the fully processed mature miR-31 were almost entirely absent in some of the lines (Lee et al., 2008). In a portion of these cases, the defect in miR-31 processing may have derived from retention of the miR-31 precursor RNA in the nucleus (Lee et al., 2008), thereby precluding its endonucleolytic cleavage by the cytoplasmically confined Dicer endonuclease. These findings are particularly noteworthy, as this mode of regulation was observed for only a very small minority of individual miRNAs within a given cell type; in contrast, many other miRNAs in the same cell type were not regulated by this post-transcriptional mechanism (Lee et al., 2008). It will be of critical importance to discern whether post-transcriptional regulation of miR-31 is a peculiarity of certain genetically abnormal tumor cell lines or, alternatively, if this mode of control is an important determinant of the levels of functionally active miR-31 in a variety of normal and malignant cells. If post-transcriptional regulation of miR-31 processing is indeed a widespread means of titrating the functional levels of this miRNA, then the report-based screening approach described above is likely to fail to detect certain biologically important regulators of mature miR-31 levels. Moreover, a further topic for future work would involve deciphering the relevance of post-transcriptional control of mature miR-31 levels in primary tissue specimens derived directly from human cancer patients.

Another mechanism by which miR-31 expression might be downregulated in breast carcinomas is physical deletion of the miR-31-encoding genomic locus. Indeed, deletion of the *mir-31* locus has been observed in a variety of types of human carcinomas (Beroukhim et al., 2010). This observation is of particular interest in light of the fact that 9p21.3 – the chromosomal region within which the miR-31 gene resides – harbors the genomic loci encoding several *bona fide* tumor suppressor genes (p16, p14[ARF], and p15) (Sherr and McCormick, 2002), in addition to the metastasis suppressor miR-31. In fact, *mir-31* is located less than 450 kb from these neighboring tumor suppressor-encoding loci (Beroukhim et al., 2010). Consequently, even small deletions in the 9p21.3 region are likely to simultaneously abrogate the function of multiple gene products relevant to carcinoma pathogenesis. It is therefore striking that 9p21.3 is the single most frequently deleted chromosomal region across a wide variety of human cancers originating from a diverse array of tissue types (Weir et al., 2007; Beroukhim et al., 2010). Moreover, it is interesting that p16 – the best-studied of the three validated 9p21.3 tumor suppressors – is known to be inactivated predominantly by "regional mechanisms" (e.g., deletion or DNA methylation) rather than "local mechanisms" (e.g., point mutation) in human tumor specimens (Boström et al., 2001). I hypothesize that 9p21.3 deletions are so frequent because they represent an efficient means by which incipient tumor cells can concomitantly abolish the functions of multiple gene products that would otherwise act to oppose malignant progression.

In response to these findings, I am currently working with Andrea Richardson and Zhigang Wang – both faculty at Brigham and Women's Hospital – to further investigate the clinical relevance of 9p21.3 deletions for metastatic progression in human breast tumors. More specifically, we are characterizing the frequency of 9p21.3 deletions in a case-controlled cohort of human breast cancer patients of known metastasis outcome, determining which cancer-

relevant locus or loci (miR-31, p16, p14^{ARF}, and/or p15) is disrupted by each 9p21.3 deletion, and then deciphering the association between deletion of the various potential combinations of these genes and the propensity for metastatic relapse (data not shown). I speculate that these studies may unearth information of potential utility to the diagnosis of human carcinomas of the breast, and may also provide further mechanistic insights regarding the startlingly high prevalence of 9p21.3 deletions in clinically arising tumors.

I believe that future work will reveal a variety of cellular mechanisms by which mature miR-31 expression levels are controlled. Current evidence suggests that these mechanisms of modulation will include traditional transcriptional regulation, epigenetic control, physical deletion of the genomic locus encoding this miRNA, and post-transcriptional strategies that alter the efficiency of processing of the miR-31 precursor RNA to its mature form.

What are the Roles of miR-31 in Normal Organismal Development and Physiology?

The work reported herein has focused almost exclusively on the consequences of altered miR-31 functional activity in carcinoma cells. Hence, the studies reported in Chapters Two, Three, Four, and Five largely fail to illuminate the likely roles of miR-31 in normal cellular and organismal biology. Comprehending the contributions of miR-31 to normal development and physiology therefore represents a topic of great interest for future studies.

Work emanating from several other laboratories has begun to investigate the functions of miR-31 in normal physiology. For example, miR-31 has been found to be under-expressed in T regulatory (T_{reg}) cells, as compared to the levels of this miRNA in other T cell populations (Rouas et al., 2009). Of interest, miR-31 was found to be capable of directly targeting the mRNA encoding the forkhead box P3 (FOXP3) transcription factor, a master regulator of T_{reg} cell

differentiation and functional activity (Rouas et al., 2009). Thus, it is plausible that miR-31 antagonizes a T_{reg} phenotype by suppressing the expression levels of this important transcription factor.

A role for miR-31 during inflammatory responses has been suggested based on the observation that the cytokine TNF was capable of enhancing miR-31 expression in endothelial cells, resulting in suppression of the endothelial adhesion molecule E-selectin (Suárez et al., 2010). This downregulation of E-selectin led, in turn, to reduced physical interactions between endothelial cells and neutrophils *in vitro*, ultimately triggering negative feedback control of inflammatory signaling (Suárez et al., 2010). These findings therefore raise the possibility that miR-31 levels are dynamically regulated in response to acute stressors in order to mount an appropriate inflammatory response.

Yet other investigators have evaluated changes in miR-31 expression patterns in multipotent progenitor cells and stem cells upon induced differentiation. For example, miR-31 was one of three miRNAs whose expression levels decreased in human unrestricted somatic stem cells upon osteogenic differentiation (Schaap-Oziemlak et al., 2009). Another group observed reduced miR-31 expression in rat adipose-derived stem cells that had been triggered to undergo adipogenic differentiation; in this study, several known adipogenic differentiation genes were identified among the computationally predicted downstream targets of miR-31, although no attempt was made to experimentally validate these computational predictions (Tang et al., 2009). Others found that the addition of exogenous BMP-2 stimulated miR-31 expression levels in mesenchymal stem cells (Sun et al., 2009). These authors also reported that ectopic expression of miR-31 prevented the differentiation of mesenchymal stem cells into adipocytes, a phenotype likely mediated – at least in part – by the capacity of miR-31 to directly target the gene encoding

CCAT/enhancer-binding protein-alpha (CEBPA), an established promoter of the adipocytic differentiation program (Sun et al., 2009).

Taken together, these studies begin to provide evidence that miR-31-mediated signaling events are of fundamental importance in a diverse array of normal cell types. However, these prior studies provide only rudimentary insight regarding the full spectrum of likely roles for miR-31 in normal development and physiology. Definitive resolution of the normal cellular and organismic functions of miR-31 therefore necessitates the creation of more sophisticated genetic models of altered miR-31 function.

For these reasons, I am currently in the process of generating miR-31-deficient murine genetic model systems. More specifically, I have already derived a traditional knockout vector targeting the miR-31-encoding genomic locus and I am also now in the process of creating a Cre-loxP conditional knockout vector against *mir-31* (data not shown). Working with the MIT Koch Institute ES Cell and Transgenics Core Facility, the traditional knockout vector has been electroporated into murine embryonic stem cells and I am now identifying successfully targeted clones suitable for blastocyst injections (data not shown).

I speculate that the miR-31-deficient mice that will ultimately be generated from this work will represent an important tool for dissecting the contributions of miR-31 function to both embryonic development and the homeostatic maintenance of various adult tissues. Moreover, these miR-31-knockout mice may prove useful for further refining our understanding of the roles of miR-31 in disease pathogenesis. For example, the miR-31-deficient animals could be crossed with well-characterized mammary carcinoma transgenic murine models (e.g., MMTV-Neu mice or PyMT mice) in order to obtain stringent genetic evidence concerning the contributions of miR-31 activity to both primary tumor development and subsequent metastatic progression. In

this respect, the miR-31 conditional knockout mice will be of particular value, as they will allow me to conduct metastasis intervention studies analogous to those described in Chapter Five – but now using a genetic miR-31-deficient experimental system.

Similarly, the dox-inducible miR-31 transgenic mice that were created in collaboration with Thomas Andl of Vanderbilt University and described above may also prove useful for dissecting the roles of miR-31 in normal development and physiology. Very preliminary initial characterization of these mice reveals a variety of apparent abnormalities in multiple tissue types in the wake of long-term dox-dependent induction of miR-31 (data not shown). In the future, it will be critical to cross the inducible miR-31 transgenic mice to animals carrying various tissue-specific reverse tetracycline-controlled transactivator (rtTA) or tetracycline-controlled transactivator (tTA) elements and then activate miR-31 expression in a spatially defined manner at various specific timepoints during development, as well as in adult mice. For example, if the dox-inducible miR-31 transgenic mice were bred to animals bearing a mammary-specific dox-responsive element, I could discern the effects of miR-31 on normal mammary gland development or, alternatively, the effects of modulating miR-31 expression during important physiological processes such as pregnancy.

To complement insights that might be obtained from the miR-31 knockout mice and the dox-inducible miR-31 transgenic mice, I have also initiated *in vitro* studies to investigate the roles of miR-31 in normal human mammary epithelial cells. For example, I found that MCF10A cells contain relatively high levels of endogenous miR-31 (data not shown), and I have now generated MCF10A cells that stably express either constitutive or dox-inducible miR-31 sponge constructs (data not shown). MCF10A cells are an established line of spontaneously immortalized, untransformed human mammary epithelial cells; importantly, when cultured under

appropriate conditions, MCF10A cells form three-dimensional structures that closely recapitulate the glandular architecture of normal breast epithelial tissue (Debnath and Brugge, 2005). Brugge and colleagues have previously demonstrated that this system is a powerful and tractable tool for ascribing the functional impact of genetic factors of interest on numerous aspects of epithelial cell biology (Debnath and Brugge, 2005). Future work will therefore assess the effects of perturbing miR-31 functional activity in MCF10A three-dimensional culture models.

The Contributions of miR-31 to Other Pathological Conditions

The research outlined in this thesis has focused on the role of miR-31 in one specific pathological condition: cancer. However, the work of others has implicated aberrant miR-31 activity in the pathogenesis of several other disease states. For example, miR-31 expression was found to be diminished during the course of ischemia-induced retinal neo-vascularization (She et al., 2008). Mechanistically, the authors proposed that miR-31 might elicit these angiogenesis-related phenotypes via its capacity to downregulate the expression levels of PDGFb and HIF1_ – two known neo-vascularization-promoting factors. Additionally, the authors reported that injection of miR-31 RNA precursor mimetics significantly decreased the extent of ischemia-induced retinal neo-vascularization and choroidal neo-vascularization *in vivo* in mice (She et al., 2008). Together, these observations suggest that miR-31 functions as a negative regulator of nutrient deprivation-induced neo-vascularization.

Another report, which employed a transgenic rat model, has indicated that miR-31 is downregulated upon the onset of polycystic kidney disease (Pandey et al., 2008). This study also suggested that computationally predicted miR-31 target genes involved in the processes of calcium signaling and cell cycle regulation exhibited changes in their mRNA levels that

coincided with downregulation of miR-31 during the course of polycystic kidney disease pathogenesis (Pandey et al., 2008). Thus, miR-31 may affect the progression of polycystic kidney disease by targeting effector molecules involved in core signaling pathways associated with this malady.

Other groups have reported that miR-31 expression is diminished in granulocytes from patients afflicted with primary myelofibrosis, relative to the levels of miR-31 present in granulocytes from unaffected individuals (Guglielmelli et al., 2007). Consequently, certain aspects of hematopoietic homeostatic maintenance may be modulated by the actions of miR-31.

Finally, miR-31 was upregulated by more than 70-fold in a mouse model of muscular dystrophy, as compared to the levels of this miRNA in wild type littermates (Greco et al., 2009). The authors of this study proposed that miR-31 may promote skeletal muscle regeneration upon tissue insult; however, experimental validation of this mechanistic model was not provided (Greco et al., 2009). Hence, hyper-activation of miR-31 – and not just the reduced expression of this miRNA – can contribute to the progression of human diseases.

Assessed collectively, the above-described studies reveal that aberrant miR-31 signaling occurs in a variety of pathological conditions and may play a functional role in mediating these disease phenotypes. Future studies will be necessary to explore the contributions of miR-31 to the etiologies of these diseases in greater detail, as well as to define additional roles for this miRNA in the onset and maintenance of various other pathologies. Notably, the miR-31-deficient murine genetic systems that I am endeavoring to generate – as described above – may prove useful for elucidating miR-31's functional contributions to these various disease states.

An Experimental System for the Unbiased Discovery of Genes Relevant for Breast Cancer Metastasis

While miR-31 appears to represent a key regulator of metastatic progression in breast carcinomas, a number of additional genetic factors are also certain to play critical roles in controlling aspects of the invasion-metastasis cascade during breast cancer pathogenesis. Therefore, in Chapter Six, I undertook to determine the identity of additional genes whose encoded products function in the acquisition of metastatic competence. In order to do so, I established an experimental system that allowed me to preserve and assay the functionally critical, intrinsic intercellular diversity that pre-exists within tumor cell populations. More specifically, I derived a relatively large number of single-cell clones (SCCs) from a heterogeneous bulk population of metastatic human breast cancer cells. I then characterized their phenotypic diversity with regard to several metastasis-relevant parameters of interest (including *in vitro* cell motility and *in vivo* metastasis formation) and performed gene expression profiling on those SCCs that displayed noteworthy phenotypic differences. Together, these analyses have elucidated a number of candidate regulators of the processes of interest.

One assumption that the successful utilization of this SCC-based screening system is predicated upon is that the various SCCs are relatively stable at a genomic level. Importantly, the SCCs appear to be stable even after extended *in vitro* culture, as the phenotypic behaviors of the SCCs in the described *in vitro* and *in vivo* assays have proven robust even after long intervening intervals of *in vitro* passage (data not shown). However, in the future, it will be important to directly demonstrate that this functional robustness is accompanied by relative genomic stability; to do so, I will compare the global gene expression profiles of early-passage and late-passage samples drawn from the same SCC. Similarly, one might wish to derive a relatively large

number of individual clones from a single SCC and subsequently assess the extent of genetic diversity and functional heterogeneity that exists amongst these various "clones of a clone" in order to address this point further.

With regard to the proof-of-concept screen conducted in Chapter Six to identify putative regulators of *in vitro* cell motility, several lines of experimentation are still ongoing. First, additional phenotypic characterization of the biological consequences of perturbing RhoJ expression is currently underway. More specifically, both gain-of-function and loss-of-function approaches are being taken to investigate the effects of altering RhoJ levels on *in vitro* invasion, *in vitro* proliferative kinetics, *in vivo* primary tumor formation, and *in vivo* metastatic capacity (data not shown). Together, these experiments are anticipated to provide further resolution concerning the spectrum of RhoJ's impacts on malignancy-associated attributes. Additionally, more refined mechanistic studies regarding the particular biochemical activities of RhoJ that underlie its impact on *in vitro* cell motility, as well as the identity of important downstream effectors of RhoJ-evoked suppression of cell migration, will soon be undertaken.

Second, additional candidate genes identified by the *in vitro* motility screen will be assayed in greater detail in future work. To this end, shRNA vectors targeting a number of these mRNAs of interest have been created and transduced into appropriate target cells (data not shown). Analogous to the experiments conducted involving RhoJ, both gain-of-function and loss-of-function approaches will be performed to determine whether the activity of each of these factors is either necessary or sufficient to impact *in vitro* cell motility. In certain cases, the results obtained from these assays may prompt me to conduct more detailed follow-up experiments. For example, several of the genes implicated in my initial screen encode transcription factors of unknown function. An important topic for future studies would therefore involve enumerating

the rosters of downstream effectors of these transcription factors whose deregulation is likely to account for the observed phenotypic impacts of perturbation of the transcription factors themselves. This might be accomplished, for example, by combining data obtained from microarray-based gene expression profiling upon overexpression or shRNA-mediated suppression of the transcription factor of interest with independently conducted genome-wide chromatin immunoprecipitation analyses of the promoter sequences occupied by the transcription factors under investigation.

Similarly, the functional consequences of altering the expression levels of many of the candidate genes identified in the screen for novel regulators of *in vivo* metastasis outlined in Chapter Six remain unexplored. At present, shRNA hairpins targeting many of the genes of interest have been cloned and then introduced into appropriate target cells (data not shown). In the future, a number of experiments – including *in vivo* spontaneous metastasis assays – will be conducted using these genetically modified cells. Based on the outcome of these studies, more detailed investigation of the particular step(s) of the invasion-metastasis cascade impacted by a subset of these genes may prove fruitful. Moreover, the mechanistic bases responsible for any observed phenotypes will need to be dissected in detail.

Concerning the more general utility of the SCC system, in the future, it will be possible to expand upon my previous analyses by assaying additional phenotypes of interest, such as sensitivity to chemotherapeutic agents, enrichment for tumor-initiating cells (TICs), regulation of the EMT, *in vivo* tumor neo-angiogenesis, *in vivo* cell proliferation, and resistance to various forms of stress-induced apoptosis. Moreover, miRNA expression profiling could be performed to complement the previously conducted mRNA microarrays in an endeavor to implicate novel miRNAs whose functions are relevant for the processes of interest. Taken together, the data

currently amassed suggest that this SCC-based screening platform may represent a valuable tool for the identification of novel genes that contribute to malignancy-associated attributes; therefore, future utilization of this experimental system appears to be warranted.

Final Perspective

Collectively, the research described in this thesis has endeavored to (1) elucidate novel genes that regulate breast cancer metastasis, (2) determine the cell-biologic consequences conferred by the altered expression of these molecules, and (3) uncover the mechanistic underpinnings for these genetically dictated phenotypic changes. The insights attained from these studies have implications for our understanding of metastatic progression and provide evidence that may aid in our comprehension of the cellular origin and subsequent genetic evolution of incipient metastatic carcinoma cells. Moreover, this work identifies previously unappreciated genetic factors that may one day serve as clinically useful prognostic biomarkers for aggressive malignancy and/or potential therapeutic targets for the remediation of metastatic carcinomas.

REFERENCES

Asangani IA, Rasheed SA, Nikolova DA, et al. (2008). MicroRNA-21 post-transcriptionally downregulates tumor suppressor Pdcd4 and stimulates invasion, intravasation and metastasis in colorectal cancer. Oncogene *27*, 2128-2136.

Bandrés E, Cubedo E, Agirre X, et al. (2006). Identification by real-time PCR of 13 mature microRNAs differentially expressed in colorectal cancer and non-tumoral tissues. Mol Cancer 2006 *5*, 29.

Beroukhim R, Mermel CH, Porter D, et al. (2010). The landscape of somatic copy-number alterations across human cancer. Nature *463*, 899-905.

Blenkiron C, Goldstein LD, Thorne NP, et al. (2007). MicroRNA expression profiling of human breast cancer identifies new markers of tumor subtype. Genome Biol. *8*, R214.

Boström J, Meyer-Puttlitz B, Wolter M, et al. (2001). Alterations of the tumor suppressor genes CDKN2A (p16(INK4a)), p14(ARF), CDKN2B (p15(INK4b)), and CDKN2C (p18(INK4c)) in atypical and anaplastic meningiomas. Am J Pathol *159*, 661-669.

Brueckner B, Stressemann C, Kuner R, et al. (2007). The human let-7a-3 locus contains an epigenetically regulated microRNA gene with oncogenic function. Cancer Res *67*, 1419-1423.

Calin GA, Sevignani C, Dumitru CD, et al. (2004). Human microRNA genes are frequently located at fragile sites and genomic regions involved in cancers. Proc Natl Acad Sci USA *101*, 2999-3004.

Coussens LM, Fingleton B, and Matrisian LM. (2002). Matrix metalloproteinase inhibitors and cancer: trials and tribulations. Science *295*, 2387-2392.

Creighton CL, Fountain MD, Yu Z, et al. (2010). Molecular profiling uncovers a p53-associated role for microRNA-31 in inhibiting the proliferation of serous ovarian carcinomas and other cancers. Cancer Res *70*, 1906-1915.

Debnath J and Brugge JS. (2005). Modeling glandular epithelial cancers in three-dimensional cultures. Nat Rev Cancer *5*, 675-688.

Desmedt C, Haibe-Kains B, Wirapati P, et al. (2008). Biological processes associated with breast cancer clinical outcome depend on the molecular subtypes. Clin Cancer Res. *14*, 5158-5165.

Dykxhoorn DM, Wu Y, Xie H, et al. (2009). miR-200 enhances mouse breast cancer cell colonization to form distant metastases. PLoS One *4*, e7181.

Fidler IJ. (2003). The pathogenesis of cancer metastasis: the 'seed and soil' hypothesis revisited. Nat Rev Cancer *3*, 453-458.

Greco S, De Simone M, Colussi C, et al. (2009). Common micro-RNA signature in skeleton muscle damage and regeneration induced by Duchenne muscular dystrophy and acute ischemia. FASEB J 23, 3335-3346.

Grimson A, Farh KK, Johnston WK, Garrett-Engele P, Lim LP, and Bartel DP. (2007). MicroRNA targeting specificity in mammals: determinants beyond seed pairing. Mol Cell *27*, 91-105.

Guglielmelli P, Tozzi L, Pancrazzi A, et al. (2007). MicroRNA expression profile in granulocytes from primary myelofibrosis patients. Exp Hematol *35*, 1708-1718.

Guo J, Miao Y, Xiao B, et al. (2009). Differential expression of microRNA species in human gastric cancer versus non-tumorous tissues. J Gastroenterol Hepatol *24*, 652-657.

Gupta GP and Massagué J. (2006). Cancer metastasis: building a framework. Cell *127*, 679-695.

Gupta GP, Nguyen DX, Chiang AC, et al. (2007). Mediators of vascular remodeling co-opted for sequential steps in lung metastasis. Nature *446*, 765-770.

Huang Q, Gumireddy K, Schrier M, et al. (2008). The microRNAs miR-373 and miR-520c promote tumour invasion and metastasis. Nat Cell Biol *10*, 202-210.

Hüsemann Y, Geigl JB, Schubert F, et al. (2008). Systemic spread is an early step in breast cancer. Cancer Cell *13*, 58-68.

Kondo N, Toyama T, Sugiura H, Fujii Y, and Yamashita H. (2008). miR-206 Expression is down-regulated in estrogen receptor _-positive human breast cancer. Cancer Res. *68*, 5004-5008.

Kota J, Chivukula PR, O'Donnell KA, et al. (2009). Therapeutic microRNA delivery suppresses tumorigenesis in a murine liver cancer model. *Cell 137*, 1005-1017.

Krek A, Grün D, Poy MN, et al. (2005). Combinatorial microRNA target predictions. Nat Genet *37*, 495-500.

Kumar MS, Erkeland SJ, Pester RE, et al. (2008). Suppression of non-small cell lung tumor development by the let-7 microRNA family. Proc Natl Acad Sci USA *105*, 3903-3908.

Landgraf P, Rusu M, Sheridan R, et al. (2007). A mammalian microRNA expression atlas based on small RNA library sequencing. Cell *129*, 1401-1414.

Lee EJ, Baek M, Gusev Y, Brackett DJ, Nuovo GJ, and Schmittgen TD. (2008). Systematic evaluation of microRNA processing patterns in tissues, cell lines, and tumors. RNA *14*, 35-42.

Liu X, Chen Z, Yu J, Xia J, and Zhou X. (2009). MicroRNA profiling and head and neck cancer. Comp Funct Genomics, 837514.

Liu CJ, Tsai MM, Hung PS, et al. (2010). miR-31 ablates expression of the HIF regulatory factor FIH to activate the HIF pathway in head and neck carcinoma. Cancer Res *70*, 1635-1644.

Lujambio A, Calin GA, Villanueva A, et al. (2008). A microRNA DNA methylation signature for human cancer metastasis. Proc Natl Acad Sci USA *105*, 13556-13561.

Ma L, Reinhardt F, Pan E, et al. (2010). Therapeutic silencing of miR-10b inhibits metastasis in a mouse mammary tumor model. Nat Biotechnol *28*, 341-347.

Ma L, Teruya-Feldstein J, and Weinberg RA. (2007). Tumour invasion and metastasis initiated by microRNA-10b in breast cancer. Nature *449*, 682-688.

Maglione JE, Moghanaki D, Young LJ, et al. (2001). Transgenic polyoma middle-T mice model premalignant mammary disease. Cancer Res *61*, 8298-8305.

Massagué J. (2008). TGF_ in cancer. Cell *134*, 215-230.

Mattie MD, Benz, CC, Bowers J, et al. (2006). Optimized high-throughput microRNA expression profiling provides novel biomarker assessment of clinical prostate and breast cancer biopsies. Mol Cancer *19*, 5-24.

McClatchey AI. (2003). Merlin and ERM proteins: unappreciated roles in cancer development? Nat Rev Cancer *3*, 877-883.

Motoyama K, Inoue H, Takatsuno Y, et al. (2009). Over- and under-expressed microRNAs in human colorectal cancer. Int J Oncol *34*, 1069-1075.

Muller WJ, Sinn E, Pattengale PK, Wallace R, and Leder P. (1988). Single-step induction of mammary adenocarcinoma in transgenic mice bearing the activated c-neu oncogene. Cell *54*, 101-115.

Nagrath S, Sequist LV, Maheswaran S, et al. (2007). Isolation of rare circulating tumour cells in cancer patients by microchip technology. Nature *450*, 1235-1239.

Pandey P, Brors B, Srivastava PK, et al. (2008). Microarray-based approach identifies microRNAs and their target functional patterns in polycystic kidney disease. BMC Genomics *9*, 624.

Pantel K, Brakenhoff RH, and Brandt B. (2008). Detection, clinical relevance and specific biological properties of disseminating tumour cells. Nat Rev Cancer *8*, 329-340.

Polyak K and Weinberg RA. (2009). Transitions between epithelial and mesenchymal states: acquisition of malignant and stem cell traits. Nat Rev Cancer *9*, 265-273.

Rouas R, Fayyad-Kazan H, El Zein N, et al. (2009). Human natural Treg microRNA signature: role of microRNA-31 and microRNA-21 in FOXP3 expression. Eur J Immunol *39*, 1608-1618.

Sahai E and Marshall CJ. (2002). Rho-GTPases and cancer. Nat Rev Cancer *2*, 133-142.

Sanchez-Carbayo M, Socci ND, Lozano J, Saint F, and Cordon-Cardo C. (2006). Defining molecular profiles of poor outcome in patients with invasive bladder cancer using oligonucleotide microarrays. J Clin Oncol *24*, 778-789.

Sathyan P, Golden HB, and Miranda RC. (2007). Competing interactions between micro-RNAs determine neural progenitor survival and proliferation after ethanol exposure. J Neurosci. *27*, 8546-8557.

Schaap-Oziemlak A, Raymakers RA, Bergevoet SM, et al. (2009). MicroRNA has-miR-135b regulates mineralization in osteogenic differentiation of human unrestricted somatic stem cells (USSCs). Stem Cells Dev, Epub ahead of print.

Schaefer A, Jung M, Mollenkopf HJ, et al. (2010). Diagnostic and prognostic implications of microRNA profiling in prostate carcinoma. Int J Cancer *126*, 1166-1176.

Semenza GL. (2003). Targeting HIF-1 for cancer therapy. Nat Rev Cancer *3*, 721-732.

She J, Yang X, Xie B, et al. (2008). MicroRNAs regulate ocular neovascularization. Mol Ther *16*, 1208-1216.

Sherr C and McCormick F. (2002). The RB and p53 pathways in cancer. Cancer Cell *2*, 103-112.

Si ML, Zhu S, Wu H, Lu Z, Wu F, and Mo, YY. (2007). miR-21-mediated tumor growth. Oncogene *26*, 2799-2803.

Smith SC and Theodorescu D. (2009). Learning therapeutic lessons from metastasis suppressor proteins. Nat Rev Cancer *9*, 253-264.

Sørlie T, Perou CM, Tibshirani R, et al. (2001). Gene expression patterns of breast carcinomas distinguish tumor subclasses with clinical implications. Proc Natl Acad Sci USA *98*, 10869-10874.

Steeg PS. (2003). Metastasis suppressors alter the signal transduction of cancer cells. Nat Rev Cancer *3*, 55-63.

Steeg PS. (2006). Tumor metastasis: mechanistic insights and clinical challenges. Nat Med *12*, 895-904.

Suárez Y, Wang C, Manes TD, and Pober JS. (2010). Cutting edge: TNF-induced microRNAs regulate TNF-induced expression of E-selectin and intercellular adhesion molecule-1 on human endothelial cells: feedback control of inflammation. J Immunol *184*, 21-25.

Sun F, Wang J, Pan Q, et al. (2009). Characterization of function and regulation of miR-24-1 and miR-31. Biochem Biophys Res Commun *380*, 660-665.

Takeshita F, Patrawala L, Osaki M, et al. (2010). Systemic delivery of synthetic microRNA-16 inhibits the growth of metastatic prostate tumors via downregulation of multiple cell-cycle genes. *Mol Ther 18*, 181-187.

Tang YF, Zhang Y, Li XY, Li C, Tian W, and Liu L. (2009). Expression of miR-31, miR-125b-5p, and miR-326 in the adipogenic differentiation process of adipose-derived stem cells. OMICS *13*, 331-336.

Tavazoie SF, Alarcón C, Oskarsson et al. (2008). Endogenous human microRNAs that suppress breast cancer metastasis. Nature *451*, 147-152.

Thiery JP. (2002). Epithelial-mesenchymal transitions in tumour progression. Nat Rev Cancer *2*, 442-454.

Trang P, Medina PP, Wiggins JF, et al. (2010). Regression of murine lung tumors by the let-7 microRNA. *Oncogene 29*, 1580-1587.

Usvasalo A, Ninomiya S, Räty R, et al. (2010). Focal 9p instability in hematologic neoplasias revealed by comparative genomic hybridization and single-nucleotide polymorphism microarray analyses. Genes Chromosomes Cancer, Epub ahead of print.

Veerla S, Lindgren D, Kyist A, et al. (2009). MiRNA expression in urothelial carcinomas: important roles of miR-10a, miR-222, miR-125b, miR-7, and miR-452 for tumor stage and metastasis, and frequent homozygous losses of miR-31. Int J Cancer *124*, 2236-2242.

Voorhoeve PM, le Sage C, Schrier M, et al. (2006). A genetic screen implicates miRNA-372 and miRNA-373 as oncogenes in testicular germ cell tumors. Cell *124*, 1169-1181.

Weir BA, Woo MS, Getz G, et al. (2007). Characterizing the cancer genome in lung adenocarcinoma. Nature *450*, 893-898.

Wellner U, Schubert J, Burk UC, et al. (2009). The EMT-activator ZEB1 promotes tumorigenicity by repressing stemness-inhibiting microRNAs. Nat Cell Biol *11*, 1487-1495.

Wong TS, Liu XB, Wong BY, Ng RW, Yuen AP, and Wei WI. (2008). Mature miR-184 as potential oncogenic microRNA of squamous cell carcinoma of tongue. Clin Cancer Res *14*, 2588-2592.

Wong QW, Lung RW, Law PT, et al. (2008). MicroRNA-223 is commonly repressed in hepatocellular carcinoma and potentiates expression of Stathmin1. Gastroenterology *135*, 257-269.

Wszolek MF, Rieger-Christ KM, Kenney PA, et al. (2009). A microRNA expression profile defining the invasive bladder tumor phenotype. Urol Oncol, Epub ahead of print.

Xiao C, Calado DP, Galler G, et al. (2007). MiR-150 controls B cell differentiation by targeting the transcription factor c-Myb. Cell *131*, 146-159.

Yan LX, Huang XF, Shao Q, Huang MY, Deng L, Wu QL, et al. (2008). MicroRNA miR-21 overexpression in human breast cancer is associated with advanced clinical stage, lymph node metastasis and patient poor prognosis. RNA *14*, 2348-2360.

Yu F, Yao H, Zhu P, al. (2007). Let-7 regulates self renewal and tumorigenicity of breast cancer cells. Cell *131*, 1109-1123.

Zhang Y, Guo J, Li D, et al. (2009). Down-regulation of miR-31 expression in gastric cancer tissues and its clinical significance. Med Oncol, Epub ahead of print.

Zhang L, Huang J, Yang N, et al. (2006). MicroRNAs exhibit high frequency genomic alterations in human cancer. Proc Natl Acad Sci USA *103*, 9136-9141.

Zhu S, Wu H, Wu F, et al. (2008). MicroRNA-21 targets tumor suppressor genes in invasion and metastasis. Cell Res *18*, 350-359.